STUDY S-267

UNCERTAINTIES OF EQUATIONS OF STATE OF EXPLOSIVELY LOADED ROCK SALT

W. David Barfield

February 1968

INSTITUTE FOR DEFENSE ANALYSES
SCIENCE AND TECHNOLOGY DIVISION

IDA

IDA Log No. HQ 67-6572
Copy 43 of 100 copies

170

STUDY S-267

UNCERTAINTIES OF EQUATIONS OF STATE OF EXPLOSIVELY LOADED ROCK SALT

W. David Barfield

February 1968

INSTITUTE FOR DEFENSE ANALYSES
SCIENCE AND TECHNOLOGY DIVISION
400 Army-Navy Drive, Arlington, Virginia 22202

Contract DAHC15 67 C 0011
ARPA Assignment 10

"It may well be that the results are no more incorrect than the true uncertainties in the problem would otherwise ensure."

H.W. Lewis and S.B. Treiman,
"Seismic Signals from Nuclear Explosions in Overdriven Cavities"

"We fully realize that error estimates are difficult and uncertain things but they are nevertheless worthy of one's best effort."

E.R. Cohen and J.W.M. Dumond,
"Our Knowledge of the Fundamental Constants of Physics and Chemistry in 1965"

ACKNOWLEDGMENTS

The author thanks personnel of the IDA Library for courteous cooperation in furnishing a bibliography on properties of alkali halides and rocks as well as dozens of articles and reports on which the present study is based. Helpful conversations with B.E. Cummings, G.J. MacDonald, Humbert Morris, Ivan Nelson, F.W. Niedenfuhr, F.B. Porzel and other members of the Science and Technology Division are happily acknowledged. Mrs. Marion Fickett furnished a graph-plotting computer program; Joan Begelman and Vera Wilson assisted with programming the numerical calculations. Sandra Wynne and Mrs. Lotte Goldman facilitated the translation of some of the references. Thanks are due to F.B. Porzel, members of the Physics Research Division of IIT Research Institute, Dr. T.H. Schiffman, Assistant Director, and members of the IITRI research group and Dr. Fred Holzer, of the Lawrence Radiation Laboratory, for reading the manuscript and furnishing helpful comments.

ABSTRACT

In connection with a general investigation of uncertainties in prediction capability for close-in ground motion due to buried explosions, rock salt (halite) is selected as an example of rock-like material for purposes of assessing uncertainties associated with methods for determining material properties and with models of material behavior. Uncertainties of techniques for "laboratory" measurement of shock and static compressibility and plastic flow properties and uncertainties of four different equations of state for highly compressed NaCl are discussed.

CONTENTS

I.	Introduction	1
II.	Uncertainties in Dynamic and Static Compressibility Measurements	3
	A. Uncertainties in Shock Measurements	3
	1. Pure NaCl	3
	2. Naturally Occurring Rock Salt	15
	B. Uncertainties in Static Compression Measurements for Rock Salt	21
III.	Uncertainties of Plastic Flow Measurements	27
	A. Results of Plastic Flow Measurements	29
	B. Sources of Experimental Error	33
	C. Fracture Phenomena Uncertainties	35
IV.	Uncertainties of Theoretical Equations of State	57
	A. Free Volume Theory: Equation of State of Al'tshuler et al. (1965)	58
	B. Equation of State of Kormer et al. (1965)	72
	C. Mie-Grüneisen Equation of State: Decker's Equation	75
	D. Equation of State of Rogers (1964) and Cook (1963)	91
V.	Summary	107
	Appendix A - Uncertainties of "Laboratory" Shock Compression Measurements for Solids	109
	Appendix B - Properties of Rock Salt in Salt Domes	131
	Appendix C - Uncertainties in Hugoniot Measurements for Pusher Materials	135
	Bibliography	147

CHAPTER I

INTRODUCTION

I. INTRODUCTION

In connection with a general investigation of uncertainties in prediction capability for close-in ground motion due to buried explosions, rock salt (halite) was selected as an example of rock-like material for purposes of assessing uncertainties associated with methods for determining material properties and with models of material behavior. Studies of pure and relatively simple solids such as alkali halides serve to demonstrate the minimum uncertainty associated with methods and techniques for measurement of mechanical properties of rocks, free from complications of variability of composition, water content, porosity, etc.* Similarly, the uncertainties associated with models** of mechanical and thermodynamic behavior are probably smaller for alkali halides than for other rock-like materials. Results for pure NaCl and naturally occurring rock salt are compared.

It is convenient to consider four regions of thermodynamic/mechanical behavior: the close-in high-temperature region,*** the strong shock region, the "subhydrodynamic" region of stress levels sufficiently low that the stress is not well represented by a scalar pressure and sufficiently high that the approximations of linear elasticity theory are not appropriate, and the elastic region.

---

* There remain complications of variability of grain size and orientation, strain history, etc.

** "Model" is used here to mean "macroscopic flow model" (i.e., instead of "microscopic model of the physical flow mechanism").

*** I.e., the close-in region heated by direct contact with a nuclear explosion or--in the case of an explosion in a cavity--the fireball.

The present study discusses uncertainties of techniques for "laboratory"* measurement of mechanical properties in the strong shock and subhydrodynamic or plastic flow regions, and uncertainties of equations of state for the highly compressed region.**

It is hoped that in addition to giving insight into the order of magnitude of the uncertainties associated with knowledge of material properties, the results of this study will also prove useful by suggesting areas where additional research is indicated.

---

* A somewhat arbitrary distinction is made between "laboratory" tests - meaning experiments in which samples of material under study are subjected to static, dynamic, impact or explosive loading--and "field" tests--in which the energy of the explosive source is (more or less) coupled to the entire natural medium *in situ*.

** It was necessary to limit the scope of the present investigation so as to preclude discussion of uncertainties of plastic flow models, elastic measurements, thermodynamic description of the vaporized-expanded region, and effects of nuclear radiations on material properties.

CHAPTER II

UNCERTAINTIES IN DYNAMIC AND STATIC COMPRESSIBILITY MEASUREMENTS

II. UNCERTAINTIES IN DYNAMIC AND STATIC COMPRESSIBILITY MEASUREMENTS

A. UNCERTAINTIES IN SHOCK MEASUREMENTS

1. Pure NaCl

The dynamic compressibility ("Hugoniot") measurements for pure NaCl are summarized in Table 1. The $P(\eta)$* Hugoniot points derived from the experimental data have been replotted on a large scale in Fig. 1 to facilitate comparison and assessment of uncertainties. It is fortunate that measurements have been made in different laboratories over a large range of pressures, using somewhat different techniques. These techniques, however, are basically variations on the same theme, so there exists the possibility of systematic errors common to all the measurements.**

The residual minimum uncertainty in the shock measurements for rock salt is that associated with the precision of the measurement of the shock wave and free-surface velocities, which is of the order of 0.5 to 2 percent. For various reasons discussed in the following pages--mainly, the scatter in the data for both rock salt and "pusher" materials--it is likely that the experimental results are characterized by somewhat larger uncertainty. If enough information were available to make an adequate analysis of the uncertainties, the results could be conveniently summarized by means of "uncertainty bands"

---

* $\eta = 1 - \rho_o/\rho$.

** For the benefit of readers not familiar with techniques used for Hugoniot measurements for solids, a brief description of experimental methods is given in Appendix A, along with a discussion of associated uncertainties.

BLANK PAGE

on Fig. 1, for example. A quantitative way of doing this--which, however, would not be completely free of subjective influence (through the choice of weights)--would be by means of a least-squares analysis. This has not been done in the present report, for various reasons.*

The information relevant to the experimental error is collected, and various effects contributing to the uncertainty are identified and estimated, where possible. Factors considered in estimating uncertainty include:

(a) Basic precision of Δt, Δx measurements;
(b) Scatter of data and reproducibility;
(c) Comparison of results of different investigators;
(d) Consistency of results for different materials;
(e) Number of approximations entering analysis, and corrections;
(f) Corrections for approximations of measurement (e.g., non-zero flash-gap closure time);**
(g) Uncertainties in pusher material p(V) loci;***
(h) Density of points along curve (both for rock salt and pusher material,, number of measurements;
(i) Possibility of systematic error.

Except in the region near what has been interpreted as a polymorphic transition around 300 kilobars, there is no systematic deviation in the results of the different investigators. The consistency of the results for different materials and for NaCl, in particular, indicates that if it is assumed there is no undiscovered source of important

---

* Partly because complete experimental information is not available in some pressure ranges and partly because of the sparseness of data points in some regions for both halite and pusher materials, the possibility of systematic error (see text), the time constraint, and a judgment that the estimation of an upper limit on the uncertainty would be sufficient for the contemplated application. See note in Appendix C about least-squares analysis of dynamic compressibility data.

** See Appendix A.

*** Summarized in Appendix C.

systematic error,* for pressures in the range of 50 to 1000 kilobars, ±20 percent would be an upper limit on the uncertainty in pressure for a given compression. The "scatter" of the data indicates that over most of the pressure range just specified a reasonable "fit" to the data of Fig. 1 would probably lie within a few percent of the true values.

In the next few paragraphs the various factors contributing to uncertainty in the results of the experiments summarized in Table I are discussed. It is necessary to consider each pressure range in some detail.

According to Christian (1957), the probable error associated with the points of Experiment 1 (Table 1) is "the minimum consistent with the method, ±1/2%" (in velocities). "The accuracy of the [P(V) Hugoniot] curves is ±1% in the measured change of the relative volume, or ±4% in pressure at the highest points. In general, no difficulty is encountered in defining a Hugoniot curve which is consistent with both methods."** These error estimates are roughly consistent with the estimated ±1 percent error claimed for the 24ST Al (u_s, u_p)*** curve (Experiment B, Table C-1 of Appendix C) on which the interface solutions are based.† Note that the interface solution points corresponding to rarefaction wave pressures <134 kilobars are based on extrapolation of

---

*Possible sources of systematic error are discussed in Appendix A.

**That is, free-surface and reflection methods.

***u_s = shock velocity; u_p = mass velocity.

†More precisely, the interface solutions are based on the rarefaction adiabat derived from the Hugoniot.

Table 1. SHOCK COMPRESSION MEASUREMENTS FOR PURE NaCl*

	Method	Pusher	Pusher Hugoniot Reference**	Approximations in Analysis***	Pusher Adiabat	Pressure Range, Kilobars	Reference	Experiment
Single Crystals and Pressed Samples	Free Surface	-	-	"Doubling"	(Not Used)	52-270	Christian, UCRL-4900 (1957); van Thiel (1966)	1
	Reflection	24ST Al	B	Corrected For Adiabat; Extrapolation	Fickett (Unpublished)			
	Reflection (With Flying Plate)	Copper, Aluminum, Iron (Low-C Steel)	J,M, K, L	Interpolation, Mirror(?)	JETP 11, 573	50-790	Al'tshuler, et al., JETP 12, 10(1961)	2
Single Crystals and Pressed Samples	Reflection	(24ST Al?)	(B,D,G?)	?	?	48-803	van Thiel (1966); Alder (1963);	3
Single Crystals and Porous Samples	Reflection (with Flying Plate And Screen)	Iron (Screen), Aluminum (Screen)	L,Q, K	Interpolation, Mirror (?)	JETP 11, 573	276-4030	Kormer, et al., JETP 20, 811,(1965)	4
Single Crystals	Reflection	Aluminum, Titanium	?	Mirror (?)	?	108-252	Hauver and Melani (1965); van Thiel (1966)	5
Single Crystals	Reflection	Aluminum, Titanium	?	Mirror (?)	?	225-462	Hauver and Melani (1965); van Thiel (1966)	6

*See Fig. 1.
**Refer to table of pusher Hugoniot measurements in Appendix C.
***See Appendix C.

the aluminum Hugoniot data.* The uncertainty due to the use of the "doubling" approximation in the free-surface data reduction has not been estimated. Since $\rho_o c_o^2$ for NaCl is smaller (factor 4) than for iron, it would be expected that the "doubling" approximation would become poor at somewhat lower pressures for NaCl than for iron. (See discussion in Appendix A.) The lowest pressure points lie close to the isothermal compressibility curve as determined by Bridgman (1954).

The data** of Experiment 2 depend upon adiabats for copper, aluminum, and iron, based on polynomial fits to P(V) Hugoniot curves.*** In particular, these data depend on points in the unmeasured regions of the metal Hugoniots between one atmosphere pressure and the lowest measured points of the experiments cited in Table C-1 of Appendix C.†

---

*The uncertainty in the Al rarefaction adiabats was not estimated in Christian (1957). It was shown in Walsh (1955) that under very general assumptions about equations of state (see Appendix A), the value of

$$u_r = \int_0^{P_1} \left(\frac{-dV}{dP}\right)_S^{\frac{1}{2}} dP$$

with the integral being taken along the rarefaction adiabat, lies within ±3 percent of

$$u_p = \sqrt{P_1 (V_o - V_1)}$$

for shocks in Al ($100 < P_1 < 400$ kilobars), thus bounding the error in u_p (P_1) due to the deviation of the Al adiabat from the Hugoniot in the interface solutions.

**"The wave velocities--measured over reference bases of 4-8 mm--were accurate to ±1%" (Al'tshuler et al., 1961).

***See discussion of "reflection method" in Appendix A.

†Specifically, the data depend upon points of the Hugoniots for copper corresponding to u_p = ~0.15 and 0.37 km/sec, iron at u_p = ~0.51, 1.03, ~1.5, 2.8 km/sec, and "Russian aluminum" in the range $100 < P_{Al} < 700$ kilobars. See graphs in Appendix C.

Fifth and seventh degree polynomial fits for $P_H(V/V_o)$ were used for the interpolation. Except in the case of iron, the first three coefficients of the fits were determined using data for parameters at normal conditions (isothermal compressibility, Grüneisen constant $\gamma_o(V_o)$, and $d(\log \gamma)/dV$). The (u_p, u_s) loci derived from the fits for copper and iron pass within the "uncertainty bands" shown in Figs. C-3 and C-4 of Appendix C, except for iron at the lower velocities. (The fit passes through the point at $u_p = 1.0$ (Experiment H), which is probably high in mass velocity.) It is unclear whether corrections were made for the deviation of the rarefaction adiabats from the mirror reflections of the iron Hugoniot.* Thus, the uncertainty in the data of Experiment 2 could well be more than a few percent (±5 percent or more).

Since a complete description of Experiment 3 was not given in Alder (1963), it is not possible to assess the uncertainty associated with those data. Disagreement of >10 percent (in pressure at about 200 to 220 kilobars) with the data of Experiments 2 is noted. The uncertainty could be comparable with the uncertainty in the rarefaction adiabats for whatever pusher material was used.

---

*A correction of 6.3 percent (in P or u_s for a given u_p) which was apparently made for the highest iron point at $u_p = 1.5$ km/sec could have been for this reason. (I.e., the pressure given in Al'tshuler et al. (1961), 790 kilobars, is 6.3 percent higher than the value that would be obtained using the $u_s - u_p$ relation of Fig. C-3 of Appendix C; 1.5 km/sec is the value of the mass velocity "reflected" with respect to mass velocity of 2.8 km/sec in screen due to shock; actual rarefaction mass velocity is 2.8 + (2.8 - 1.5) = 4.1 km/sec.)

The points shown for Experiment 4 represent the mean of 15 to 50 time measurements.* Aluminum** and Fe*** were the intermediate materials. As was the case for Experiment 2, the data of Experiment 4 depend upon rarefaction adiabats based on polynomial fits to iron ($2.0 \lesssim u_p \lesssim 5.5$ km/sec) and aluminum ($1.4 \lesssim u_p \lesssim 10$ km/sec, $280 < P < 4930$ kilobars) Hugoniot data. For iron in the region of interest the fit lies near the center of the uncertainty band in Fig. C-3 of Appendix C. As was the case in Experiment 2 a small correction was made to the pressures, probably to take account of the deviation of the rarefaction adiabats from the mirror-reflected Hugoniot. For the case of iron at u_p = 2 km/sec,† this correction amounted to 4 percent.

---

*"The value of the shock wave velocity was determined from a series of 5 to 8 tests, in each of which the time was recorded 6 to 8 times. From 15 to 50 measurements, we eliminated those values whose probability--found from the normal distribution--did not exceed 1/2n (the Chauvenet criterion). In practice, the number of measurements rejected by the application of this criterion did not exceed 2% of the total. A check showed that the use of the criterion 1/n...increased the accuracy of the results obtained but had practically no effect on the average value of the measured time." The precisions quoted for the shock velocity measurements were in the range 1-2%. The fractional uncertainty in P_{screen} is related to that in the shock velocity in the screen by

$$\frac{\Delta P}{P} \approx \frac{1}{P} \frac{dP}{du_s} \Delta u_s = \frac{2V_o^2 P_H'(V)}{u_s^2 + P_H'(V)V_o^2} \frac{\Delta u_s}{u_s}$$

$$\approx 2 \frac{\Delta u_s}{u_s}$$

for iron near u_s = 3.6 km/sec (P_{NaCl} = 1.17 Megabars), for example. (I.e., this is uncertainty in P_{screen} due to uncertainty in measurement of u_s in screen--it assumes no uncertainty in Hugoniot for screen material.)

**New measurements slightly refined the parameters of the Al Hugoniot obtained in earlier work (Kormer et al., 1965, presumably Experiments K and S).

***Low-carbon steel.

†There is a real need for more iron Hugoniot measurements in the high pressure region.

The uncertainty in the data of Experiment 4 could be comparable with that of the iron data and aluminum data (which also depend on the iron Hugoniot--see Table C-1 of Appendix C) on which they depend. Additional uncertainty is introduced by the interpolation.* The uncertainties due to the corrections for deviation of the rarefaction adiabats from the reflected Hugoniots would be expected to be small since the maximum deviations are 10 percent. The lowest point of Experiment 4 agrees well with a point of Experiment 2 (Fig. 1).

It is not possible to evaluate the uncertainties associated with the results of Experiments 5 and 6, since a published description is unavailable. The Hugoniot points correspond to consistently higher pressures than were found in Experiments 1, 2, and 3 (Fig. 1).

Alder (1963) reports that experiments at 120 kilobars (Experiment 1) with single crystals oriented with the (100) axis (edge of cube) and the (111) axis (diagonal) perpendicular to the shock gave the same compression, within experimental accuracy.** The shift of the 100 Hugoniot at about 270 kilobars (Fig. 2) was interpreted by Alder as representing a polymorphic phase transition from the face-centered (6 nearest neighbors) to the more dense (for same pressure) body-centered (8 nearest neighbors) structure. The transformation is a simple displacement type, equivalent to compression of the unit cell of a face-centered crystal along the diagonal axis. Alder reports that near 270 kilobars "a single crystal oriented with the (111) axis perpendicular to the shock front transforms at a lower pressure to the body-centered form than one that has the (100) axis so orientated. At the volume corresponding to 270 kilobars, it was found in three separate

---

* There is a real need for more iron Hugoniot measurements in the high pressure region.

** The ratio of velocities of elastic longitudinal waves is given by

$$v_{100}/v_{111} = \left[\frac{3c_{11}}{c_{11} + 2c_{12} + 4c_{44}}\right]^{\frac{1}{2}} = 1.08 \ ,$$

where the experimental values for the elastic stiffness constants reported by Spangenberg and Haussühl (1957,1960) have been used.

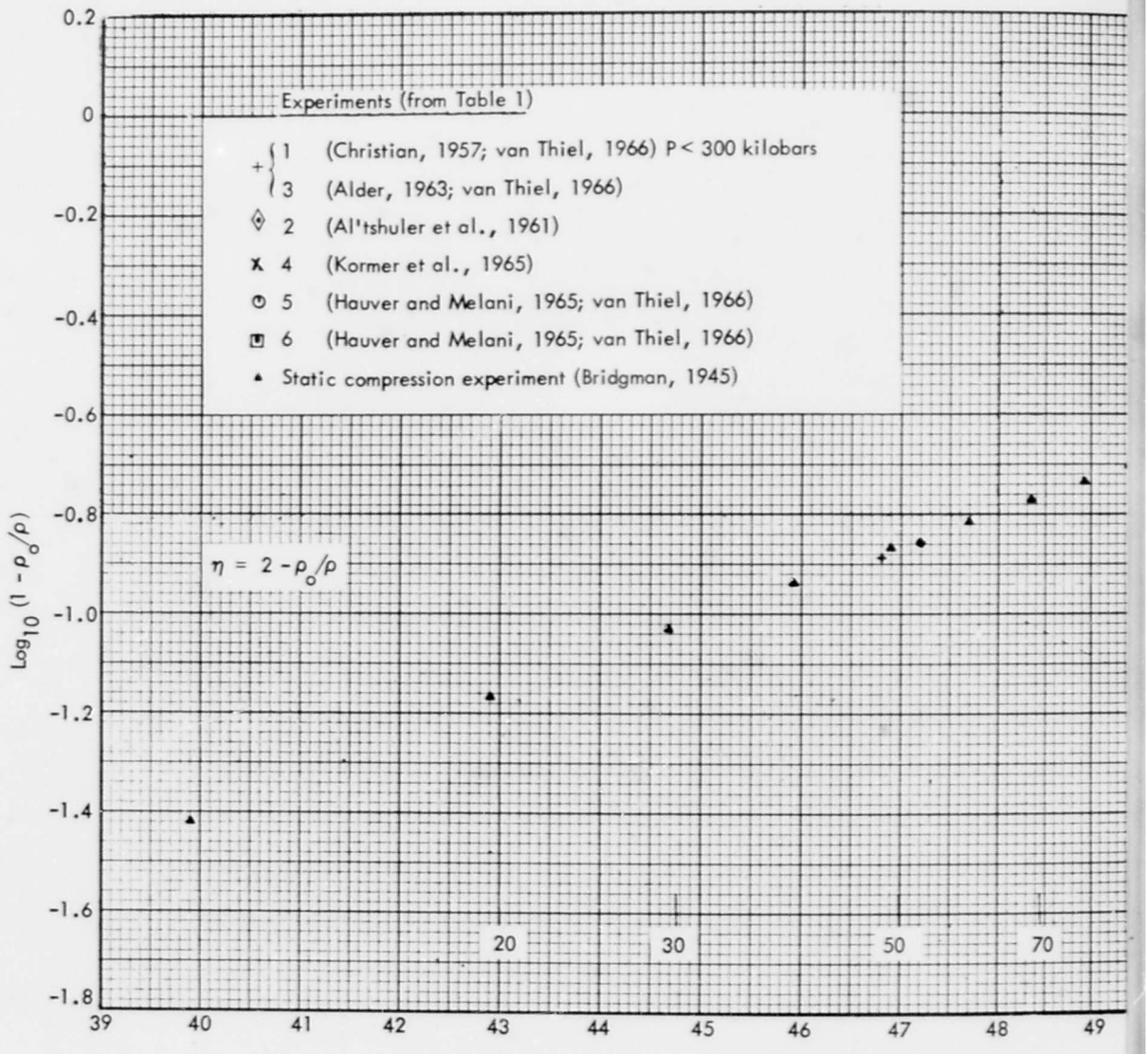

FIGURE 1 Results of Hugoniot Measurements for Pure NaCl. (The points shown for Experiments 1 and 3 were taken from the tabulation of van Thiel, 1966, and in some cases represent small changes from the data of the original references (Christian and Alder.)

R7-10-67-21

A

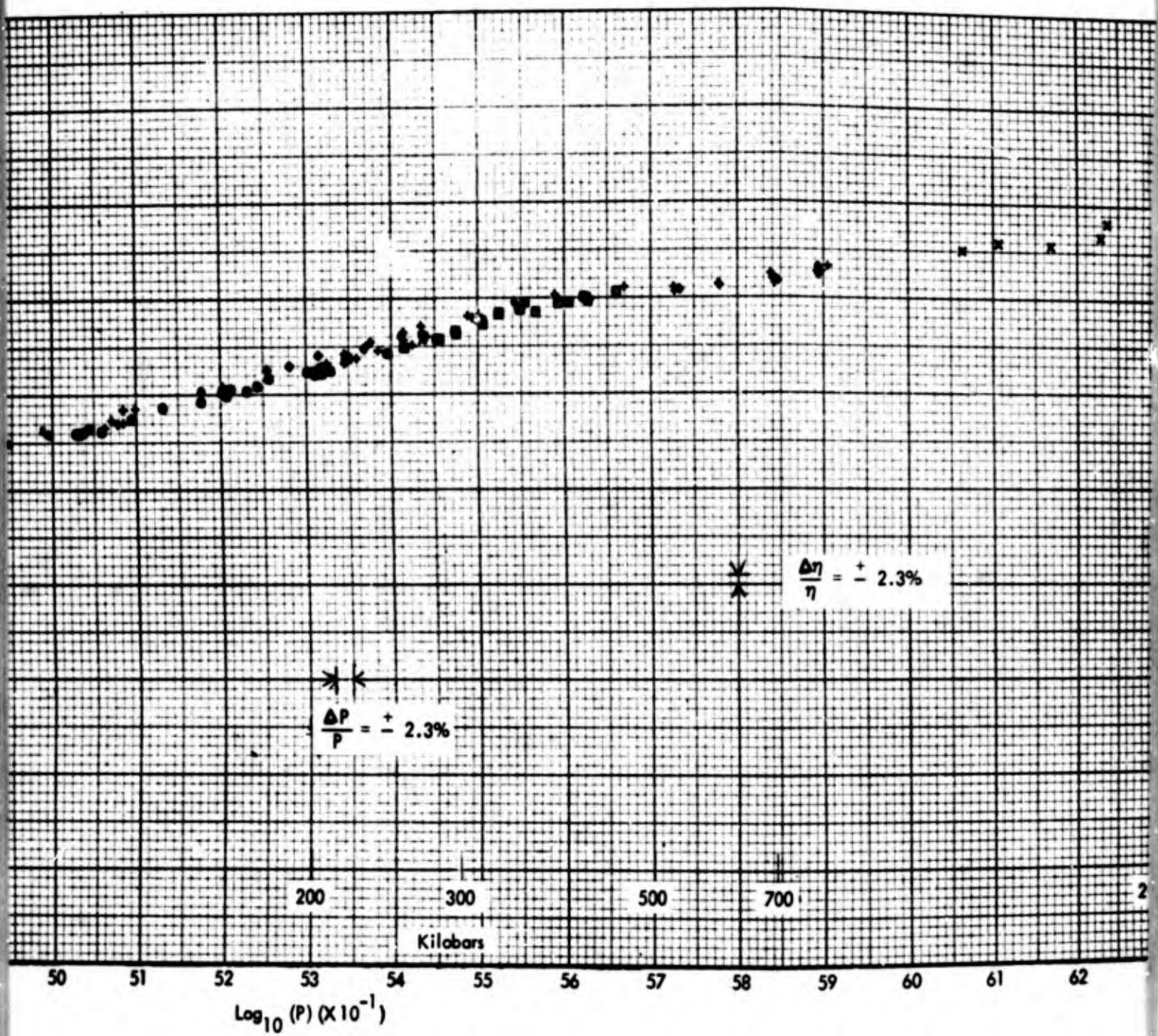
$\frac{\Delta\eta}{\eta} = \pm 2.3\%$
$\frac{\Delta P}{P} = \pm 2.3\%$
200
300
500
700
Kilobars
50
51
52
53
54
55
56
57
58
59
60
61
62
$\text{Log}_{10}(P)(X10^{-1})$

B

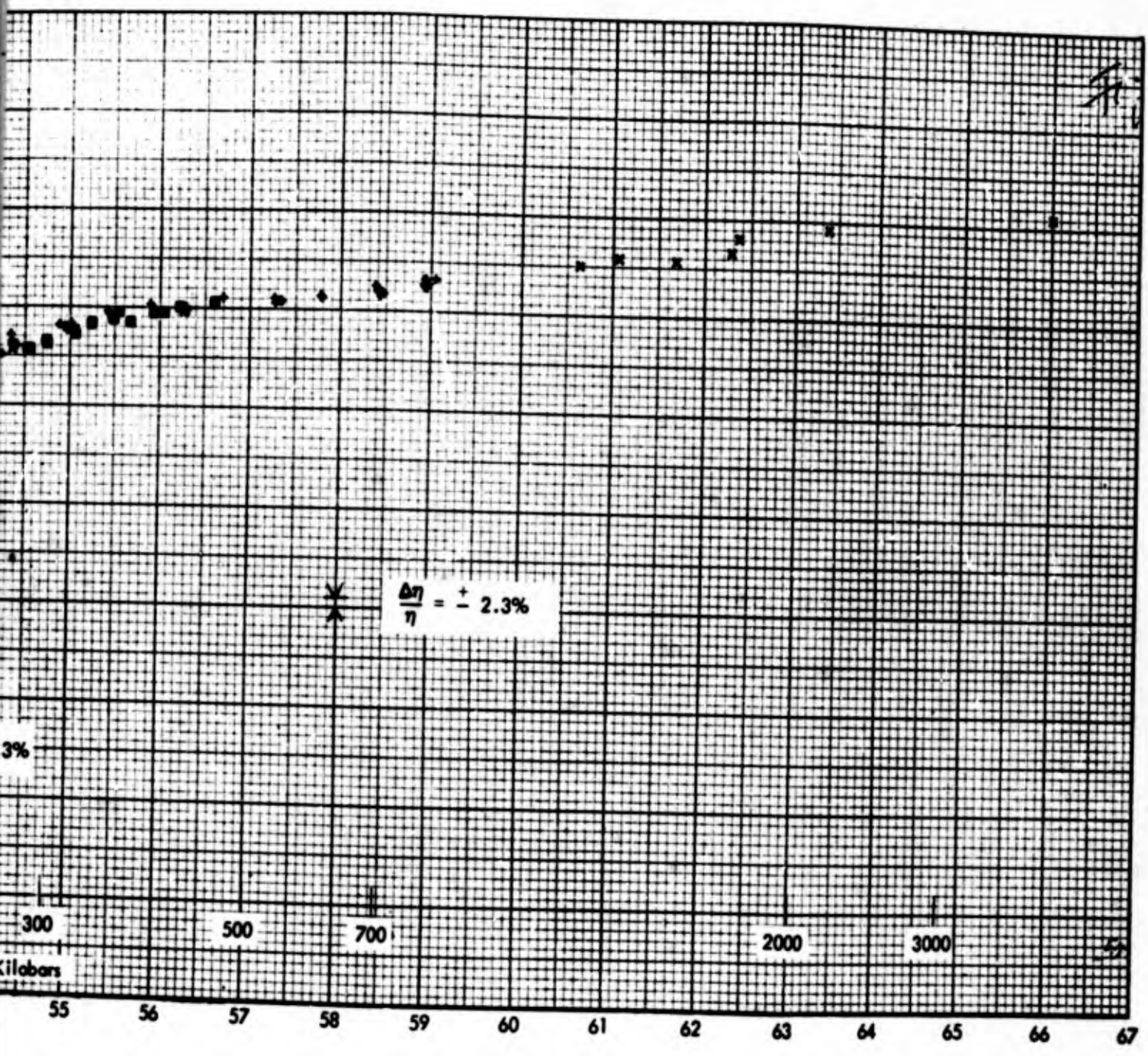
$\frac{\Delta\eta}{\eta} = \pm 2.3\%$
3%
300
500
700
2000
3000
Kilobars
55
56
57
58
59
60
61
62
63
64
65
66
67

C

BLANK PAGE

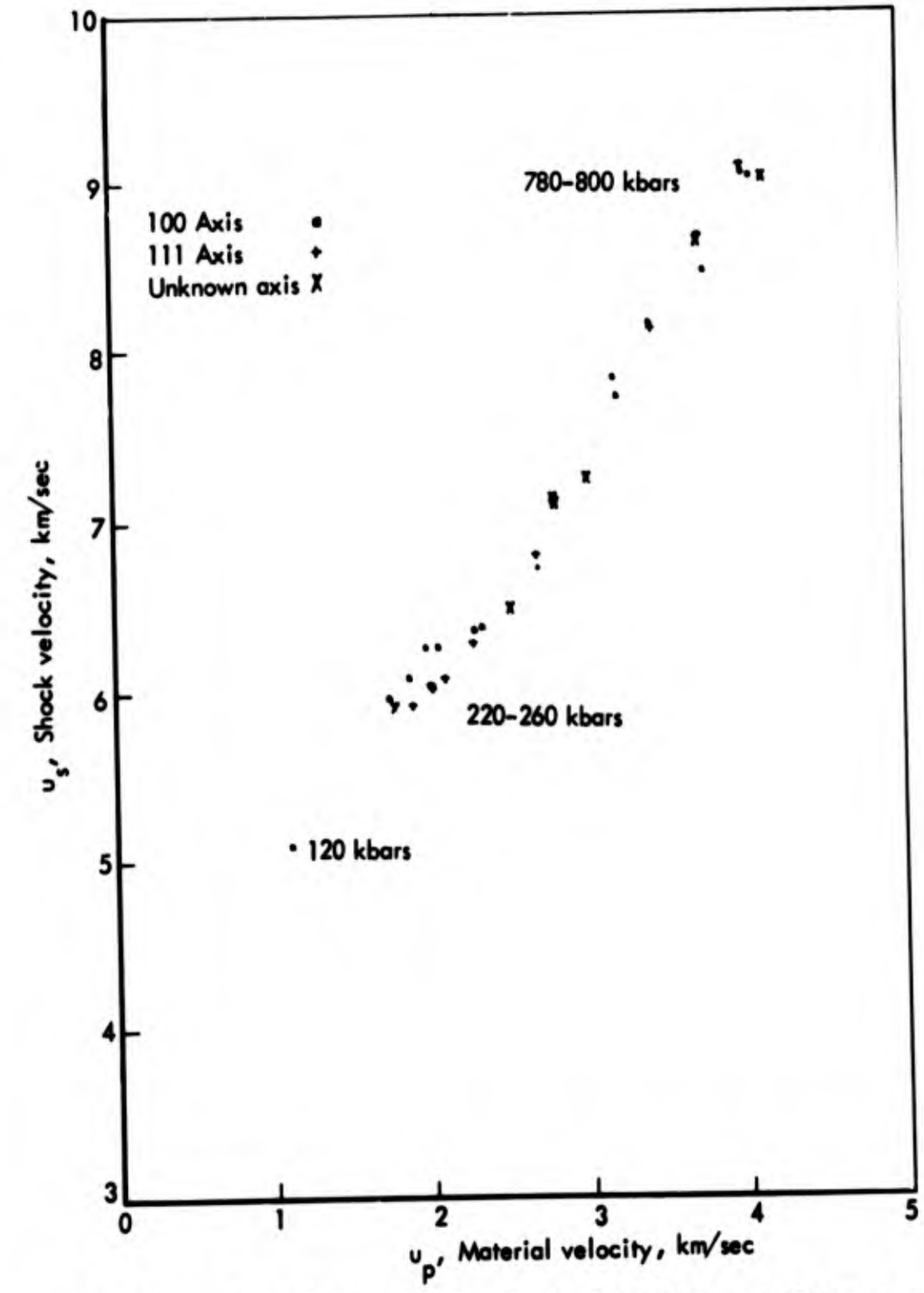

FIGURE 2 Shock Compression Data for Single NaCl Crystals Oriented with 100-Axis and 111-Axis Perpendicular to Shock (Experiment 3, van Thiel, 1966). In Fig. 1 the same data points are not distinguished from results obtained using pressed NaCl.

R7-10-67-22

experiments that the difference in pressure between the two differently arranged single crystals was three times the probable error and that pressed powder gave intermediate results. In view of the previously mentioned perfect agreement at lower pressure (120 kilobars), there appears to be a time requirement somewhat greater than 1 μsec at 270 kilobars in transferring the energy from the (100) to the (111) direction, since the process is accompanied by a relative displacement of the atoms and not just a uniform shortening of distances . . . . A little over-driving will also transform the (100)-oriented material, although an accurate quantitative measure of this has yet to be made." The Russian measurements, on the other hand, do not show a break in the slope of the Hugoniot in this pressure region.* Al'tshuler (1965) suggests that the difference may be due to different sample sizes used in the experiments: "for samples of larger dimensions make it possible to register later stages of the transformation process. To check in this assumption, Al'tshuler et al. (1961) undertook special experiments in which they registered the parameters of a 400-kilobar shock wave in NaCl as the latter propagated through the sample . . . On the whole, the experiments confirmed the presence of the very start of the transformation process but did not lead to quantitative agreement with . . . [Experiment 3]. In direct contradiction of . . . [Experiment 3] was also the effect of the crystallographic orientation." Results of Experiment 6 indicate a transition near 280 kilobars. The transition observed in Experiment 4 at about 1.7 Megabars was interpreted as being from less dense states of liquid NaCl corresponding to an initial non-equilibrium structure of a "lattice" liquid with a coordination number equal to 6 uniformly over the entire volume to denser states corresponding to an equilibrium state of a mixture of two coordinations, with 6 and 8 neighbors (Al'tshuler, 1965).

---

*The one point of Experiment 2 in the region of interest could have an error of ±5 percent or more, as discussed above.

Results of dynamic compressibility measurements for porous samples* show considerably lower compressions (relative to uncompressed non-porous material) corresponding to given pressures (Figs. 3 and 4) than for non-porous specimens.

2. Naturally Occurring Rock Salt

Hugoniot measurements for naturally occurring rock salt are summarized in Table 2 and the results are plotted in Fig. 5. Since complete descriptions of Experiments 1 through 4 are not available, little can be said about the uncertainties of the results, except that they might be expected to be at least as large in magnitude as the uncertainties in the measurements on pure salt made in the same laboratory.

The measurements with the wedge technique (Experiments 5 through 9) are probably considerably more uncertain. In the experiments on halite "shock arrival and free-surface arrival traces were rough because inhomogeneities in the rock disturbed the waves in the wedges. Since, for interpretation of wedge shots, the wavefront must be steady state, the oscillations in the arrival traces must be regarded as errors. The traces may be regarded as approximating functions to the smooth traces which would result from shooting a homogeneous wedge" (Grine, 1961). The shock arrival data were approximated by least-squares fits of parabolas. Shock velocities were then derived from the parabolas. "The large errors in slope [of smoothed curve] cause large errors in derived shock velocity."

The scatter in the data is likely mainly due to sample-to-sample variability of composition (not determined).** An additional possible source of significant uncertainty is variation in water content between in situ samples and samples as measured "in the laboratory."*** Porosity may also be a significant variable in some cases.†

---

*Prepared by pressing powders.

**Appendix B presents information about properties of naturally occurring rock salt.

***Water content not specified: a significant amount of moisture could have been picked up by the samples after removal from the sites.

†See Fig. 4 and Appendix B.

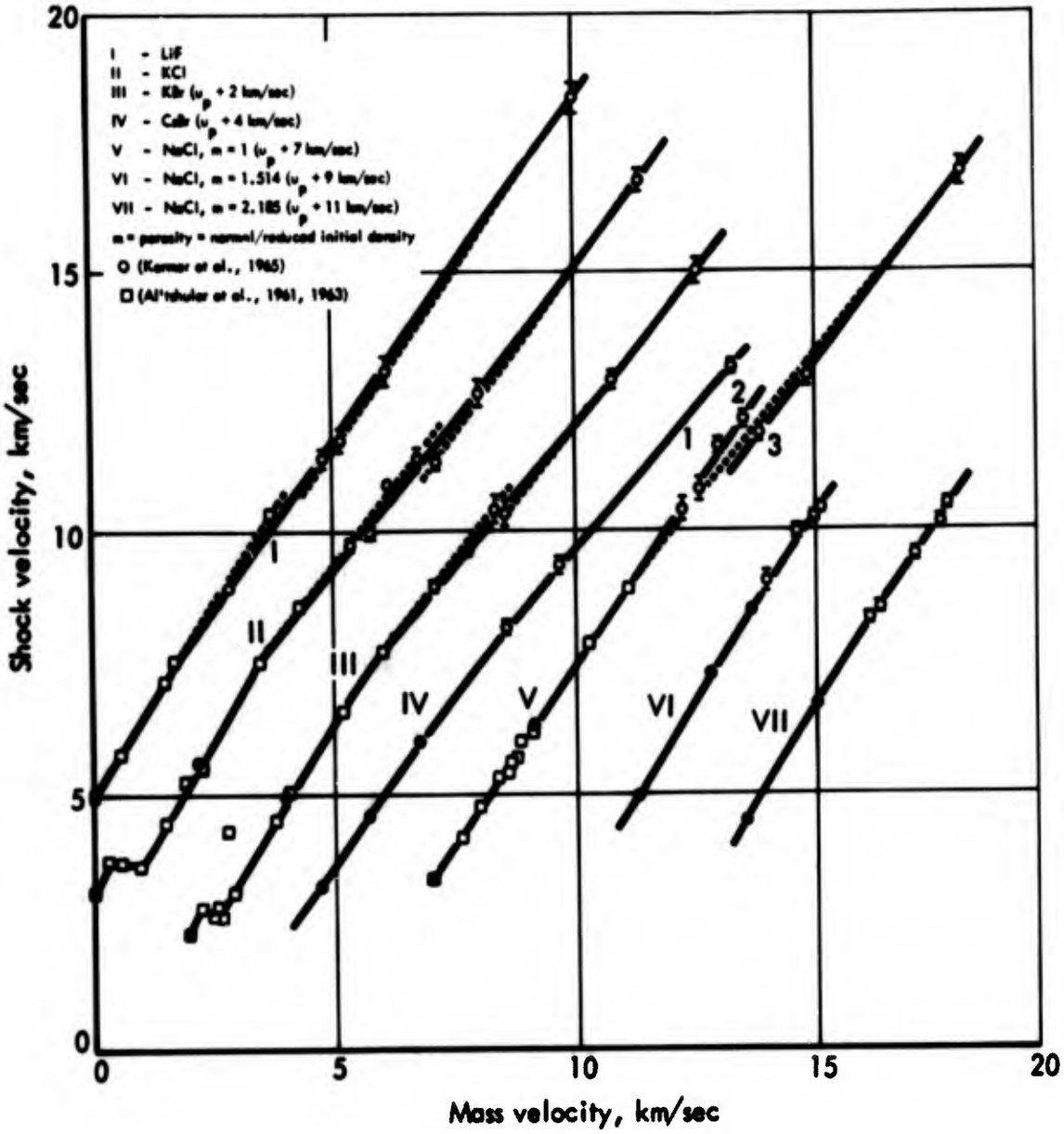

FIGURE 3 Shock Velocity Versus Mass Velocity Data for Several Alkali Halides, Including Porous NaCl. (Figure from Kormer et al., 1965)

R7-10-67-24

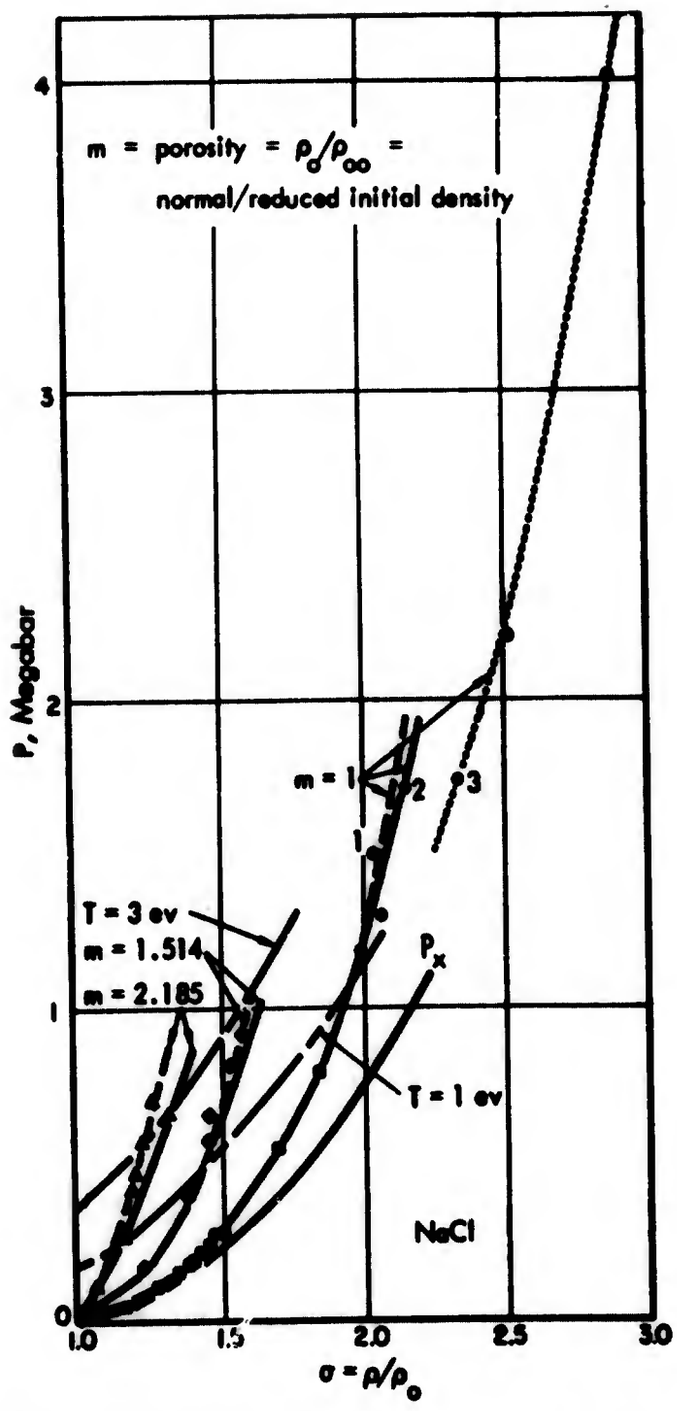

FIGURE 4 Hugoniot Curves for Normal and Porous NaCl (Kormer et al., 1964). Also shown are experimental points from the same reference. (The continuous curve includes contribution of electrons to pressure and energy, not included in dashed curve.) The dotted curve corresponds to the (u_s, u_p) relation of the preceding figure. Also shown are computed isotherms corresponding to temperatures of 3 ev, 1 ev, 0 ev ("P_x").

R7-10-67-25

Table 2. HUGONIOT MEASUREMENTS FOR VARIOUS ROCK SALTS*

Experiment	Sample Description	Composition,** Grain Size	Method	Pusher	Approximations in Analysis	Pressure Range, Kilobar	Reference	Experiment
1	Louisiana (Carey mine)	See Appendix B 1/4" - 3/4" (?) (Merrill, 1960)	?	?	?	89-709	Lombard, UCRL-6311, (1961)	1
2	?	?	?	?	?	126-856	Lombard, UCRL-6311, (1961)	2
3	New Mexico Potash	?***	?	?	?	865-882	Lombard, UCRL-6311, (1961)	3
4	Mississippi, Tatum dome "Salmon Salt"	?	?	?	?	0-1000†	Holzer, UCRL-12219, (1965)	4
5-10	Louisiana (Carey mine)	See Appendix B 1/4" - 3/4"(?) (Merrill, 1960)	Wedge	-	(See text and Appendix A)	6-117	Grine, UCRL-13004, (1961)	5-10

*See Fig. 5.
**Appendix B presents information of properties of natural rock salt.
***89% NaCl, 7% $Ca_2MgK_2(SO_4)_4 \cdot 2H_2O$, 1% $CaSO_4$, 3% silt and clay (?)(Rawson 1963)
†Results given as smooth curve.
NOTE ADDED IN PRESS: Results of H.E.-streak camera experiments run on core samples of halite from the Salado formation in the stress range 2.7 to 15 kilobars are reported in Dennen (1963).

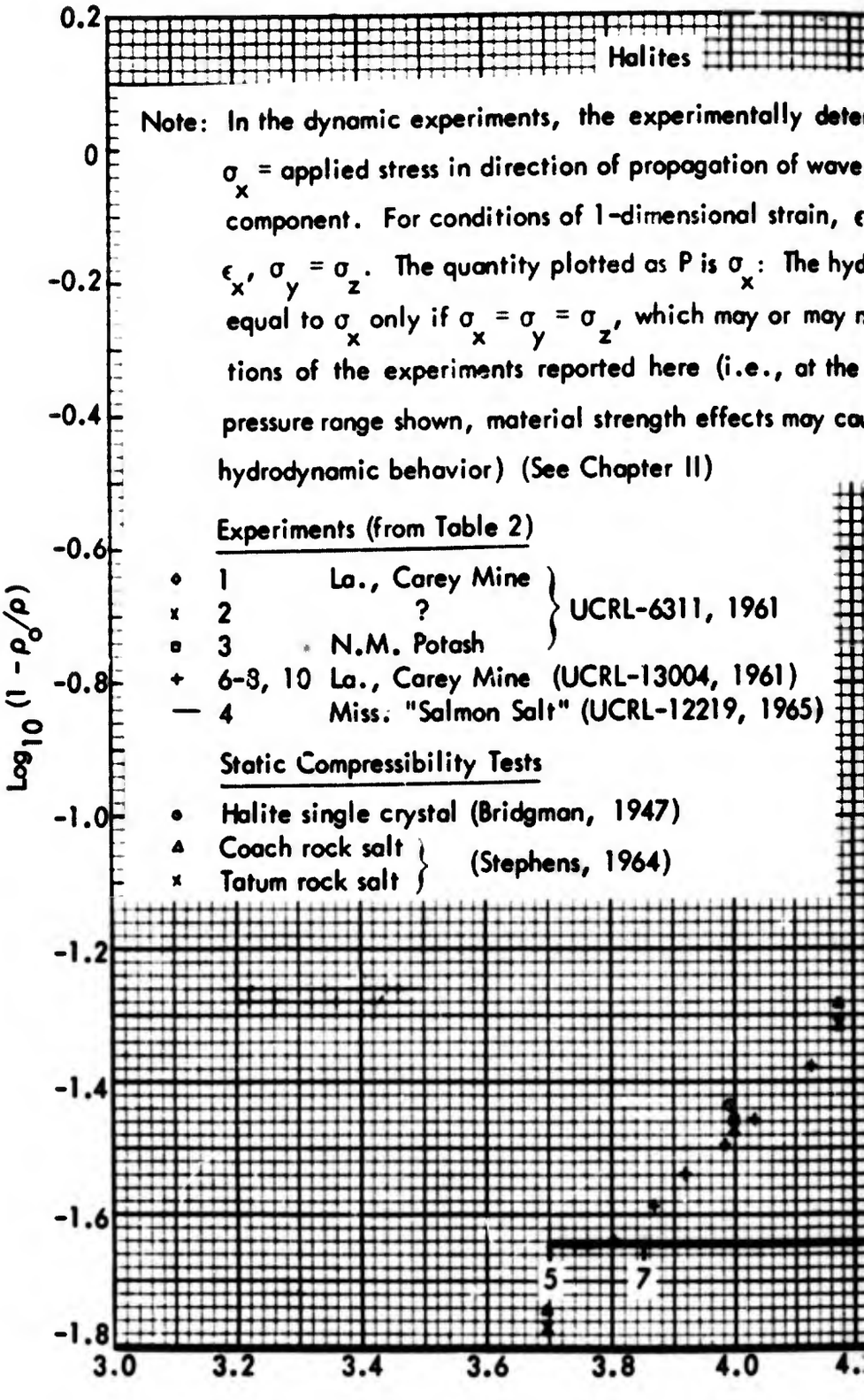

FIGURE 5 Results of Hugoniot Measurements for Various Naturall
Rock Salts. The Hugoniot data for Salmon salt (Expe
given as a smooth curve (Holzer, 1965). The data of
5 and 9 (shots 7383 and 7467), reported as "less reliab
rough oscilloscope traces (Grine, 1961), are omitted f

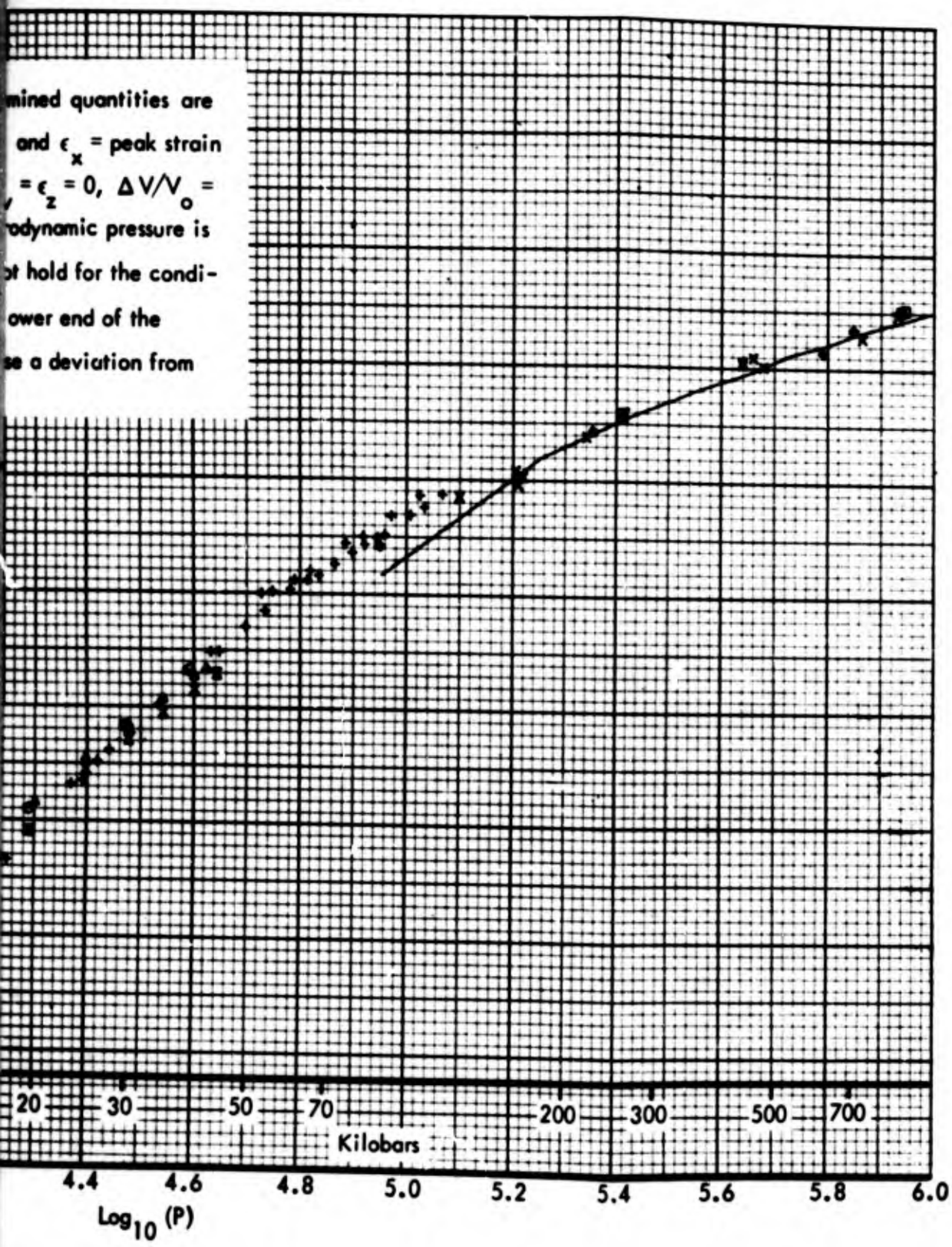

Occurring
ment 4) were
periments
" due to
clarity.

Since the velocity of a shock in rock salt becomes less than the velocity of compressional elastic waves (~4 km/sec) in the uncompressed material for shock pressures less than about 50 kilobars, it would be expected that such weak shocks would be preceded by an elastic precursor. The precursor, which would be expected to have an amplitude of the order of the yield strength of rock salt in compression (~1 kilobar) has not been observed.*

B. UNCERTAINTIES IN STATIC COMPRESSION MEASUREMENTS FOR ROCK SALT

Hydrostatic measurements of NaCl compressibility were made by Bridgman in two sets of experiments: Experiment I (1940) to 50,000 atm; Experiment II (1945) to 100,000 atm. (See Fig. 1, from Experiment II.)** The piezometers were calibrated by means of an Au

---

* Grine (1961) states that such a precursor "could have been easily missed" by the raised-mirror method of observation. NOTE ADDED IN PRESS: The author has been informed that the elastic precursor was observed in experiments carried out at Stanford Research Institute in 1963-1964 by Gregson and Doran.

** A polymorphic transition reported as experimentally observed at 20,000 kg/cm^2 is apparently a misprint in Born and Huang (1954).

standard;* the final compressibility curve was taken as the smoothed mean of measurements made with two different piezometers. "The final results are . . . strictly differential results between the substance in question and gold, assuming for the latter an extrapolation [above 30,000 kg/cm^2] by Murnaghan's formula." (Bridgman, 1948) The values of 50,000 atm adopted in II for $\Delta V/V_o$ for 21 halogen compounds are

---

*Above 30,000 kg/cm^2, simple determinations of the thrust of the piston, corrected as well as may be for friction, and of the area on which the piston acts, corrected as well as may be for distortion by various calculations and by blank runs in which certain compressibilities are assumed by extrapolation, are about all that can be attempted. I believe that pressures up to 100,000 can be determined within 2 or 3 percent. Up to 30,000, where pressure is transmitted by a true liquid, electrical leads can be got into the apparatus, and the scale of the experiment is comfortable, there is no reason why pressure should not be measured as accurately as up to 12,000, or with an accuracy of 0.1 percent or even better."

"The thrust is measured internally from the change of electrical resistance of a 'grid' of hardened steel mounted so as to take the thrust. The change of electrical resistance of the grid consists of a term arising from the hydrostatic pressure and another term depending on the superposed one-sided thrust. The hydrostatic pressure is accurately known from a manganin gauge mounted with the 30,000 chamber, so that the term arising from the superimposed thrust can be found by difference. The effect of thrust on the resistance of the grid has to be found by a calibration, which involves a correction for the effect of pressure on the thrust coefficient. The electrical parameters of the apparatus were such that the thrust at 100,000 could be determined to 0.5 percent."

"There are corrections for elastic distortion which cannot be exactly calculated and which have to be determined by blank runs with the more incompressible substances, assuming that the compressibility of them is known by extrapolation from measurements in the range up to 40,000 or 50,000. At the maximum pressure the cross section of the [carboloy] piezometer increases by approximately 3 percent." (Bridgman, 1952)

"The greatest source of error [in the highest pressure static measurements] is in determining the pressure attained, because the friction within the apparatus is difficult to estimate. The volume change must be calculated with the aid of a differential technique and is subject to possible consistent errors due to uncertainties in the compressibility of iron and carboloy. The additional problems of strength, creep, and distortion of the apparatus are avoided in the dynamic method . . ." (Christian, 1957)

consistently slightly larger (3 percent for NaCl) than in I, interpreted as due to systematic errors in I. The values of the difference between the two individual measurements and the mean $\Delta V/V_o$ at 100,000 atm ranged from 1 to 4.5 percent for the compounds studied (3.3 percent for NaCl).

The compressibility of pure NaCl in the low-pressure range is given adequately by data from the International Critical Tables (Vol. 3, 1928).

$$\beta = -\frac{1}{V_o}\left(\frac{\partial V}{\partial P}\right)_T = 4.18 \times 10^{-6} \text{ bar}^{-1}$$

$$\frac{1}{\beta}\left(\frac{\partial \beta}{\partial P}\right)_T = -0.20 \times 10^{-4} \text{ bar}^{-1}$$

$$\frac{1}{\beta}\left(\frac{\partial \beta}{\partial T}\right)_P = 7 \times 10^{-4} \text{ deg}^{-1}$$

at 25°C and 1 atm. Values for $\Delta V/V_o$, calculated below, using these coefficients are close to the measurements at 10,000 and 20,000 atm reported by Bridgman (1945).**

P 10^3 kg/cm^2	$(\Delta V/V_o)_B$	$(\Delta V/V_o)_{ICT}$
10	0.038	0.037
20	0.068	0.066

Results obtained by Bridgmen (1948) for rock salt using a different apparatus (Bridgman, 1945, II) are shown in Fig. 5. The single crystal specimen* from the Harvard geology department collection was

*Mineralogical and petrographic analyses not given.

ground to the shape of a truncated cone. "Each substance involves two applications of maximum pressure, a preliminary 'seasoning' application and the second stepwise application, up and down in steps of approximately 2000 kg/cm^2 . . ."

Smoothed results of more recent measurements for rock salt with 98.6 percent NaCl by Stephens (1964) are also shown in Fig. 5. Au was again used as a calibration standard; the measurements of Bridgman (1949) for Au to 30 kilobars (Fig. 6)* were extrapolated by two different unspecified procedures to 50 kilobars. Results for a sample of Tatum salt (containing 15.7 percent $CaSO_4$) are shown in Fig. 5.** The cores were not given special dehydration treatment, although they may have experienced significant dehydration (or deliquescence) during whatever time elapsed before the measurements.*** "Most of the samples were seasoned by a prepressing to 40 kilobars before taking the final data." Figure 7 shows results of compressibility measurements on two samples of halite from the COWBOY test site at the Carey Co. mine† (Guide and Warner, 1960). The specimens were cast into blocks of epoxy and machined to rectangular solids with salt exposed at the ends; after being jacketed in thin copper foil, the compressibility was determined with a quoted accuracy of 10 to 12 percent by means of a procedure described by Fatt (1958).

The comparisons of dynamic and static compressibility measurements for aluminum and pure NaCl are discussed above and in Appendix C. (See Fig. 1 of this chapter, and Fig. C-13 of Appendix C.)

---

* A "hysteresis loop" with width equal to 0.5 percent of the maximum distortion was noted for the gold measurements (not shown in Fig. 6). "The hysteresis for this specimen is undoubtedly real."

** The smoothed results for Tatum salt agree within 6 percent with compressibilities calculated from measured compressibilities of NaCl and $CaSO_4$, assuming additivity of volumes.

*** The author thanks F.B. Porzel for calling his attention to the importance of humidity effects.

† A chemical analysis and other properties of the samples are presented in Appendix B.

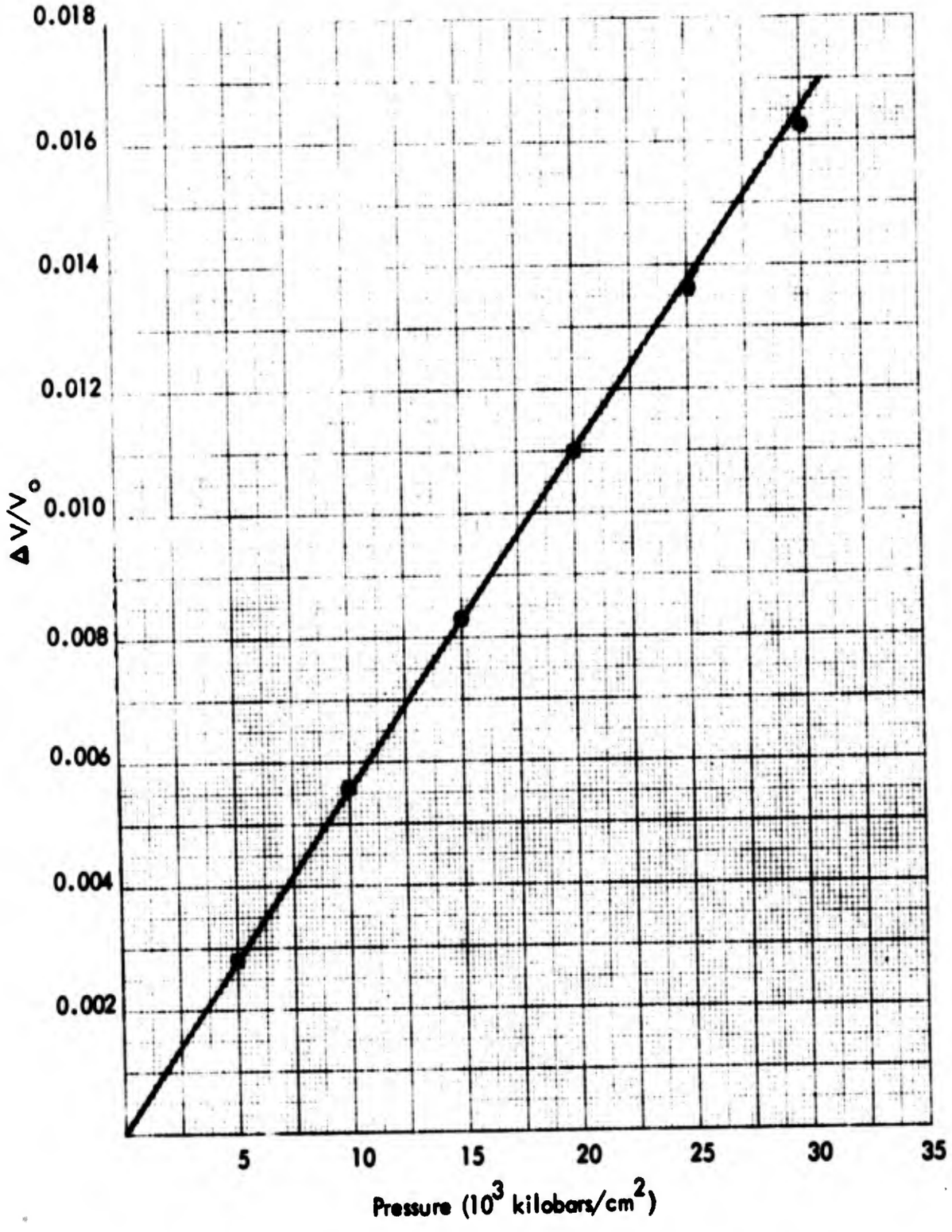

FIGURE 6 Static Compressibility Measurements for Gold (Bridgman, 1949)

RT-10-67-26

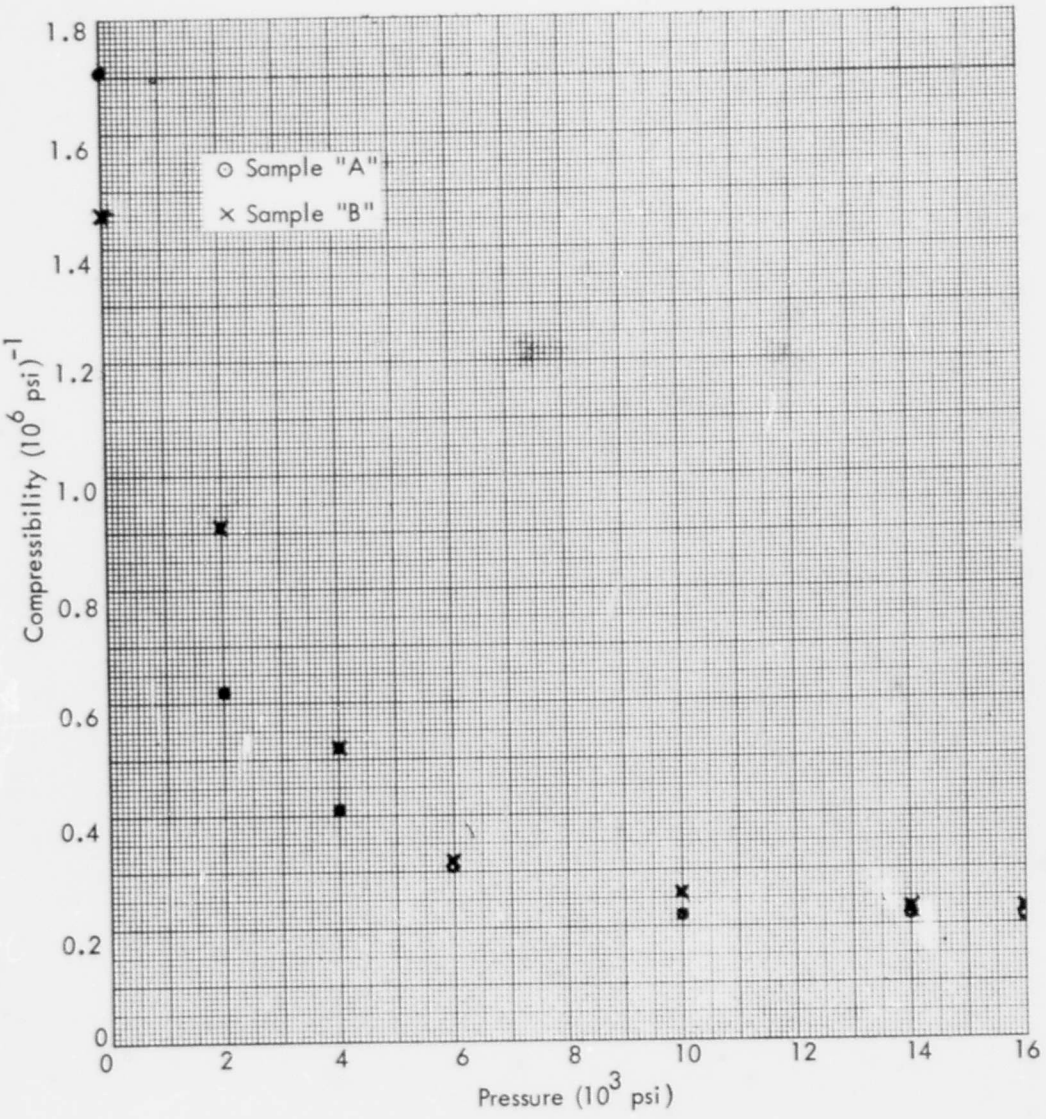

FIGURE 7 Compressibility Measurements for COWBOY Test Site Salt, Carey Co. Mine (Guide and Warner, 1960)

R7-10-67-27

CHAPTER III

UNCERTAINTIES OF PLASTIC FLOW MEASUREMENTS

BLANK PAGE

III. UNCERTAINTIES OF PLASTIC FLOW MEASUREMENTS

Except for field tests with explosive loading, only static tests have been employed to investigate flow properties of rock salt in the subhydrodynamic region.* These tests include hydrostatic compression, uniaxial tension, combined stress ("triaxial"), and bend tests. Since results of these static tests have been used as guides for determining flow parameters (plastic yield strength, for example) used in

---

*Strictly speaking, the results of Experiments 5 to 10 of Table 2, Chapter II, probably represent an exception to this statement. Results discussed below indicate that rock salt will not support differential stresses greater than about 1.5 kilobar, at least for confining pressures less than about 2 kilobars in axial compression. For stresses much greater than this "yield stress," the response can be treated as approximately hydrodynamic with an error of the order of yield stress/pressure. On the basis of the simple elastic-plastic flow model, it would be expected that a weak shock in rock salt would be preceded by an elastic shock with amplitude of the order of the yield strength of the material. The amplitude of such an elastic precursor would be too small to be measured by dynamic testing methods currently in use, e.g., the wedge technique (Chap. II "Uncertainties in Dynamic and Static Compressibility Measurements"). Experiments investigating effects due to high strain rates in metals (Hauser, Bell, 1961), and a few rocks, and ceramic materials have been reported. The same physical mechanism--migration of dislocations--is the basis of plastic flow of metals and ionic crystals. Investigations on dry limestone and gabbro rocks reported by Serdengecti and Boozer (1961) found that, for a given state of stress (up to 20,000 psi confining pressure) and temperature (up to 300°F), the axial compressive stress required for failure of the rock increases by 10 to 15 percent as the strain rate is increased over the range 10^{-5}/sec to 1/sec, and the type of failure observed changes from ductile to brittle. Shook and Niedenfuhr (1964) found that the stress to cause bending brittle failure of ceramic rods was essentially the same for impact loadings (force increased linearly with time to failure load in the range of 3000 to 11,000 lb in times like 50 to 100 μsec, corresponding to 0.3 to 0.5 cycle of resonant flexural vibration) and "static" tests (loading rate ~23 lb/sec).

calculations of response to impulse loading,* the experimental uncertainties are assessed in the following paragraphs. Since the uncertainties are large, the assessment is semi-quantitative.**

Nonreproducibility and sample-to-sample variation characterized the results of plastic flow investigations, both for salt of high purity and for naturally occurring rock salt.*** No attention seems to have been given by any of the investigators to possible humidity effects: Anhydrite, a principal impurity of natural rock salt in salt domes, takes on water of crystallization, becoming transformed to gypsum ($CaSO_4 \cdot 2H_2O$). It is a commonly used drying agent. In addition, NaCl is deliquescent for relative humidities greater than 75 to 80 percent in the temperature range 0 to 100°C.† Moisture has a significant effect on the plastic flow properties (Fig. 1). Strain rate and sample size effects have not been investigated. A certain nonreproducibility is to be expected in the case of polycrystalline

---

* Note that the simple model of plastic flow described by the von Mises (strain-rate-independent) yield condition implies that a plastic strain-rate-stress relation ("flow rule") is valid (Freudenthal and Geiringer, 1958). If the model is valid, the yield parameter can be determined in static tests.

** It was necessary to limit the scope of the present investigation so as to preclude discussion of the correlation of the various measurements reported in this chapter by means of plastic flow models, and the uncertainties associated with such models.

*** Appendix B presents information on properties of naturally occurring rock salt. In connection with the question of reproducibility, the following comment from Goldsmith and Austin (1964) seems pertinent: "On the other hand, careful selection of a single rock type... with attention to details of physical structure in all respects will give accurately reproducible data, regardless of the locality from which the samples are collected, indicating that the concept of nonreproducibility of properties of geologic materials is a myth." Contrast the experiences of the investigators who subjected rock salt monocrystals to bending tests, finding variability of factors 2 to 5 (in stress for the same plastic strain, Figs. 18 to 20). Unfortunately, not enough results of the triaxial tests on natural rock salt were given for fixed values of the constraints to make possible a meaningful assessment of the reproducibility.

† National Research Council, "International Critical Tables," 1928, Vol. I, p. 67.

samples. Such samples are not rheologically isotropic. In no case was there reported the depth from which a sample of natural rock salt was removed.*

A. RESULTS OF PLASTIC FLOW MEASUREMENTS

Triaxial tests on various rock salts are summarized in Table 1 and the results are shown in Figs. 2-15, 24-25.** Results by Handin (1953), shown in Fig. 2, for the lower range of 2τ (=differential stress) appear to agree with the results of Schmidt (1937) for triaxial compression of naturally occurring halite (Fig. 9D)--at least for confining pressures greater than 100 kg/cm^2. The latter specimens show stiffer response than several samples of "artificial" rock salt of high purity tested in the same way (Fig. 9).*** Note especially the absence of a well-defined elastic limit or yield point for most curves for the triaxial tests on polycrystalline samples. This is perhaps not surprising, considering the variation of about a factor of 2 in yield points found in bend tests on as-grown monocrystals and annealed cleavages reported by Schlichta (1966)† (Figs. 18 to 20).

---

*This information would have made possible an estimate of the static overburden pressure to which the specimen was subjected in situ.

**The maximum shear stress levels occurring in the experiments by Goguel (1948) and Schmidt (1937) are comparable with those calculated by Patterson (1964) to occur in the wall of the Project DRIBBLE "decoupling" cavities due to the static overburden loading.

***Except series "O" and "n". Note the variation in stiffness found for the different series.

†In the 4-point bend tests (Fig. 21), the outer fiber of the crystal should be approximately subject to pure tension loading (Timoshenko and MacCullough, 1940). The tests were conducted at deflection rates of 0.05 mm/min, equivalent to outer-fiber strain rates of 1.5 to 3×10^{-5}/sec. Schlichta conjectures that "the variation in the stress-strain curves of the as-grown crystals is caused by a defect which simultaneously raises the yield stress and the work-hardening rate. The most likely sources of such variation are the dislocation density and the impurity concentration. The density of dislocations does affect the yield stress and the work-hardening rate, but in opposite directions ... Therefore, this explanation does not seem likely. On the other hand, a divalent ion, such (Continued)

Table 1 -- TRIAXIAL TESTS ON ROCK SALT

Reference	Fig. No.	Sample Description***	Uncompressed Sample Dimension	Type of Test	Confining Pressure Range (atm)	Max Shear Stress Range $(\sigma_1-\sigma_3)/2$ (atm)	Strain Rate (%/min)	Sensitivity
Handin (1953)	2 & 3	Natural rock salt from Hockley mine, Texas; polycryst.(?); 1/4 in.-3/4 in.(?)* grain size	~0.5 in. diam x 1 in.	Compression Extension	1-2800 500-5100	0-1200 0-1300	~2	~1% (friction-limited)
Goguel (1948)	4 to 6	"Sel de pigeon" from Varangéville (France); polycryst.; average grain size ~mm	~cm	Compression	0-500**	0-400	(?)	
	7 to 8	Monocryst. cleavage (rectangular cross section)	~cm(?)	Compression	0-300**	0-400	(?)	
Schmidt (1937)	9	"Liniensalz" from Stassfurter Berlepschschacht (Germany); "coarse-grained)	6 cm diam x 15 cm	Compression	0-500	0-200		~20 kg/cm^2
	9 to 14	"Artificial" rock salt (pressed, annealed industrial common salt); average grain diam 0.158 mm ("series O") and 0.138 mm ("series A")	30 mm diam x 75 mm	Compression	0-600	0-300		
		"Artificial" rock salt (pressed, annealed, high-purity powdered rock salt); average grain diam 0.181 mm ("series n") and 0.108 mm ("series K")		Extension	0-200	0-200		
Serata (1961)	15	"Rock salt"	1.75 in. diam x 3.5 in.	Compression (with lateral strain restricted)	0-820	0-255	?	?
Handin (1958)	24 25	As grown pure NaCl monocrystal ("optical quality")	0.5-in diam. x 1 in.(a axis)/cylinder axis	Compression Extension	1000 2000	0-350 (24°C) 0-170 (150°C) 0-55 (300°C)	?	~1%

*Merrill, no date; see also Appendix B.
**Confining pressure increased during a single run.
***Complete petrographic data not available.

Points from Figs. 4, 5, and 7 have been replotted in Fig. 16, along with the curves of Fig. 9D, to facilitate comparison of the results of the triaxial tests at the lower stress levels. Apparent envelopes of Mohr stress circles constructed from the data of Handin (1953), Schmidt (1937), and Serata (1961) are compared in Fig. 17.* In other tests (Bridgman, 1964), circular cylinders cut from natural rock salt were "pulled under a hydrostatic pressure of 420,000 psi to a reduction of area of 20 percent under a superposed 'true' tension as calculated on the final diameter of 7300 psi. At the necked part, there was no loss of optical homogeneity--no evident slip planes or other evidence of crystal structure, and the cross section remained round."**

Wuerker (1956) lists without source citation the following data:

	Grain Size, mm	Compressive Strength, psi	Tensile Strength, psi
Rock Salt (La.)	25-40	5000	
Rock Salt (N.M. potash, halite-sylvite mixture)	10-30	4180	402

Figure 22 shows results of a uniaxial tension test performed on one of the cylindrical specimens of "artificial" rock salt used for

---

(Continued) as calcium, is capable of raising both the yield stress and the Stage I work-hardening rate ... Moreover, nothing is known about the other variable quantities in the crystals such as the anion concentrations, vacancy concentrations, or dislocation densities." In addition, humidity effects could have played a role: "All of the crystals were stored for over a year before testing, sometimes in a dessicator, and sometimes in the open air under widely varying conditions of humidity and NO_2 or ozone concentrations [from smog] ... In fact, the crystal surfaces became somewhat dull as a result of atmospheric etching." The cleavages and predeformed crystals were water polished before testing.

* The apparent disagreement between the results of Handin and the others is probably mainly due to the fact that the other tests were not carried to sufficiently high stress levels.

** The specimen was mounted between steel pull pieces; the central portion was covered by a 0.007-in. thick copper sheath.

the triaxial tests by Schmidt (1937). This test gave smaller strains, although the results might be expected to differ from the bend test results (see below) because of the method of preparation of the samples, and also from the triaxial extension tests on samples prepared in the same way. (The values of Young's modulus in the zero-strain limit [5.0×10^5 kg/cm^2] determined from the uniaxial tension results are comparable with other determinations.) Figure 10 shows results of an extension test experiment (German: "Umschlingungsversuch") in which confining pressure was increased while axial stress was held constant (-)--so that the material elongates in the axial direction as in a tension test--compared with the more usual experiment (/). Results of loading-unloading and stress-reversal tests (Figs. 11 to 13) on pure NaCl carried out with the same apparatus used for the results shown in Fig. 9 show characteristic work-hardening.* The curves of Fig. 12 demonstrate that the workhardening is not independent of the confining pressure for small deformations. Figure 13 gives results of experiments studying temperature effects.**

The lack of reproducibility found for the plastic behavior of the annealed cleavages in the bend tests (Fig. 19) was interpreted by Schlichta (1966) as being due to predeformation arising from the cleaving. Both the yield stress and the tension stress required for a given strain in the bend tests appear to be an order of magnitude smaller than those found in the results of the triaxial tests on monocrystal samples (Figs. 24 and 25).***

Results of measurements of the temperature dependence of the critical shear stress of NaCl (single crystals?) are shown in Fig. 23.

---

* "Work-hardening in a simple tension experiment means that the stress is a monotonically increasing function of increasing strain" (Fung, 1965).

** The physical mechanism of the plastic deformation and work-hardening of NaCl has been studied by many investigators; Davidge and Pratt (1964) include a brief review of the work.

*** Crystals that were water-polished before being subjected to bend tests did not show the enhanced ductility characteristic of crystals bent under water (Fig. 1).

No details of the experimental arrangements used or discussions of the uncertainties associated with the points in Fig. 23 are given by Eshelby (1958) or Seeger (1958). Hardening curves for single crystals at temperatures up to 600°C are given by Seeger (1958) and Joffe (1924).

Results of triaxial tests carried out on confined dry pure NaCl monocrystals at various temperatures by Handin (1958) are shown in Figs. 24 and 25. (See also, Table 1.)* Note the lack of a well-defined yield point in some cases. The strains corresponding to given differential stress levels are generally larger than were found for the polycrystalline samples of mineral halite tested with the same apparatus (Handin, 1953), but smaller than in the results of the bend tests of Schlichta (1966). Again, no results were given that would demonstrate reproducibility.**

Results reported by Stepanow (1934) for moistened single crystal specimens deformed 50 percent under tension loading at room temperature (corresponding stress ≈ 3.3 kg/mm^2) seem to be consistent with results of bend tests discussed above.

B. SOURCES OF EXPERIMENTAL ERROR

Probably the largest sources of error in the bend and combined stress tests are corrections for friction and distortion of apparatus and the (unknown) deviations of the stress fields from pure uniaxial (bend tests) or triaxial conditions ("end effects"); also, in the bend tests, the magnitude of the effective outer-fiber tension is subject to some uncertainty, associated with the approximate solution of the

---

*The same apparatus used for the tests reported in Handin (1953) was used. The samples were jacketed in copper and correction was made to the applied load for the contribution of the copper jacket, based on measurements of stress-strain relations for copper.

**The apparent dropping off of the 300-degree curve in Fig. 25 at large strains is due to "necking" of the sample; a constant cross section was assumed for the data reduction.

statics problem.* There is also the question of whether equilibrium was reached at each loading step (Fig. 26).**

According to Handin (1953), force, piston displacement, and confining pressure measurements were made with an accuracy of 0.25 percent and a sensitivity of 0.1 percent; corrections of unspecified magnitude were made for piston friction (found to be about 1 percent of load) and elastic distortion of the apparatus.*** The force is converted to true differential stress on the specimen by dividing by the cross-sectional area determined from the original area and measured change in length, assuming no volume change. This procedure probably leads to no appreciable error until the strain becomes very large and the specimen necks down or "assumes a barrel shape." (The curves in the figures were carried to only 40 percent strain because of the uncertainty of computing the stress for greater strains.) No estimate was made of corrections for deviation from true triaxial stress states due to shear stresses at the ends of the test sample, arising from friction with piston faces. Results for Yule marble obtained with the apparatus were found to agree with results obtained by Griggs (1961) for a test under the same conditions (Fig. 27). Figure 28 shows the effect of exposure of rock salt to the confining liquid (kerosene).

Contact of the sample with the confining medium was avoided in the tests reported by Schmidt (1937) by encasing the sample with 0.1-mm thick annealed copper foil. Goguel (1948) accomplished the same

---

* A useful application of two-dimension computer codes might be to obtain estimates of corrections for these effects. The errors could also be estimated by running tests with samples of different dimensions.

** Schmidt (1937) adopted the procedure of holding the load constant at each level until no length change greater than 0.001 mm occurred during a 5-min period. It was found, however, that this rule could not be practically followed at shear stress levels greater than 200 kg/cm^2 (Fig. 14).

*** Determined by a run on steel. The calibration results were not given by Handin.

thing in his experiments by means of a thin rubber sleeve and coating of varnish. Schmidt noted that the test samples were stored in a dessicator over sulfuric acid.

A somewhat different experimental arrangement was employed for the triaxial tests reported by Serata (1961). Lateral strain of the cylindrical rock salt sample was restricted by a close-fitting aluminum collar. From a measurement of the tangential strain at the outer surface of the collar by means of strain gauges,* the lateral stress at the inner surface was inferred by assuming elastic deformation of the collar (Fig. 29). Details of the testing machine, axial pressure measurements, and techniques used for reduction of friction on the surfaces of the sample are not described by Serata. Calibration results, strain gauge readings, and dimensions, and elastic modulus for collar material are not reported. In similar tests carried out on three paraffin cylinders with different height/diameter ratios "it was found that the effects from specimen size and the height-radius ratio can be reduced to an insignificant level, if proper measures for reducing friction on all sides of a specimen are taken."

C. FRACTURE PHENOMENA UNCERTAINTIES

There seems to have been no systematic investigation of fracture and crushing phenomena for rock salt. Some fracture points are indicated in the triaxial and bend tests results (Figs. 3, 18 to 20). Results of impact tests given by Johnston, Stokes, and Li (1959) carried out on 1.25 in. x 0.2 in. x 0.2 in. cleavages of optically pure NaCl and LiF at strain rates ~40/sec** indicate a transition from brittle fracture to ductile fracture (i.e., preceded by plastic deformation) in the temperature range 0.6 to 0.65 T_M (350 to 380°C for NaCl). (See Fig. 30.) Results of tension tests carried out by Voigt

---

*Three "type SR-4" gauges were employed. "A good agreement among the strains measured by the three different circuits of the same cell was achieved."

**Impact bending load at mid-span with swinging pendulum.

(1893) on specimens confined to CO_2 gas at pressures up to 850 psi indicate that the superposed tensile load required to fracture is independent of pressure and that "the fracture is a clean brittle break with no trace of plastic flow. Evidently the pressures were not high enough to bring about the plasticity which is exhibited at higher [confining] pressures" (Bridgman, 1964). The last result appears inconsistent with the results of the 4-point bend tests discussed above.

No results of plastic flow or yield measurements on uncrushed or crushed rock salt subjected to previous dynamic loading seem to have been reported. Some plastic yield, tensile, and crushing strengths data for virgin and crushed "Salmon salt"* are reported by Holzer (1963) without source citation (Table 2).**

Table 2 -- MATERIAL STRENGTH DATA FOR SALMON SALT (Holzer, 1963)

	Kilobars
Plastic Yield Criteria	
Fast rising pulse	0.5
Slow rising or falling off	0.14
Crushed	0.05
Tensile Strength	0.03
Crushing Strength	
Uncracked	30
Cracked	0.34

* Presumably from Tatum salt dome, Mississippi.

** "No attempt will be made here to review how each [datum] is determined. No good experimental techniques exist for determining some of the constants, and approximate numbers must be used. For others, satisfactory values can be obtained from the literature." In the report by Holzer the crushing strengths data for uncracked and cracked (i.e., due to tension loading) material were reversed (L. Rogers, private communication).

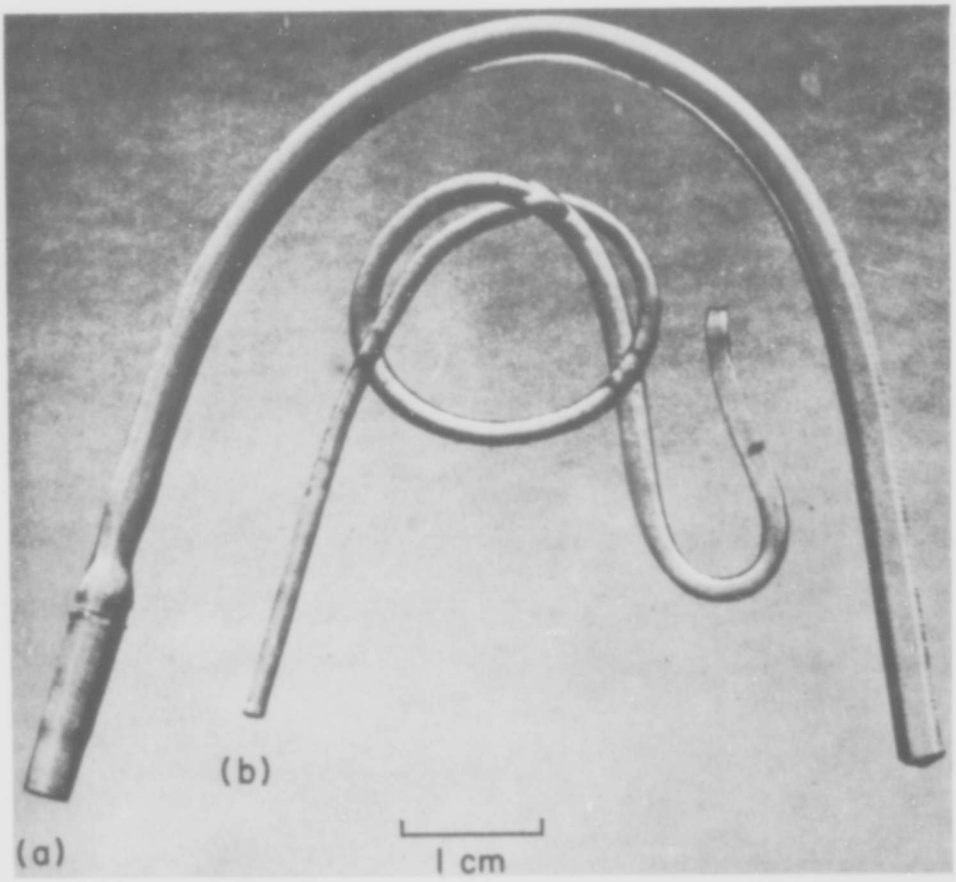

FIGURE 1 As-Grown NaCl Crystals Bent (A) in Air, and (B) Under Water (Schlichta, 1966)

RI2-12-66-1

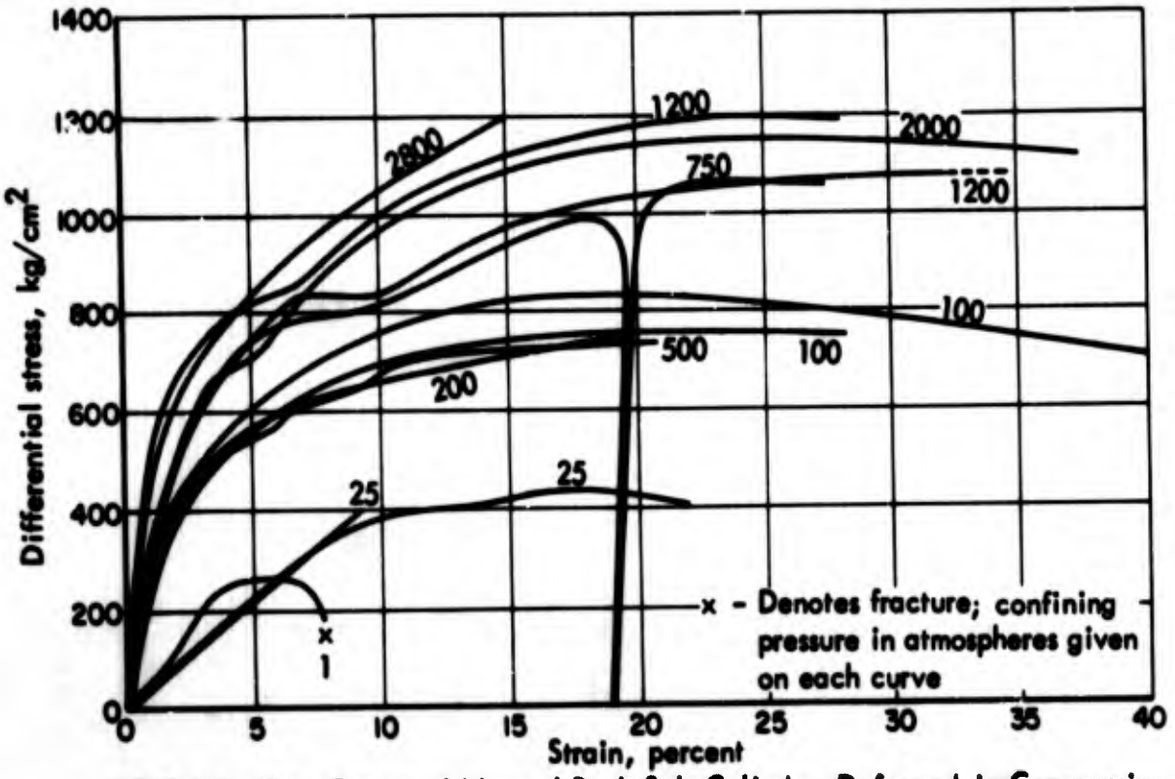

FIGURE 2 Flow Curves of Natural Rock Salt Cylinders Deformed in Compression (Handin, 1953)

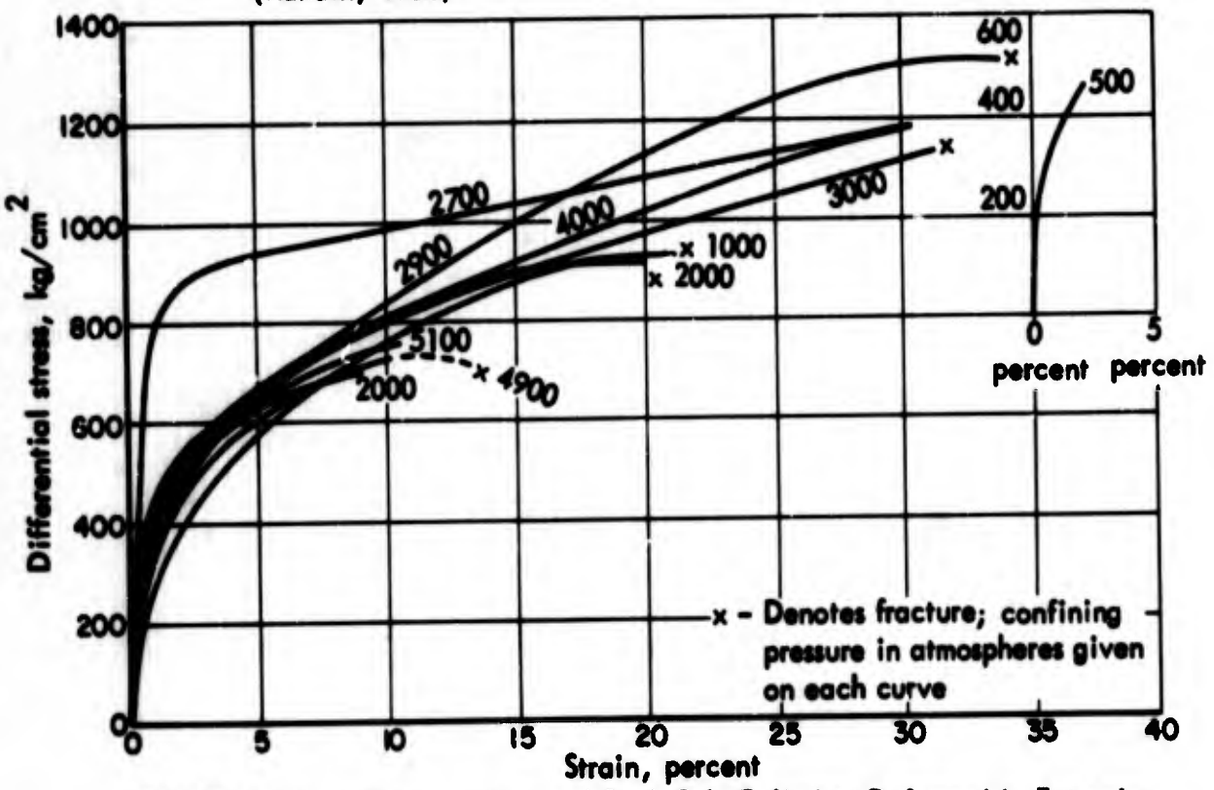

FIGURE 3 Flow Curves of Natural Rock Salt Cylinders Deformed in Extension (Handin, 1953)

RIS-12-66-2

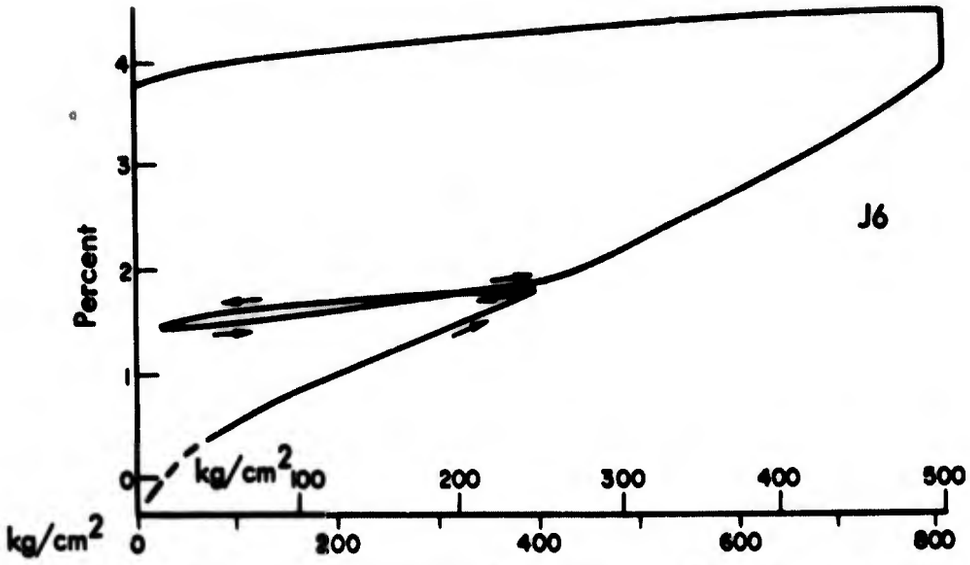

FIGURE 4 Flow Curve of Natural Polycrystalline Rock Salt Cylinder Deformed in Compression (Goguel, 1948). The Upper Abscissa Scale Gives the Confining Pressure (kg/cm^2); the Lower Scale Gives the Axial Stress. Note the Creep that Occurred While the Constraints were Held Constant for an Unspecified Period of Time, Corresponding to a Differential Stress Level of About 300 kg/cm^2

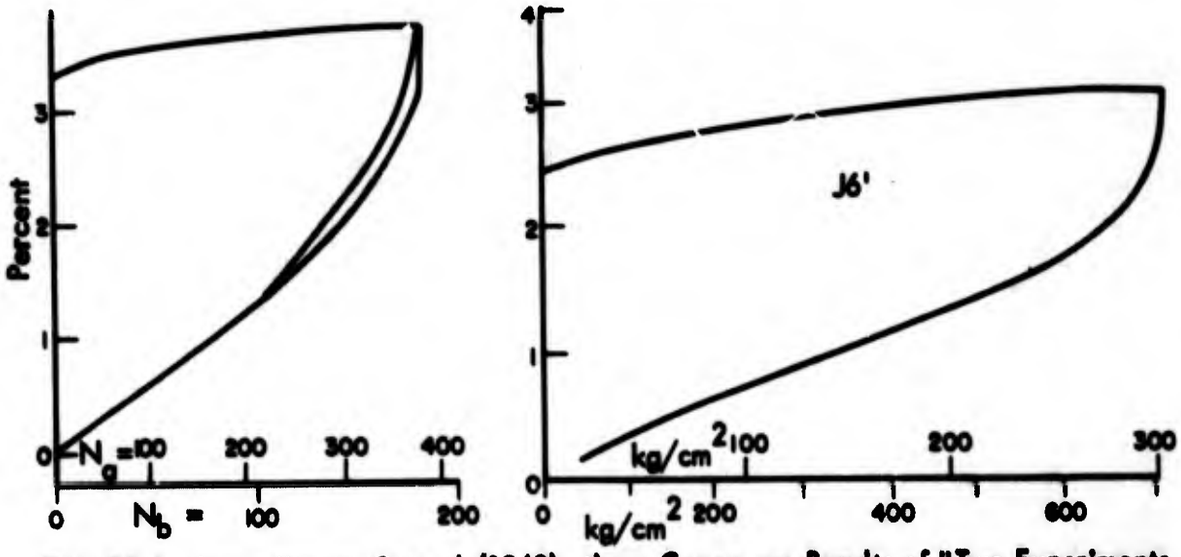

FIGURE 5 According to Goguel (1948), these Curves are Results of "Two Experiments [on Polycrystalline Rock Salt] Showing, by the Increase of the Pressure-Deformation Curve, the Existence of a Rapid Deformation for Salt." The Arrow Indicates a Poorly Defined "Knee" of the Curve which "Seems to Correspond to a Change in the Regime of Deformation. If the Pressure Continues to Increase, la déformation se poursuit, mais reste toujours progressive sans s'accélerer, ni sans rien qui ressemble à une rupture." Compare Fig. 7.

R12-12-66-3

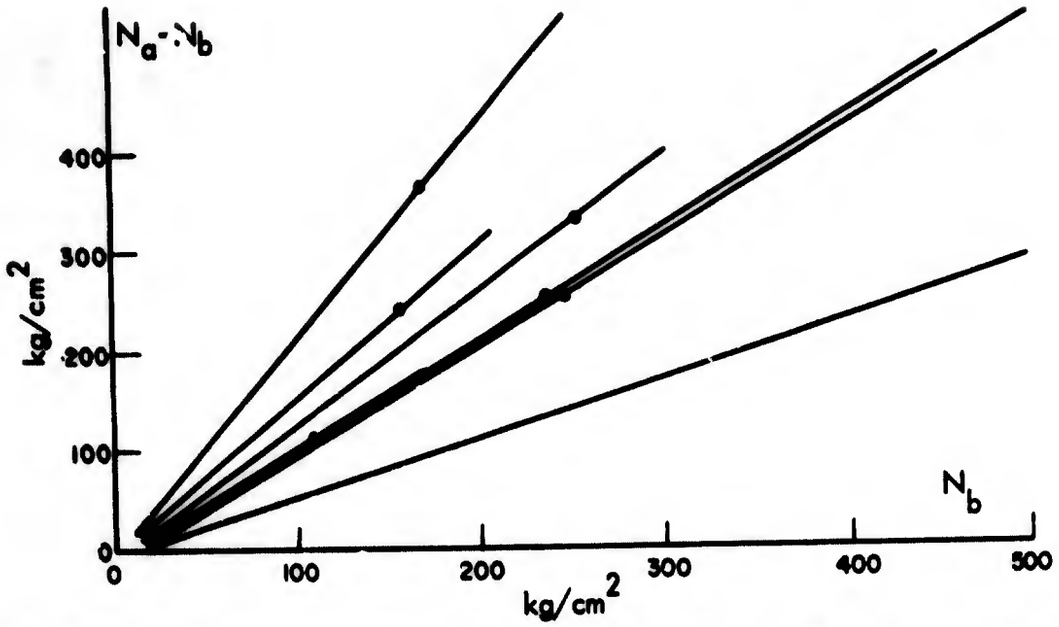

FIGURE 6 The Points Shown Correspond to the "Knees" of the Flow Curves for Several Experiments on Polycrystalline Rock Salt, as in the Preceding Figure (Goguel, 1948).

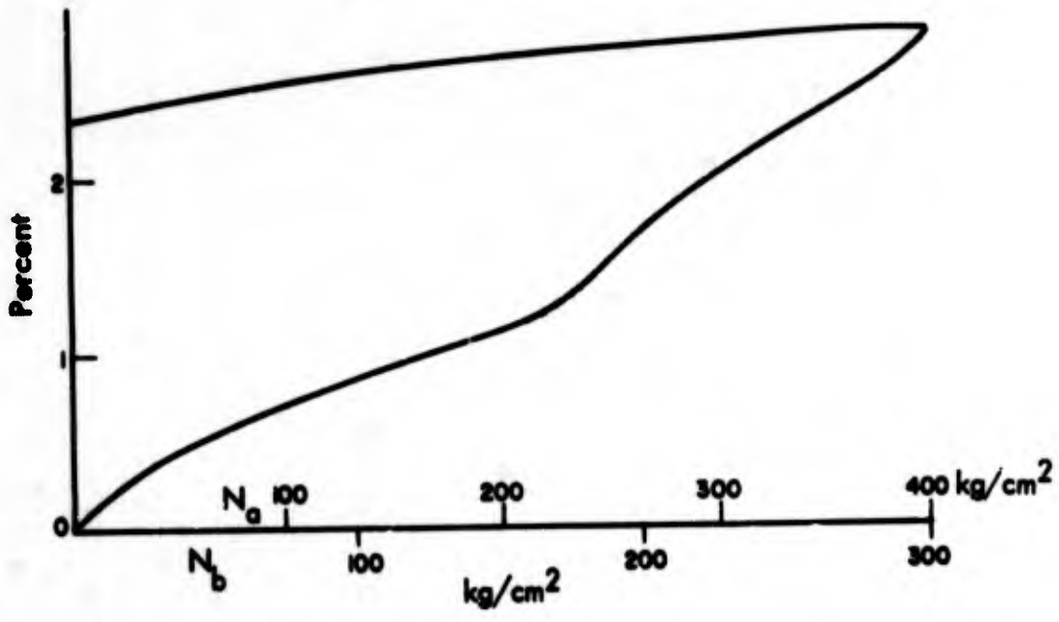

FIGURE 7 Example of Deformation of a Rock Salt Monocrystal (Goguel, 1948). Compare Fig. 5. In this Case the "Knee" is Sharply Defined. "Beyond this Limit of Plasticity, Which Seems to Decrease Slightly When the Mean Pressure Increases (Fig. 8), the Crystal can be Deformed Indefinitely, in a Plastic Fashion."

R12-12-66-4

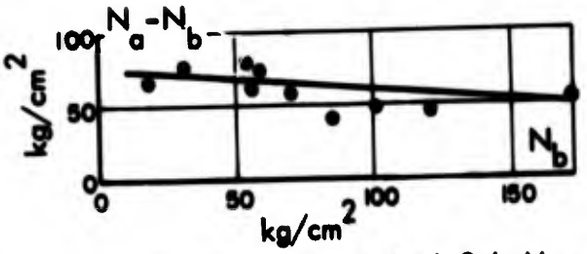

FIGURE 8 Results of Several Experiments on Rock Salt Monocrystals. The Circles Represent the Constraints for which the "Rapid Plastic Deformation" Begins (Goguel, 1948). (See preceding figure)

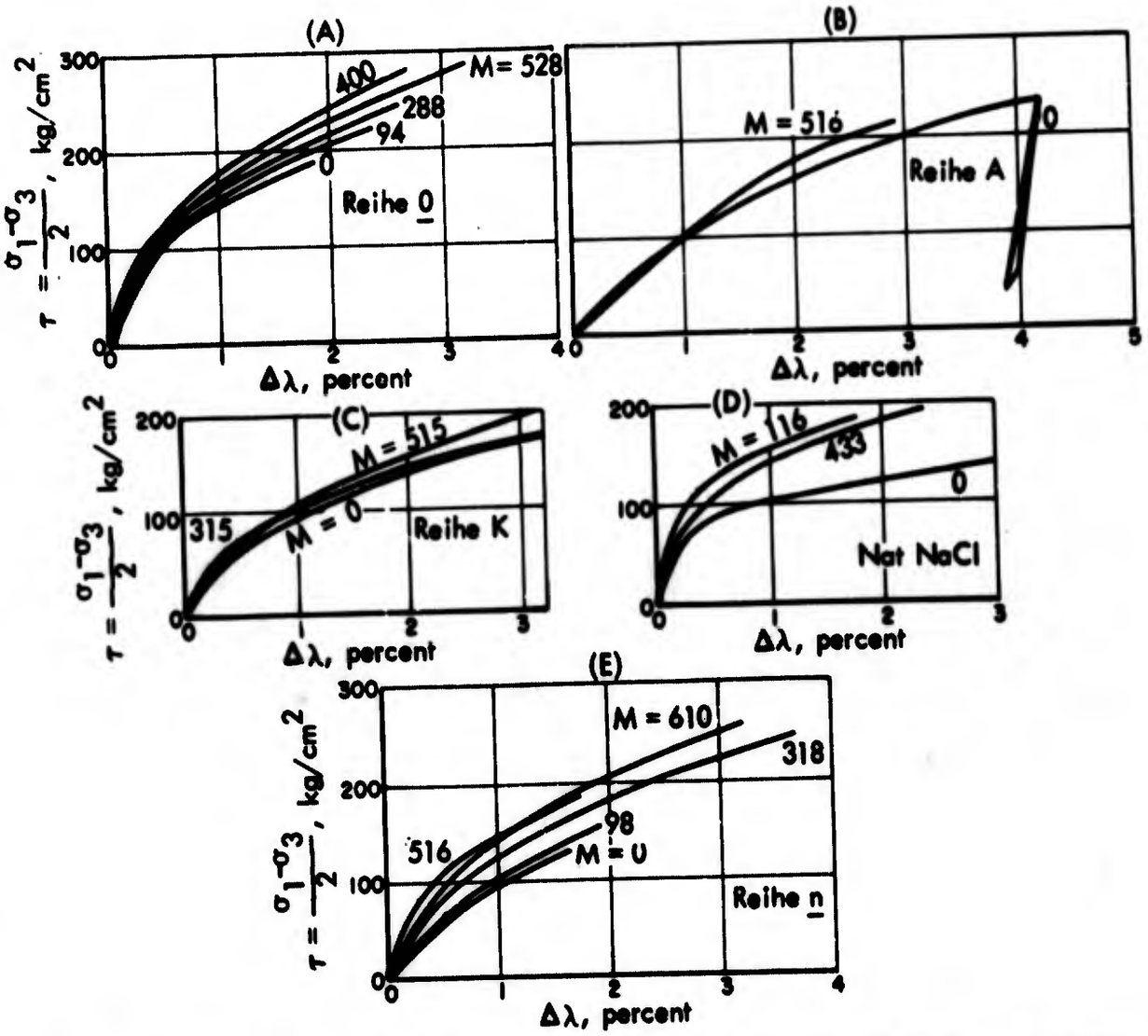

FIGURE 9 Flow Curves of Rock Salt Cylinders Deformed in Compression (Schmidt, 1937). Figure 9(D) Shows Results Obtained for Natural Rock Salt; Other Results are for Cylinders of Pressed, Annealed Rock Salt Powder ("Artificial" Rock Salt). The Curves are Labeled with the Value of the Confining Pressure ("Manteldruck") in kg/cm^2; Unit for τ = Maximum Shear Stress in kg/cm^2. $\Delta\lambda$ = Axial Strain.

R12-12-66-3

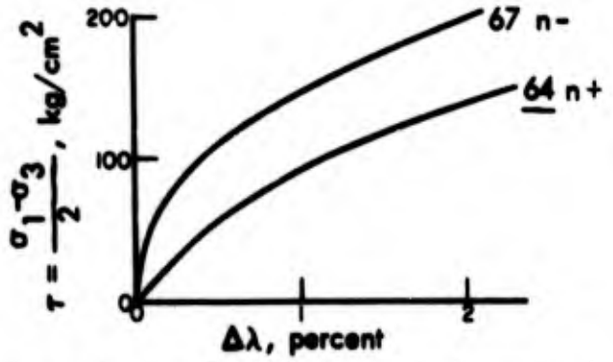

FIGURE 10 Flow Curves for Test Piece Deformed in Extension (-) and Compression (+) (Schmidt, 1937). In the Extension Case, a Small Effective Axial Stress of 8.5 kg/cm^2 was Due to Friction.

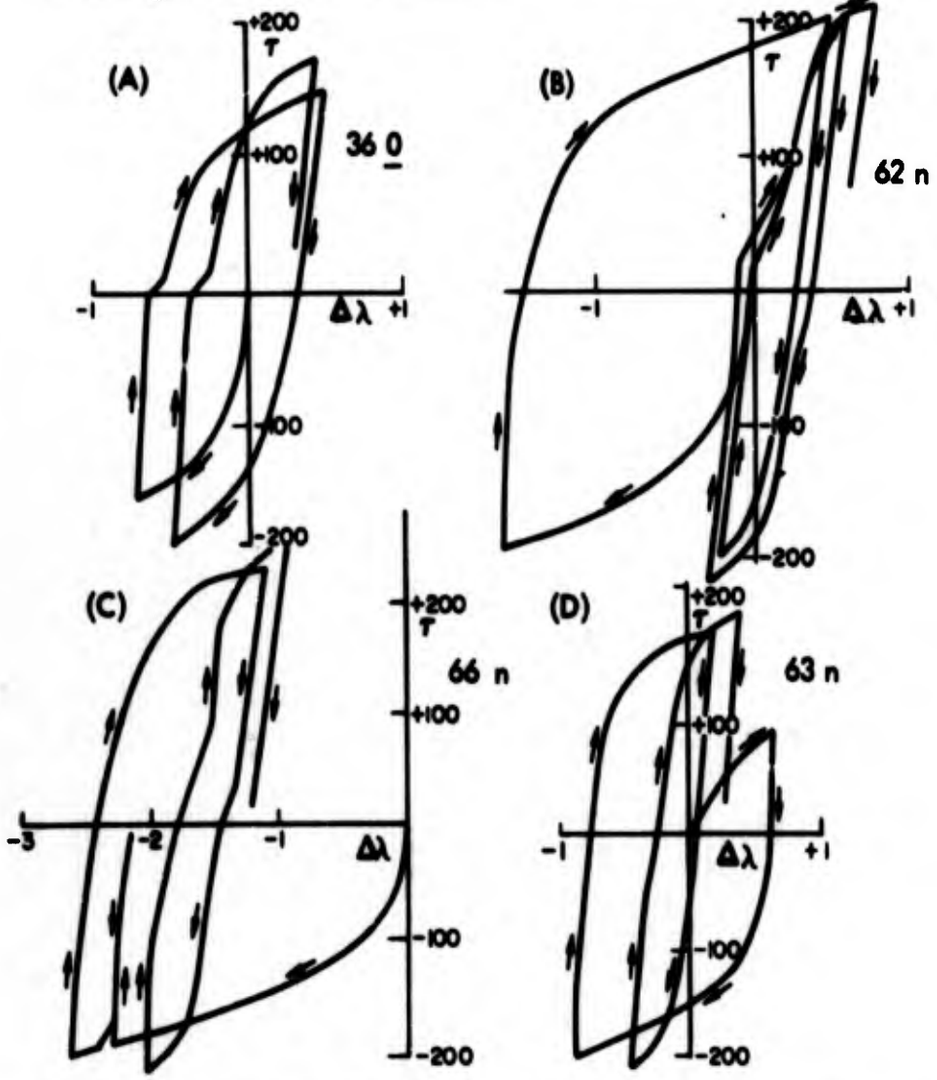

FIGURE 11 Rock Salt Under Stress Reversal (Schmidt, 1937). A Positive Strain Corresponds to a Shortening Along the Axis of the Cylindrical Test Piece. $\tau = (\sigma_1 - \sigma_3)/2$ = Maximum Shear Stress (kg/cm^2). The Apparent Discontinuity in Slope at the Extension → Compression Transition is Due to "Play" in the Piston Screws.

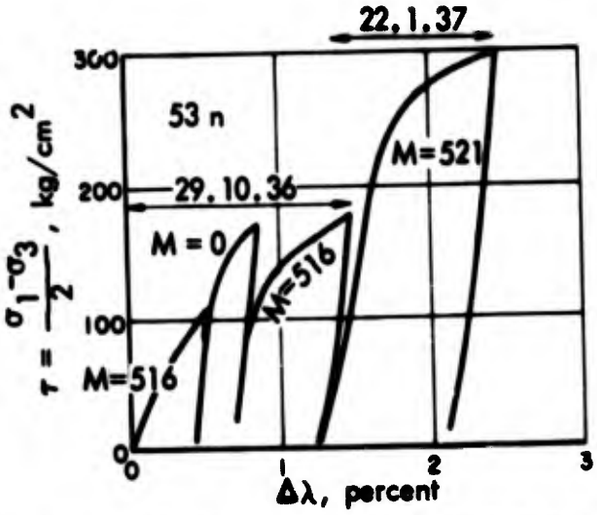

FIGURE 12 Flow Curves for Rock Salt Cylinder Deformed in Compression (Schmidt, 1937). The Test Piece was Allowed to "Rest" for a Three-Month Period After Three Triaxial Load Tests.

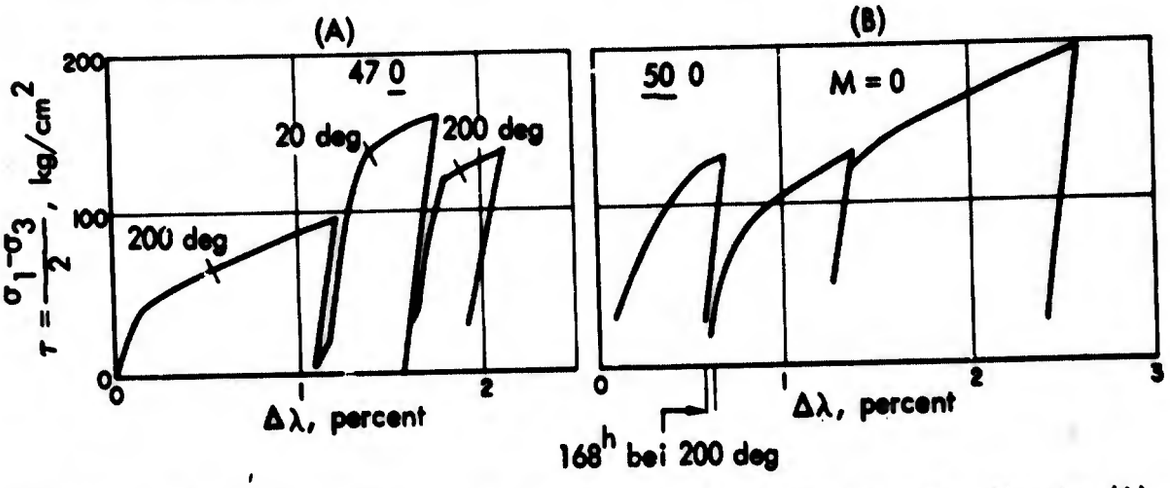

FIGURE 13 Results of Uniaxial Compression Tests on Rock Salt Cylinders, Showing (A) Deformation of Heated Test Piece and (B) Effect of Annealing (Schmidt, 1937)

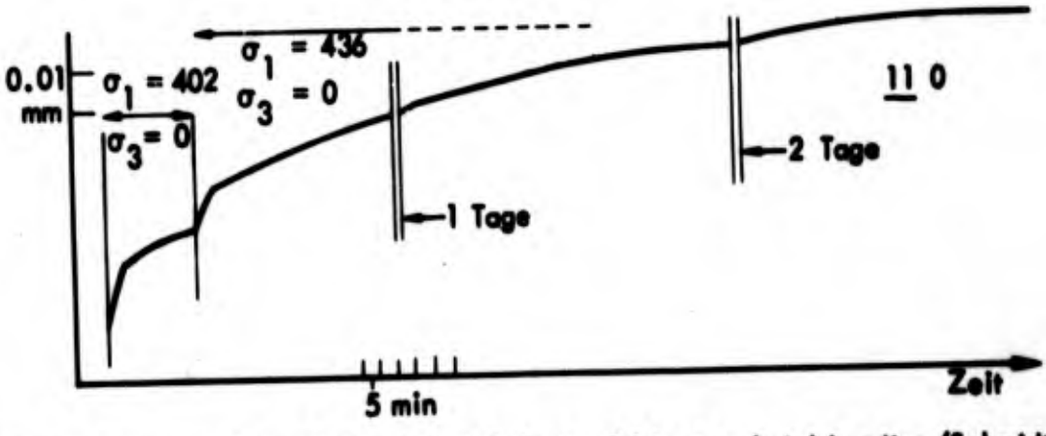

FIGURE 14 Strain vs. Time for Rock Salt Cylinder Subject to Axial Loading (Schmidt, 1937)

R12-12-66-0

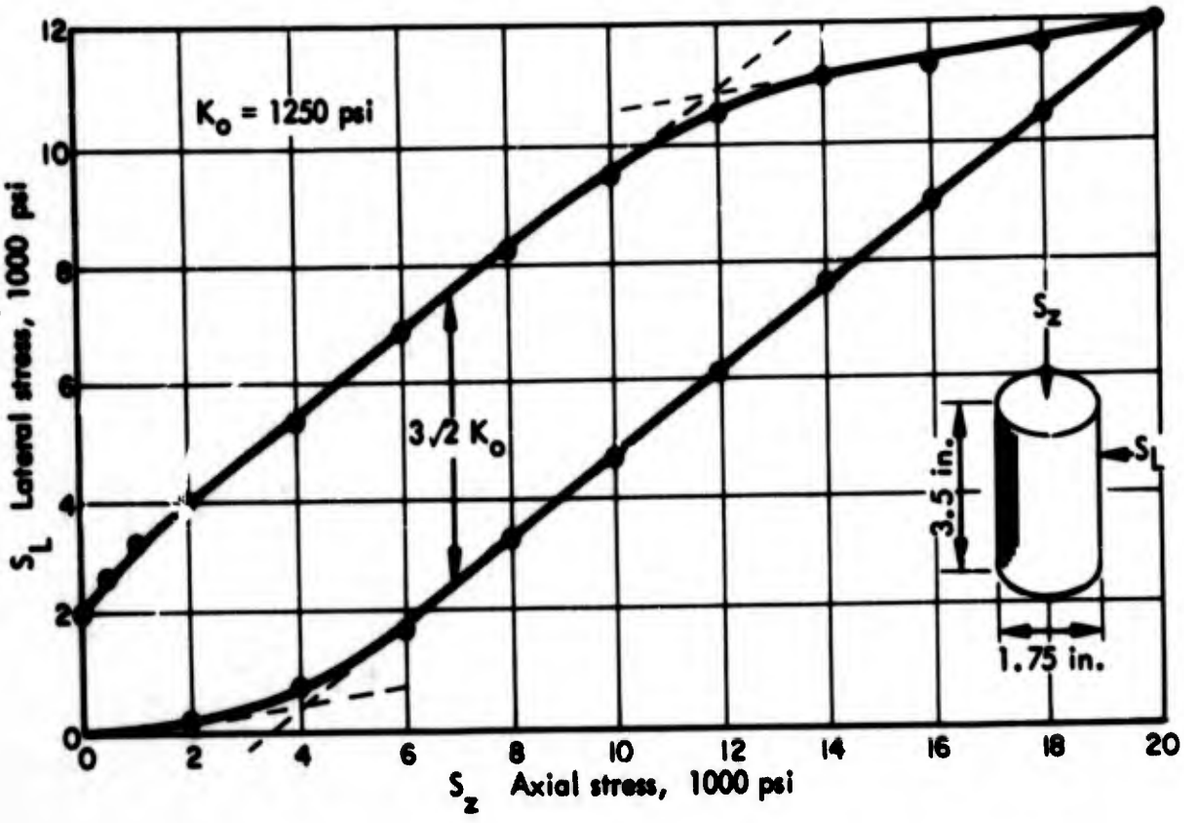

FIGURE 15 Results of Triaxial Test on Rock Salt Cylinder (Serata, 1961). The Lateral Expansion of the Cylinder was Restricted by an Aluminum Collar.

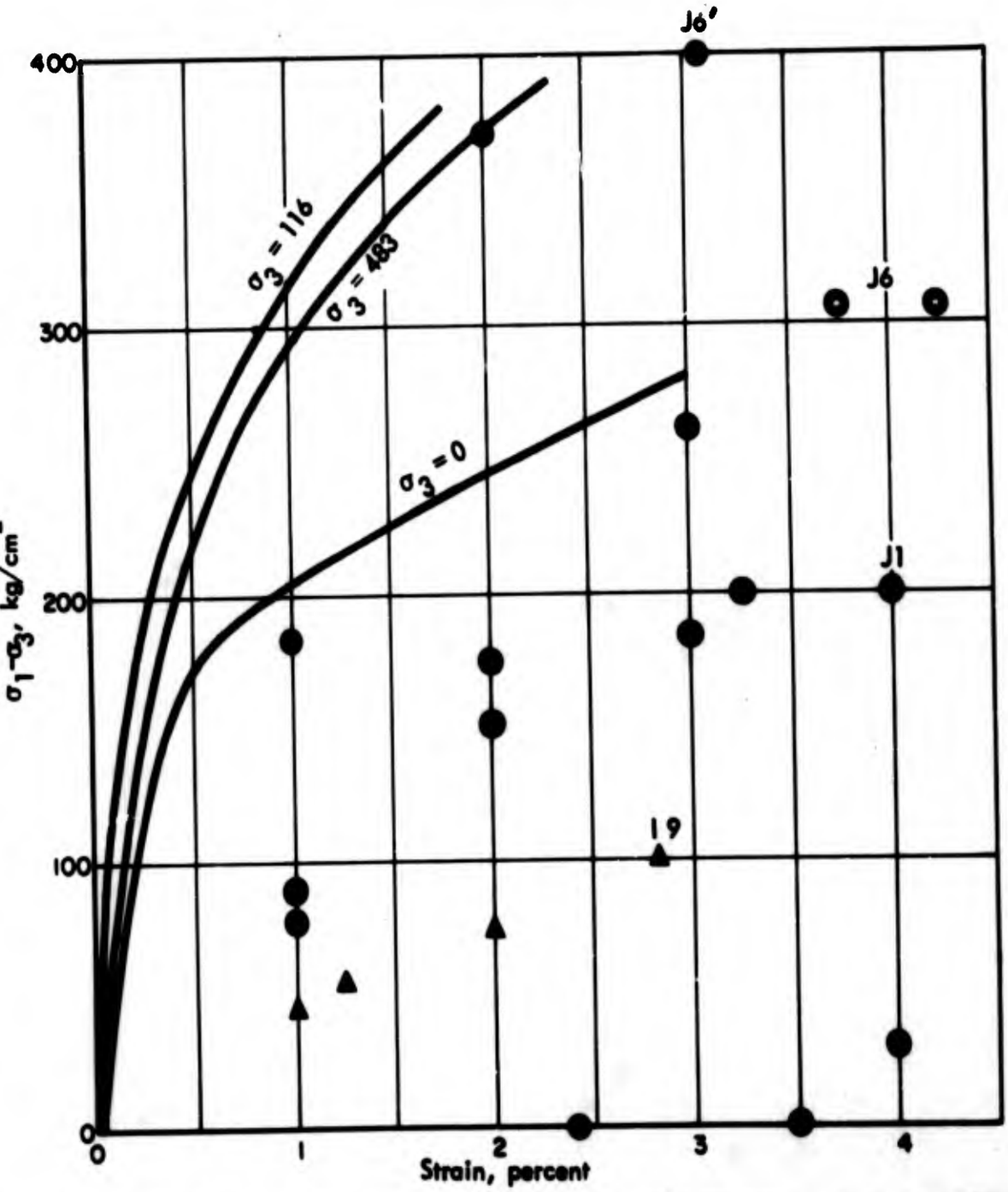

FIGURE 16 The Results of Triaxial Tests at Low Stress Levels (Figures 4, 5, 7, and 9(D)) have been Replotted to Facilitate Comparison. The Continuous Curves are Replotted from Fig. 9(D). Sample 19 was a Monocrystal; the Other Results are for Polycrystalline Samples of Natural Halite. Note that the Experiments of Figs. 4, 5, and 7 were not Carried out at Constant Confining Pressure. (A Fairly Large Error was Introduced by the Replotting.)

R12-12-66-10

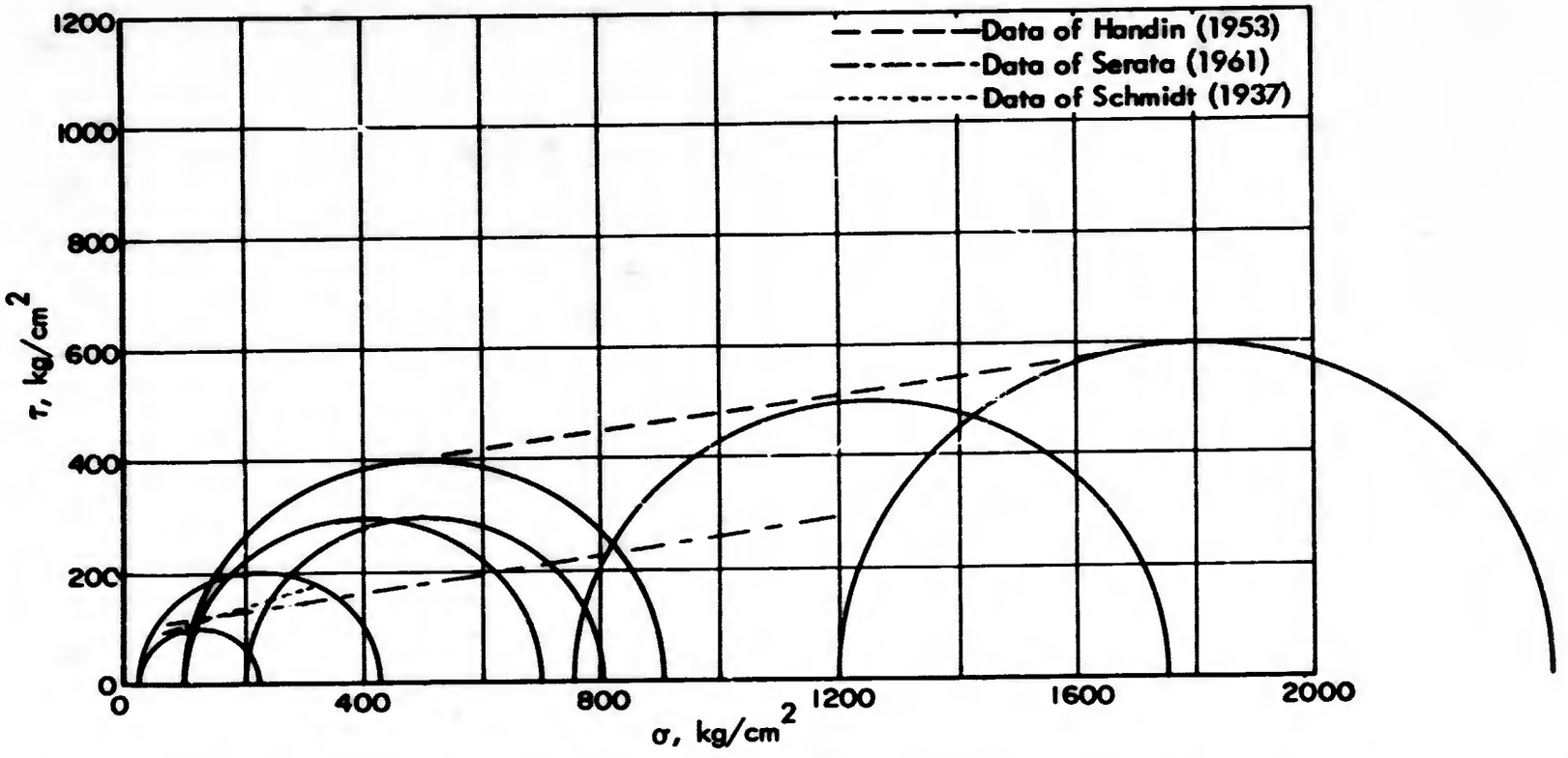

FIGURE 17 Mohr Stress Circles Corresponding to Data of Handin (1953) in Fig. 2. Also Shown are Apparent Envelopes of Stress Circles (not shown) Constructed from Data of Schmidt (1937) and Serata (1961). The Mohr Circle Describing a State of Stress has Radius $(\sigma_1-\sigma_3)/2$ and Center $(\sigma_1+\sigma_3)/2$.

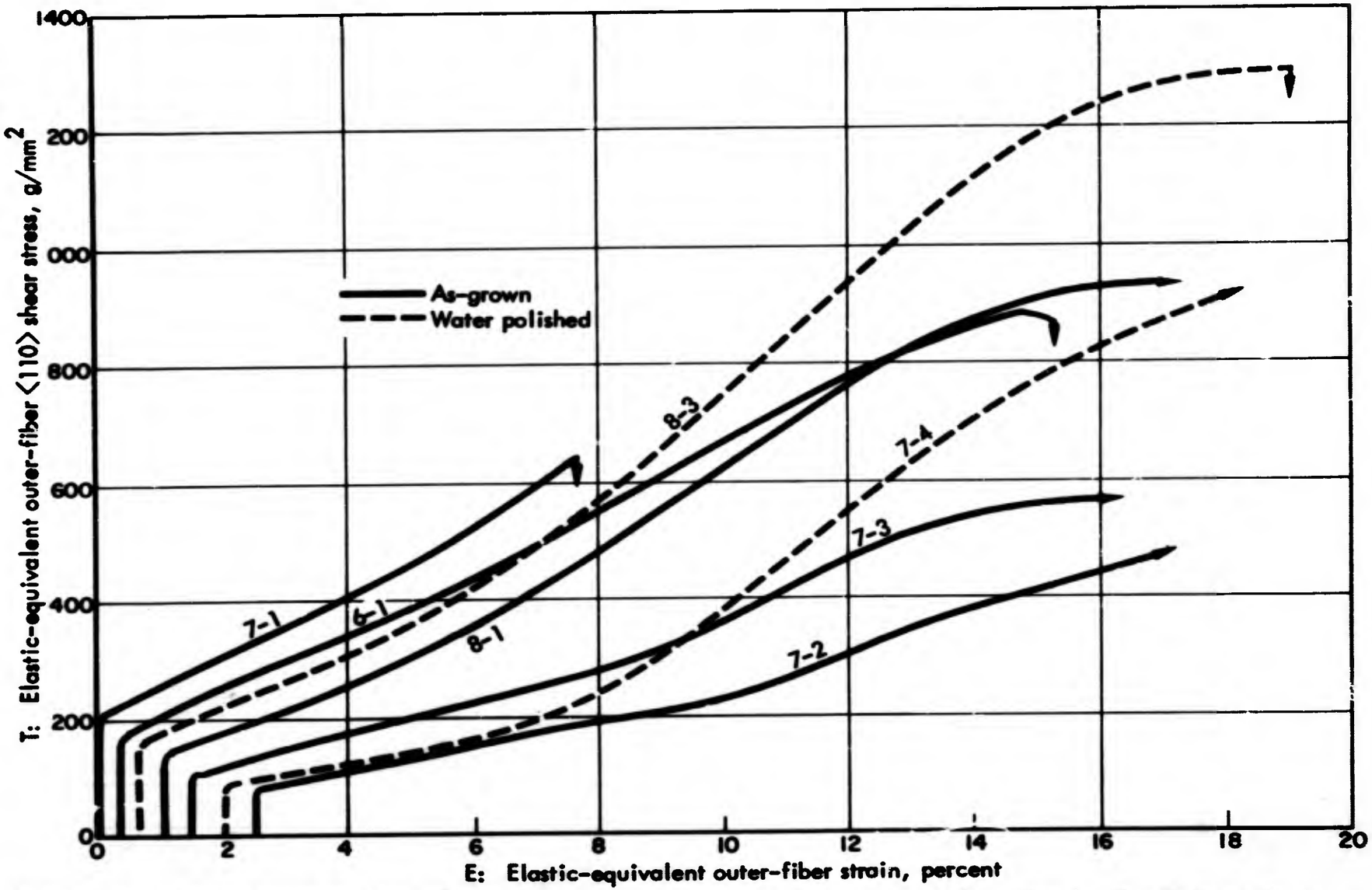

FIGURE 18 Elastic-Equivalent Stress-Strain Curves for As-Grown NaCl Crystal Rods (Bend Tests). The Ordinate Scale Can be Multiplied by a Factor 0.2 to Give Elastic Equivalent Outer Fiber Tensile Stress in kg/cm . "The Values of [Stress] and [Strain] at High Strains Must be Regarded as Having Qualitative Significance Only..." A Downward-Pointing Arrow Indicates Fracture (Schlichta, 1966).

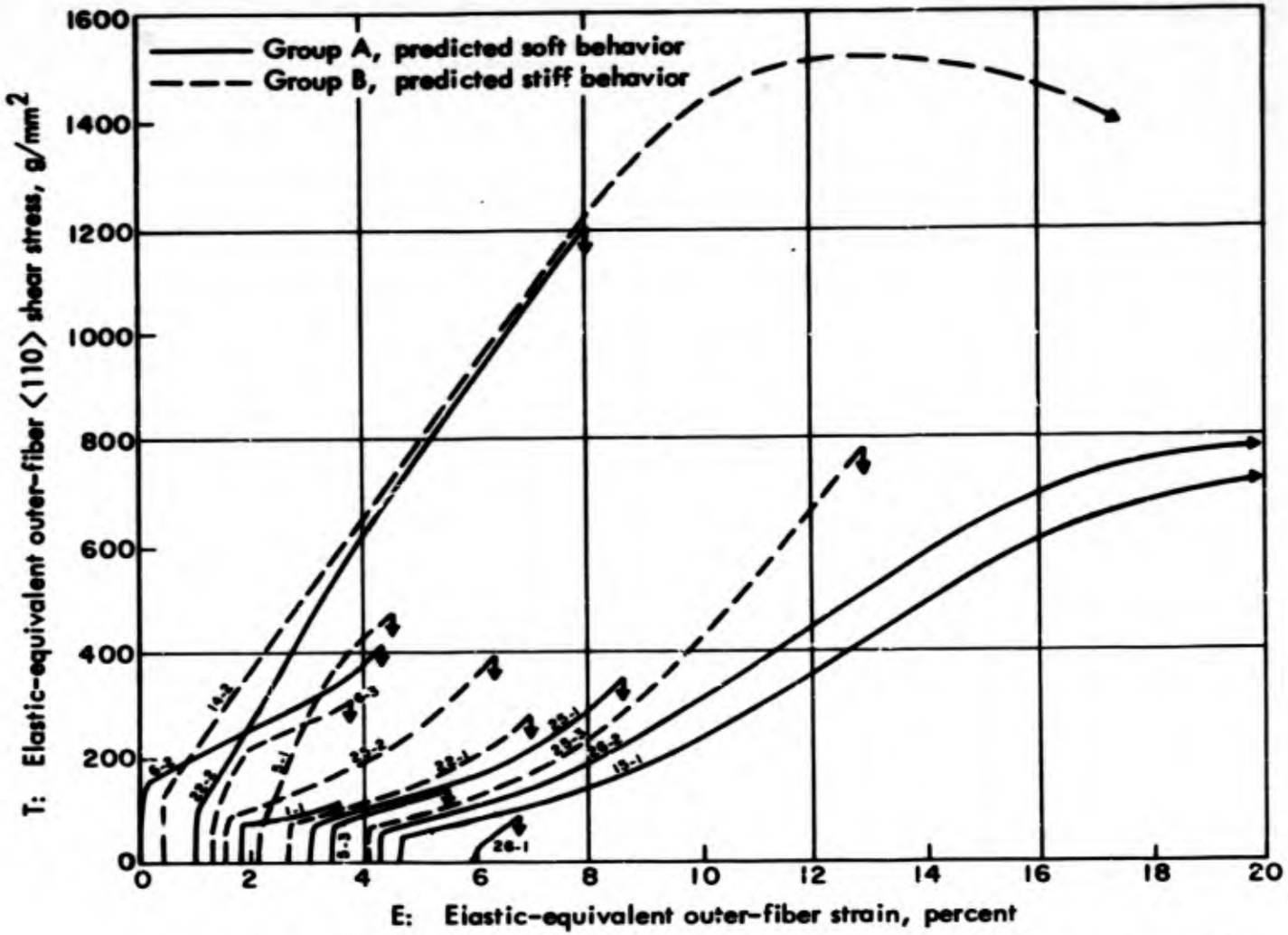

FIGURE 19 Elastic-Equivalent Stress-Strain Curves for Annealed Cleavages of NaCl (Bend Tests). The Ordinate Scale Can be Multiplied by a Factor 0.2 to Give Elastic Equivalent Outer Fiber Tensile Stress in kg/cm^2 (Schlichta, 1966).

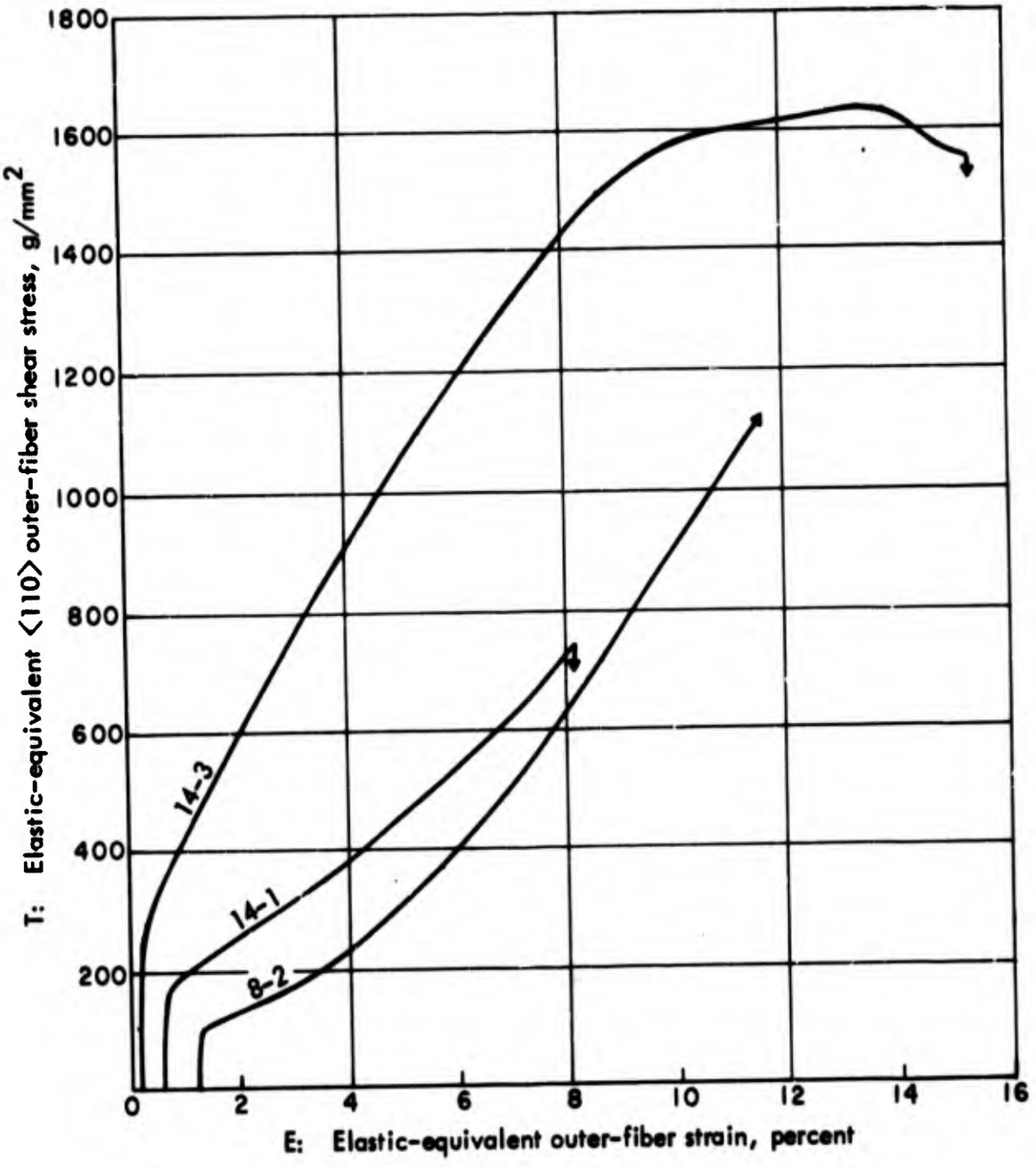

FIGURE 20 Elastic-Equivalent Stress-Strain Curves for Predeformed NaCl Crystal Rods (Bend Tests). The Ordinate Scale Can be Multiplied by a Factor 0.2 to Give Elastic Equivalent Outer Fiber Tensile Stress in kg/cm^2 (Schlichta, 1966).

RI2-12-66-14

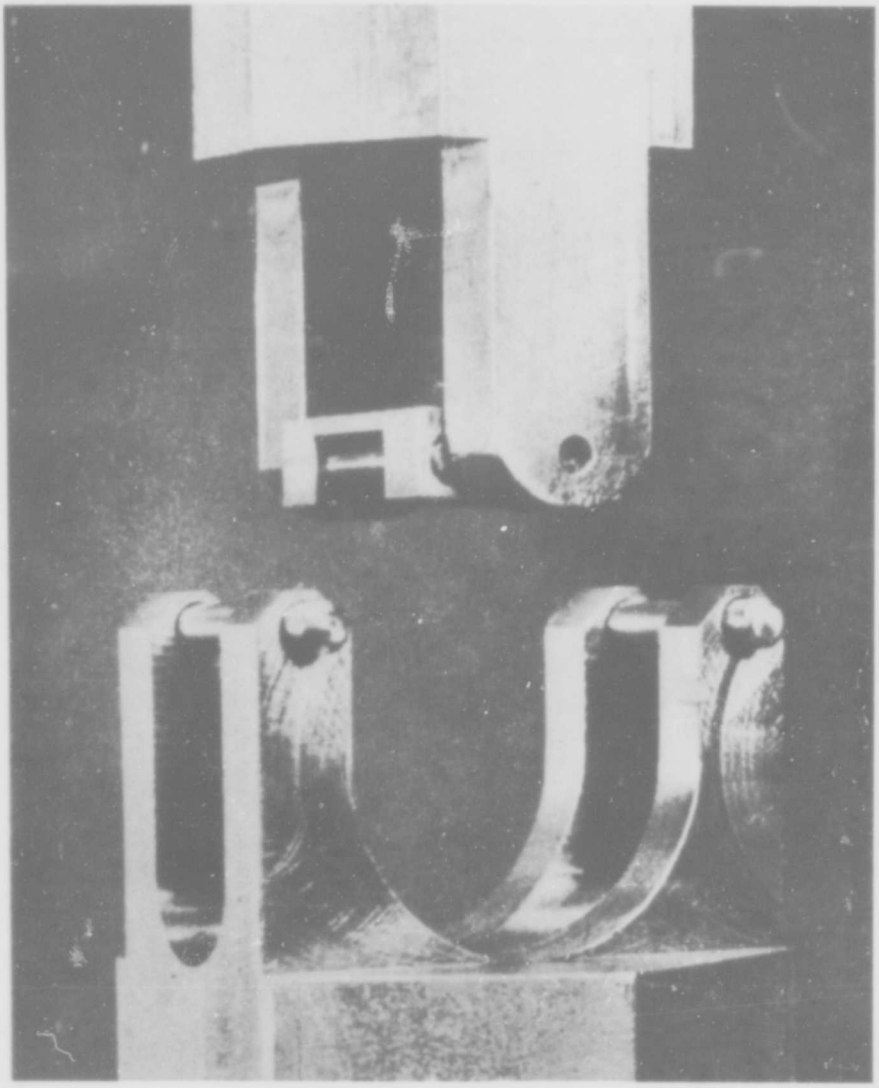

FIGURE 21 Jig Used for Four-Point Bend Tests (Schlichta, 1966).

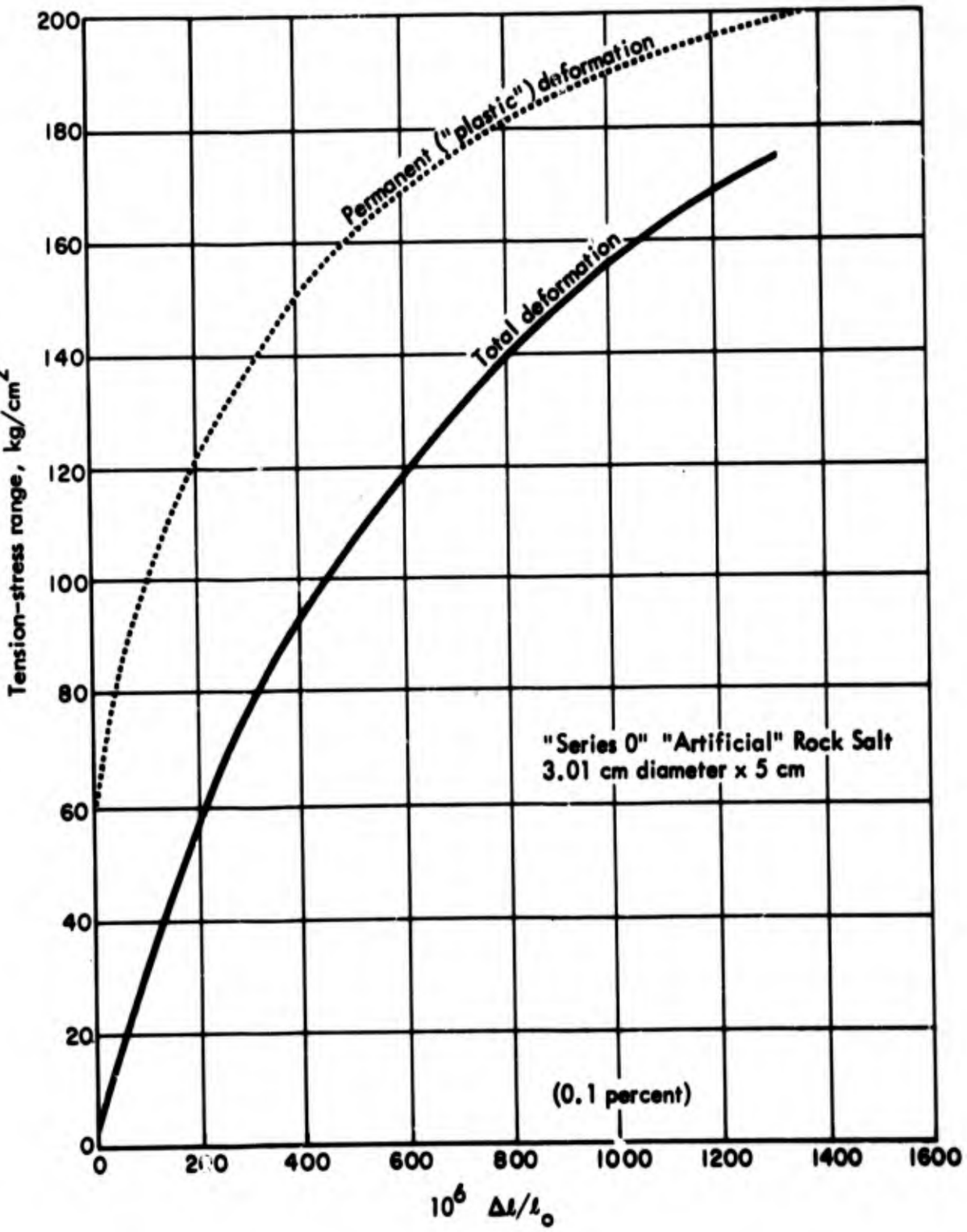

FIGURE 22 Results of Uniaxial Tension Test on Rock Salt Cylinder (Schmidt, 1937). Compare Fig. 11(A).

R12-12-66-16

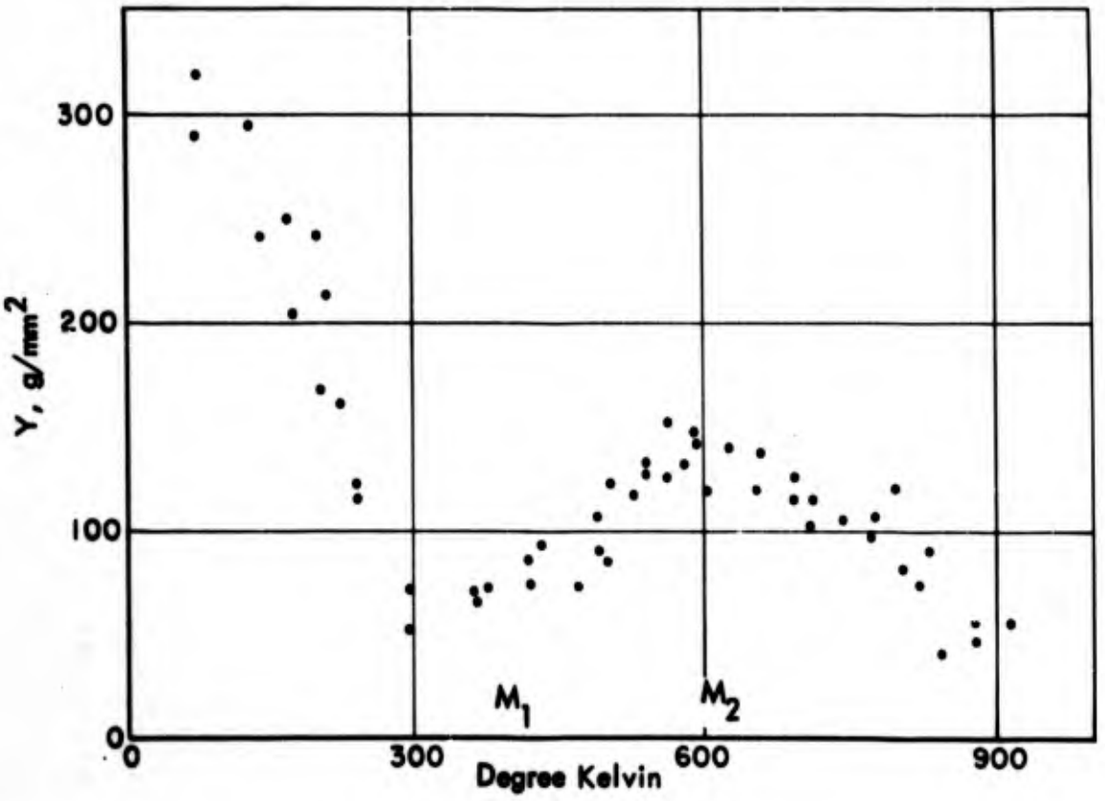

FIGURE 23 Yield Stresses of Rock Salt (Single Crystal?) Specimens at Various Temperatures (Eshelby, 1958). Earlier Measurements by Ekstein (1935) Gave Critical Shear Stresses Exceeding those Shown by 15 to 130 Percent in the Temperature Range 270 to 600°C. Other Measurements by Grafand Klatte (Unpublished Data Quoted by Seeger, 1958) Ranged from 0 to 70 Percent Higher in the Temperature Range 600 to 870°C.

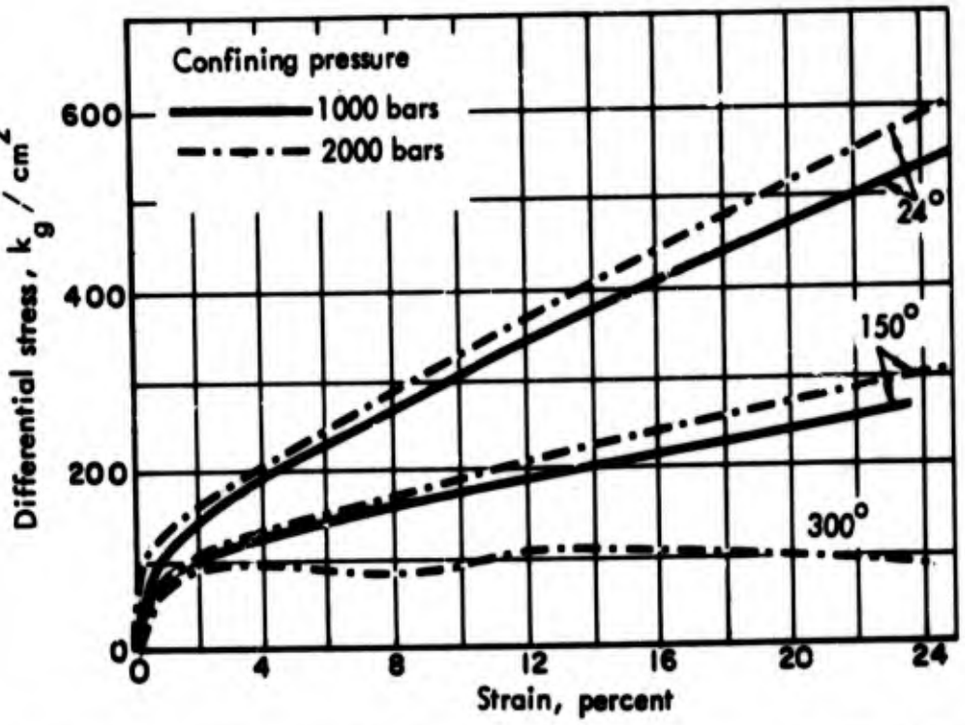

FIGURE 24 Stress-Strain Curves for NaCl Single Crystals Deformed Dry in Compression at 1,000 and 2,000 Bars Confining Pressure and at Different Temperatures. Figure from (Handin 1958).

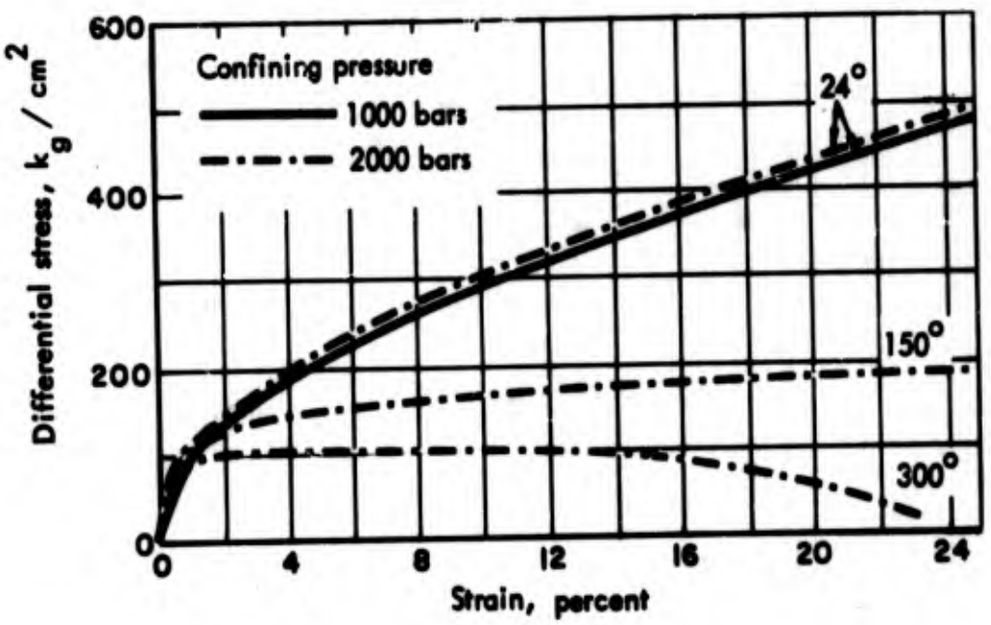

FIGURE 25 Stress-Strain Curves for NaCl Single Crystals Deformed Dry in Extension at 1,000 and 2,000 Bars Confining Pressure at Different Temperatures. Figure from (Handin 1958).

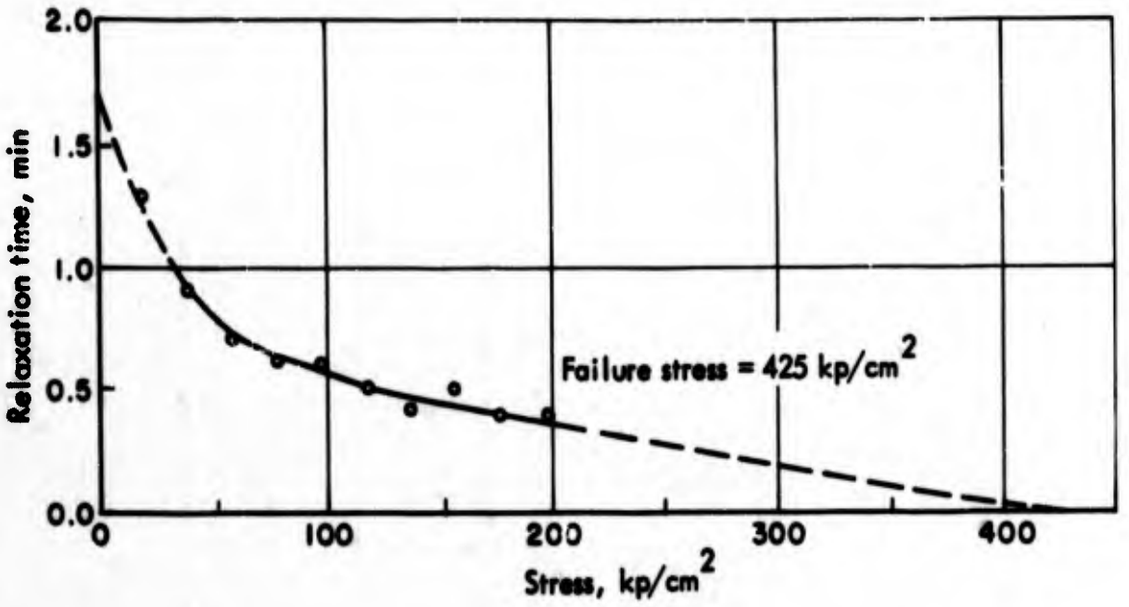

FIGURE 26 Relaxation Time, Hard Rock Salt (Höfer, 1964). The Stress Unit here is Probably Kiloponds [sic]/cm^2. 1 kp = 1 kg Force (Polski Komitet Normalizacyjny, Vocabulary of Mechanics in Five Languages, 1962).

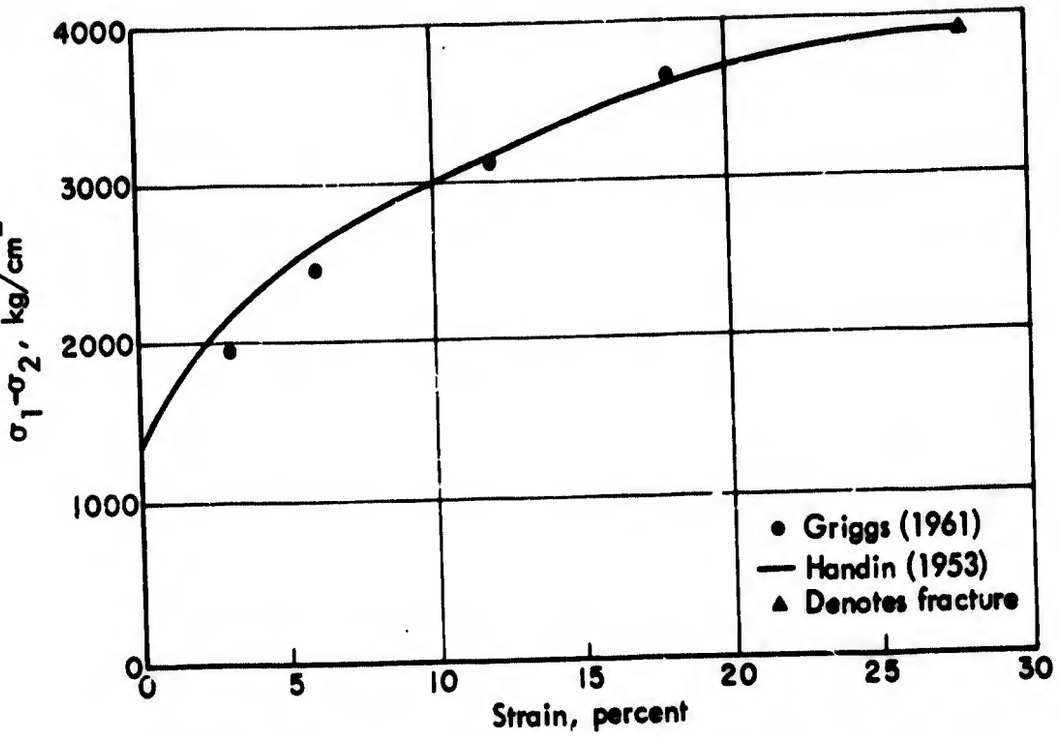

FIGURE 27 Flow Curves for Yule Marble Deformed in Extension. Confining Pressure = 5200 atm.

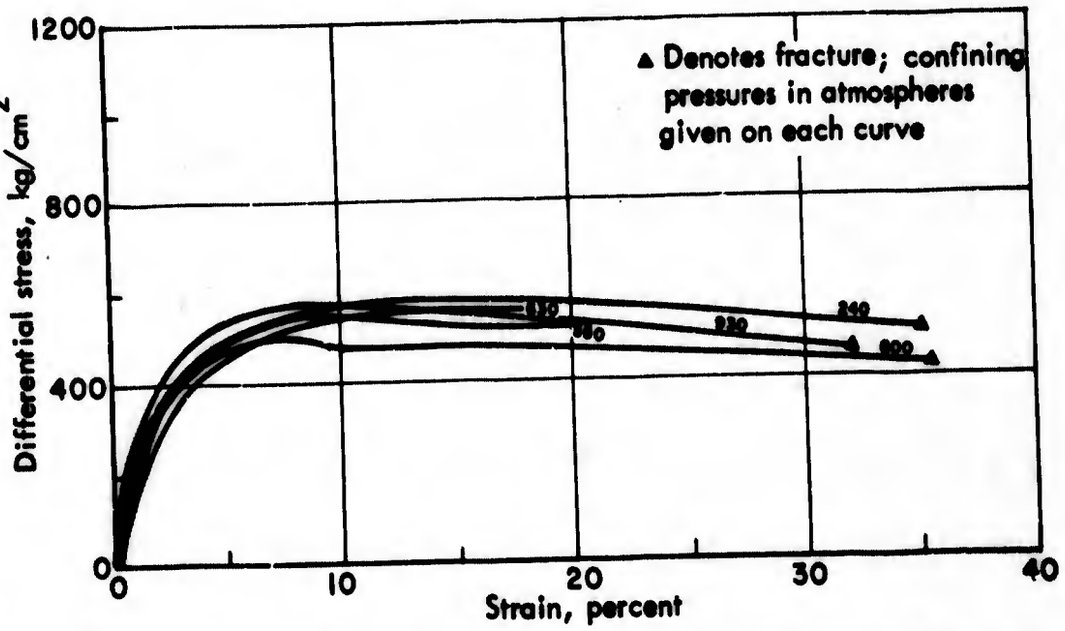

FIGURE 28 Flow Curves of Natural Rock Salt Cylinders Deformed in Compression with Specimens Exposed to Confining Liquid (Kerosene) (Handin, 1953).

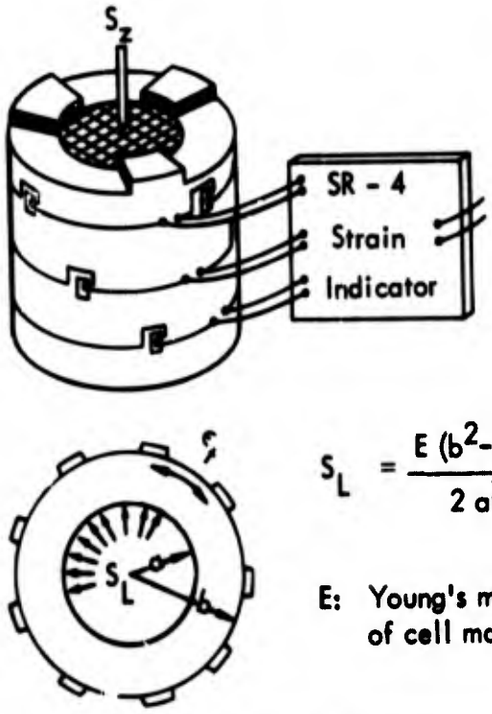

FIGURE 29 Triaxial Test Cylinder Used for Measurements Reported by Serata (1961)

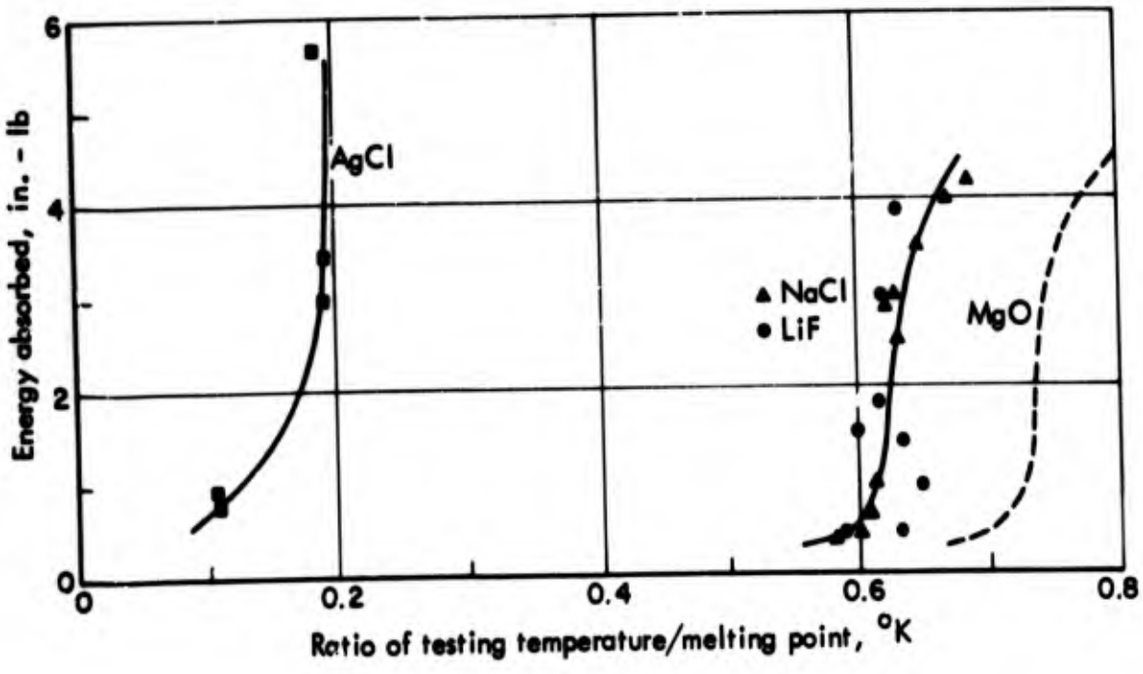

FIGURE 30 Results of Impact Tests on Ionic Crystals (Johnston, Stokes, and Li, 1959)

CHAPTER IV

UNCERTAINTIES OF THEORETICAL EQUATIONS OF STATE

IV. UNCERTAINTIES OF THEORETICAL EQUATIONS OF STATE

Ideally, an equation of state should be based on a physically reasonable statistical-mechanical model and should involve only atomic constants (i.e., no parameters to be determined by comparison with measurements of mechanical or thermodynamic properties). Such an equation should be capable of predicting the mechanical/thermodynamic properties over the entire range of pressure, density, and temperature with high accuracy; the model should be consistent with models capable of predicting other properties, e.g., optical or electrical. Theoretical equations of state, relating the thermodynamic variables for NaCl under conditions of hydrostatic or hydrodynamic loadings, have been proposed which range from simple fits to compressibility data in various ranges to something less than the ideal equation of state just described.

Four different equations of state developed to describe the thermodynamic states of compressed NaCl or NaCl-like solids are discussed below.* The theoretical models on which the equations are based are described briefly; more complete discussions can be found in the various sources cited. Our purpose here is to identify and emphasize the assumptions and approximations which enter the theoretical models and which contribute to the uncertainties. Unfortunately, in most cases it would be very difficult to estimate the sizes of the associated uncertainties. Comparisons are made both among the complete equations of state and with the experimental compressibility data. Some results of analyses of sensitivity to the uncertainties in various parameters which enter the equations are given.

---

*The time constraint on the present report precluded discussion of the region $|<V/V_o$, a universal equation of state for solid materials developed by Gogolyev (1963), or pressure-density relations developed by Porzel (1958) and Knopoff (1965).

An inadequacy common to all of the equations discussed is their failure to describe phase changes which may occur on decompression following sufficiently strong shocks, and the polymorphic transition indicated by the shock compressibility data for NaCl in the vicinity of P = 250 to 350 kilobars or 1.7 Megabars.*

A. FREE VOLUME THEORY: EQUATION OF STATE OF AL'TSHULER ET AL.(1965)

Of the four equations of state discussed in this chapter, an equation proposed by Al'tshuler et al. (1963) based on a classical statistical mechanical model, the "free volume theory" (FVT) originally developed by Lennard-Jones and Devonshire (1937) as a model for dense gases and liquids, approaches most closely the ideal model discussed at the beginning of this section. In the FVT model, a molecule--or ion--"wanders" in the "free volume" bounded by other molecules. The motion of the wanderer is determined by the potential field of all other molecules--considered in first approximation to be at rest at the centers of their respective "cells"--and the constraints represented by the cell "boundaries."

Al'tshuler et al. represent the interaction energy of ions E_c (v) at T = 0 in the form of the sum of the Madelung attraction potential and the Born-Mayer repulsion potential:

$$E_c = -A\left\{x^{-1/3} - \frac{1}{q}\exp\left[q\left(1-x^{1/3}\right)\right]\right\} . \qquad (1)$$

Here, $x = \rho_K/\rho$, ρ_K = density at P = 0, T = 0; $A = N\alpha e^2/r_K\mu$, N = Avogadro's number, α = Madelung constant, r_K = distance of separation of ions of opposite charge at P = 0, T = 0; q = "parameter characterizing the degree of smearing of the filled electron shells." From Eq. 1,

$$P_c = -\frac{dE_c}{dv} = \frac{A\rho_K}{3}\left\{x^{-2/3}\exp\left[q\left(1-x^{1/3}\right)\right] - x^{-4/3}\right\} . \qquad (2)$$

*See Chapter II of this report and Fumi and Tosi (1962).

For $T > 0$, the cell model or FVT equation of state can be written in the Mie-Grüneisen form:*

$$P = P_c + \frac{\bar{\gamma}(v,T)}{v}\left[E - E_c(v)\right]$$

$$\text{with} \qquad E - E_c = \zeta \frac{6RT}{\mu} D(T/\theta) \,. \tag{4}$$

In these expressions

$P_c(v)$ = pressure at $0°K = -\frac{dE_c}{dv}$

$E_c(v)$ = energy at $0°K$

$\bar{\gamma}(v,T)$ = Grüneisen "constant," defined by Eq. 3

μ = molecular weight

$D(x) = 3x^3 \int_0^{1/x} \frac{y^3\, dy}{e^y - 1}$ = Debye function tabulated in Abramowitz and Stegun, 1964)

---

*That is, the cell model expressions for P and E are used to determine

$$\bar{\gamma} = \frac{P - P_c}{E - E_c} V \quad \text{and} \quad \zeta = \frac{E - E_c}{(E - E_c)_{\text{Debye}}} \,.$$

The quantity $(E - E_c)_{\text{Debye}}$ is given by Eq. 4 with $\zeta = 1$. Values of $\bar{\gamma}$ and ζ have been computed and tabulated in Al'tshuler et al. (1963) as explicit functions of dimensionless temperature and inter-ionic spacing (Table 1). Note temperature dependence of $\bar{\gamma}$. As $T \to 0$,

$$\bar{\gamma} \to \gamma_o = -\frac{v}{2} \frac{\frac{d^2}{dv^2}\left(P_c\, v^{4/3}\right)}{\frac{d}{dv}\left(P_c\, v^{4/3}\right)} = \frac{1}{6} \frac{q^2 x^{2/3} - 2qx^{1/3} - 2}{qx^{1/3} - 2}$$

where $x = \rho_K/\rho$. In the usual Mie-Grüneisen equation, γ is assumed independent of temperature.

θ = Debye temperature = 281°K for NaCl (Born and Huang, 1954)

ζ = "correction for anharmonicity" ($\zeta \to 1$ at low temperatures)

Table 1. CALCULATED VALUES OF THE COEFFICIENTS ζ and $\bar{\gamma}$ as FUNCTIONS OF THE NONDIMENSIONAL SPECIFIC VOLUME (η) AND TEMPERATURE (τ)

	η		$\bar{\gamma}$				ζ			
τ	7.0	8.0	9.0	10.0	12.0	7.0	8.0	9.0	10.0	12.0
0	1.100	1.278	1.453	1.626	1.969	1	1	1	1	1
$1.5 \cdot 10^{-5}$	1.092	1.257	1.399	1.494	1.517	0.993	0.987	0.967	0.931	0.818
$3.0 \cdot 10^{-5}$	1.086	1.239	1.357	1.398	1.385	0.989	0.975	0.945	0.898	0.782
$6.0 \cdot 10^{-5}$	1.074	1.211	1.299	1.332	1.243	0.983	0.957	0.915	0.859	0.727
$9.0 \cdot 10^{-5}$	1.061	1.186	1.257	1.271	1.146	0.974	0.943	0.895	0.833	0.684
$1.5 \cdot 10^{-4}$	1.046	1.150	1.195	1.184	1.026	0.951	0.922	0.856	0.785	0.630
$2.4 \cdot 10^{-4}$	1.030	1.103	1.127	1.097	0.927	0.944	0.895	0.817	0.726	0.589
$4.2 \cdot 10^{-4}$	1.018	1.036	1.031	1.978	0.834	0.877	0.836	0.738	0.653	0.554

$\eta = q\,(V/V_{oK})^{\frac{1}{3}}$. For NaCl, $\tau = T\,(°K)/(0.5623 \times 10^8)$.

Al'tshuler's equation of state involves two empirically determined parameters:

q = parameter occurring in Born-Mayer repulsion potential, and

V_{oK} = specific volume of the cold (T = 0) crystal;

q and V_{oK} are related* through the compressibility K:

$$V_o - V_{oK} \approx - K V_o P_c (V_o, V_{oK}, q) , \qquad (5)$$

where $P_c = -dE_c/dV$ = pressure at T = 0 and V_o = normal specific volume.

*The relationship is obtained by elimination of P_H between the Hugoniot relation $P_H(V_o, V)$ derived from Al'tshuler's equation of state and

$$P_H(V_{oK}) \approx \frac{1}{K} \frac{V_o}{V_{oK}} - 1 \qquad (K = \text{compressibility})$$

A critical discussion of the FVT is available in Hirschfelder et al. (1954), where it is pointed out that the model has two general defects: Firstly, there is no correlation between motions of molecules in neighboring cells. (However, the FVT should be a better approximation than the Einstein model for a solid, in this respect.) Secondly, the FVT model allows no free interchange of molecules between cells. This restriction introduces an error which is approximately corrected by the addition of "communal entropy:" $(\Delta S)_{c.e.} = R$. Although it is likely that the communal entropy should be added gradually as the material changes from more to less dense (or from compressed solid to dense gas, in the case of alkali halides), FVT as employed by Al'tshuler uses the low density limiting case $(\Delta S)_{c.e.} = R$, which would be expected to introduce an error since the volume derivative of the communal entropy parameter contributes to the pressure.

Other approximations inherent in FVT include the expression of the probability density in configuration space as a product of functions of coordinates of one molecule only, the assumption--for purposes of evaluating the configuration integral--that the molecules are located at the centers of the cells ($s(\vec{r}) = \delta(\vec{r})$), neglect of effects of other than nearest neighbors, and the use of a sphericalized free volume. There is some uncertainty about inclusion of a multiplying factor $\frac{1}{2}$ in the power of the integrand of the configuration integral. (See discussion in Al'tshuler et al., 1963.) Approximations in the expression assumed by Al'tshuler for the energy of the cold crystal are discussed in Sec. C, Decker's equation.

Al'tshuler's equation ignores contributions of electronic excitations, which are unimportant below about 1 ev temperature. (See discussion of Kormer's equation, below.)

The values of the parameters g and V_{oK} which best represent shock compressibility data in the pressure range of 20 to 1000 kilobars (Al'tshuler et al., 1961, 1963)* were determined for the various

*See also Chapter II of this report, "Uncertainties in Dynamic and Static Compressibility Measurements."

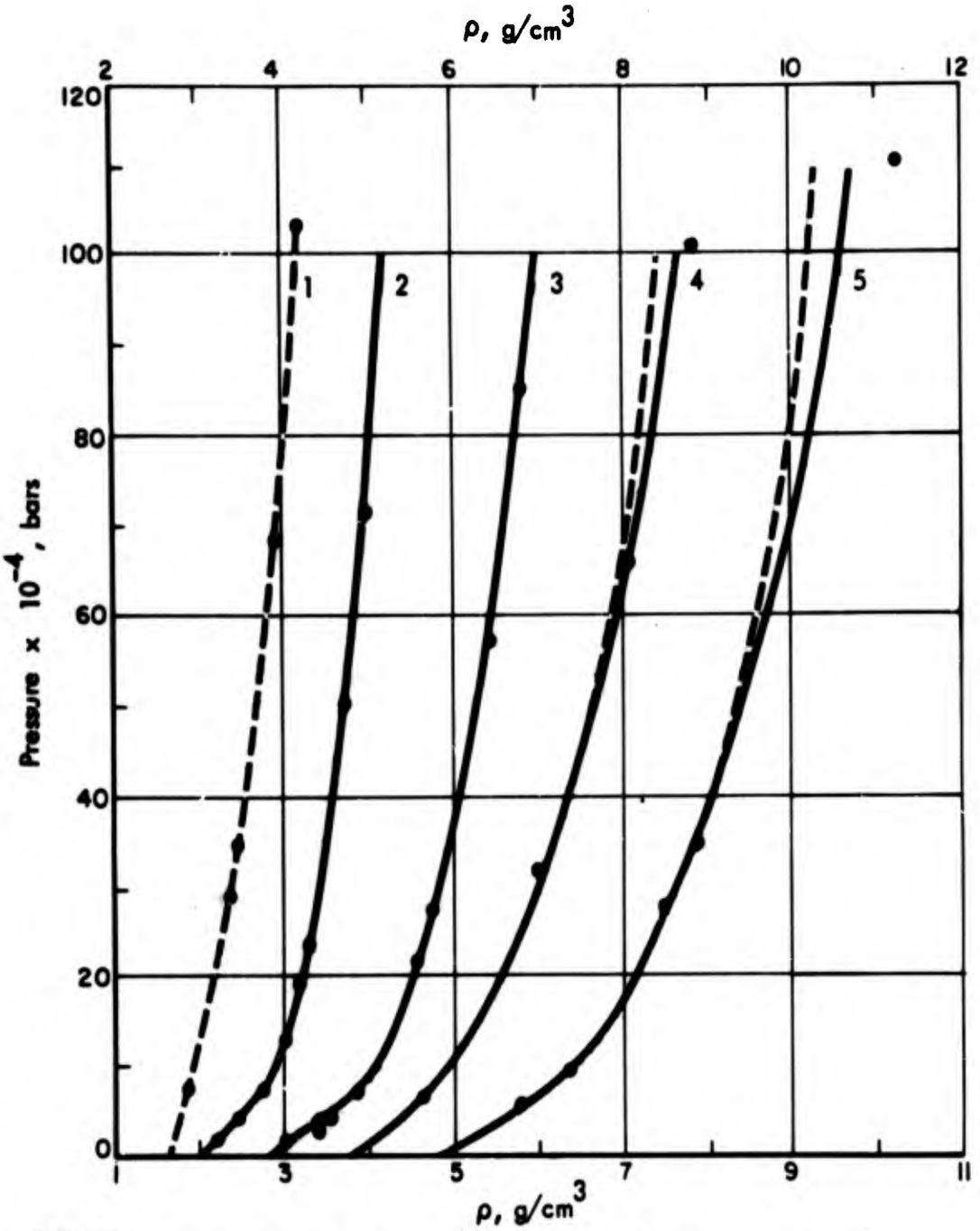

FIGURE 1 Hugoniot Curves for LiF (1), KCl (2), KBr (3), NaI (4), CsI (5) Calculated from Equation of State of Al'tshuler et al. (1963), Continuous Curves, and Compared with Experimental Data Points Reported in Same Reference. Figure from (Al'tshuler 1963).

The dashed curves represent the harmonic approximation, i.e., calculated using the $T \rightarrow 0$ FVT expression for $\gamma(V)$.

alkali halides (Fig. 1 and Table 2). For comparison, values of q determined in Born (1954) on the basis of the Debye model, the Mie-Grüneisen equation of state and the measured compressibility and, in some cases, values determined from the Bridgman isotherms are given in Table 3, from Al'tshuler et al (1963).*

Table 2. VALUES OF PARAMETERS ρ_k AND q FOR AL'TSHULER EQUATION DETERMINED FROM RESULTS OF SHOCK COMPRESSION EXPERIMENTS (Al'tshuler et al., 1961, 1963)

Compound	ρ_k, g/cm^3	q	$\frac{\rho_k A}{3} \cdot 10^{-10}$, bar	$\frac{A\mu^q}{2qN_a k} \cdot 10^{-8}$	$\beta_o \cdot 10^{12}$, bar^{-1}	γ_o (q)*
LiF	2.700	7.60	42.154	-	1.35	1.78
NaCl	2.210	9.20	10.939	0.5623	4.16	1.50
KCl Phase I	2.041	10.22	7.074	-	5.65	1.67
KCl Phase II	2.367	10.00	7.956	1.0000	-	-
NaI	3.781	9.70	6.381	0.7672	6.94	1.59
KBr Phase I	2.819	10.48	5.868	-	6.68	1.72
KBr Phase II	3.190	10.00	6.388	0.9467	-	-
CsI	4.668	10.90	3.755	1.8744	10.79	1.60

*Values of γ_o (q) given in the last column were calculated on the basis of free volume theory (except for LiF).

Al'tshuler's equation is compared with experimental Hugoniot data for normal and porous NaCl in Fig. 2; the complete equation of state (shock Hugoniot and rarefaction adiabats) is shown in Fig. 3, where it is compared with Kormer's equation of state (below). Figures 4 and 5 demonstrate the sensitivity to the parameter q.**

---

* The entire table is reproduced to show the consistency of the data determined for the several alkali halides studied.

** Unless otherwise identified, equation of state calculations reported in this chapter were made by the author.

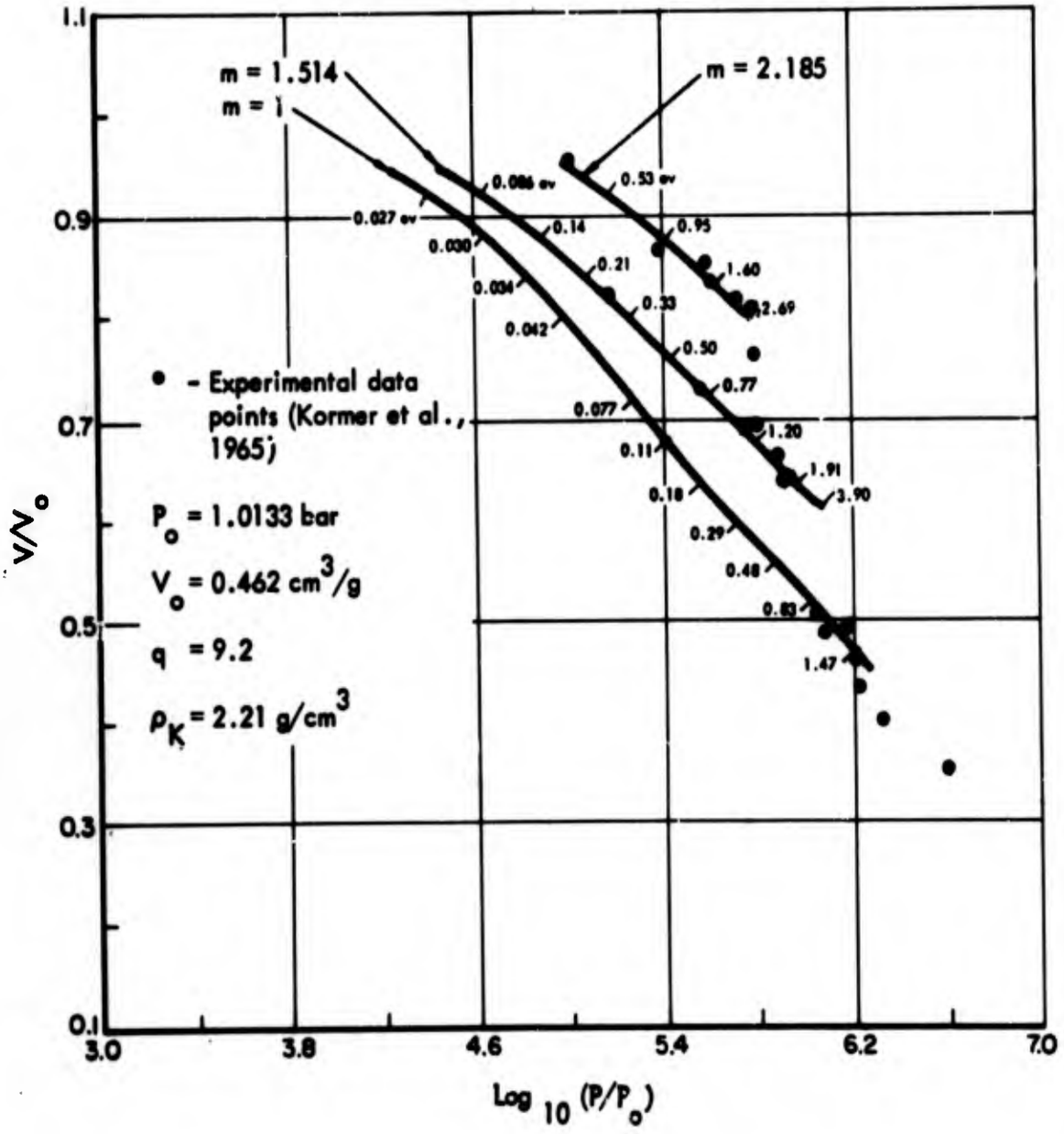

FIGURE 2 Hugoniot Curves for Pure Rock Salt of Various Porosities ($m = V_{oo}/V_o$) Calculated Using the Equation of State of Al'tshuler et al. (1963).

The porous Hugoniots are calculated by solving the equation of state P(V,E) simulanteously with the Hugoniot relation $E-E_o = (P+P_o)(mV_o - V)/2$. In Kormer's equation, the effective mass was assumed to be given by $m^* = (m_o/2)\delta(\Gamma + 2/3)$. (See Kormer et al., 1965.)

R7-10-67-2

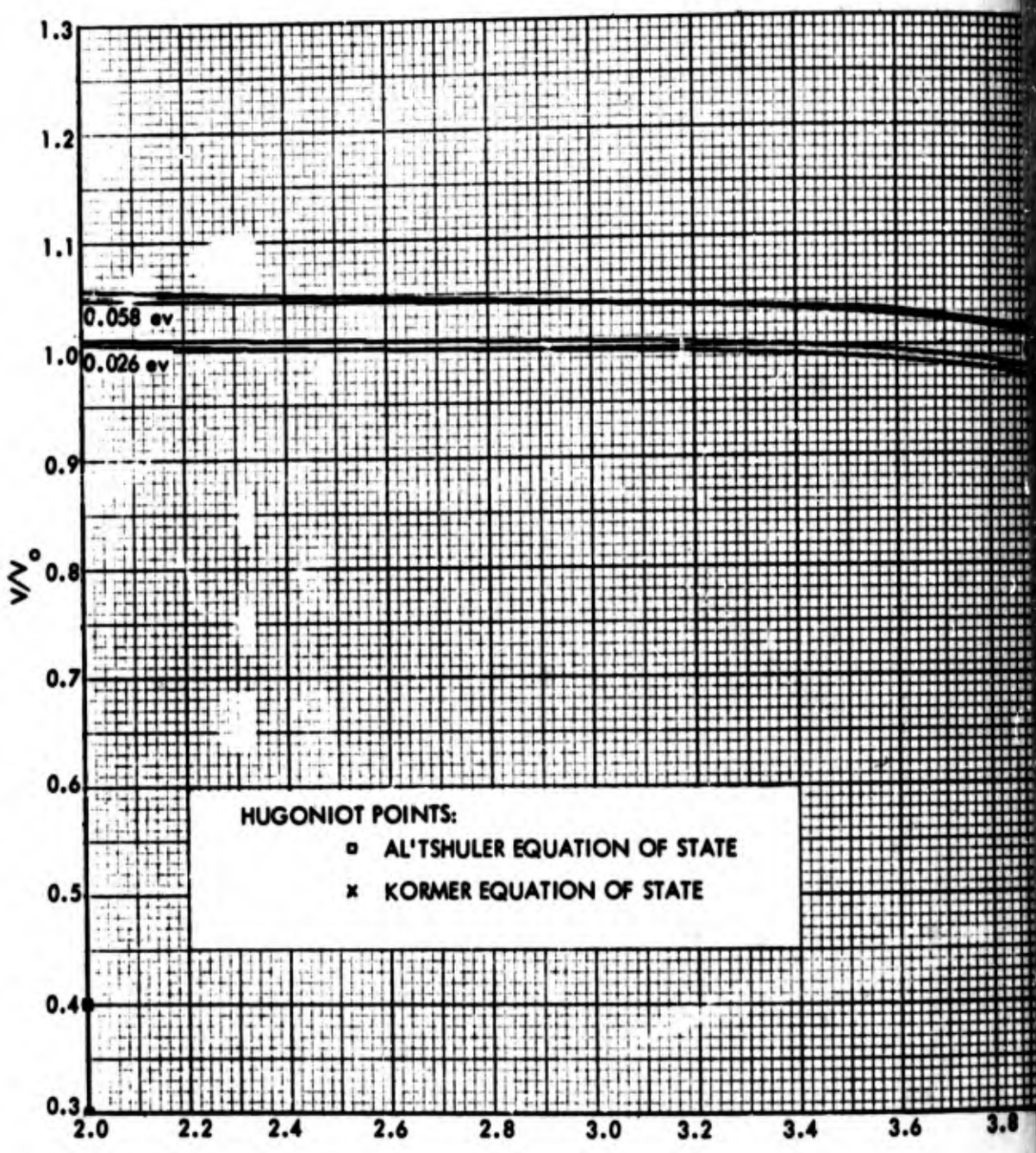

FIGURE 3 Complete Equations of State of Al'tshuler et al. (1963), and Kormer et al. (1965).

87-10-67-3

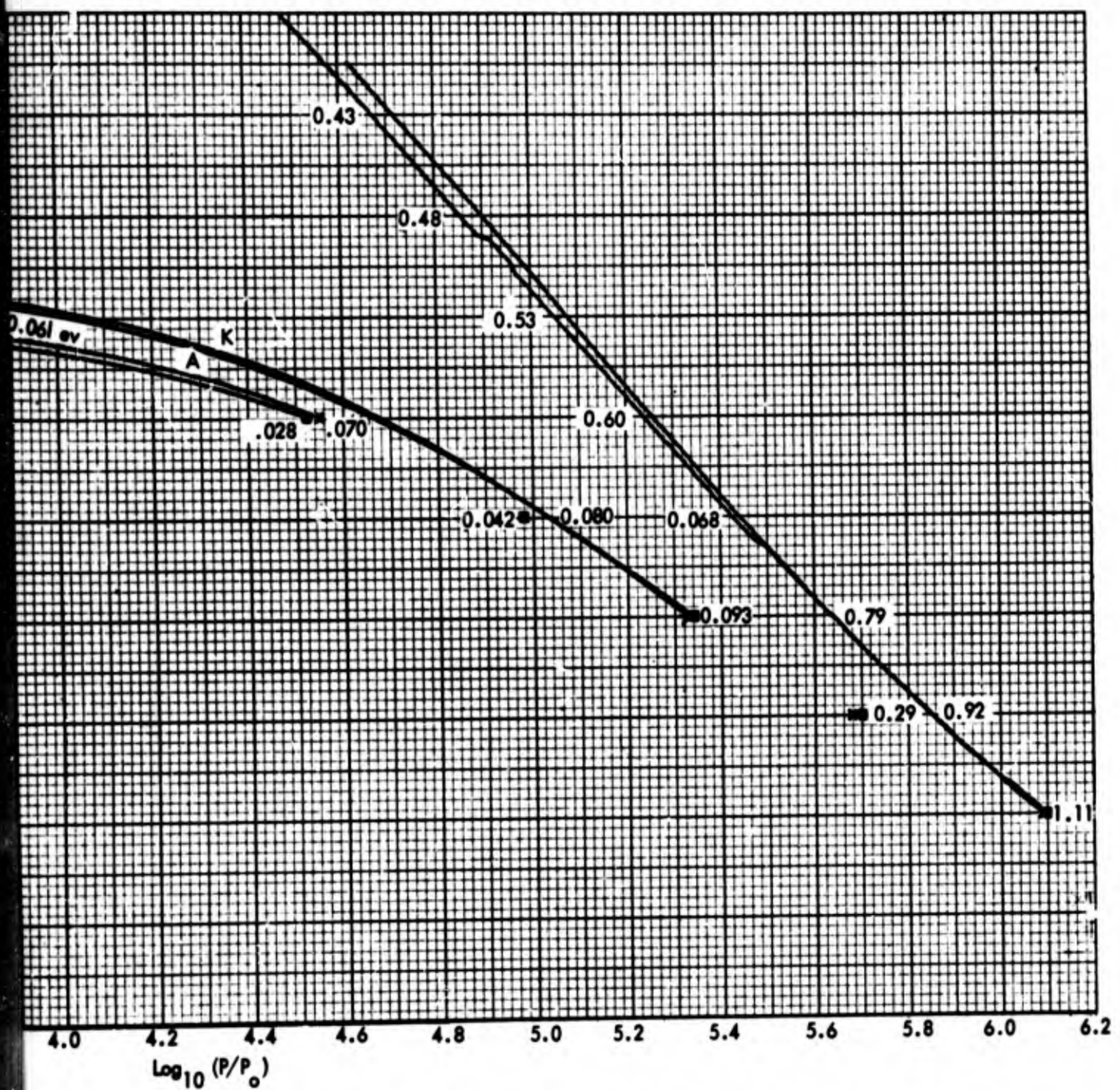

In addition to Hugoniot points, 3 decompression adiabats are shown for each equation. Temperatures shown are calculated from Al'tshuler's equation. (Compare Figs. 15 and 18.) Second-order bivariate interpolation (6 points) was used in the tables given in Al'tshuler (1963) for the quantities $\bar{\gamma}$, ξ. (See Appendix C.) The adiabats for the Al'tshuler equation were calculated by numerical integration of

$$\left.\frac{\partial T}{\partial V}\right)_S = \left[\left.\frac{\partial P}{\partial V}\right)_S - \left.\frac{\partial P}{\partial V}\right)_T\right] \Big/ \left.\frac{\partial P}{\partial T}\right)_V$$

where

$$\left.\frac{\partial P}{\partial V}\right)_S = \left[-P - \left.\frac{\partial E}{\partial V}\right)_P\right] \Big/ \left.\frac{\partial E}{\partial P}\right)_V$$

For the Kormer equation, adiabats were obtained by solving the equation $S(T, V) = S_1 = \text{constant}$, by iteration.

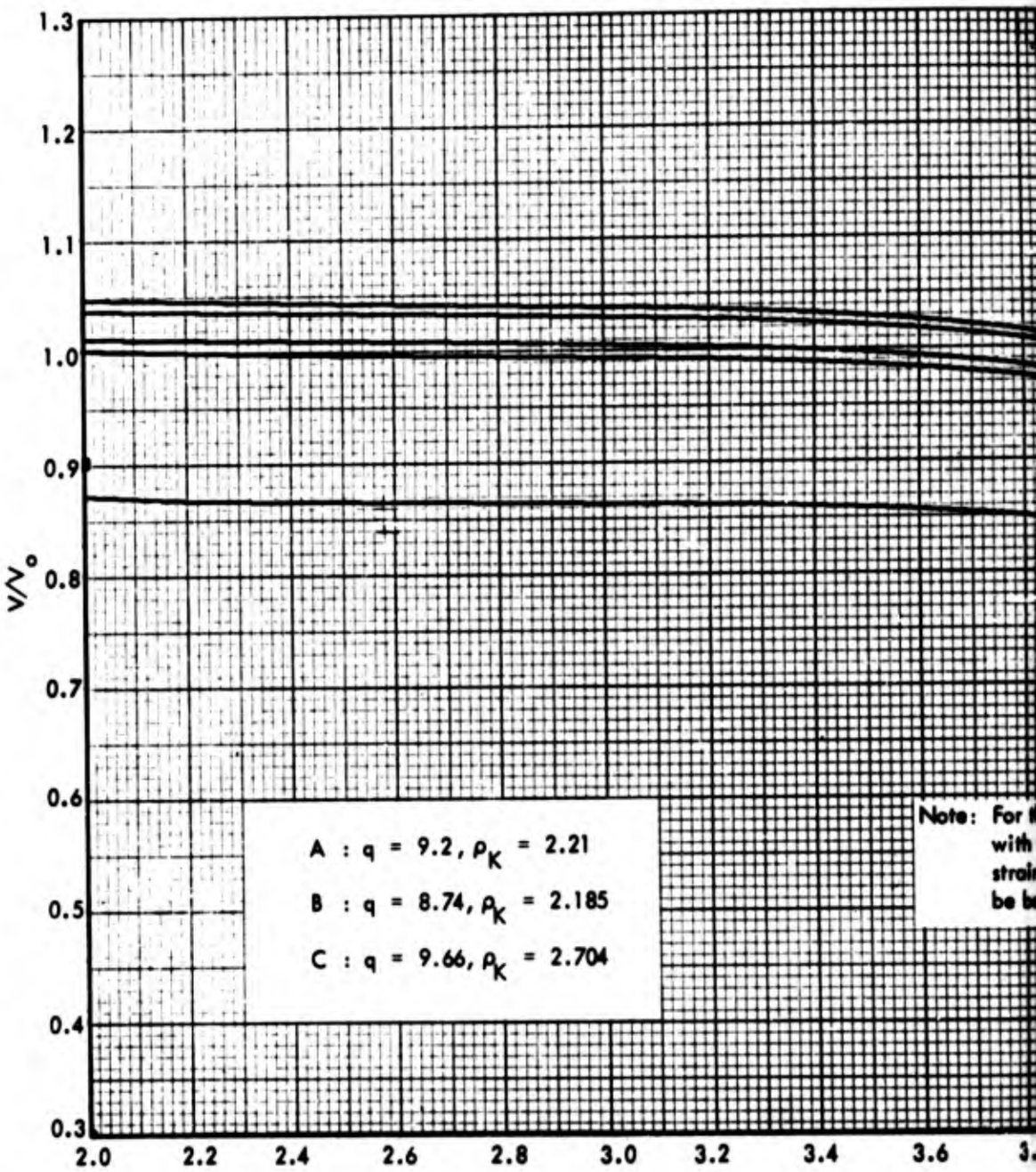

FIGURE 4 Hugoniot Points and Decompression Adiabats Demonstrating Sensitivity of Results of Al'tshu Equation of State to 5 Percent Changes in the Ionic Repulsion Parameter q.

(Also indicated are the corresponding values of ρ_K = density (g/cm^3) of the cold (T = 0) crystal, as determined by Eq. 1 with K = 4.16/Megabars)

R7-10-67-4

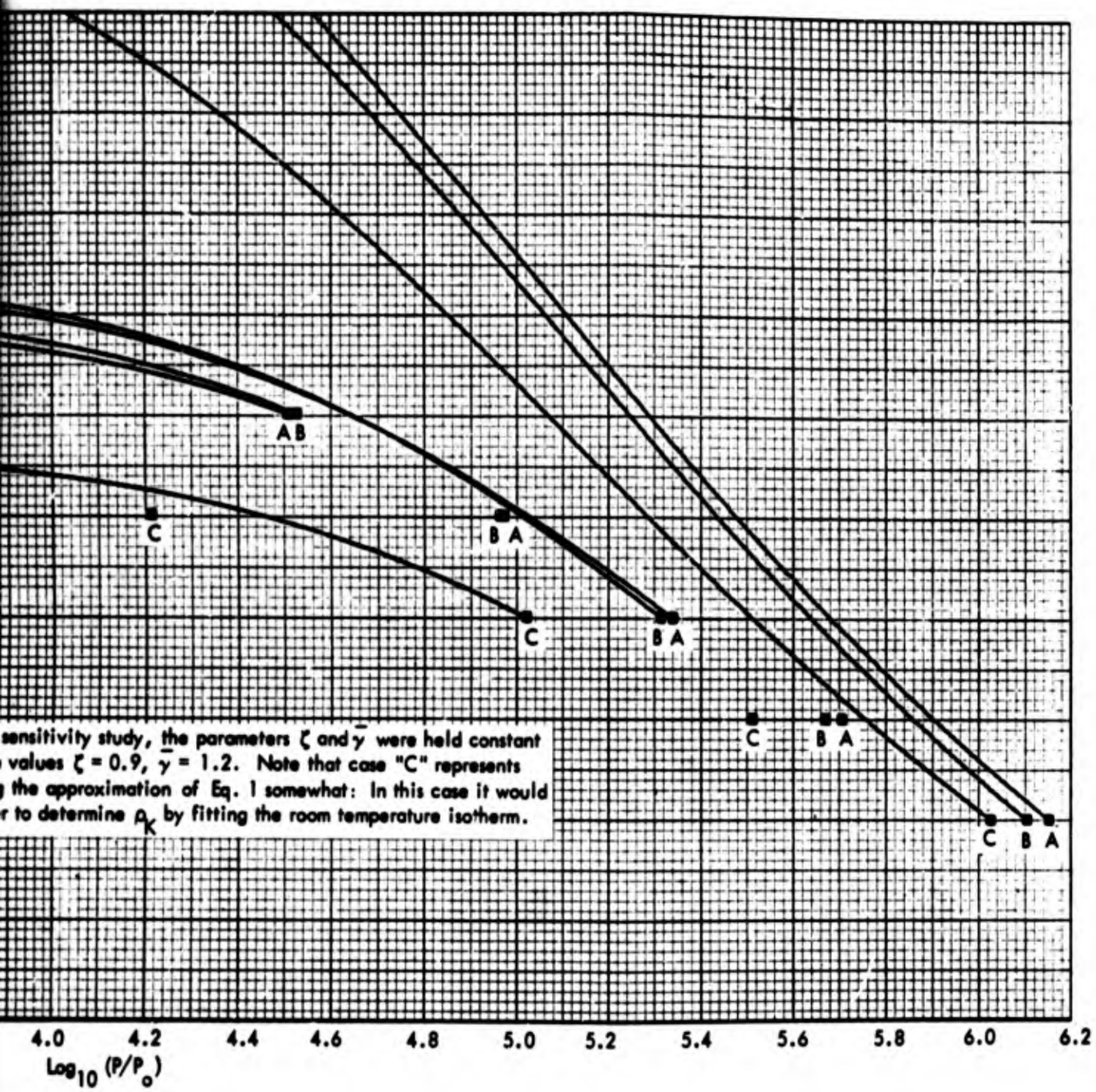

sensitivity study, the parameters ζ and $\bar{\gamma}$ were held constant
values $\zeta = 0.9$, $\bar{\gamma} = 1.2$. Note that case "C" represents
the approximation of Eq. 1 somewhat: In this case it would
to determine ρ_K by fitting the room temperature isotherm.

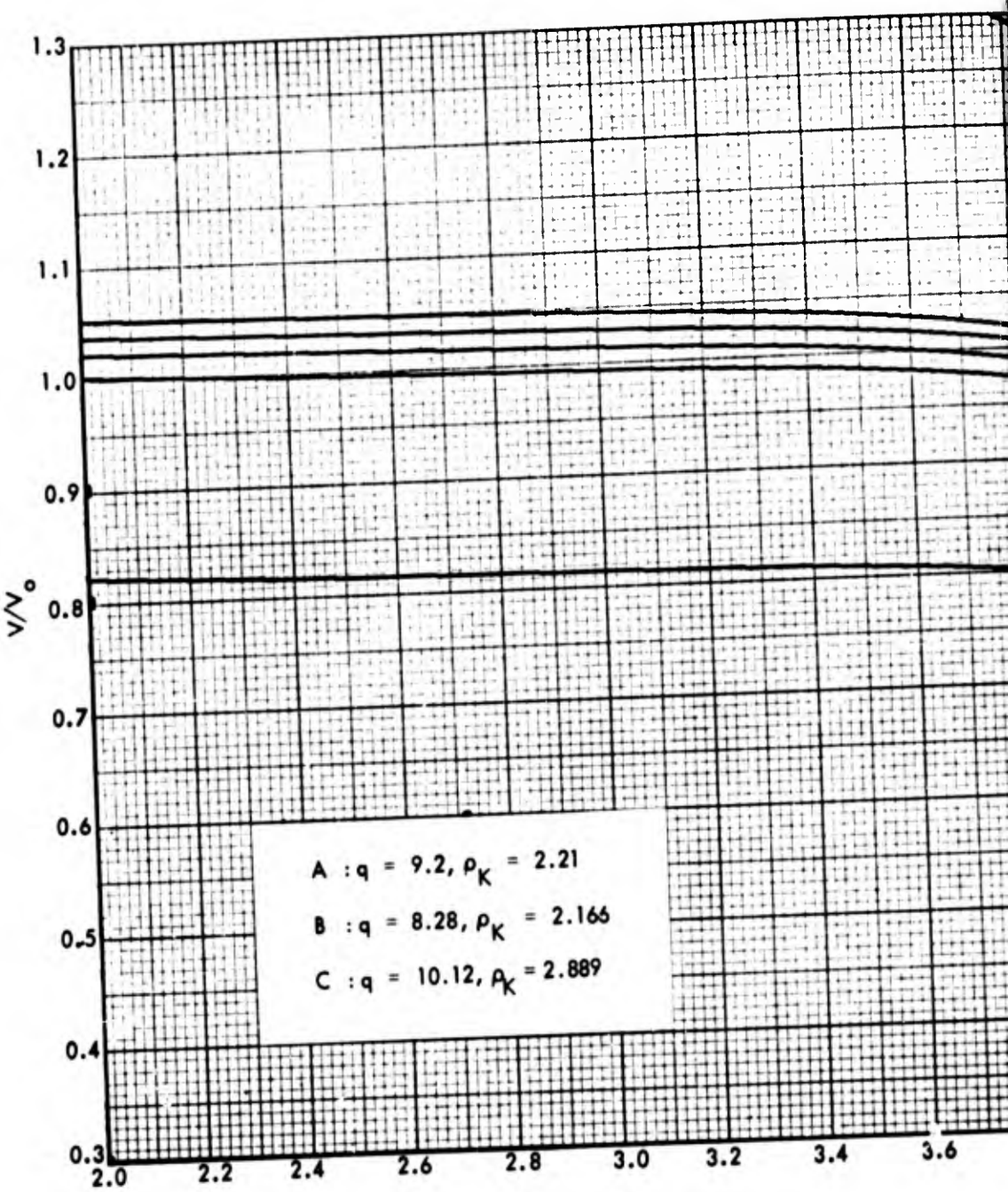

FIGURE 5 Hugoniot Points and Decompression Adiabats Demonstrating Sensitivity of Results Equation of State to 10 Percent Changes in the Ionic Repulsion Parameter q. (Se

R7-10-67-6

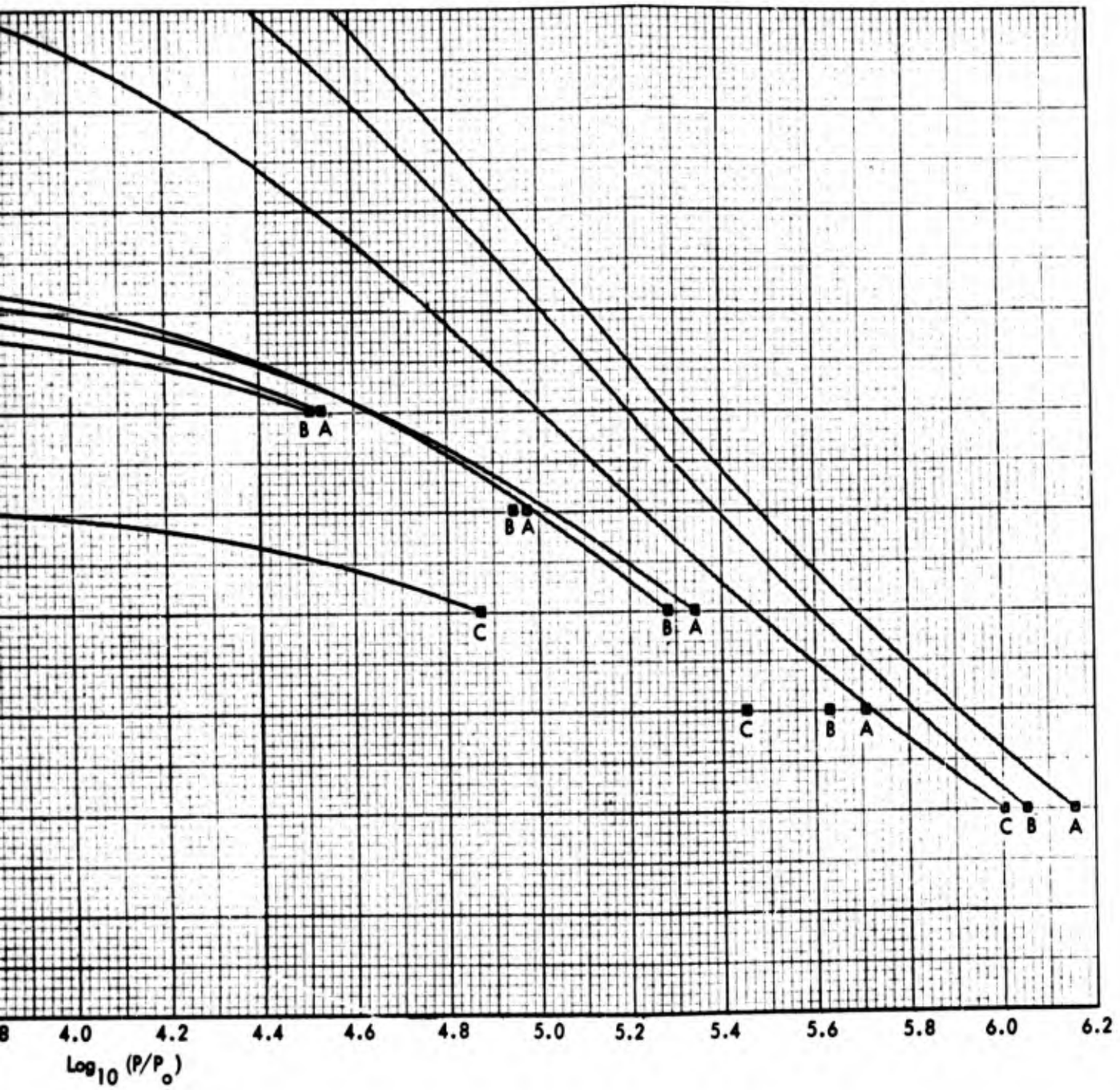

l'tshuler
ure 4.)

Empirically determined values of the Grüneisen constant for normal conditions

$$\gamma_o = \alpha_V / \beta_o \, c_V \rho_o \, ,$$

where α_V = volume thermal expansion coefficient, β_o = compressibility, and c_V = specific heat, are given in the last column of Table 3. For comparison, values of $\gamma_o(q)$ as determined theoretically on the basis of FVT by Al'tshuler et al. (1963), are also shown.

Table 3. VALUES OF COMPRESSIBILITY,* PARAMETER q, AND GRÜNEISEN CONSTANT FOR HALIDES

Compound	$\beta_K \cdot 10^{12}$, bar^{-1}	q**	γ_o (q)***	$\gamma_{o\,exper}$†
LiF	1.44	6.92	1.09	1.72
		7.00	1.11	
LiCl	3.20	7.93	1.28	1.54
NaF	1.99	8.33	1.34	1.57
NaCl	3.98	8.88	1.44	1.43--1.56
		9.4	1.53	
NaBr	4.70	9.32	1.52	1.55--1.48
		9.40	1.53	
NaI	6.45	9.29	1.52	1.59
		9.70	1.59	
KF	3.10	9.13	1.49	1.46
KCl	5.26	10.09	1.65	1.34
KBr	6.17	10.28	1.69	1.43--1.58
KI	7.75	10.64	1.75	1.58
RbCl	6.21	10.31	1.69	1.25
RbBr	7.35	10.27	1.68	1.27
RbI	8.70	10.99	1.81	1.50
CsF	3.94	13.63	2.26	1.49
CsCl	5.26	12.10	2.00	1.87--2.01
		12.40	2.06	
CsBr	6.17	12.15	2.00	1.93--1.98
		11.50	1.90	
CsI	7.43	12.64	2.11	2.01--1.88
		11.80	1.94	

*From Born and Huang, 1954, p. 54.
**The values of q were determined by making use of the compressibilities β_K. The second value of q listed for some cases was determined from Bridgman isotherms.
***The corresponding values of $\gamma_o(q)$ calculated on the basis of FVT are given in column 4.
†Experimental values of γ_o in column 5 are from Born and Huang (1954) and handbook data (A'tshuler et al., 1963).

The disagreements between experimental and theoretical values of γ_o for potassium and rubidium salts and CsF are interpreted by Al'tshuler et al. (1963) as being due to instability of these lattices, which are transformed into other modifications by a small increase of pressure. Differences between calculated and experimental values for the highest compressions in NaI and CsI (Fig. 1) were interpreted as being due to inadequate representation of the interaction potential or the effect of electron excitation. The lack of agreement of the values of γ_o determined for LiCl and NaF and of the static and dynamic determinations of q for LiF* were not discussed. For all except the smallest molecular weight halides--LiF, LiCl, and NaF--it was found that the transition from FVT to Slater's or Dugdale-MacDonald's formulas** for γ_o increases the disagreement between calculated and experimental values. The representation of the results of the dynamic measurements by FVT and the agreement of the static and dynamic determinations of the parameter q are remarkable for NaCl, KCl, NaI, and KBr.

B. EQUATION OF STATE OF KORMER ET AL. (1965)

An equation of state developed by Kormer et al. (1965) gives results nearly identical with Al'tshuler's equation in the region of temperatures $\lesssim$ 1 ev. Above 1 ev, there is a small systematic deviation due to the inclusion by Kormer's equation of terms accounting for the contribution of electronic excitations.***

Kormer's equation of state is given by

$$F = E_c(\rho) + 6RT \log\left[\frac{\theta(\rho)}{T}\ (1 + z)^{\frac{1}{2}}\right]$$

$$- \frac{4kT}{\rho}\left(\frac{2\pi m^* kT}{h^2}\right)^{3/2} e^{-w/2kT}$$

---

* For LiF, the value of γ was found from Slater's expression (Slater, 1939) rather than FVT.

** See below.

*** The effect of electronic excitations is large for C_sB_r (Fig. 7) and CsI (Fig. 1).

with

$$\theta(\rho) = \text{const.}\ \rho^{1/3}\left(\frac{dP_c}{d\rho} - n\,\frac{2}{3}\,\frac{P_c}{\rho}\right)^{1/2}$$

$$z = \ell RT\left[\frac{dP_c}{d\rho} - n\,\frac{2}{3}\,\frac{P_c}{\rho}\right]^{-1} = \ell RT/c_c^{\,2}$$

In these expressions, F = total free energy, E_c = energy of "cold" (T = 0) crystal, R = gas constant per gram, ρ_K = density at T = 0° $m^*(\rho) = (m_e^* m_h^*)^{\frac{1}{2}}$ = geometric mean of effective electron and hole masses,† $w(\rho)$ = width of energy gap between filled band and conduction band, M = molecular weight, ℓ = empirical constant, n = 1 for Dugdale-MacDonald theory, C_c = velocity of compressional waves. The pressure and internal energy are given by

$$P = -\left(\frac{\partial F}{\partial V}\right)_T$$

$$E = F - T\left(\frac{\partial F}{\partial T}\right)_V .$$

The quantity z interpolates smoothly between the solid ($z \to 0$) and gas ($z \to \infty$) phases: For $z \ll 1$ the equation for E(P,V) reduces to the Mie-Grüneisen equation†† with the Dugdale-MacDonald (1953) γ, whereas, for $1 \ll z$, it assumes the form of the equation of state of a monatomic ideal gas, with an additional term proposed to represent the contribution of electrons thermally excited to the conduction band. (For an intrinsic semi-conductor the concentration of such electrons is

$$2\,(2\pi\, m^*\, kT/h^2)^{3/2}\, e^{-w/2kT}$$ (Kittel, 1966, p. 307)) .

---

†For example, Kittel (1966), p. 277ff.

††See discussion of Sec. C.

The parameters w and m^* were assumed to have a volume dependence given by

$$w = w_o \, \delta^{\Gamma}$$

$$m^* = m_o \, \delta^{2/3 + \Gamma} ,$$

with w_o = forbidden bandwidth under normal conditions,

	LiF	NaCl	KCl	KBr	CsBr
ρ_o, g/cm^3	2.65	2.165	1.992	2.752	4.45
6R, joules/g-deg	1.923	0.8535	0.6693	0.4194	0.2355
w_o, eV	11.5	7.7	7.5	6.6	6

m_o = free electron mass,* and Γ = empirical constant found from best description of the Hugoniot data at high temperatures.

	ℓ	Γ	ρ_K, g/cm^3	a_1, Mbar	a_2, Mbar	a_3, Mbar	a_4, Mbar	a_5, Mbar
LiF	12	0	2.694	-0.428	0.438	-1.69	1.68	0
NaCl	9	0	2.218	-0.071	0.052	-0.693	0.712	0
CsBr	12	-0.5	4.583	-0.26	1.921	-4.392	3.431	-0.7

Kormer's equation utilizes a 4 or 5 parameter polynomial fit to P_c (ρ/ρ_K), the cold (T = 0) compressibility curve; other parameters determined by matching the experimental Hugoniot data include ℓ and w_o, m_o, Γ. The constants in the fit for P_c were determined to best fit the Hugoniot points for nonporous samples and the values of volume compressibility, Grüneisen constant, and binding energy of the substance in its normal state.

*For NaCl, m_o was taken equal to one-half of the free electron mass, in order to best describe the high-temperature data.

According to Kormer (1965), the cold compression curve found in this way agreed with the curve of Al'tshuler (1963), described by the Born-Mayer potential for NaCl. The value of ℓ was found from the low temperature parts of the Hugoniot for porous samples. Kormer's equation is compared with Hugoniot data for normal and porous alkali halides in Figs. 6 to 9. Figure 18 shows the complete equation of state.*

C. MIE-GRÜNEISEN EQUATION OF STATE: DECKER'S EQUATION

An equation of state which has been widely used for solids, the so-called Mie-Grüneisen equation, is developed on the basis of the Debye model. It is usually written in the form

$$P + \frac{dW_L}{dV} = \gamma(V,T)\,\frac{W_{vibr}}{V}$$

where W_L represents the energy of the static solid in its electronic ground state (the "lattice energy") and W_{vibr} is the "vibrational energy."** The quantity

$$\gamma(V,T) = \frac{V}{T}\,\frac{[\partial(F_{vibr}/T)/\partial V]_T}{[\partial(F_{vibr}/T)/\partial T]_V} \qquad (6)$$

*Isentropic adiabats, rather than isotherms, were selected for making the comparisons among equations of state. The shocked material decompresses along an adiabat $P(V,S_1)$, where S_1 = constant = entropy of shocked material.

**In an alternative formulation,

$$P + \frac{dW_c}{dV} = \gamma_2(V,T)W_{th}\ , \qquad (6')$$

W_c is the nonthermal ("cohesive") energy of the solid at T = 0 and W_{th} represents the thermal energy. The difference between the two formulations corresponds to splitting the free energy in different ways:

$$F = \underbrace{U_{static} + \tfrac{1}{2}\sum_i h\nu_i + kT\sum_i \log\left(1 - e^{-h\nu_i/kT}\right)}$$

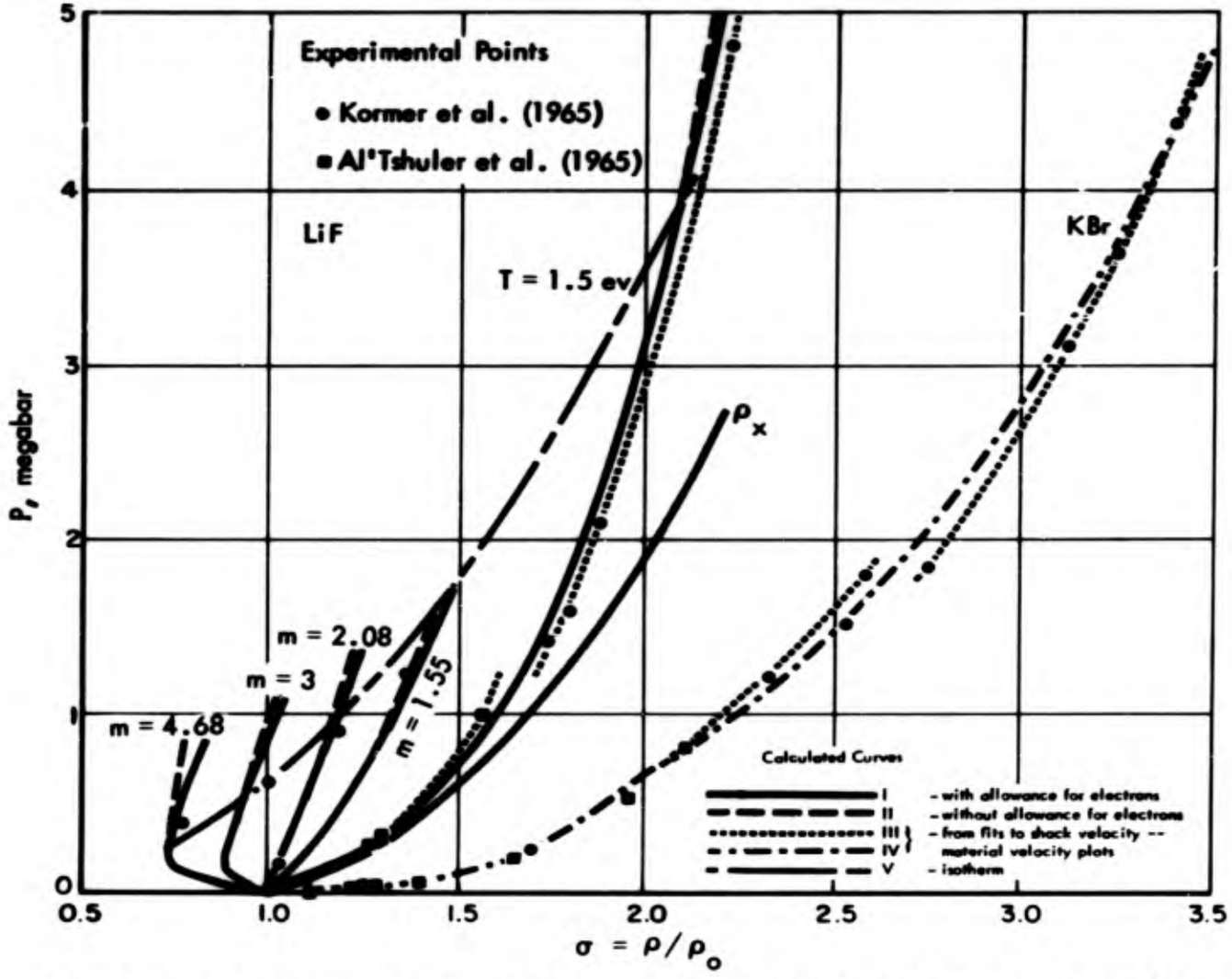

FIGURE 6 Shock Compression Data and Hugoniot Curves Calculated Using Equation of State of Kormer, et al. (1965), for LiF and KBr. Figure from (Kormer 1965).

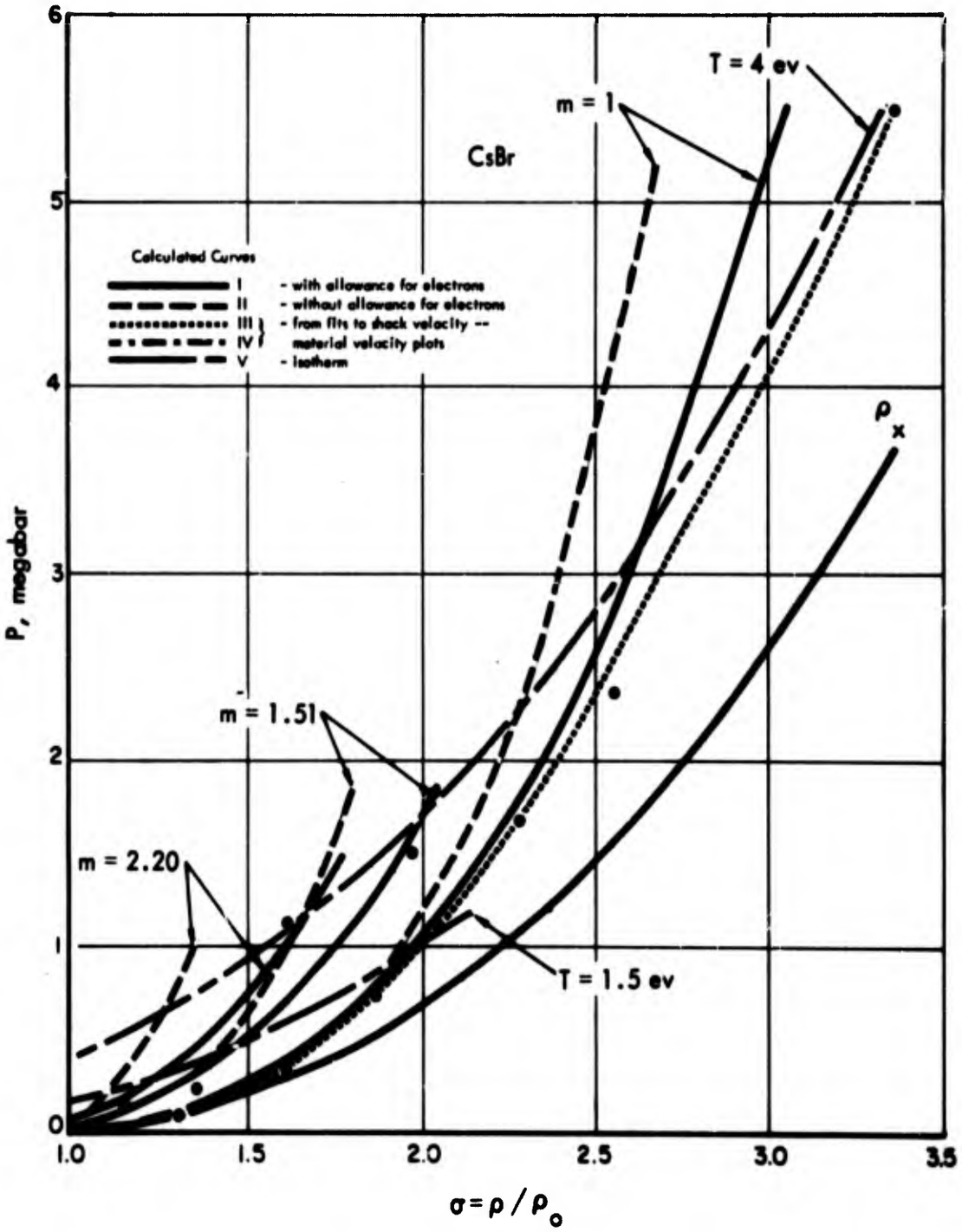

FIGURE 7 Shock Compression Data and Hugoniot Curves Calculated Using Equation of State of Kormer et al. (1965), for CsBr. (See Figure 6.) Figure From (Kormer 1965).

R7-10-67-7

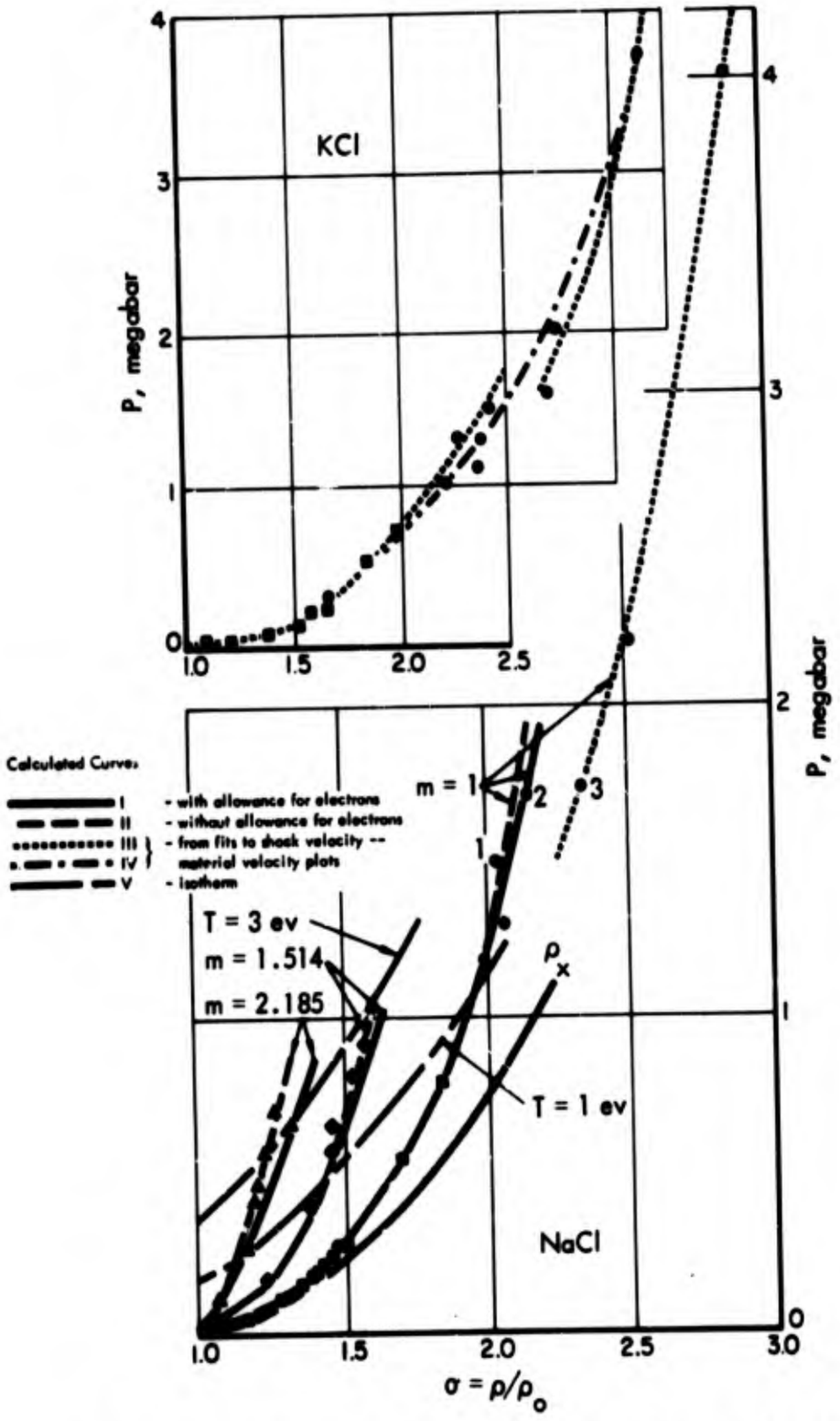

FIGURE 8 Shock Compression Data and Hugoniot Curves Calculated Using Equations of State of Kormer et al. (1965), for KCl and Normal and Porous NaCl. (See Figure 6.) Figure from (Kormer 1965).

R7-10-67-8

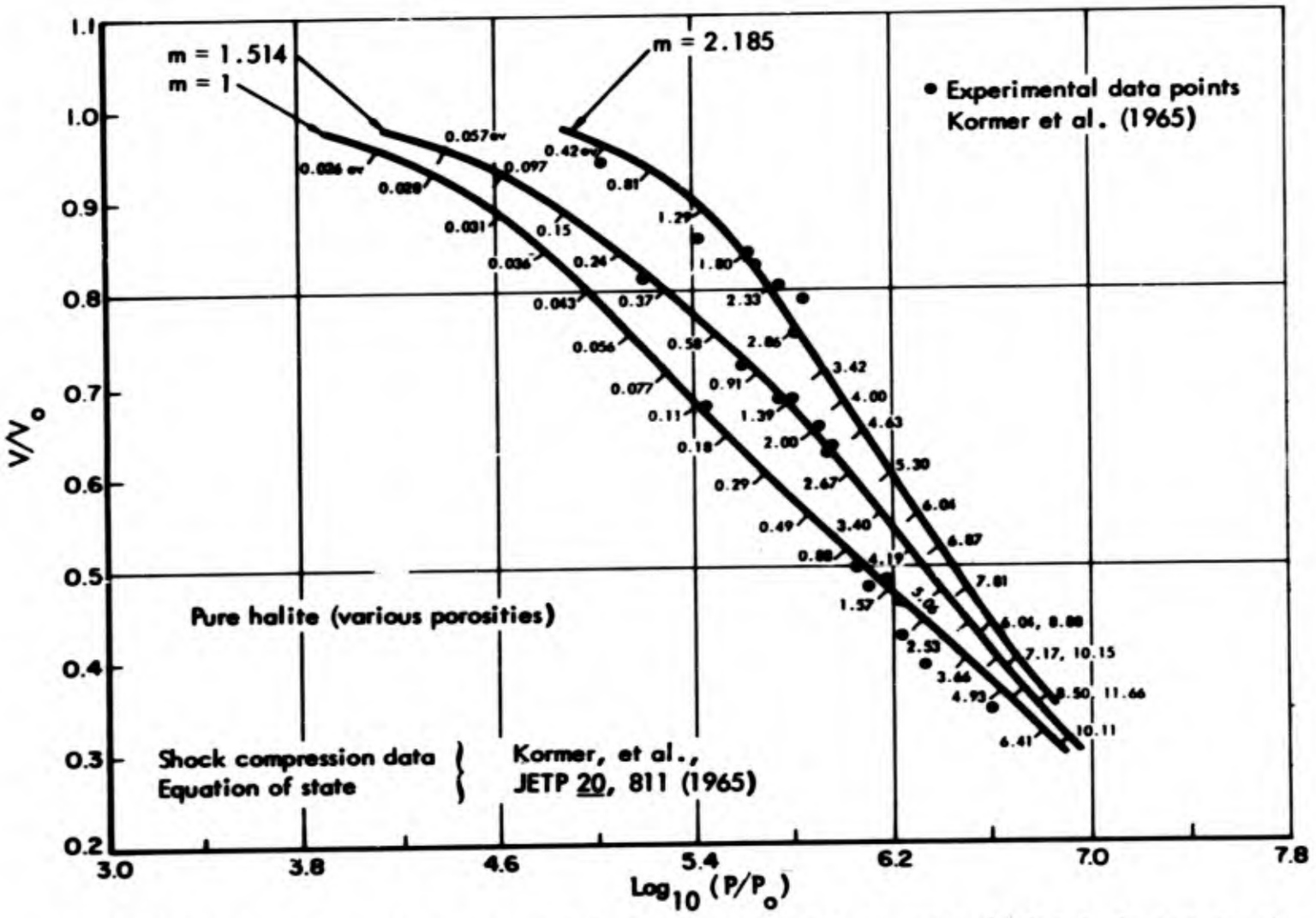

FIGURE 9 Hugoniot Curves for Pure Rock Salt of Various Porosities ($m = V_{oo}/V_o$) Calculated Using the Equation of State of Kormer et al. (1965). (See Figure 2.)

is given by the Debye model as the temperature-independent expression*

$$\gamma_D(V) = - \frac{d \log \theta_D}{d \log V} \quad .$$

The volume dependence of γ_D is not determined by the Debye model; additional assumptions must be introduced.** Inherent in the Mie-Grüneisen equation are the assumptions underlying the Debye model

---

*The Debye model approximation requires the quantities $\gamma_i = \frac{d \log \nu_i}{d \log V}$ to be equal to the same value γ_D. Fumi and Tosi (1962) have shown that a consequence of the quasi-harmonic approximation--in which the lattice contributions to the thermodynamic functions are those of an assembly of uncoupled harmonic oscillators with frequencies dependent only on volume--for a cubic nonmetal, pertinent to the region of moderate and high temperatures where the Thirring-Stern expansions of the thermodynamic functions converge, is that the "vibrational" formulation of the Mie-Grüneisen equation of state becomes valid only at temperatures somewhat above the Debye characteristic temperature $\theta(V)$ when the vibrational energy per particle approaches 3 kT. Also, the "thermal" formulation generally would become valid in the high temperature region only at the very high temperatures hardly ever attained by a solid, where the Hildebrand approximation for the thermal energy ($\partial E_{vibr}/\partial V = 0$) becomes valid.

**Slater's (1939) expression

$$\gamma = - \frac{V}{2} \frac{\partial^2 P/\partial V^2}{\partial P/\partial V} - \frac{2}{3}$$

was obtained for an isotropic elastic body with constant Poisson's ratio. (It was assumed that $\nu_i = C/\lambda_i$, where λ_i varies as $V^{1/3}$.) Dugdale and MacDonald (1953) obtained the form

$$\gamma = - \frac{V}{2} \frac{\partial^2 (PV^{2/3})/\partial V^2}{\partial (PV^{2/3})/\partial V} - \frac{1}{3} \quad .$$

An alternative derivation (Rice et al., 1958) of their result, applicable for materials of cubic symmetry, involved the simplifying assumption that all the interatomic force constants which govern the small amplitude thermal vibrations change in the same proportion with volume. The Slater and Dugdale-MacDonald expressions for γ are compared with static and dynamic compressibility data for metals in Rice et al., 1958. Compare expression for effective γ_o = low temperature limit of $V(P-P_c)/(E-E_c)$, derived on the basis of FVT by Vashchenko and Zubarev (1963).

(independent harmonic oscillators, Debye frequency distribution, equal γ_i's).

Decker's (1965) equation of state is written in the "vibrational" Mie-Grüneisen form. The internal energy of the static crystal

$$E_c = N_o \left(- \frac{Aq^2}{r} - \frac{C}{r^6} - \frac{D}{r^8} + 6b\, e^{-r/\rho} \right.$$

$$\left. + 6b_- \, e^{-\sqrt{2}r/\rho_-} + 6b_+ \, e^{-\sqrt{2}r/\rho_+} \right)$$

includes terms representing the Madelung energy, van der Waals forces (dipole-dipole and dipole-quadrupole interactions) and Born-Mayer repulsion forces due to overlap of ion core wave functions (6 nearest and 12 next-nearest neighbors). (In the above expression N_o = Avogadro number, A = Madelung constant, q = electronic charge, r = interionic spacing.) The vibrational energy is assumed to be given by the Debye model as

$$E - E_c = \frac{2.25}{M} R\theta + \frac{6RT}{M} D\,(\theta/T) \, .$$

An assumed linear dependence of Grüneisen parameter on interionic spacing,

$$\gamma = \gamma_o + \lambda\,(r-r_o)/r_o \, ,$$

gives a volume dependence of the Debye parameter as the integral of

$$-\frac{1}{3}\frac{d\,(\log\,\theta)}{d\,(\log\,r)} = \gamma_o + \lambda\,\frac{r-r_o}{r_o} \, .$$

Three parameters appearing in Decker's equation were determined by an iterative procedure involving comparison with experimental data for compressibility at 1 atm and room temperature* and linear thermal

*The value $(4.27 \pm 0.04) \times 10^{-12}$ cm^2/dyne was used. See note added in press at end of chapter.

expansion coefficient at 1 atm between 0 and 800°C. Other constants and the values include:

r_o = lattice parameter at 1 atm and 25°C

= 2.8205 Å (Siegbahn, 1931)

θ_o = Debye constant = 290 ± 12°K

(Yates and Panter, 1962)

γ_o = Grüneisen ratio = 1.59 ± 0.16

(Yates and Panter, 1962)

$\frac{\alpha_+ + \alpha_-}{2\alpha_+}$ = ratio of ionic polarizabilities = 6.331

(Tressman, et al., 1953)

$\frac{\alpha_+ + \alpha_-}{2\alpha_-} = 0.543$

r_+ = ionic radius = 0.95 ± 0.10 Å (Pauling, 1960)

r_- = 1.81 ± 0.18 Å

C = coefficient of dipole-dipole term =

$(1.80 \pm 0.36) \times 10^{-58}$ erg-cm^6 (Mayer, 1933)

D = coefficient of dipole-quadrupole term =

$(1.79 \pm 0.90) \times 10^{-74}$ erg-cm^8 (Mayer, 1933)

It was assumed that the parameters ρ, ρ_+, ρ_- occurring in the Born-Mayer repulsion terms for unlike and like ions are proportional to the sum of the ionic radii:

$$\frac{\rho_\pm}{\rho} = \frac{2r_\pm}{r_+ + r_-} .$$

The interaction parameters b, b_+, b_- were assumed to be inversely proportional to the sum of the polarizabilities of the respective ions:

$$\frac{b_{\pm}}{b} = \frac{\alpha_{+} + \alpha_{-}}{2\alpha_{\pm}} \quad .$$

According to Decker, it is possible to make somewhat arbitrary assumptions here because the like-ion repulsion terms represent a small part of the total repulsion, and the calculated values of ρ and $\underline{b}$ tend to compensate for different choices of b_{+}/b, b_{-}/b, ρ_{+}/ρ, and ρ_{-}/ρ.

In addition to the assumptions and approximations involved in the Mie-Grüneisen equation of state, as discussed above, Decker's equation involves the approximation of the representation of the interaction by means of the Born-Mayer form.

Decker (1965) made comparisons between calculated (Decker's equation) and experimentally determined values of coefficient of linear thermal expansion versus T at P = 0 (Fig. 10), isothermal compressibility versus T at P = 0 (Fig. 11), volume change versus P at 25°C (Fig. 12), and high-pressure shock measurements (Table 4, and Fig. 13).

Table 4. PRESSURES FOR SHOCK-COMPRESSED NaCl EQUATION OF STATE OF DECKER (1965) COMPARED WITH MEASUREMENTS OF AL'TSHULER ET AL. (1961)

V_o/V^*	T (°K)	P_H (meas.) (kbar)	P (calc.) (kbar)
1.22	380	78	74.8
1.32	550	134	133.8
1.43	920	208	208.7
1.53	1500	311	308.6

*V_o is the volume at atmospheric pressure and 25°C.

On the basis of these comparisons, Decker views his equation as accurate to within 2 percent for pressures in the range 0 to 150 kilobars

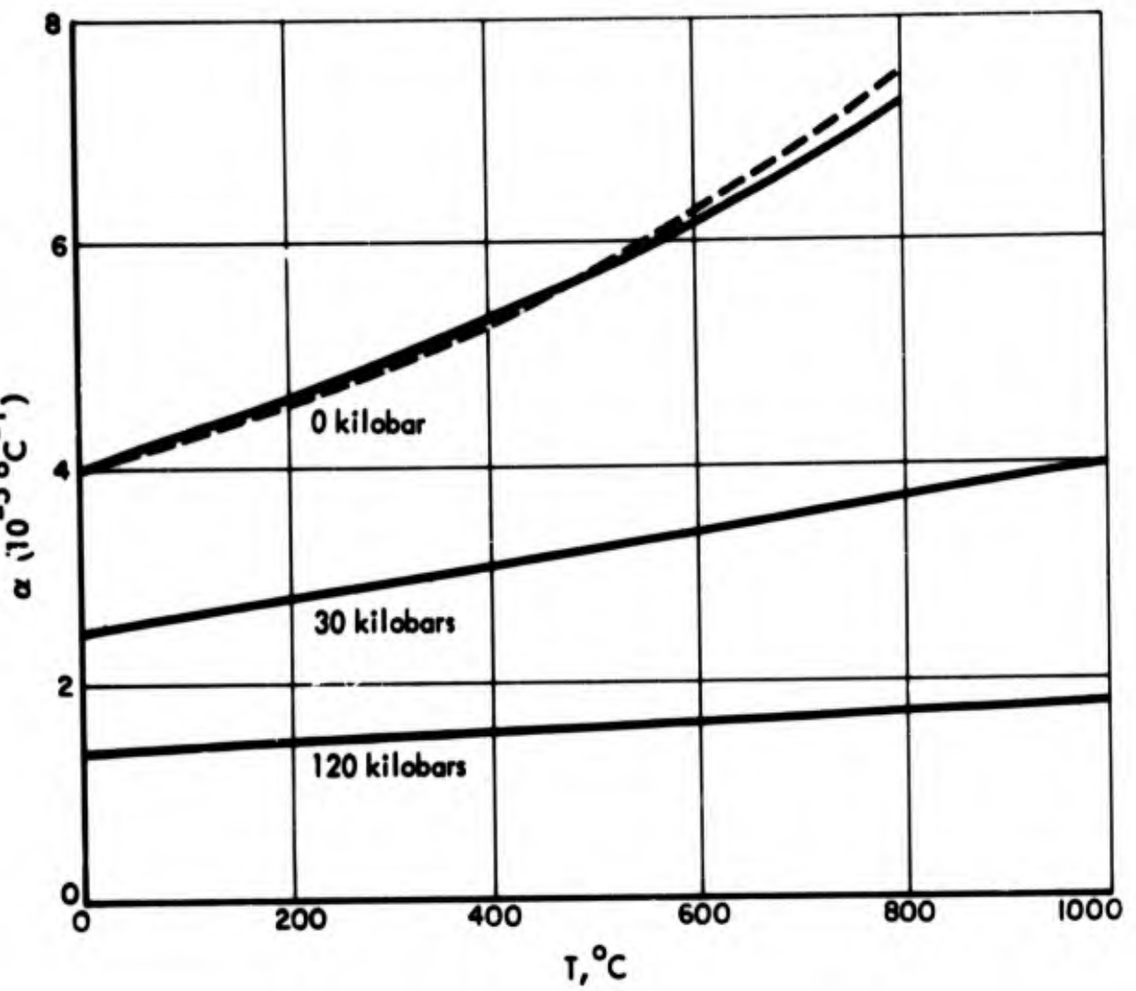

FIGURE 10 Coefficient of Linear Thermal Expansion of NaCl vs Temperature Along 3 Isobars, Computed Using Equation of State of Decker (1965).

(The dashed line is a fit to unpublished atmospheric pressure experimental data of Enck.) Figure from (Decker 1965).

R7-10-67-10

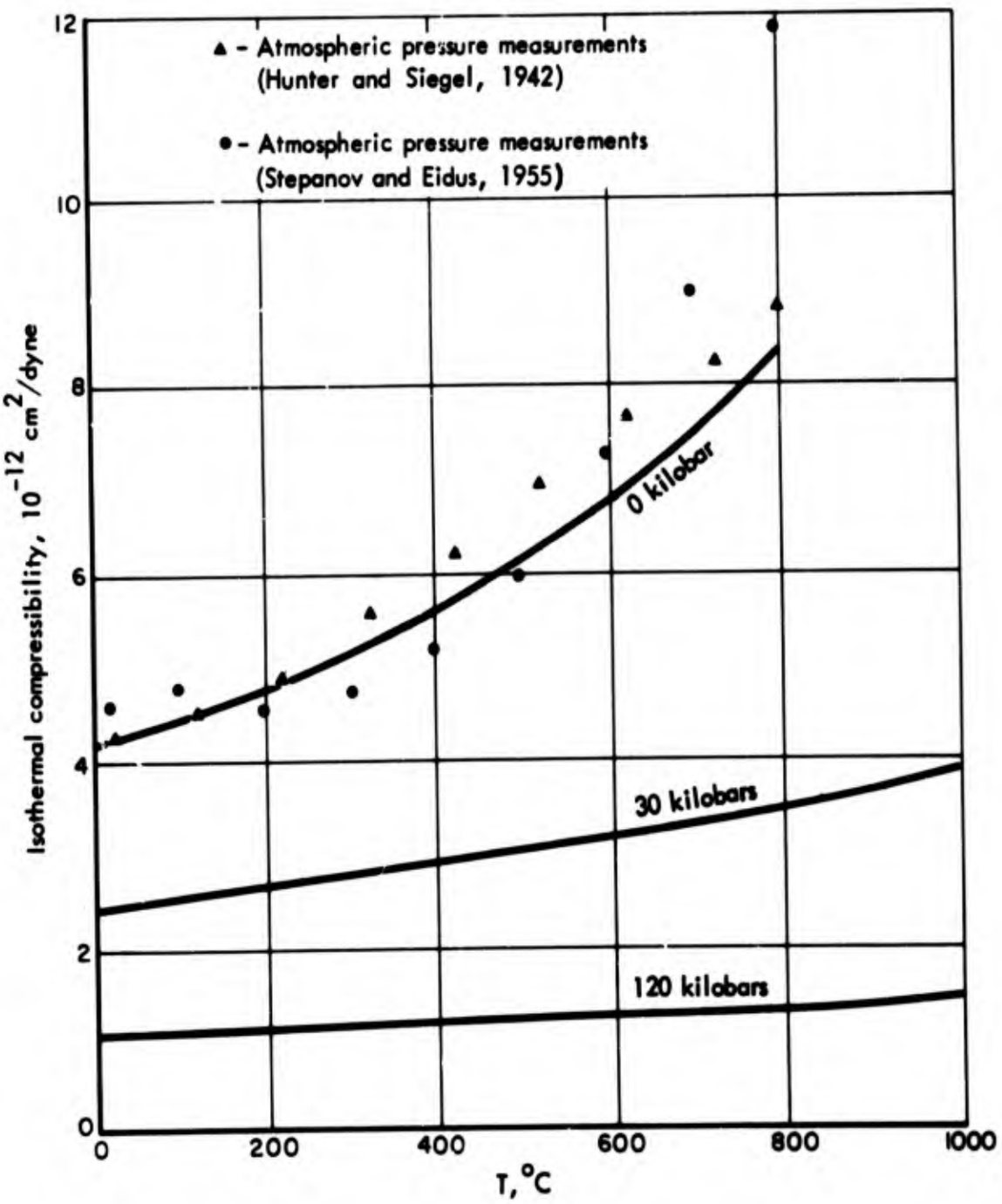

FIGURE 11 Isothermal Compressibility of NaCl vs Temperature Along 3 Isobars, Computed Using Equation of State of Decker (1965). Figure From (Decker 1965).

R7-10-67-11

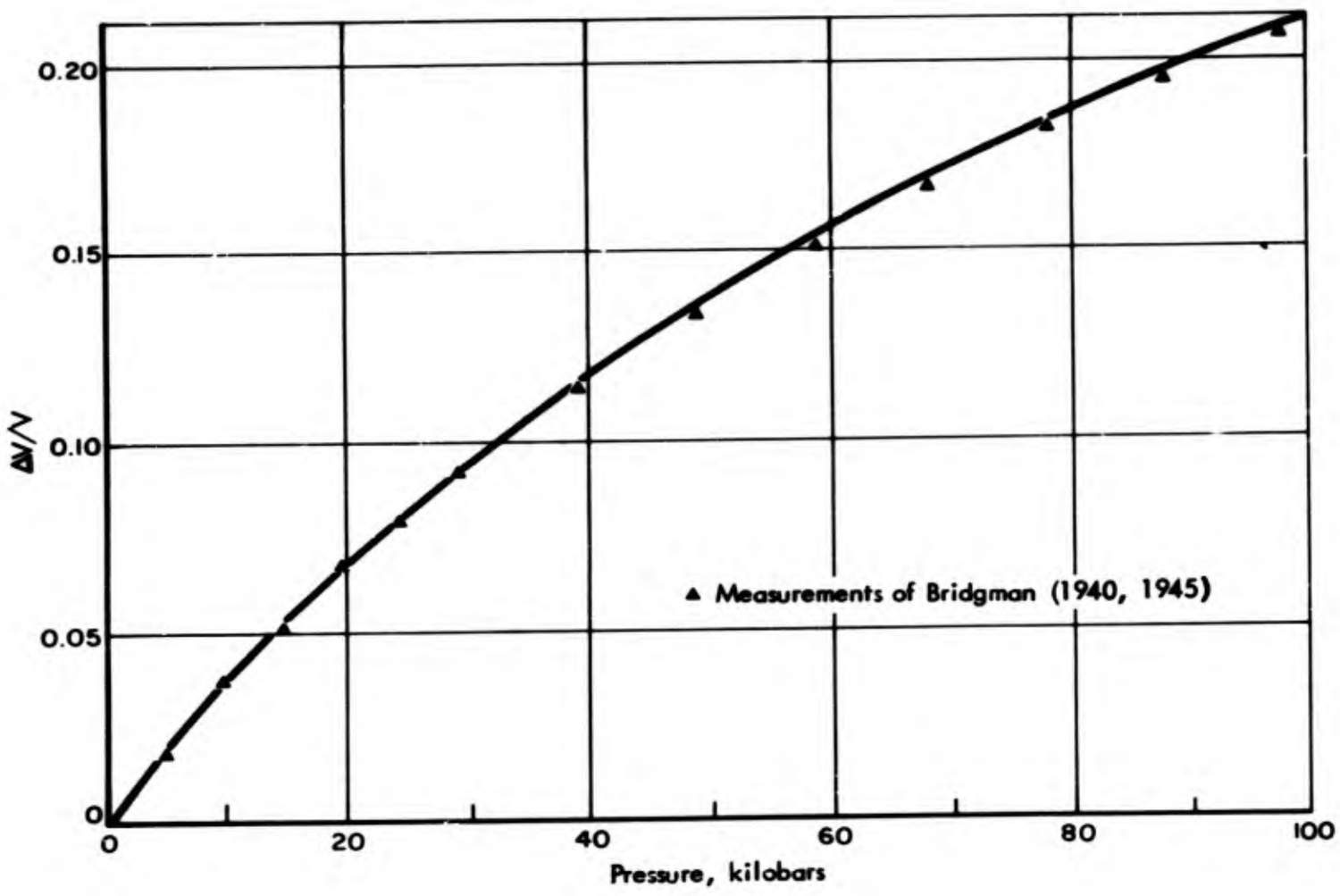

FIGURE 12 Volume Change vs Pressure for NaCl at 25°C, Computed Using Equation of State of Decker (1965). Figure from (Decker 1965).

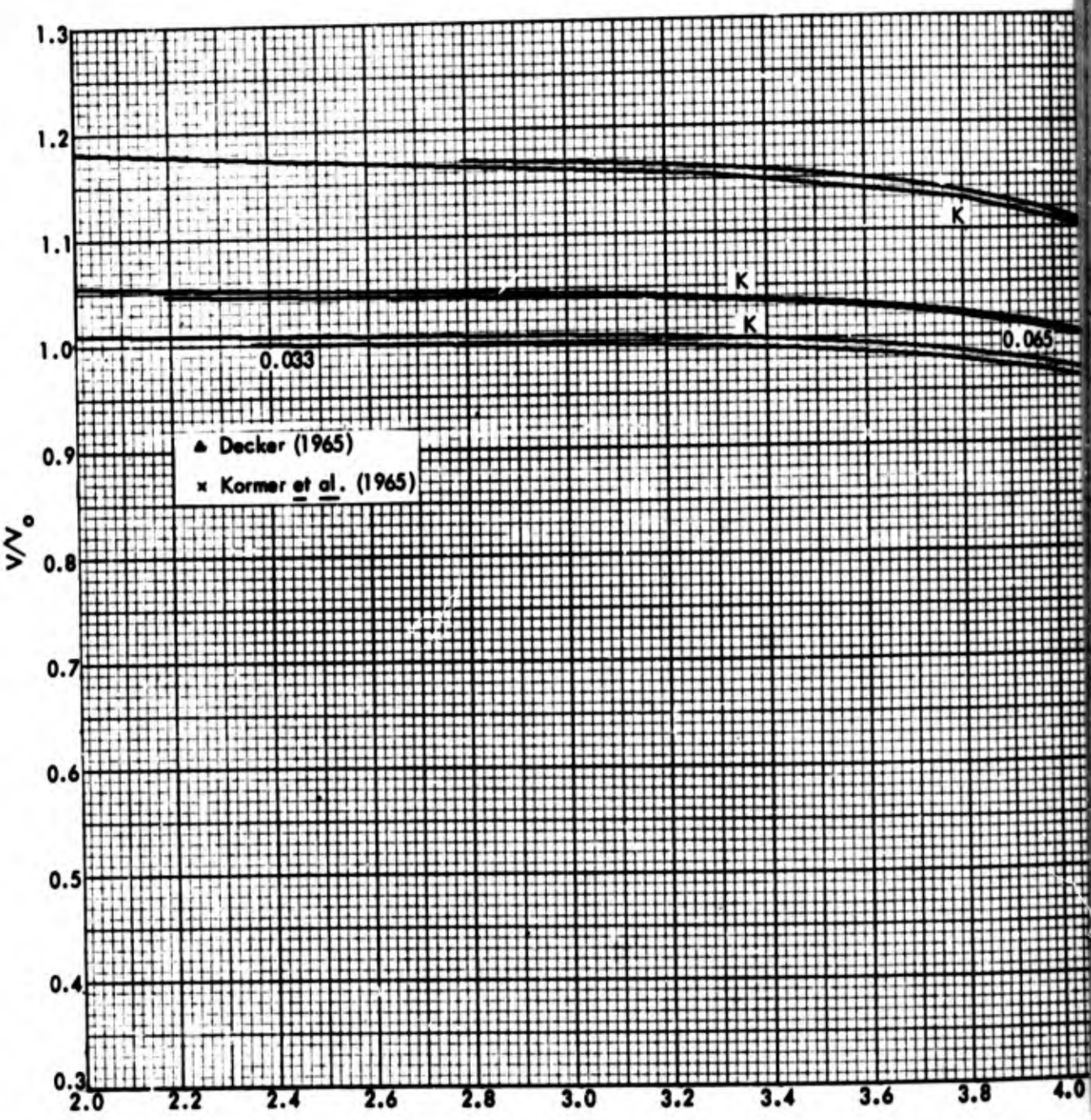

FIGURE 13 Complete Equations of State of Decker (1965) and Kormer (1965) Compared. In addition to Hugoniot points, decompression adiabats are shown for each equation. The adiabats for Decker's equation were computed by numerical integration of

$$(\partial P/\partial V)_S = \left[- P - \left(\frac{\partial E}{\partial V}\right)_P \right] \Big/ \left(\frac{\partial E}{\partial P}\right)_V$$

Temperatures shown were calculated from Decker's equation. (Compare Fig. 18)

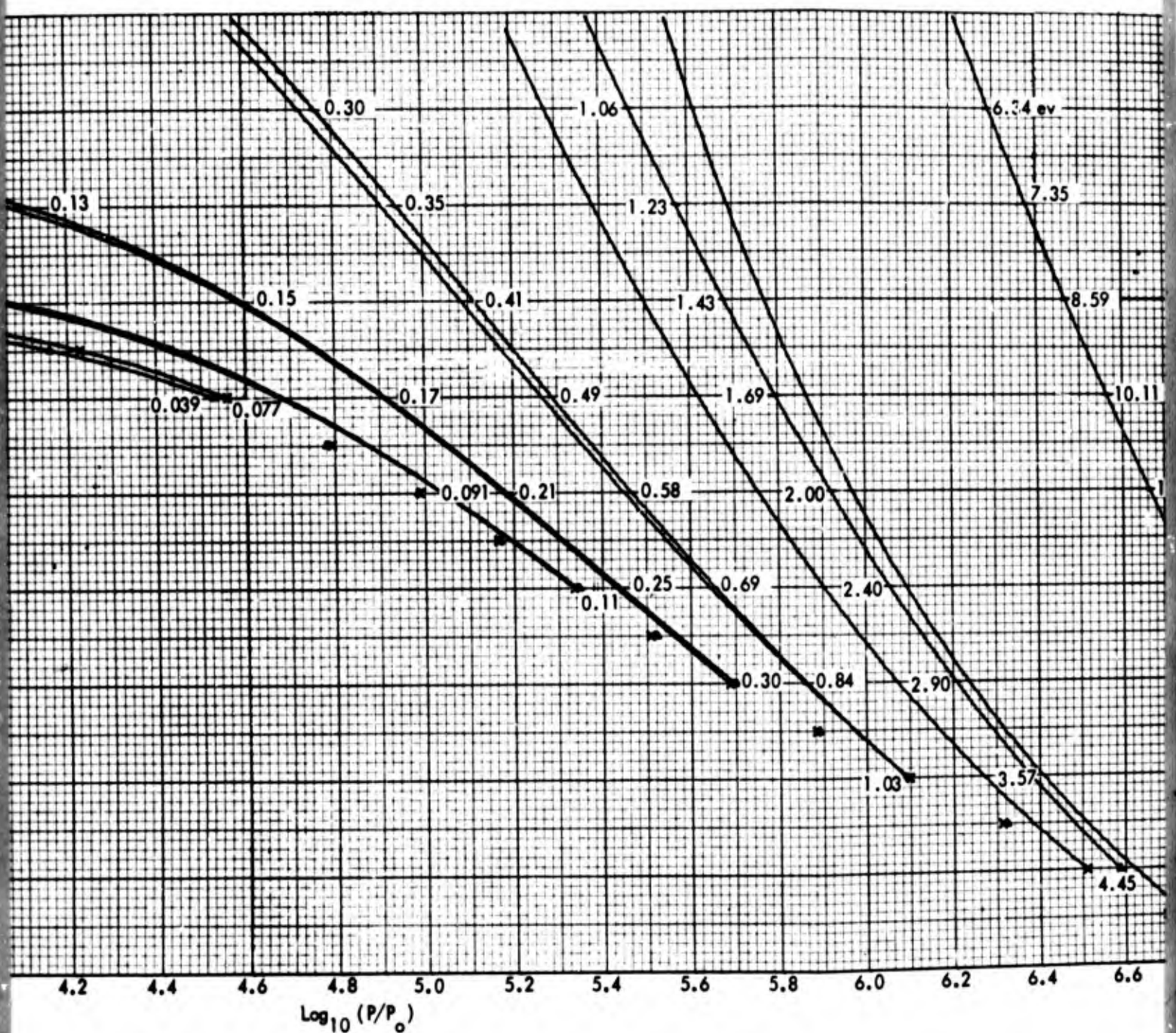
0.30
1.06
6.34 ev
0.13
0.35
1.23
7.35
0.15
0.41
1.43
8.59
0.039
0.077
0.17
0.49
1.69
10.11
0.091
0.21
0.58
2.00
0.25
0.69
2.40
0.11
0.30
0.84
2.90
1.03
3.57
4.45
4.2
4.4
4.6
4.8
5.0
5.2
5.4
5.6
5.8
6.0
6.2
6.4
6.6
Log10 (P/Po)

β

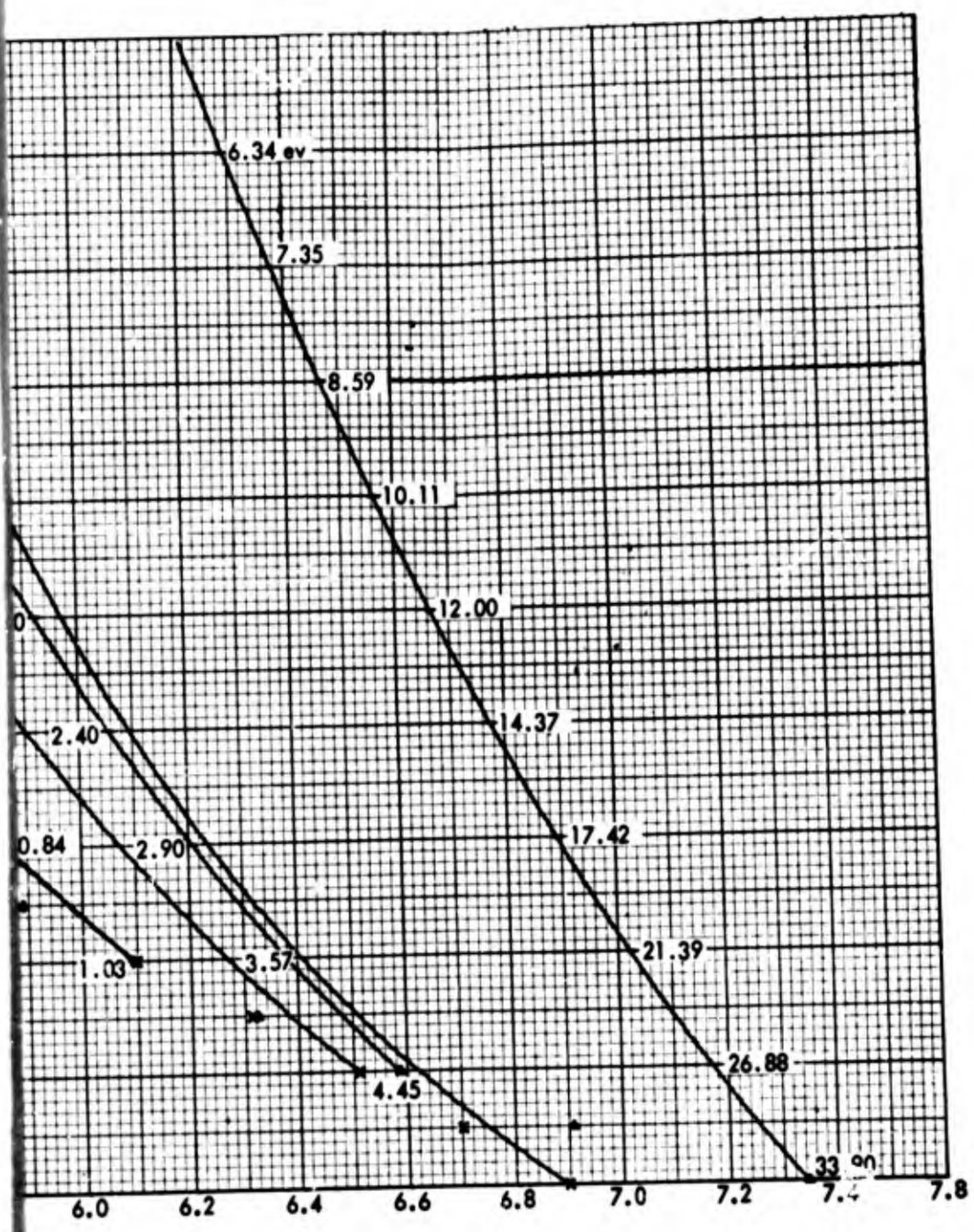
6.34 ev
7.35
8.59
10.11
12.00
14.37
17.42
21.39
26.88
33.90
2.40
2.90
0.84
1.03
3.57
4.45
6.0
6.2
6.4
6.6
6.8
7.0
7.2
7.4
7.8

C

and temperatures up to 1500°C.* Decker's equation gives an inadequate representation of Hugoniot data (Kormer et al. 1965) for porous samples at higher pressures (Fig. 13-a).

Results of an analysis by Decker (1965) of the sensitivity of the calculated pressures to the uncertainties of the various parameters showed: The range of uncertainty of the parameters r_+, r_-, C, D, θ_o does not vary P(V,T) more than ±0.30 kilobar over the range $0 \leq T \leq 1500°C$, $0 < P \leq 150$ kilobars; P(V,T) in the same range was not changed by more than ±0.10 kilobar by changing values of b_+/b to b_-/b to 1.25 and 0.75, respectively (lack of sensitivity to these parameters was interpreted as being due to compensation by corresponding changes of b, ρ); variations in γ_o are partially compensated by change in λ (however, fit to experimental thermal expansion became poor for values of γ_o at extremes of uncertainty range); 1 percent variations in K_o make ≤1.5 percent change in P(V,T) up to 150 kilobars.

D. EQUATION OF STATE OF ROGERS (1964) AND COOK (1963)

Rogers (1964)** and Cook (1963) use a form similar to the Mie-Grüneisen equation which assures agreement with the measured shock wave data:

$$P - P_H = \frac{\gamma_G}{V}(E - E_H) \quad . \tag{7}$$

In this equation, $P_H(V)$ and $E_H(V)$ are the experimental Hugoniot curves. The function $P_H(V)$ is taken to have the analytical form

$$P_H(V) = P_1\left[\left(\frac{V_o}{V}\right)^{\gamma_A + \gamma'_G} - 1\right] \quad , \tag{8}$$

---

*The time constraint on the present report precluded comparison of other equations of state with the atmospheric pressure experimental data.

**See also Holzer, 1965.

BLANK PAGE

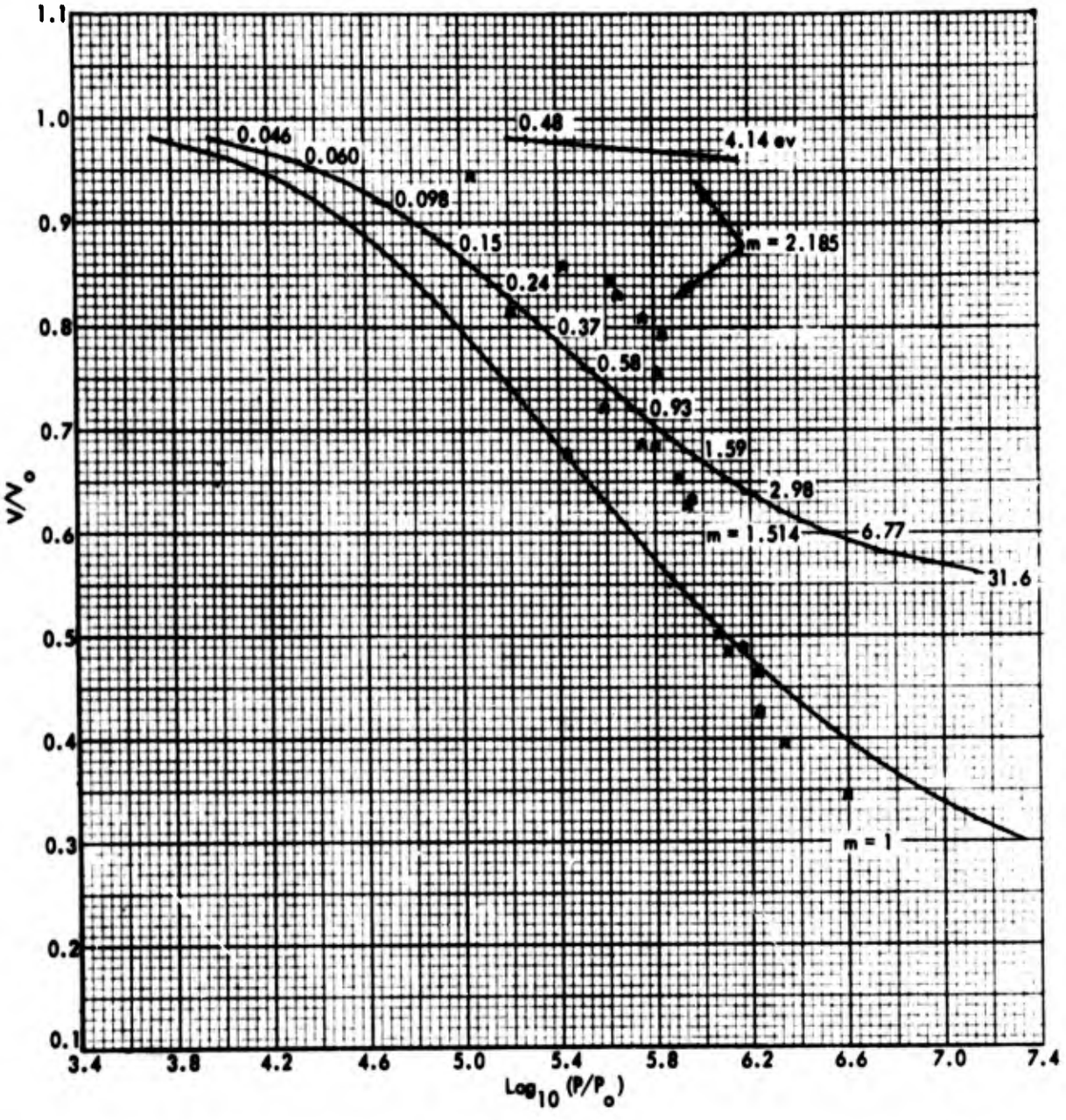

FIGURE 13-a Hugoniot Curves for Pure Rock Salt of Various Porosities Calculated Using Equation of State of Decker (1965). Also shown are experimental data points of Kormer et al. (1965).

where γ_A in the exponent is identified with the ratio of specific heats of the gaseous state of the material ($\gamma_A \to 1$ for the solid).* The above form for P(V) was found to give a good representation of the isothermal compressibility** data for a large number of solids and liquids (Cook, 1963).

The constants P_1, γ_G' are determined to best represent the compressibility data. For some materials γ_G in Eq. 3 is taken to have the constant value γ_G'; in other cases, a linear dependence on volume is assumed

$$\gamma_G(V) = \frac{V}{V_o}\,\gamma_G' \,.$$

The constant P_1 appearing in the Rogers-Cook equation is interpreted by them as the cohesive energy density of the material.***

Figure 14 shows the representation of the isothermal compressibility data of Bridgman (1940, 1945, 1949, 1954, 1957) for six alkali halides by the form of Eq. 4; it is seen that the log-log linear relationship implied by Eq. 4 does not hold in all cases. The straight line of Fig. 15 represents a least-squares best fit to isothermal compressibility and Hugoniot measurements† for pure NaCl in the region 10 kilobars $\leq P <$ 1.71 Megabars. Figure 16 shows a least-squares fit to Hugoniot data (Holzer, 1965) for "Salmon salt," presumably from Tatum dome, Mississippi.‡

---

* Note the apparent inconsistency of this interpretation with the value used for the curves of Figs. 14, 15 and 16.

** Or, in some cases, the Hugoniot data.

*** The further tentative identification of this cohesive energy density with enthalpy of vaporization is made in Holzer (1965).

† See Chapter II of this study.

‡ Holzer (1965) quoted a value P_1 = 200 kilobars; the corresponding value $\gamma_A + \gamma_G$ = 2.46, determined by a least-squares fit to the data (Fig. 17) is consistent with the quoted value (Holzer, 1965) γ_G = 1.4. This combination of values does not represent the experimental data points as well as the combination of Fig. 16.

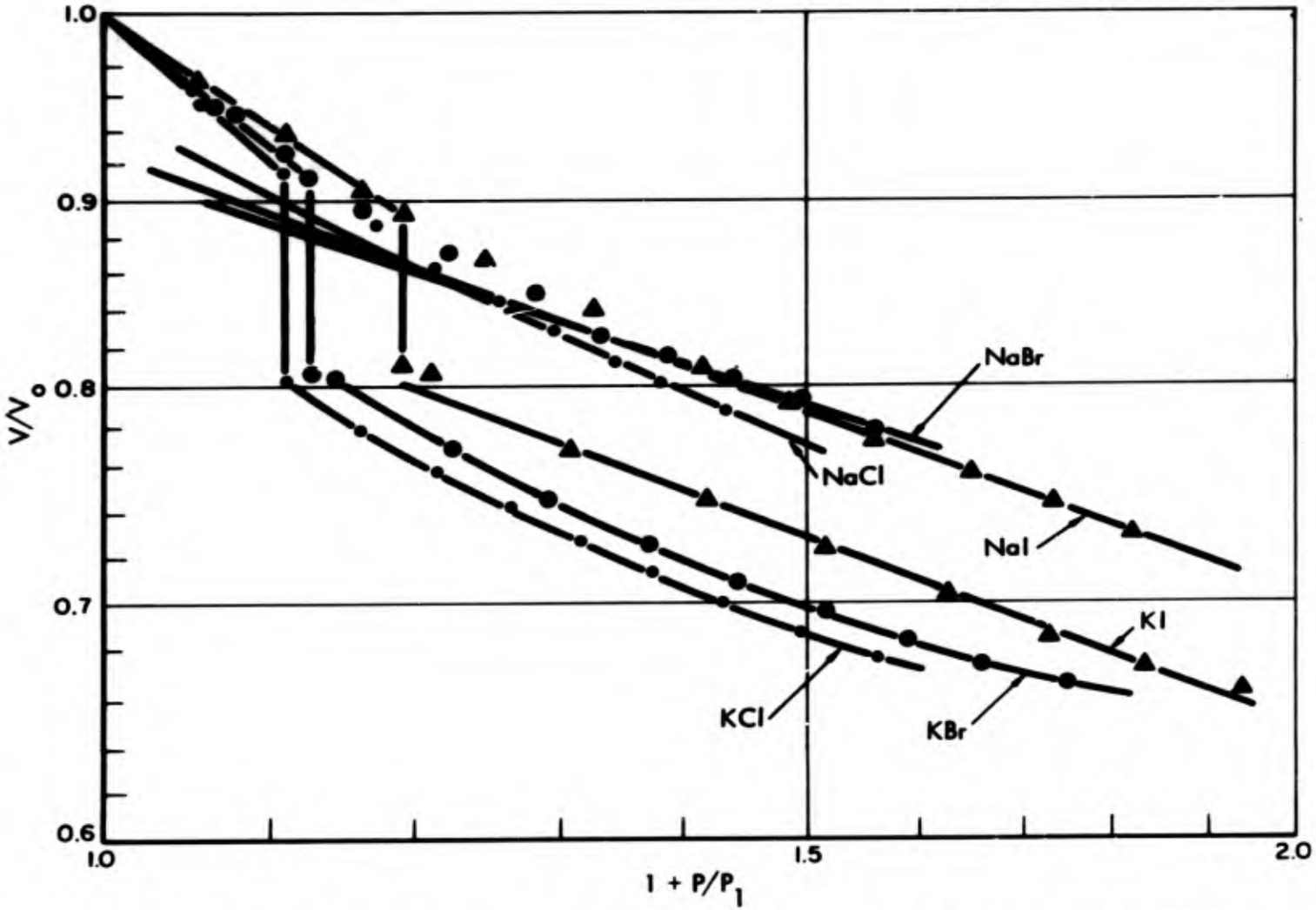

FIGURE 14 Isothermal Compressibility Data for Several Alkali Halides (Bridgman, 1940–1957) Plotted to Demonstrate Adequacy of Representation by Form of Equation 3. Figure from (Cook 1963).

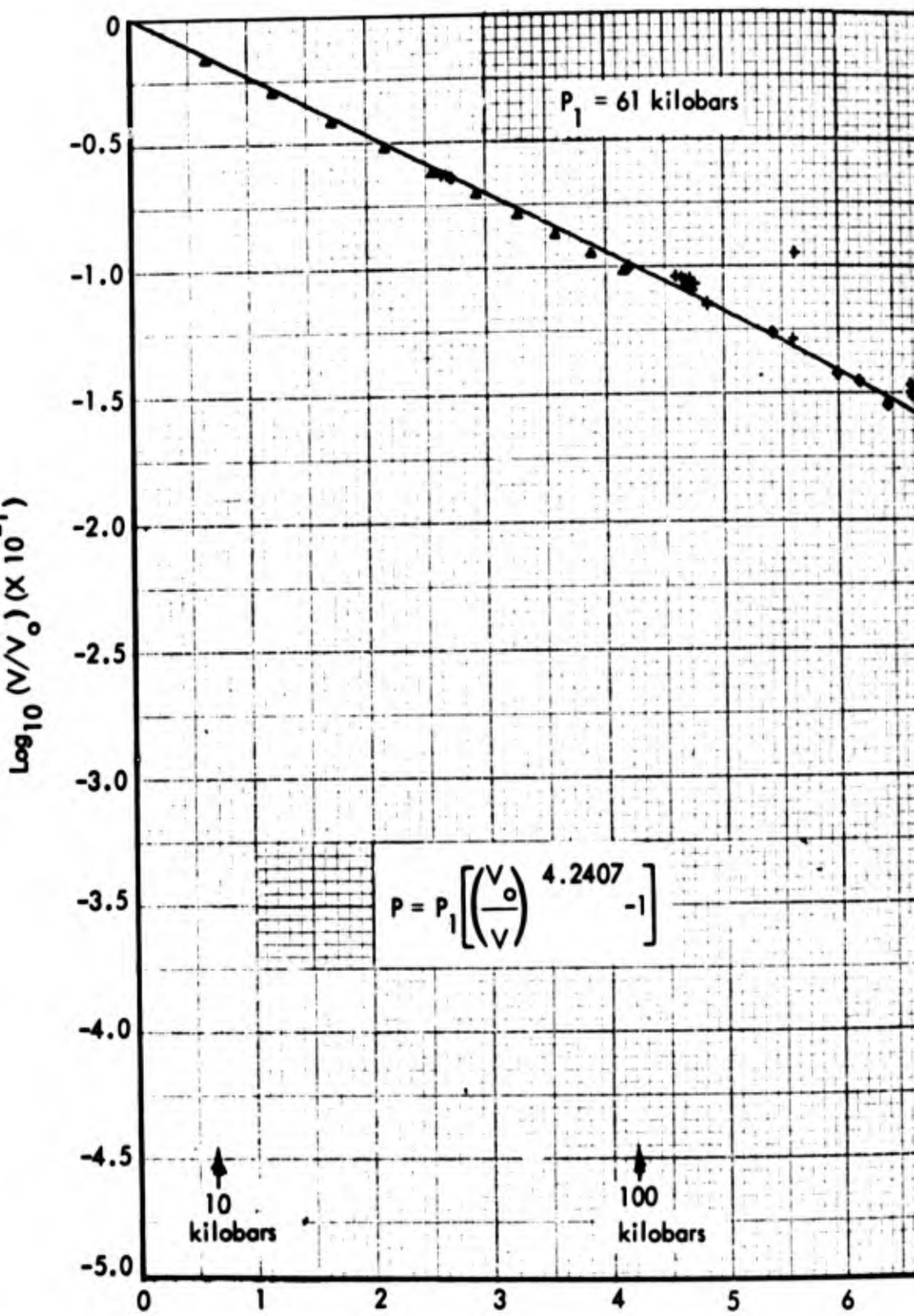

FIGURE 15 Least Squares Best Fit of Rogers-Cook Form to Experiment
NaCl. (See Fig. 1 of Chapter II.)

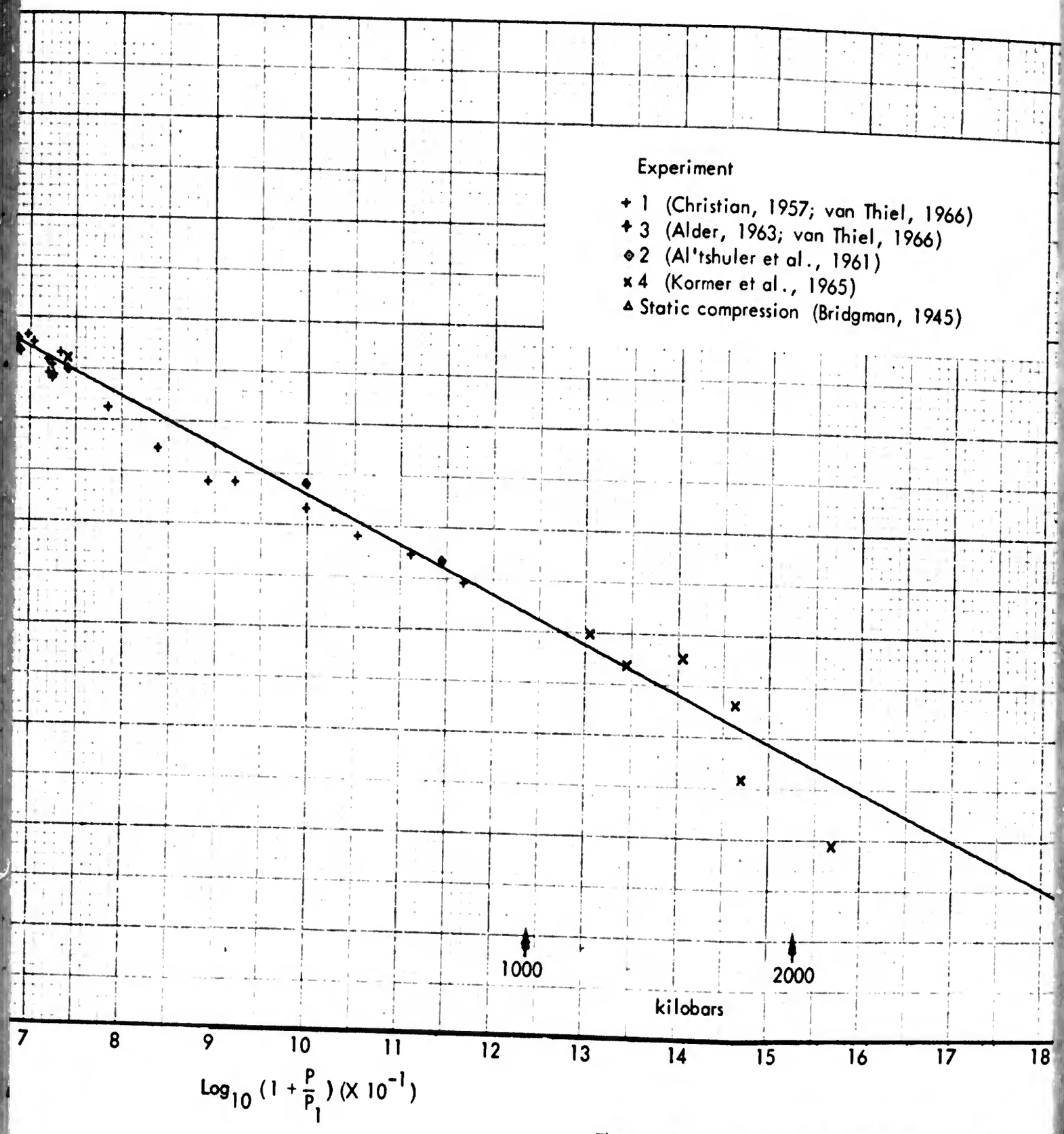

Compressibility Data for Pure

The values of the parameters were determined to minimize the quantity

$$\Sigma\left[(\gamma+\gamma)\log\left(\frac{V_o}{V_i}\right)-\log\left(1+\frac{P_i}{P_1}\right)\right].$$

The three highest pressure data points were excluded from the fit.

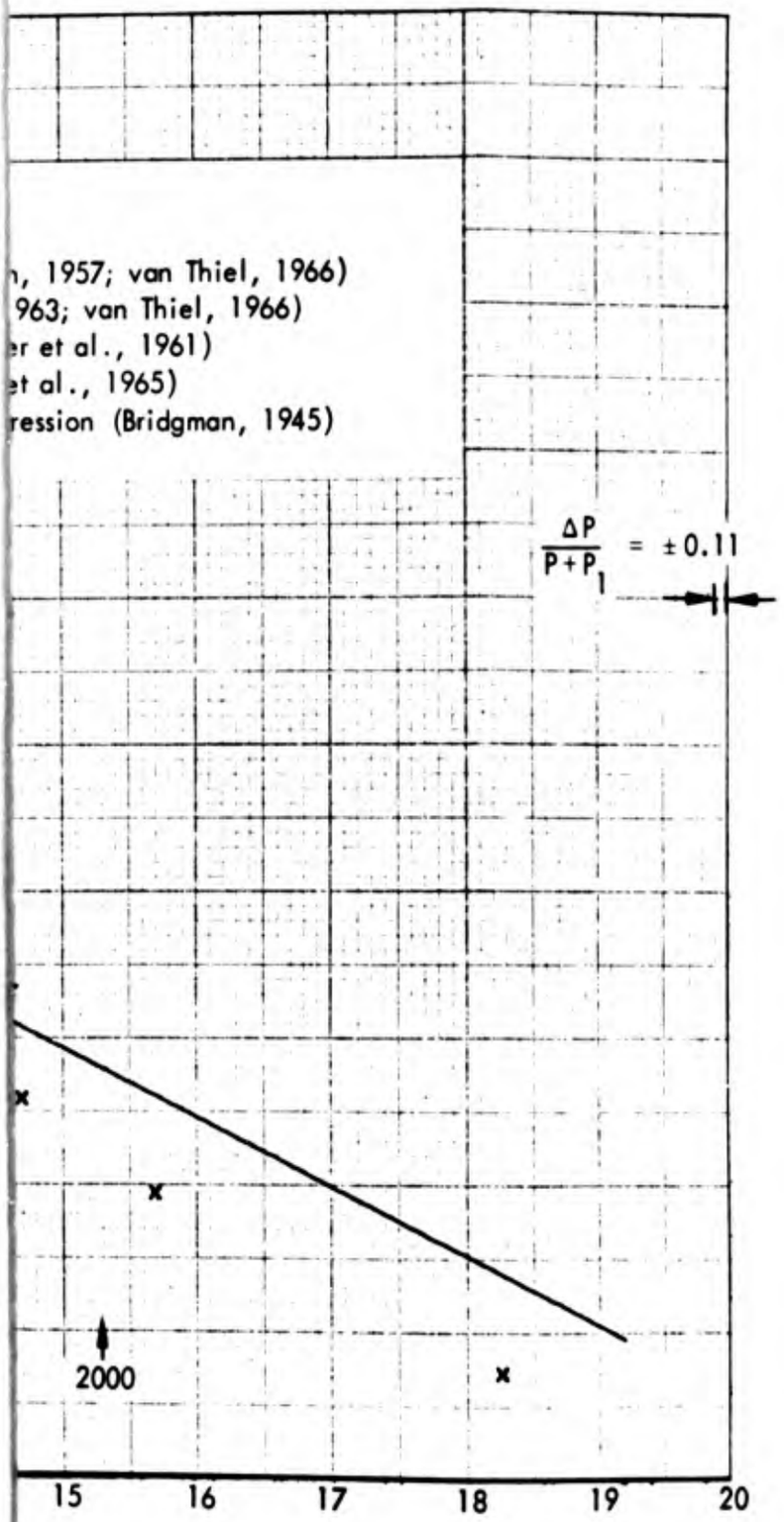

e parameters were determined to
antity

$$\left(\frac{V_o}{V_i}\right) - \log\left(1 + \frac{P_i}{P_1}\right)\Big].$$

st pressure data points were
he fit.

C

BLANK PAGE

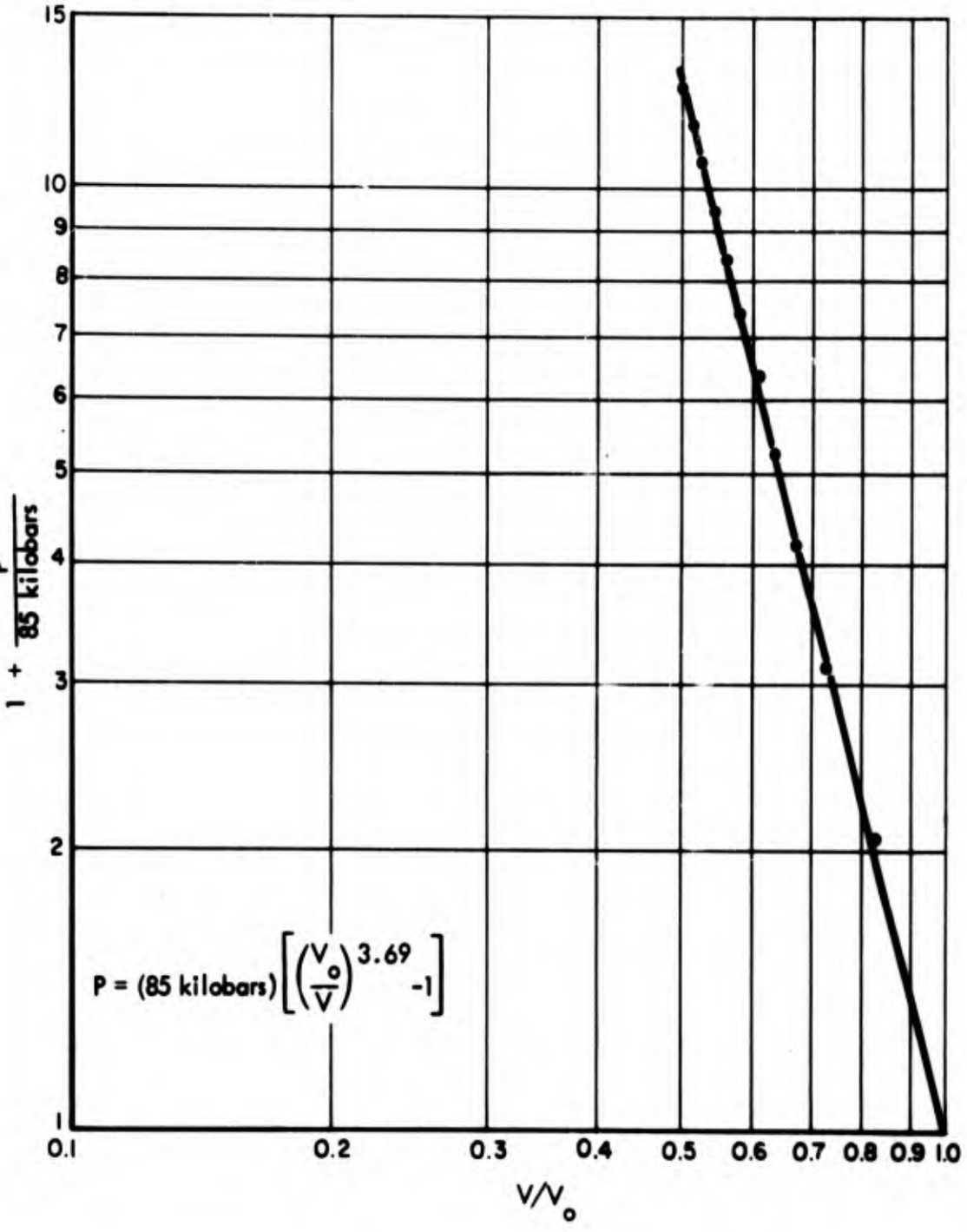

FIGURE 16 Least-Squares Best Fit of Rogers-Cook Form to Experimental Shock Compressibility Data for Salmon Salt, (Holzer, 1965).

R7-10-67-16

The parameters in the Rogers-Cook expression for dynamic compressibility (Eq. 4) are related through the bulk modulus: As $V \to V_o$,

$$P \to (\gamma_A + \gamma_G') P_1 \frac{V_o - V}{V}$$

so that the quantity $(\gamma_A + \gamma_G') P_1$ can be identified with the bulk modulus.* The table compares values of $(\gamma_A + \gamma_G') P_1$ as determined from the empirical fits of Figs. 15 to 17 with experimental values of the bulk modulus.

	P_1 (kbar)	$\gamma_A + \gamma_G'$	$(\gamma_A + \gamma_G') P_1$ (kbar)	B (kbar)
pure NaCl, ρ_o = 2.165 g/cm^3	61(1)	4.2407(1)	258	251(2)
"Salmon salt", ρ_o = 2.24 g/cm^3(3)	85(4)	3.69(4)	313	324(3)
	200(5)	2.46(5)	492	

(1) Figure 15
(2) Calculated using experimental values of elastic stiffness constants (Spangenberg and Haussühl, 1957, 1960): $3B = C_{11} + 2C_{12}$.
(3) Holzer, 1965.
(4) Figure 16.
(5) Figure 17.

The complete Rogers-Cook and Kormer equations of state are compared in Fig. 18. The Rogers-Cook equation gives an inadequate representation of the experimental results for shock compression of porous NaCl (Figs. 19 and 20).

*The author thanks F.B. Porzel for calling this relationship to his attention.

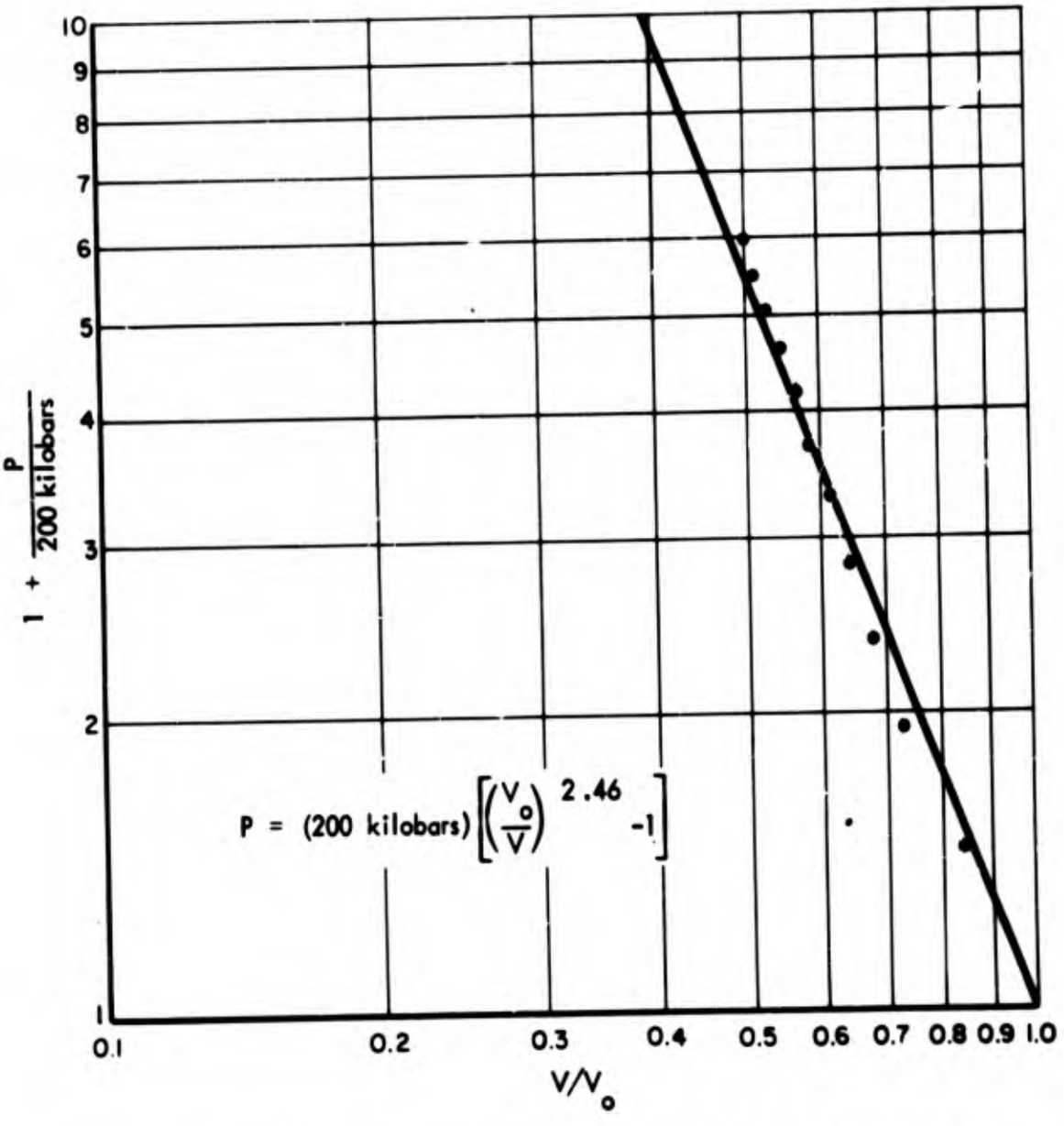

FIGURE 17 Least-Squares Best Fit of Rogers-Cook Form to Experimental Hugoniot Data for Salmon Salt (Holzer, 1965).

The parameter P_1 was held fixed at the value 200 kilobars quoted in Table 1 of Holzer (1965) for the internal energy per cm^3 of uncompressed material.

R7-10-67-17

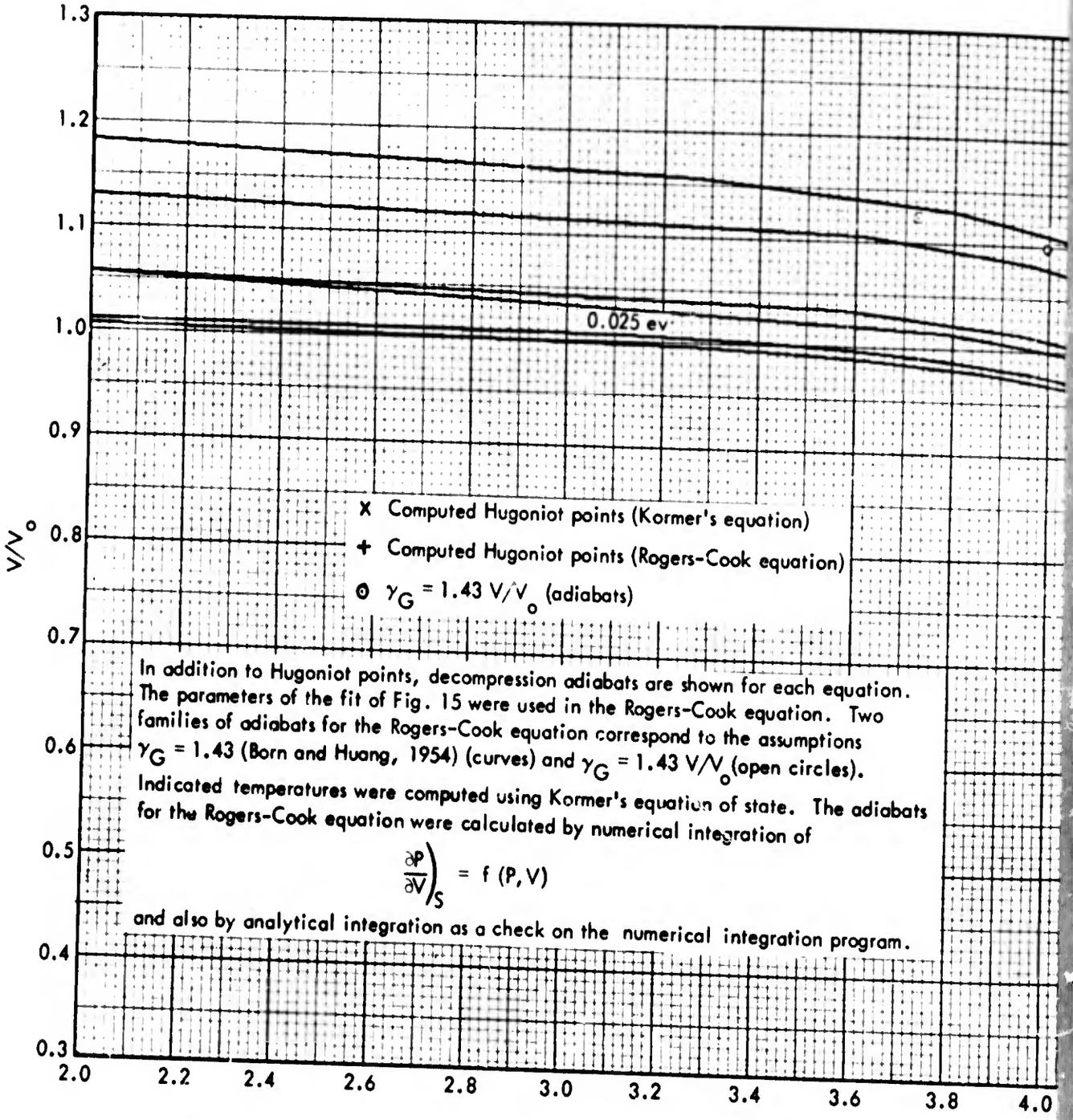

FIGURE 18 Complete Equations of State of Rogers-Cook and Kormer et al. (1965), Compared.

R7-10-67-16

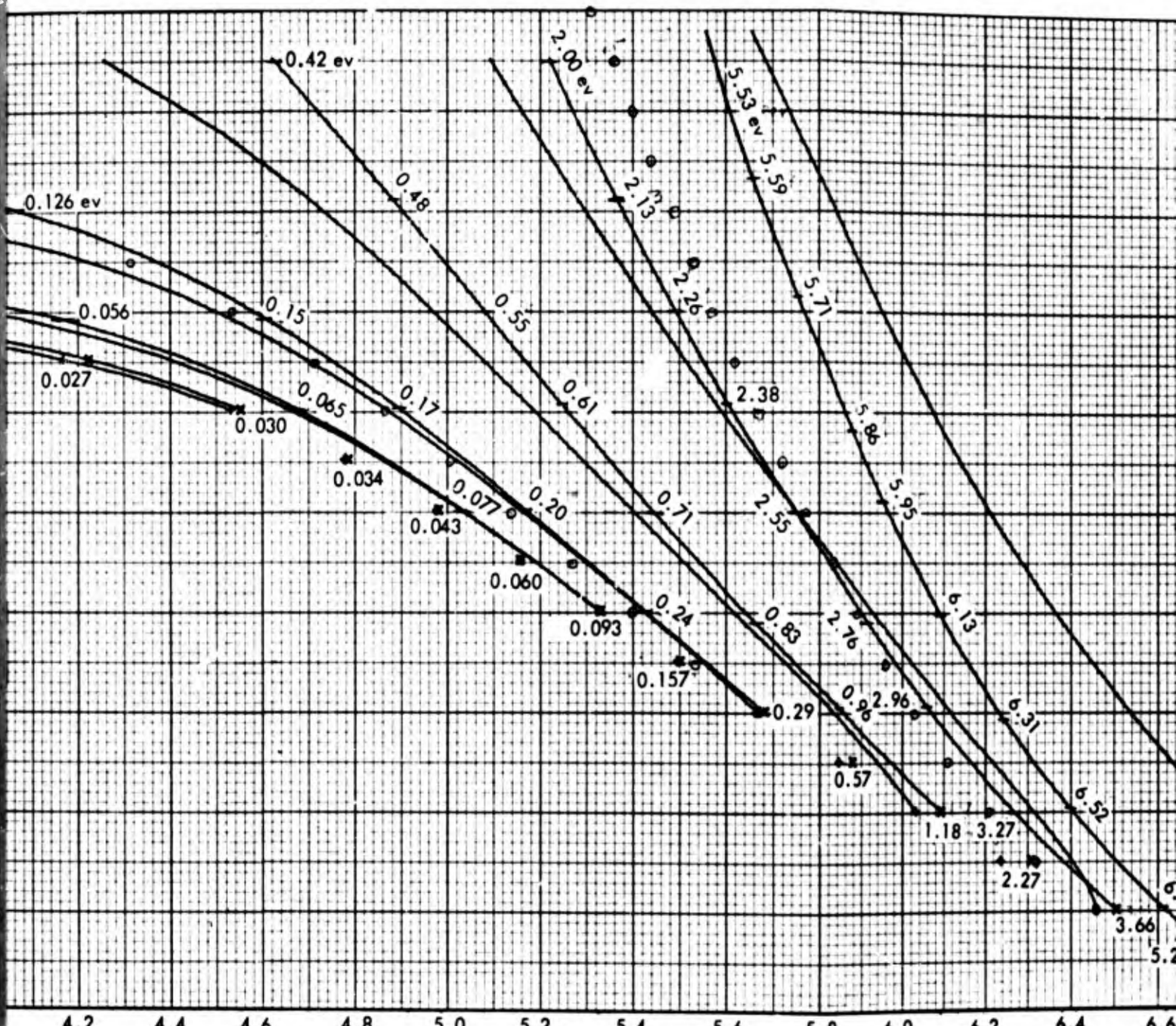
0.42 ev
0.126 ev
0.056
0.027
0.030
0.034
0.043
0.060
0.093
0.157
0.29
0.57
1.18
2.27
3.66
0.48
0.15
0.065
0.077
0.20
0.24
0.55
0.17
0.61
0.71
0.83
0.98
2.00 ev
2.13
2.26
2.38
2.55
2.76
2.96
3.27
5.53 ev
5.59
5.71
5.86
5.95
6.13
6.31
6.52
4.2
4.4
4.6
4.8
5.0
5.2
5.4
5.6
5.8
6.0
6.2
6.4
$\text{Log}_{10}(P/P_o)$

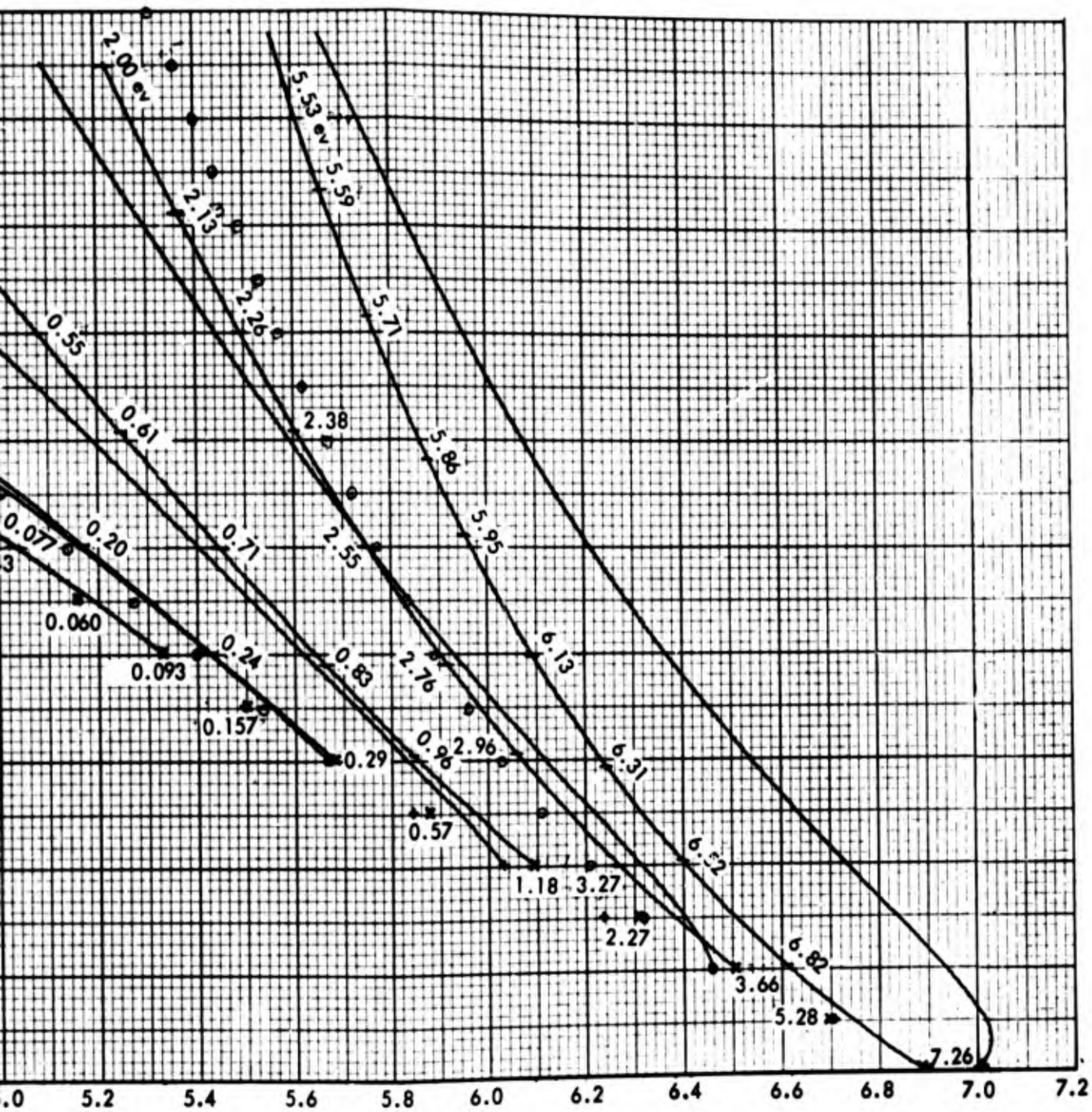
2.00 eV
2.13
2.26
2.38
2.55
2.76
2.96
3.27
3.66
5.28
7.26
5.53 eV
5.59
5.71
5.86
5.95
6.13
6.31
6.52
6.82
0.55
0.61
0.71
0.83
0.98
1.18
2.27
0.57
0.29
0.157
0.093
0.060
0.24
0.20
0.077
5.0
5.2
5.4
5.6
5.8
6.0
6.2
6.4
6.6
6.8
7.0
7.2

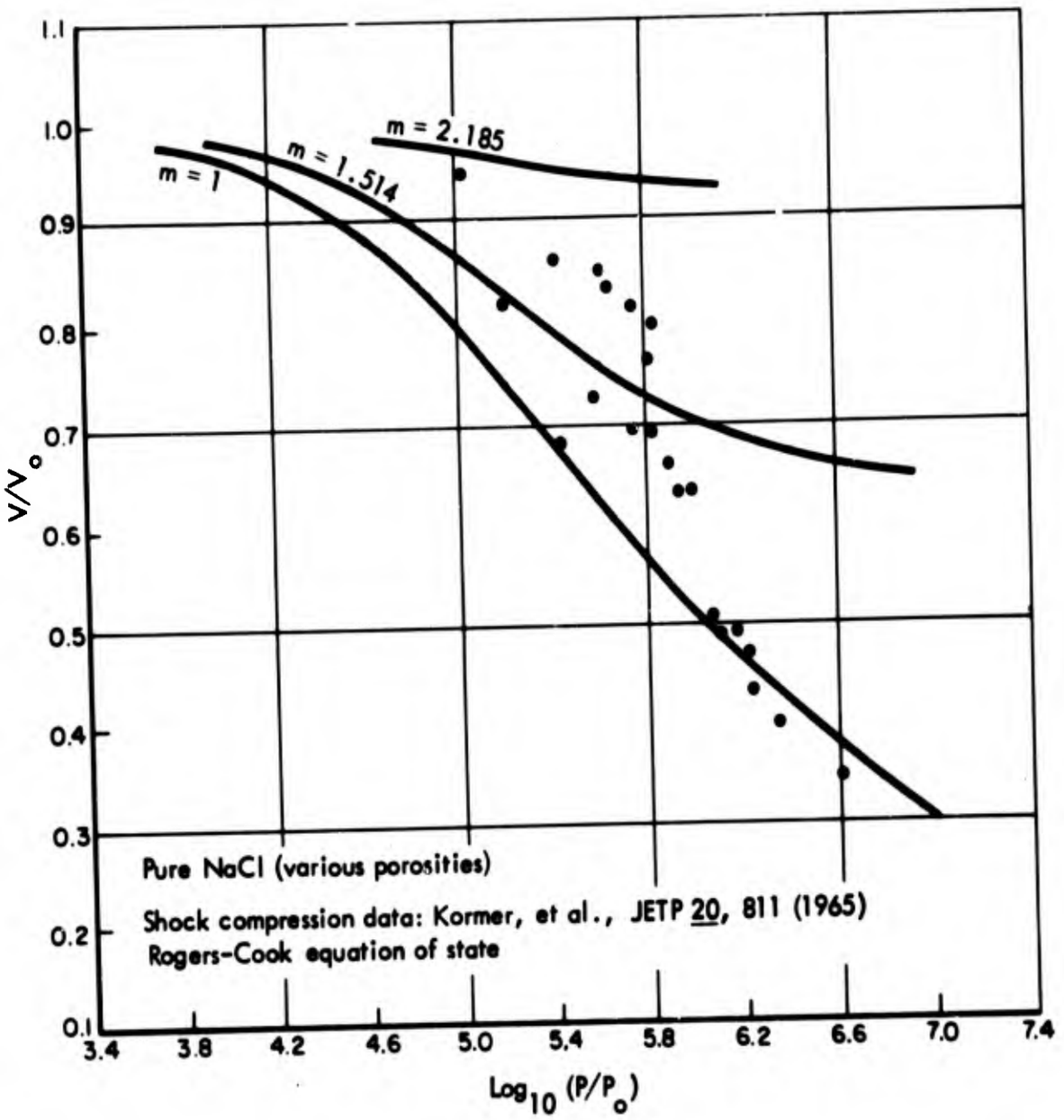

FIGURE 19 Hugoniot Curves for NaCl of Various Porosities Computed on Basis of Rogers-Cook Equation of State with Parameters of Fit of Figure 15 and γ_G = 1.43 = Constant.

Also shown are shock compression data of Kormer et al. (1965).

R7-10-67-18

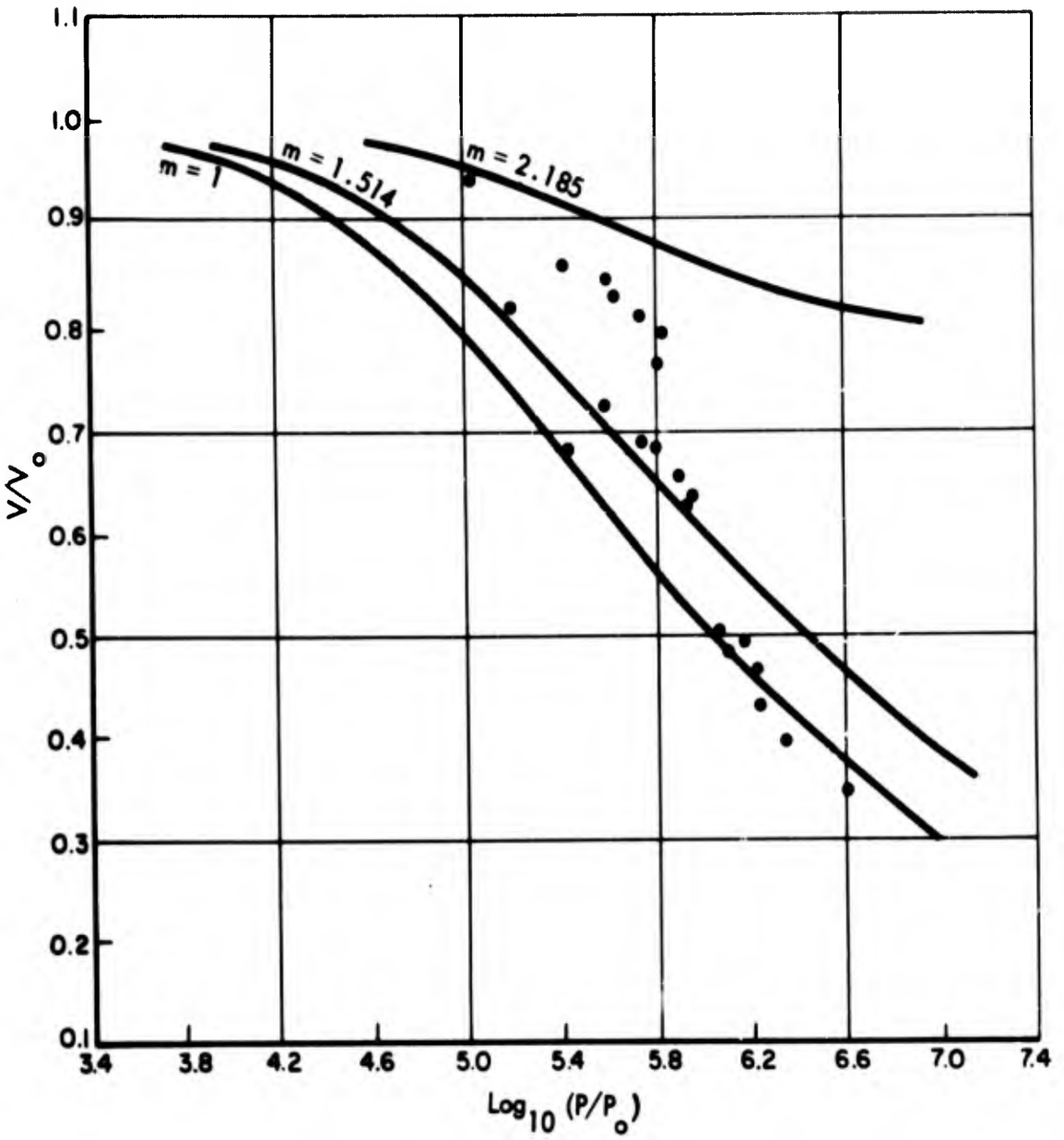

FIGURE 20 Hugoniot Curves for NaCl of Various Porosities Computed on Basis of Rogers-Cook Equation of State with Parameters of Fit of Figure 15 and $\gamma_G = 1.43\ V/V_o$.

Also shown are shock compression data of Kormer et al. (1965).

R7-10-67-20

Note added in press: Recent unpublished static compressibility measurements made on NaCl at UCLA (G. Kennedy, private communication) give pressures 2 kilobars higher than given by Decker's equation at 55 kilobars (polymorphic transition in barium) and suggest that a linear correction should be made to the pressure as given by Decker's equation using the parameter values given in this chapter. By means of a simultaneous X-ray diffraction measurement of the barium transition and NaCl compression, investigators at BYU find the same value (55 kilobars = average of values determined on increasing pressure and decreasing pressure parts of cycle) if Decker's equation is used with new parameters determined by making use of a new value of K (P = 0) recently determined by two different techniques (J.D. Barnett, private communication). According to Dr. Barnett, the new value of K improves the agreement between the isotherm as given by Decker's equation and the NaCl measurements of Bridgman and Kennedy.

CHAPTER V

SUMMARY

V. SUMMARY

If it is assumed that there is no undiscovered source of important systematic error in the shock and static experiments for pressures in the range 50 to 1000 kilobars, ±20 percent should be an upper limit on the uncertainty in the pressure for a given compression (pure NaCl). Over most of the pressure range specified, a reasonable "fit" to the data (Fig. 1, Chapter II) would probably lie within a few percent of the true values.

Results of shock and static compressibility measurements for naturally occurring rock salt and other geologic materials, made by using the same experimental techniques as those used for pure NaCl measurements, would be expected to have somewhat larger uncertainties due to the variability of composition of such materials.

Non-reproducibility and sample-to-sample variation characterized the results of plastic flow measurements, both for NaCl of high purity and for naturally occurring rock salt. Strain rate and sample size effects have not been investigated.

An inadequacy common to all of the equations of state discussed is their failure to describe phase changes which may occur on decompression following sufficiently strong shocks, and the polymorphic transition indicated by the Hugoniot data for NaCl in the vicinity of 250 to 350 kilobars or 1.7 Megabars. The agreement of the equations of Al'tshuler, et al., and Kormer, et al., with each other and with the Hugoniot data up to 1.6 Megabars for both porous and non-porous specimens, and the physical reasonableness and relative simplicity of the Lennard-Jones/Devonshire model, are factors tending to promote confidence in the predictions of these equations in the hydrodynamic, compressed region. The equations of state of Decker and Rogers-Cook

give Hugoniot curves which are not in agreement with the data for porous NaCl in the pressure ranges (100 kilobars < P) and (160 kilobars < P), respectively. Decompression adiabats calculated on the basis of the Rogers-Cook equation of state disagree substantially with adiabats calculated using Kormer's equation for shock pressures greater than about 630 kilobars.

APPENDIX A

UNCERTAINTIES OF "LABORATORY" SHOCK COMPRESSION MEASUREMENTS FOR SOLIDS

BLANK PAGE

APPENDIX A

UNCERTAINTIES OF "LABORATORY" SHOCK COMPRESSION MEASUREMENTS FOR SOLIDS

A. METHODS USING PLANE SHOCKS

Hugoniot data for rocks have been obtained by techniques involving measurements of shock transit times and free-surface velocities in samples loaded by nearly plane H.E. shocks (Fig. A-1). The determination of the Hugoniot from the measured velocities is accomplished by simultaneous solution of the Hugoniot relations

$$u_s = V_o \sqrt{\frac{P_1 - P_o}{V_o - V_1}} \tag{1}$$

$$u_p = \sqrt{(P_1 - P_o)(V_o - V_1)} \tag{2}$$

and the expression for the free-surface velocity, obtained by the method of characteristics:

$$u_{fs} = u_p + \int_o^{P_1} \left(- \frac{\partial V}{\partial P} \right)_S^{\frac{1}{2}} dP \ , \tag{3}$$

where u_s = shock velocity, u_p = material velocity behind shock, u_{fs} = surface velocity, and subscripts 0 and 1 refer to conditions ahead of and behind shock. The integration is along an adiabat, i.e., curve of constant entropy. For purposes of illustration, it can be assumed that the adiabats are known, i.e., $(\partial V/\partial P)_S$ = known function of (P, P_1, V_1). Then, the above three equations are solved for P_1, V_1, u_p in terms of the known V_o, P_o (≈ 0), and measured u_s, u_{fs}. Actually, the adiabats must be determined along with the Hugoniot (see below),

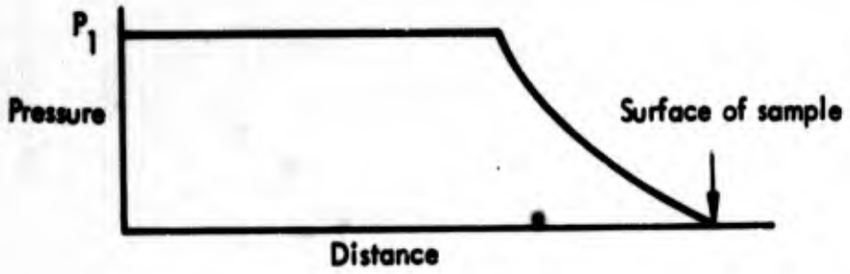

FIGURE A-1 Schematic of Pressure Profile, Free-Surface Technique

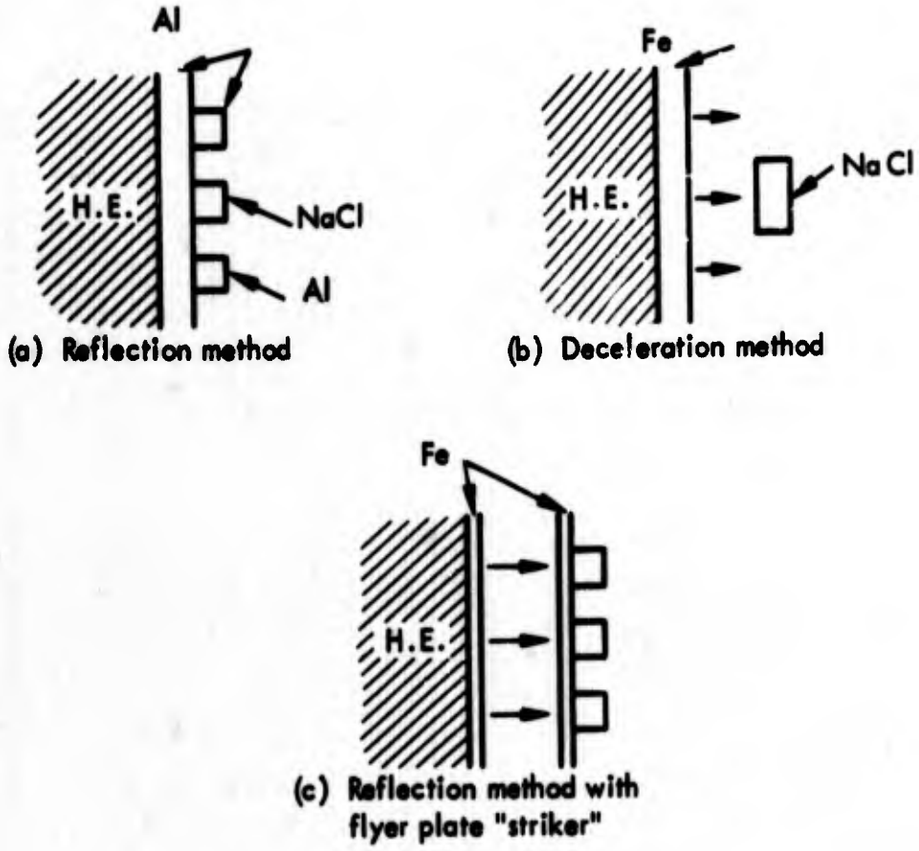

FIGURE A-2 Schematic of Experimental Arrangements for Hugoniot Measurements on Rock Samples

RR-10-67-38

so that there is an uncertainty in the Hugoniot determined in this way due to the uncertainty in the adiabats. If the approximation $u_p \approx u_{fs}/2$ is made, a correction can be made for the error introduced.*

*The "doubling" approximation is equivalent to using the (reflected) P - u_p Hugoniot for the rarefaction. (See also discussion of "reflection" method below.) Results for a large number of metals (Rice et al., 1958) indicate that it is a good approximation (few percent) to set $u_p \approx u_{fs}/2$ for pressures up to >500 kilobars. In Walsh and Christian (1955) expressions for upper and lower bounds on the ratio u_r/u_p are derived.

$$\left[u_r \equiv \int_o^{P_1} \left(-\frac{\partial V}{\partial P} \right)_S^{\frac{1}{2}} dP \right]$$

A successive approximation procedure using these expressions gives

$$0.98 < \frac{u_r}{u_p} < 1.03 \qquad \text{(Al, } 100 < P_1 < 400 \text{ kilobars)}$$

$$0.98 < \frac{u_r}{u_p} < 1.015 \qquad \text{(Cu, } 100 < P_1 < 500 \text{ kilobars)}$$

for example, corresponding to maximum possible errors in ΔV of <0.5% (±) over the indicated pressure ranges. The expression derived for the lower bound on u_r/u_p depends on the general assumptions

$$dV/dP < 0$$
$$d^2V/dP^2 > 0$$
$$V(P) \geq V_H(P)$$

for an adiabat (S = constant) V(P) connecting a point P_1 on the Hugoniot $V_H(P)$ to the line P = 0. Note that the second condition may not hold in case a phase change is induced by the shock. The author thanks F.B. Porzel for pointing out that the "doubling" approximation is a consequence of the "acoustical" behavior of solids at pressures

$$\ll \rho_o c_o^2 \left(\sim \left\{ \begin{matrix} 2000 \\ 450 \end{matrix} \right\} \text{ kilobars for } \left\{ \begin{matrix} \text{iron} \\ \text{NaCl} \end{matrix} \right\} \right),$$

for example. See also Sec. 11 of Chap. XI of Zel'dovich and Rayzer (1963). That the above condition is equivalent to $\Delta\rho \ll \rho_o$ and constant entropy is easily seen from

$$\Delta P \sim (\Delta\rho) \left(\frac{\partial P}{\partial \rho} \right)_S \ll \rho_o c_o^2 .$$

In a more sophisticated technique, the shock from an explosive source is transmitted to the sample through a plate of a material (herein referred to as the "pusher") with known (previously measured) Hugoniot (Figs. A-2a and A-3). In this "reflection" or "impedance matching" technique, the measured quantities are u_s, the velocity of the shock in the pellet of material under study, and either the free-surface velocity u_{fs} of the pusher or u_{s_1}, the shock velocity in the pusher plate. In the latter case, the intersection of a line through the origin with slope $\rho_o u_{s_1}$ and the known Hugoniot of the pusher material in the P-u_p diagram (Fig. A-3a) determines the state (P_1, u_{P_1}) behind the shock in the pusher, and the appropriate cross curve representing reflected shocks ($P > P_1$) or reflected rarefaction waves ($P < P_1$). (In the alternative method, the cross curve is determined by the measured free-surface velocity u_{fs} corresponding to $P = 0$.)* The state behind the shock in the specimen is then given by the intersection of a line through the origin with slope $\rho_o u_s$ and the cross curve through (u_{P_1}, P_1) representing reflected waves. The positions of the cross curves representing reflected shocks are mirror reflections of the P-u_p Hugoniot representing shocks from state (P_1, u_{P_1}) to pressure $P > P_1$ in the pusher material.** The portions corresponding to reflected rarefactions are determined by

$$u_p = \int_{P_1}^{P} \left(-\frac{\partial V}{\partial P}\right)_S^{\frac{1}{2}} dP \,. \qquad (3a)$$

*In Rice et al. (1958), the results of the two determinations of the cross curve are averaged. Unfortunately, these separate data--which would have been useful for assessing the uncertainty--were not given in the paper.

**It is perhaps worth pointing out that this is not the same as the Hugoniot representing shocks from P = 0 to pressure P. The approximation introduced by the use of the latter Hugoniot locus is designated "mirror" in Table C-1 of Appendix C.

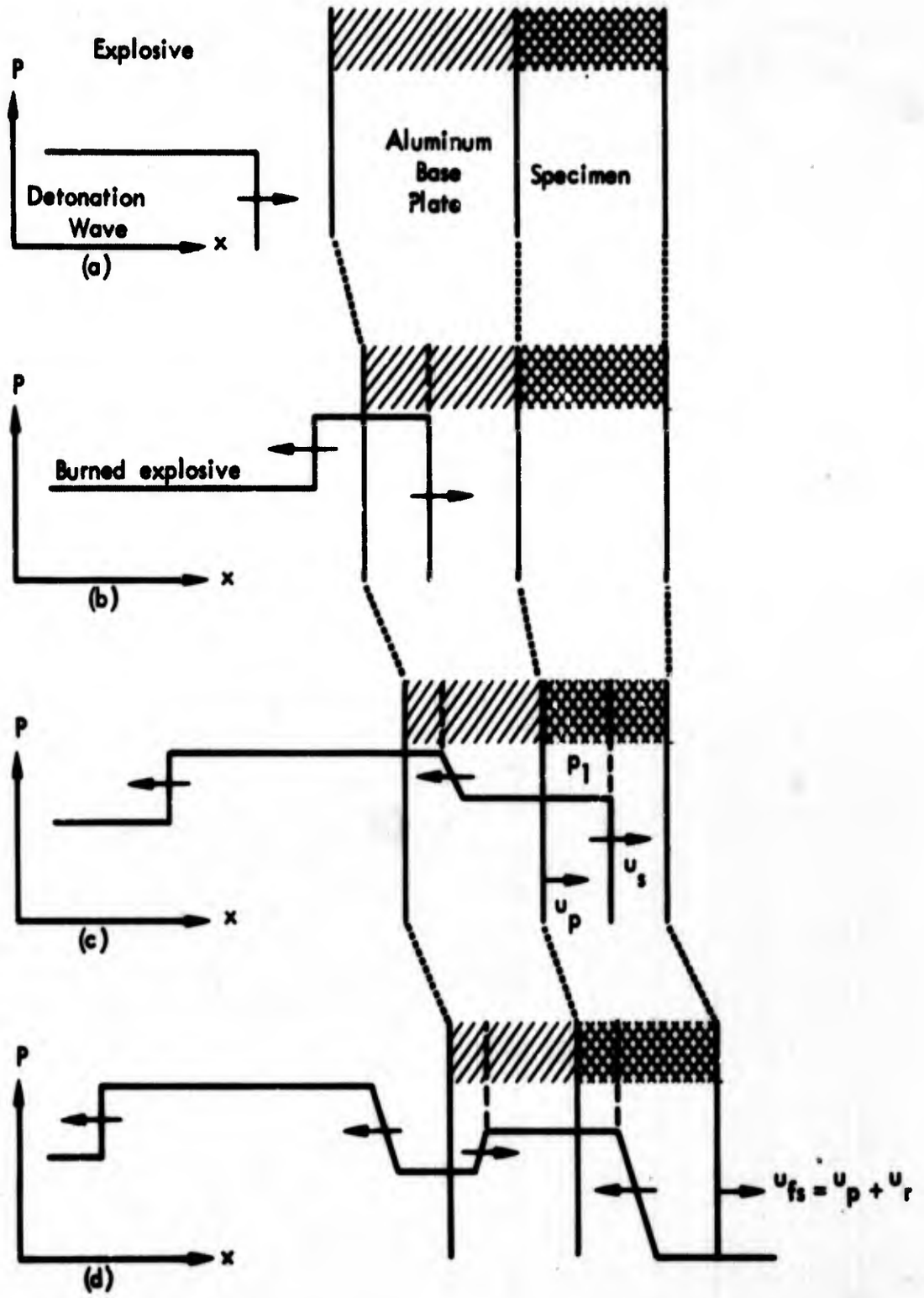

FIGURE A-3 Schematic of Pressure Wave, Reflection Method (Christian, 1957)

RT-10-67-20

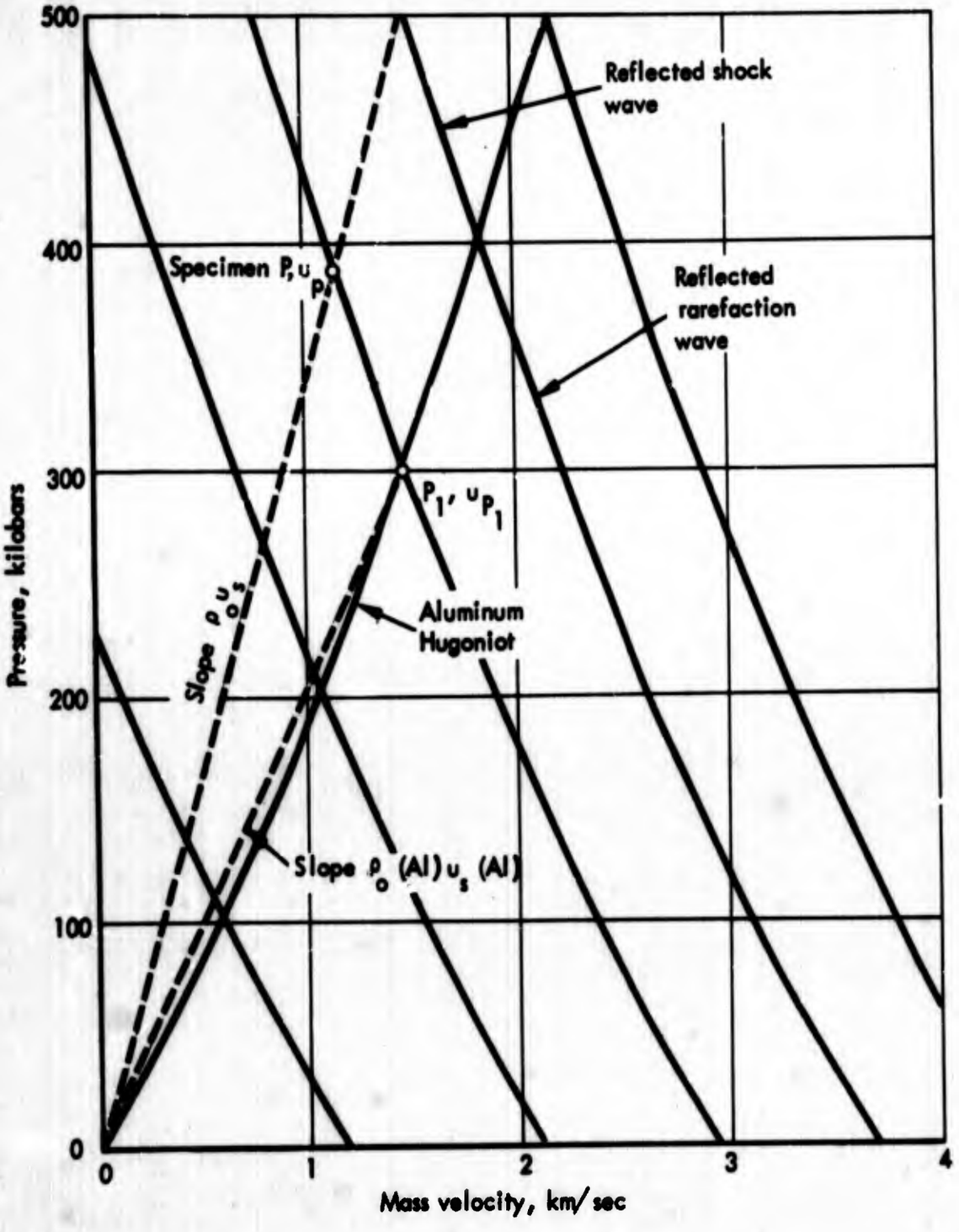

FIGURE A-3a Graphical Solution for Impedance Match Reflection Method with Aluminum Pusher

RT-10-67-30

Thus, in the latter case there will be an uncertainty in the Hugoniot for the material under study due to the uncertainty in both the Hugoniot and adiabats (constant entropy curves) of the pusher material. The uncertainty in the rarefaction cross curve will be nearly that in the (P, u_p) Hugoniot with an additional uncertainty due to the uncertainty in the difference between Hugoniot and adiabat, plus an uncertainty due to the numerical integration of Eq. 3a. Note that the equation of state of the pusher material must be known at least approximately in order to compute the cross curves for both reflected shocks and rarefactions. In most cases, no estimates of the uncertainty in the cross curves were given by the investigators who used the reflection method.*

For the calculated P-u_p 24ST Al adiabat corresponding to P_1 = 400 kilobars, the largest deviation from the Hugoniot is less than 1 percent in u_p, at P = 0 kilobars (Alder, 1963). (For all pressures $\geq$ 100 kilobars the calculated deviation is <0.2 percent.) An error of 10 percent in the difference u_p(ad.) - u_p (refl. Hug.), for example, would contribute $\lesssim$ 0.02 percent to the uncertainty in the values of u_p determined by the reflection method, for pressures $\geq$ 100 kilobars (or < 0.1 percent for the free-surface method) and $P_1 \leq$ 400 kilobars, with a comparable error in P.** The error in the numerical integration can be made practically arbitrarily small. In both cases (reflected shocks or rarefactions), errors will be introduced by interpolation between measured points on the pusher Hugoniot and its reflection.

In another technique used by Al'tshuler et al. (1958) to study shock compression of metals, a "flyer plate" is accelerated by explosive to a high velocity before colliding with a plate of the material under study (Fig. A-2b). The velocity just before impact and the

---

*However, recall discussion above of uncertainties associated with "doubling" approximation.

**"The Hugoniot locus thus determined is subject to errors due to uncertainties existing in the zero-pressure data (specific internal energy versus volume) and the volume dependence of the Grüneisen ratio. It is estimated that these effects cause uncertainties of about 0.2% at one megabar [for brass], increasing to 0.4% at two megabars, in the shock velocity at a given particle velocity." (McQueen and Marsh, 1960)

velocity of the shock in the specimen are the measured quantities. In Fig. A-4, the curve labeled "striker deceleration" is the difference between W_D, the striker velocity before impact, and the known pressure-particle velocity locus for shocks propagating into striker material at rest. The intersection of this curve with a line through the origin with slope $\rho_o u_s$ (ρ_o = density of uncompressed target specimen, u_s = measured shock velocity in specimen) determines the shocked state. In case the striker and target are the same material and negligible heating of the striker by the H.E. shock occurs, $W_D - u_1 = u_1$, or $u_1 = W_D/2$, exactly.

In a variation of the "reflection" method used for the measurements reported in Al'tshuler et al. (1958) and McQueen and Marsh (1960), an initially stationary plate in contact with pellets of the sample is struck by a flying plate (Fig. A-2c).

B. SOURCES OF EXPERIMENTAL UNCERTAINTY

The experimental methods described rest upon the basic assumptions of rheological isotropy of the material and establishment of equilibrium conditions in the shocked regions in times short compared to $\sim 10^{-7}$ sec (equivalent to shock thickness less than a few tenths of a millimeter). Results would be expected to differ from static compressibility results where equilibration times $\lesssim 10^{-6}$ sec are involved, e.g., certain polymorphic transitions.* The hydrodynamic approximation

*"The important question of equivalence for the shock-wave results and laboratory pressure-volume data is perhaps best evaluated by examination of the data plots [Hugoniot curves and, expecially, derived 20°C isotherms]. For most metals, the compatibility, if judged by downward extrapolation of the analytical fits, is quite good. This is especially true of comparisons with the recent measurements to 30 kilobars by Professor Bridgman. Several of the static measurements to 100 kilobars, however, indicate compressions which are a few percent smaller than the corresponding shock wave results. In regard to the latter comparisons, it should be noted that the approximate nature of either of the present basic assumptions (thermal equilibrium and isotropy) would cause the shock wave results to indicate too little compression, and hence is not in the desired direction to account for the small observed offsets." (Walsh et al., 1957)

"Although the atoms still have to be rearranged to form crystalline material, the agitation enormously reduces the nucleation times which frequently limit crystal growth under static conditions." (Alder, 1963)

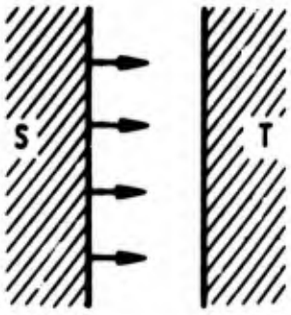

(a) Before collision

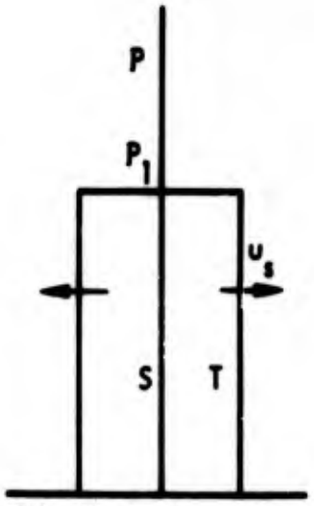

(b) Shock after collision

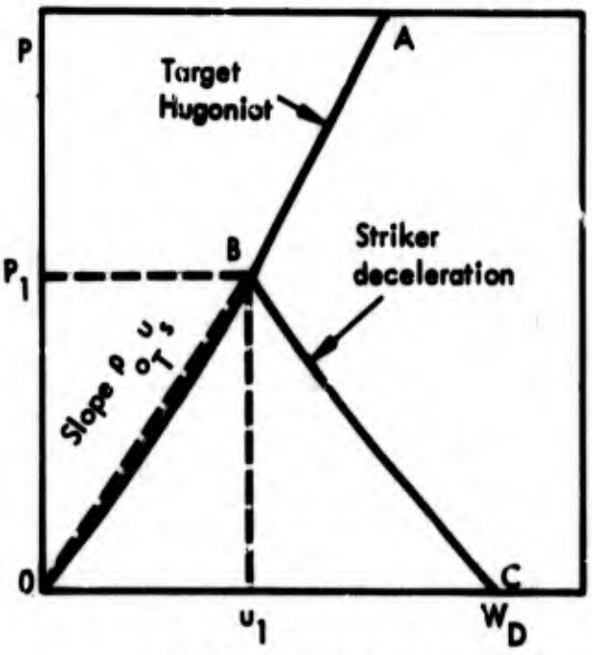

(c) $P\text{-}u_p$ diagram

W_D = Velocity of striker before collision

u_1 = Mass velocity in shocked region

u_s = Velocity of shock in target

P_1 = Shock pressure

OA = (Unknown) Hugoniot for target material

BC = (Reflected) Hugoniot for striker material

FIGURE A-4 Deceleration Method

RT-10-67-32

(scalar pressure) is valid for pressures >> material strength in compression.* It is also assumed that no cavitation occurs.**

Some possible sources of uncertainty or systematic error in the experimental methods described include:

(1) Nonuniform loading; tilt of flyer plate.
(2) Decay of driving pressure; decay of shock in screen protecting sample.
(3) Effects of unloading waves from sides of samples; effects of interacting waves; spall of flyer plate (Fig. A-5).
(4) Effect of air in free-run gap.
(5) Nonzero flash-gap closure time.
(6) Effects associated with drill holes (for pins), pins, solder and glue used to fasten specimens to plates, etc. Shorting of pins by air shock.
(7) Effects of heating; melting.
(8) Effects of ambient temperature.
(9) Nonhomogeneity or rheological anistropy of sample; effects due to grain size.
(10) Insufficient time for equilibration.
(11) Effects due to impurities.
(12) Deviation from hydrodynamic behavior at stress levels not much greater than the yield strength of the material.***

Uniformity of loading was monitored in the experiments reported in Walsh et al. (1957) by placing several pellets of "standard" material

*For example, the yield strength (maximum value of $|\sigma_x - \sigma_y|$ for plane compression in x-direction) for aluminum has been measured to be about 3 kilobars (Lundergan, 1961). I.e., at 200 kilobars the hydrodynamic approximation is about 1.5 percent in error.
**However, see discussions of "split-off" method below.
***See Chapter III, "Uncertainties of Plastic Flow Measurements."

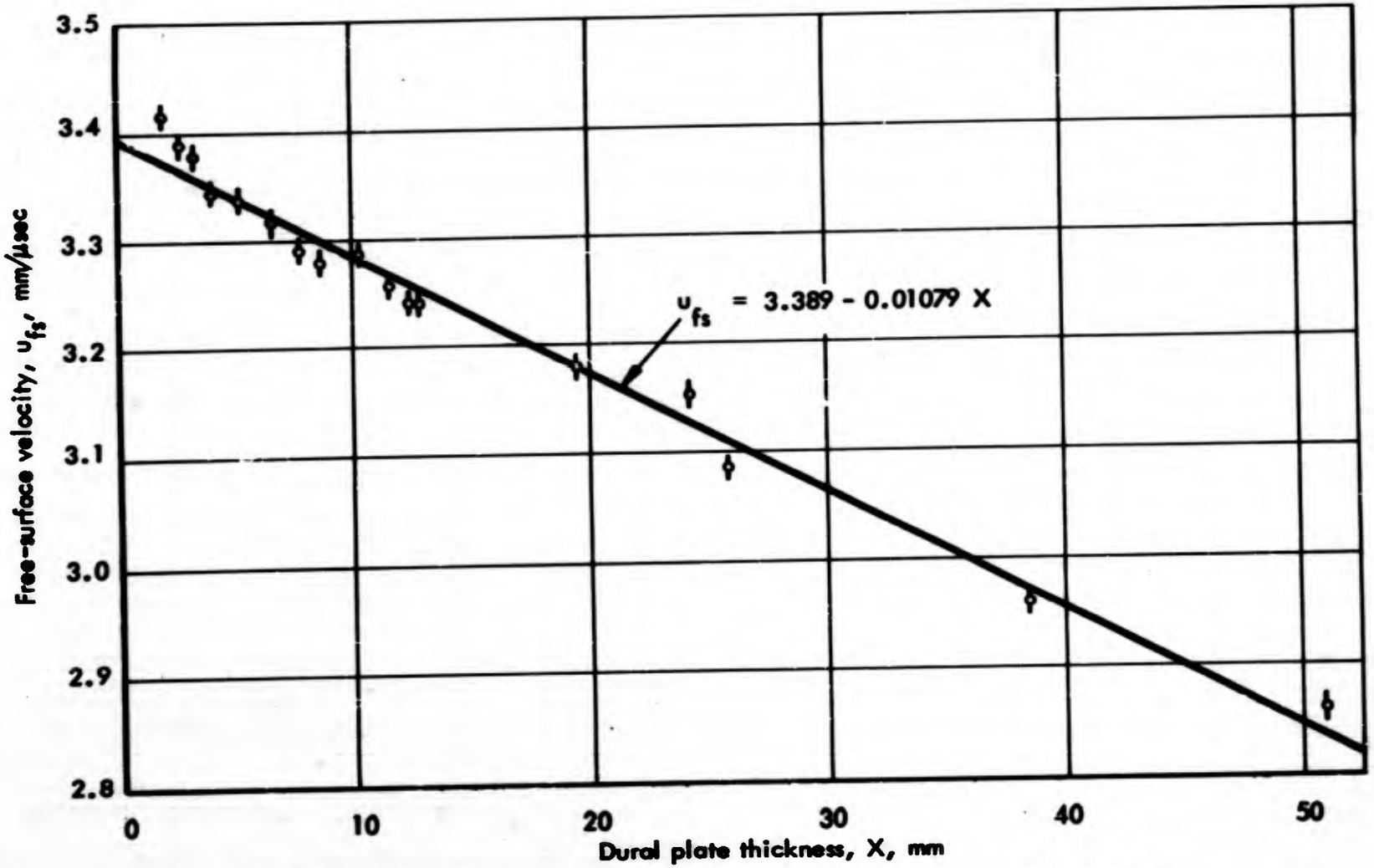

FIGURE A-5 Free-Surface Velocity as a Function of Thickness of Aluminum Plate (Deal, 1957)

in same shot with sample pellets.* The experimental arrangements were such that the driving pressure decayed with time;** this effect and that due to noninfinitesimal base length for velocity measurements were minimized by using thin plates, screens, etc., and short free-run distances, and by "centering" measurements.*** (See comments on Experiments H, J, K below.) Experiments on lead performed at the same time showed a 3 to 5 percent decrease in compression when thinner screens† and shorter base lines† were used. Smaller decreases were observed for iron and copper‡ (Figs. C-3 and C-4 of Appendix C).

---

*Movies of the motion of a grid system painted on the front face of flying plates (observed at 45°) are reported in Shreffler and Deal (1953). Unfortunately, no observations of the uniformity (i.e., across the surface of the plates) of the motion were reported.

**Except in the "flying plate" (deceleration) method. Deal (1957) has studied the decay of the pressure wave in aluminum (Fig. A-5). Note that the initial sharp spike (which has been called the "von Neumann spike") is removed by a few millimeters of Al, after which the decay is more gradual.

***The measured values of all shock velocities are the average value obtained from the transit time measurement on a 6.4 mm thick sample, which is assumed to be valid at the 3.2 mm thickness. All measurements are centered about the 3.2 mm level from the base plate surface; thus, degradation effects cancel in first order. The first order degradation in aluminum is approximately a 5 percent decrease in pressure per centimeter of shock travel, for the conditions of these experiments. This corresponds to a change in shock velocity of about 1/2 percent on passing through the samples used for shock velocity measurements. Slightly larger percentages would apply to some of the "softer" samples. No attempt has been made to measure this effect, and it will be assumed that all degradation effects cancel. The error this introduces is probably much less than 1/2 percent in shock velocity." (Christian, 1957)

†Actual thicknesses and lengths not given.

‡An obvious question that arises here is, "How does the offset vary with plate thickness?" How much more shift would occur if still thinner plates were used by both U.S. and Russian investigators? Qualitatively, in the "free-surface" or "split-off" method, since the shock velocity measurement precedes the free-surface velocity measurement (in time), too low free-surface velocities should be observed corresponding to a given measured shock velocity (unless compensated for by using thinner plates for free-surface motion measurement, i.e., "centering"). In the deceleration and reflection methods, the opposite effect would be expected to occur. Actually, in the deceleration method, the driver is still being accelerated by the explosive when it contacts the target (A'tshuler et al., 1958) to approximately compensate for the acceleration, the measurements of the driver velocity were centered, i.e., made over the same base as the shock motion messurement in the target. It would appear that the results reported in Al'tshuler (1958) were probably overcompensated.

Another effect--not discussed by the experimenters--is possible deviation of the velocity and pressure profiles behind the shock from flatness; i.e., profiles like:  . This effect, if it occurs, would result in experimentally determined mass velocities that are too low for the corresponding measured shock wave velocity in the free-surface technique. This may be an important source of systematic error in the experiments.* A phase change occurring on decompression following shock compression is another possible source of systematic error.

The experiments were designed to eliminate the effects of unloading waves from sides (by using sufficiently wide pellets) and interacting waves.** Results of an investigation by Shreffler and Deal (1963) indicate that several centimeters free-run is sufficient to insure that the pressure has decayed to a negligible level in a 0.5 cm plate driven by a 10-cm thick explosive charge. (See McQueen and March, 1960.) The effect of air in the free-run gap, while not mentioned in any of the references, is easily shown to be entirely negligible,*** at least in the case of the free-surface method. The case of the "deceleration" method may be a different matter, however, since in this case the air will be subjected to multiple shocks, which will also be transmitted

---

* A new technique making use of a manganin wire transducer has been used to check shock wave profile (Ahrens, et al. 1966, p. 25).

** For example, the flyer plate must be thick enough that effects from the face in contact with the H.E. do not weaken the shocks during the time of the measurement. (See discussion of this point in McQueen and Marsh, 1960, p. 1254.) Another question that might be raised is whether the grooves used for free-run free-surface velocity measurements (e.g., Experiments N and P) were wide enough that the center of the groove actually moved with the free-surface velocity. An estimate of the minimum ratio width/free-run gap required is $\Delta y/\Delta x > c_1/u_p$, where c_1 = sound speed behind shock in pusher plate, u_p = mass velocity behind shock. For brass, this ratio has values like 5.7/0.8 at 330 kilobars or 7.4/2.1 at 1190 kilobars (Alder, 1963). The groove dimension corresponded to $\Delta y/\Delta x \sim 12.5$ cm/0.5 cm, i.e., the groove was wide enough.

*** Imagine air as being the specimen material in the reflection method with an aluminum pusher, for example. The P - u_p Hugoniot for air is represented to a good approximation in Fig. A-3a by the u_p axis: P_{air} (3.95 km/sec) = 0.2 kilobars (Bothell and Evans, 1964).

into the metal plates. An investigation by numerical methods would be useful in order to estimate the uncertainty arising from the neglect of this effect.

In the photographic technique, small corrections were made for flash-gap closure time (Alder, 1963). Pin-contactor (Goranson et al., 1955) and photographic (Rice, et. al., 1958) results for 24ST Al agreed within 1 percent "on the average" (showing item 6 to be adequately accounted for). Air gaps due to the glued edges of the sample were assumed to be closed by the aluminum base plate moving at the free-surface velocity as measured on the standard reference pellet (Christian, 1957). Special protective caps were used in the Russian experiments to prevent shorting of pins by the air shock.

The temperature rises of strikers and screens were estimated in the Russian experiments and Experiments* D, F, E to be less than melting temperatures. For NaCl, Al, Fe and Cu, which have volume coefficients of expansion $< 1.2 \times 10^{-4}/^{o}C$ (Hodgman, 1958), a change in ambient temperature of $50^{o}C$ ($90^{o}F$) would correspond to a change of ρ_o of less than 0.6 percent.**

Experiments at 120 kilobars on single NaCl crystals with their axes oriented in various directions with respect to the shock gave the same results within experimental error (Alder, 1963), showing that the assumption of rheological isotropy is justified at high pressures.*** As for possible effects due to grain size, results for pressed NaCl showed no systematic deviation from results obtained using single crystals (Experiments 1, 3, and Fig. 1 of Chapter II).

---

* Table C-1, Appendix C.

** Corrections for ambient temperature were made in the experiments reported by Christian (1957). Presumably the assumption is made that a given pressure corresponds to the same compression on a hot day and a cold day.

*** The vicinity of a polymorphic transition represents an exception. See discussion of NaCl Hugoniot measurements.

In the "free surface" method a correction for the deviation from hydrodynamic behavior at low pressures near the free surface is appropriate,* although such a correction has not been made.

C. A METHOD OF USING CURVED SHOCKS

A wedge technique, described by Grine (1961), is useful for the lower pressure range (5 to 100 or so kilobars) and has the advantage that several Hugoniot points are obtained from each shot. Figure A-6 is a schematic of the method. The wedge is supposed to be long enough that steady-state conditions are established. Under these conditions the shock velocity at any point is given by

$$U_s = U_D \sin \theta = U_\alpha \sin \gamma ,$$

where U_D is detonation velocity in the explosive slab adjacent to the wedge of material under study, and U_α is the apparent velocity of the intersection of the shock with a plane parallel to the wedge face. From the geometry,

$$\cot \theta = \cot A + \frac{U_D}{U_\alpha \sin A} ,$$

so that U_s can be determined from measurements of U_D and U_α. The latter at various points along the wedge face is obtained from a

*The free-surface technique is referred to as the "split-off" method by the Russians: "At a certain distance from the surface the tensile stresses reach the limit of dynamic breaking strength; this leads to the formation of a crack and the splitting off of a thin plate. For matter with vanishingly small strength, the split-off plate is very thin. Under such conditions, it can be assumed that its velocity coincides with the free-surface velocity at the instant when the shock wave reaches it." (Al'tshuler et al., 1958) Split-off plate thicknesses of a few tenths of a millimeter were found for "the majority of [metals studied]." The correction due to the nonhydrodynamic unloading effect will be of the order of (material strength/shock pressure).

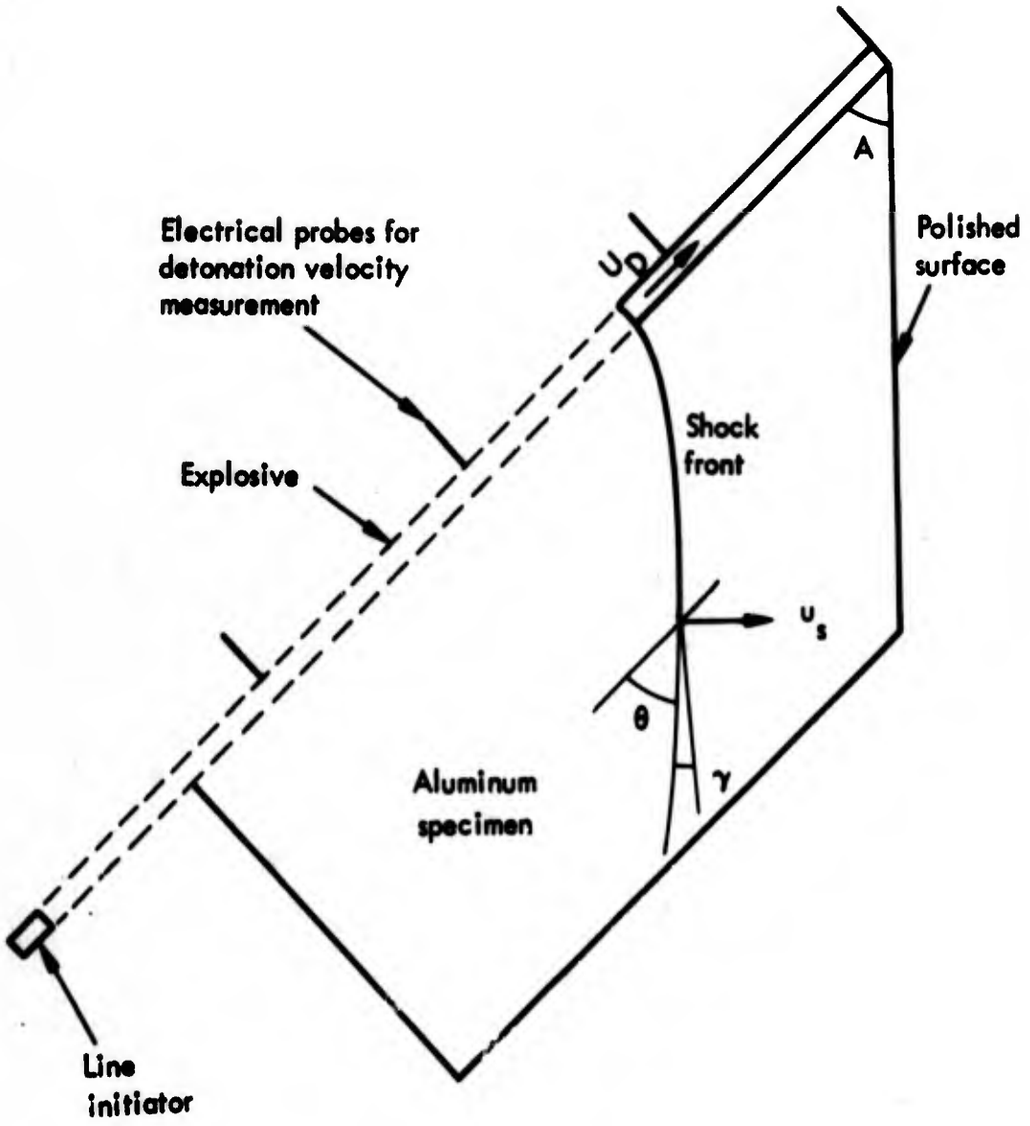

FIGURE A-6 Wedge Technique. Rock specimens can also be studied with this technique. (Figure from Grine, 1961.)

RY-10-67-31

smear camera record of the arrival of the wave at the face. At the same time, the component of free-surface velocity normal to the wedge face is measured by an optical method utilizing a mirror flat against the wedge face and another mirror raised slightly with respect to the wedge face (Fig. A-7).*

The progress of the detonation wave in the H.E. is measured with electrical pin contacts.

Because of the fairly complicated nature of the wedge method, the data reduction and analysis involve numerous assumptions, approximations, and corrections. Aside from those associated with the optical recording system,* the list includes:

(1) Assumption that steady-state condition is attained.
(2) Approximation of motion behind free surface as plane flow adjacent to region of constant state behind shock.
(3) Use of straight-line approximation to (P, V) Hugoniot as approximation for unloading adiabat.
(4) Correction for gradient (along wedge face) of normal component of surface velocity (U_n).
(5) Assumption that U_n is constant in time (after rise time of shock).
(6) Assumption that sample is rheologically homogeneous and isotropic.
(7) Assumption of uniformity of burning of H.E. charge. In case an elastic precursor is present, the situation becomes more complicated (Fig. A-8); in this case, the above list can be extended:
(8) Use of steady-state solution for reflection of plane elastic wave obliquely incident on plane free surface (i.e., to obtain material velocity behind elastic precursor).

*The method is not described in detail in Grine (1961). Recent work on the optical lever is described in Gregson (1967).

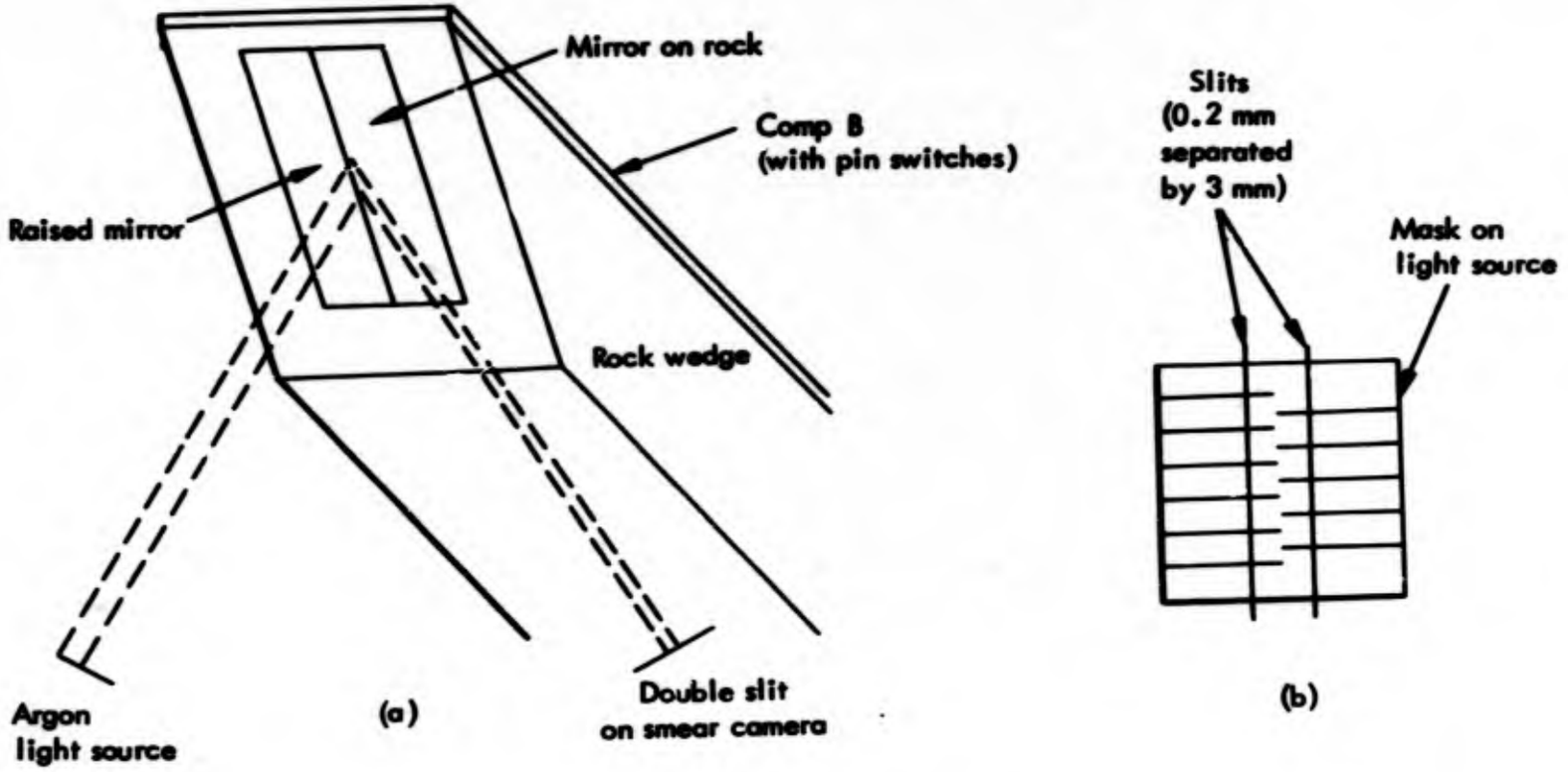

FIGURE A-7 Schematic of Wedge Experiment--Raised Mirror. (Figure from Grine, 1961)

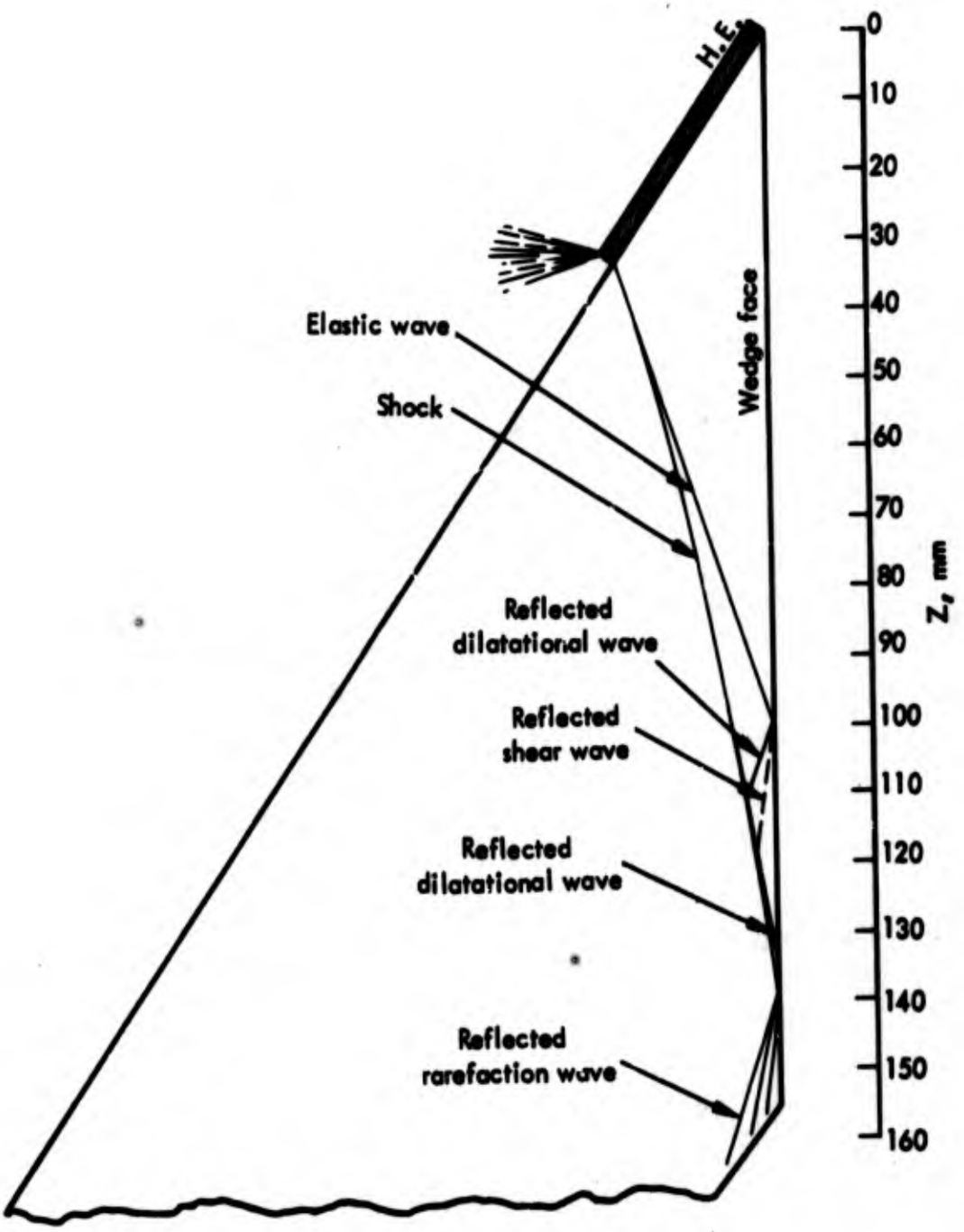

FIGURE A-8 Schematic Showing Wave Interactions for Case Where Shock is Preceded by Elastic Precursor (wedge method) [Fowles, 1960]

(9) Neglect of dilatational and shear waves "reverberating" between free surface and shock. (I.e., in applying Rankine-Hugoniot relations to determine state behind shock, state ahead of shock is assumed to be same as behind leading elastic wave.)

(10) Assumption that material unloads elastically with $d\sigma_x/de_x$ = value along elastic loading path, and then plastically.

The steady state assumption would be easily verifiable by repeating the experiment using a longer wedge, although the papers do not mention whether this was done. A machine calculation of a detonation wave propagating in an H.E. slab adjacent to an aluminum slab reported by Wilkins (1962) was not carried far enough for steady-state conditions to obtain. More refined two-dimensional machine calculations would be useful to check some of the other assumptions which enter the data reduction and analysis. A perturbation treatment of plane flow, using the angle of incidence and shock wave curvature (assumed small) as perturbation parameters, might also be a possible approach. Clearly, if the curvature of the shock front is small and the wedge angle is such that near-normal incidence obtains, the plane flow approximations improve.

A correction to the doubling approximation ($u_p \sim u_{fs}/2$) derived on the basis of approximations in the lists above, was found to be of the order of 6 percent (Fowler, 1960). A correction to $\alpha = -U_n U_\alpha$ (α = angle through which free surface is turned, U_n = free-surface velocity, U_α = apparent shock velocity along wedge face) resulting from the gradient of U_n along the wedge face was found to amount to about 5 to 10 percent.

The use of the Hugoniot as an approximation for the unloading adiabat has already been discussed.

Item 6 in the list above was not discussed in Grine (1961).

The effects of inhomogeneities of the sample show up as rough traces in the shock and free-surface arrival records. "The differences between the recorded curves and ideal smooth curves are small but the

differences between their slopes are often large. The average free-surface velocity depends on the difference in time between shock arrival and free-surface arrival traces so that small errors in the traces give only small errors in free-surface velocity. However, determination of shock velocity involves a differentiation of the shock arrival trace, either by reading slopes from the film or by numerical differentiation of the points. The large errors in slope cause large errors in desired shock velocity." (Grine, 1961)

D. OTHER METHODS

Other--much less accurate--methods involving density measurements by X-ray densitometry and pressure measurements with piezoelectric crystals appear to confirm the results for metals obtained by the photographic and pin-contactor methods (Rice et al., 1958).

A technique using porous samples* shows promise of greatly extending the region of the P-V diagram which can be reached in shock experiments (Zel'dovich and Rayzer, 1963). Higher pressures are needed to compress a porous body to the same final density as in shock compression of the normal, nonporous material. The higher pressures correspond to considerably higher temperatures.

Underground tests of conventional or nuclear explosive sources represent another technique for "Hugoniot measurements."**

---

*Prepared by pressing powders.

**Assessment of the uncertainties associated with these tests is beyond the scope of the present study.

APPENDIX B

PROPERTIES OF ROCK SALT IN SALT DOMES

APPENDIX B

PROPERTIES OF ROCK SALT IN SALT DOMES

The following information is extracted from Kupfer (1963):*

> The composition of Gulf Coast salt is remarkably pure sodium chloride (halite) with traces of calcium sulfate (anhydrite) and very little else. Despite considerable variation from mine to mine and from place to place within the mines, all of the mines maintain a grade of better than 97% NaCl, and with just a little care in choosing the proper faces to mine, grade can be maintained above 99% NaCl at most of the mines.
>
> The anhydrite content of the salt domes has commonly been quoted at 5-10%, but for the operating mines this seems high. High individual samples are sometimes quoted, ..., but these are rare and probably are inclusions. There is a need for accurate figures, but a "guesstimate" would be that the average anhydrite content is well under 3%.
>
> Taylor (1938) says that 99% of the insoluble impurities in salt are anhydrite and that the other 1%, more or less in order of abundance, includes dolomite, calcite, pyrite, quartz, iron minerals, celestite, sulfer, and traces of other minerals. Dissolved impurities include less than 1% of ions like carbonate, sulfate, calcium, magnesium, and sometimes potassium. Bloomberg and Ladenburg (1959) reported Al, Fe, Mn, K, Si, and Sr in concentrations of about 100 parts per million from what is probably the Avery mine.

---

*The author thanks Mr. Charles F. Withington of the USGS for bringing this source to his attention, and Professor R. A. Heimlich, President, Northern Ohio Geological Society, for permission to use the quoted material. The paper referred to includes an extensive bibliography. (See also Adams, 1963.)

Layering in the salt is its most distinctive physical feature in all of the mines. Most layers average 1-10 inches thick and consist of interbedded light and dark bands ... Thinner layers are common and some massive beds of white or dark salt are several feet thick ... The layers are assumed to represent original bedding ... The layers have been folded, stretched, recrystallized, and deformed ... The layers in the salt all stand essentially vertical and are isoclinally folded about vertical axes.

Grain size is coarse, distinctly crystalline, with prominent cubic cleavage everywhere apparent. Most crystals range between ¼ - ½ inch in diameter and are equant. ... Fine- to very fine-grained salt is rare. Pods of extremely coarse-grained salt occur in all the mines....

In a salt stock every transition can be found from folding to faulting, but the faults are all of the bedding-slip type. Displacements, so far, have been indeterminate. Stratigraphic separation appears to be negligible on most, although slip might be quite large.

Large, distinctive, and sharply transverse faults appear appear to be absent in most salt stocks. Probably salt, under most conditions, is too plastic to fault in this manner....

... The overall shape of halite crystals is slightly elongate in the vertical dimension, parallel to the fold axes. The ratio of the vertical to the horizontal axis is commonly about 1.5, but ratios of up to 6.0 are shown....

Shear structures, probably the result of shear folding, are abundant at Grand Saline dome and at Winnfield, but are not common features at the other mapped mines....

Not a single fracture is exposed in (Grand Saline) mine.... Porosity and permeability are effectively nil.

A chemical analysis of two samples from close to the point of one of the Project COWBOY explosions (Carey Co. mine) gave the following results (Guide and Warner, 1960):

% by Weight	Ca	Fe	SO_4	Free H_2O	Others	NaCl
(±0.01%)	1.30	0.0025	2.97	0.027	0.10	95.7

Average porosity was found to be

$$1 - \frac{\text{bulk density}}{\text{grain density}} = 0.014 \pm 0.014 \ ,$$

where the grain density was determined by weighing powdered specimens and measuring volume of kerosene displaced.

Rawson and Hansen (1965) list properties of a sample from Tatum dome (Mississippi):

	Weight, percent
NaCl	90
$CaSO_4$	10
H_2O	0.001

$\rho = 2.4$ g/cm^3

$c_p = 4550$ m/sec; $c_s = 2160$ m/sec

Rawson, et al. (1966) discussed the post-shot environment due to a 5-kt nuclear detonation ("SALMON") in Tatum salt dome (Mississippi):

> All changes in the characteristics of the salt around the cavity suggest that it is less competent than before the detonation, that the post-shot stress distribution around the cavity is variable in space, and that the stress is most intense below the cavity ... We have not been able to measure in situ stress or make meaningful laboratory measurements of the inelastic properties of this material ... No radioactive melt injection into fractures was observed above the cavity. Below the cavity, radioactive melt injection was observed out to 2.2 cavity radii [cavity radius = 17.4 ± 0.6 m]. Extensive micro-fracturing, some macro-fractures, radioactive gas penetration, decrease in sonic velocity, decrease in bulk density, and increase in permeability were observed out to about 3.7 cavity radii. The most severe degradation of mechanical properties of the salt was observed in a region 39 to 50 m below the shot point.

APPENDIX C

UNCERTAINTIES IN HUGONIOT MEASUREMENTS FOR PUSHER MATERIALS

APPENDIX C

UNCERTAINTIES IN HUGONIOT MEASUREMENTS FOR PUSHER MATERIALS

The materials which have been used as pushers in the Hugoniot measurements for rocks include aluminum, iron, and copper. The experiments for measurement of the Hugoniot curves for these materials are summarized in Table C-1. It is fortunate that measurements have been made using the several techniques described above both in this country and in the Soviet Union. The Hugoniot data for the metals used as pushers are collected and shown in Figs. A-3a and A-5b of Appendix A and Figs. C-1 through C-4 of this Appendix. Estimates of the uncertainties indicated by shading in Figs. C-3 and C-4 assume no undiscovered systematic errors common to the experiments. The rough estimates of uncertainty are based on consideration of information given below and the scatter of the experimental points, along with some judgment. Mainly, the uncertainty limits were chosen more or less as an envelope of the experimental points.* The uncertainties in P_H, V_H are related to the uncertainties in the velocities by

$$\left| \frac{\Delta(P_H - P_0)}{P_H - P_0} \right| \lesssim \left| \frac{\Delta u_s}{u_s} \right| + \left| \frac{\Delta u_p}{u_p} \right|$$

$$\left| \frac{\Delta(V_0 - V_1)}{V_0 - V_1} \right| \lesssim \left| \frac{\Delta u_p}{u_p} \right| + \left| \frac{\Delta u_s}{u_s} \right| .$$

---

* A least-squares analysis of the data would be more quantitative. Such an analysis should treat u_s and u_p symmetrically, taking into account the estimated errors in the measurements of these quantities.

Table C-1. HUGONIOT MEASUREMENTS FOR PUSHER MATERIALS

Experiment	Material	Method	"Centered"?	Approximations in Analysis[a]	Adiabat[aa]	Pusher	Hugoniot for Pusher	Plot	Pressure Range, kilobars	Reference
A	24ST Al (95% Al)	Free surface		(Not reduced?)	---	---	---	---	146-33,	Corenson et al. (Quoted in Rice et al.)
B	24ST Al	Free surface[aaa]		"Doubling"	Not used	---	---	---	134-347 (15 points)	Walsh & Christian, Phys Rev 97, 1544 (1955)
C	Copper	Free surface[aaa]		"Doubling"	Not used	---	---	Fig. A-9	185-466 (10 points)	Walsh & Christian, Phys Rev 97, 1544 (1955)
D	24ST Al	Free surface	Yes	Corrected for "doubling" approximation	Phys.Rev. 108, 316 (1957) (based on Mie-Grunaisen equation of state & Dugdale-MacDonald relation)	---	---	Fig. A-3a	100-485 (~ 100 points)	Walsh et al, Phys. Rev 108, 196 (1957)
E	Iron (< 0.8% impurity)	(1) Free surface (2) Reflection	Yes Yes	"Doubling" Corrected	(Reflected shock)	24ST Al	b	Fig. A-9	356-479 (8 points)	Walsh et al., Phys. Rev. 108, 196 (1957)
F	Copper (< 0.8% impurity)	(1) Free surface (2) Reflection	Yes Yes	"Doubling" Corrected	(Reflected shock)	24ST Al	b	Fig. A-9	216-510 (5 points)	Walsh et al., Phys. Rev. 108, 196 (1957)
G	24ST Al	Free surface (with flying plate)[f]		(Not reduced)				Fig. A-6	600-(> 1000)	McQueen (quoted in Rice et al.)
H	Iron (low-carbon steel)	(1) "Split off" (2) Deceleration (with "screen")	Yes Yes	"Doubling" (Exact)	Not used ---	--- Iron	--- ---	Fig. A-6	400-1410 300,1270-4870	A.'tshuler et al., JETP 7, 606 (1958)
J	Copper	Reflection (with flying plate)	Yes	"Mirror"(?)	(Reflected shock)	Iron	H	Fig. A-9	450,1460,3900	Al'tshuler et al., JETP 7, 614 (1958)
K	Aluminum	(1) Deceleration (Al screen)		(Exact)	---	Aluminum	---	---	693	Al'tshuler et al., JETP 11, 573 (1960)
		(2) Deceleration (Al screen)		Interpolation	(Reflected shock)	Iron	L	---	(1047,1971	
L	Iron	(1) Decelera-(? tion (iron screen)			(Reflected shock)	Aluminum	K	---	1045	Al'tshuler et al., JETP 11, 573 (1960)
		(2) Deceleration		(Exact)	---	Iron	---	Fig. A-6	1815,3566,4672	
M	Copper	(1) Deceleration (Cu screen)			(Reflected shock)	Aluminum	K		1079	Al'tshuler et al., JETP 11, 573 (1960)
		(2) Cu screen ? Fe screen		[illegible] + E.S. Corr. (?)(4187 pt.)	(Reflected shock)	Iron	L	Fig. A-9	1930 3760[g] 4187	
N	Iron	Reflection (with flying plate)	Yes	(Corrected)	J Appl Phys 31, 1253 (based on M-G & D-M)	Brass	J Appl Phys 31, 1253	Fig. A-8	477-1730	McQueen & Marsh, J. Appl. Phys. 31, 1253 (1960)
P	Copper	Reflection (with flying plate)	Yes	"Mirror"(?)	(Reflected shock)	Brass	J Appl Phys 31, 1253	Fig. A-9	875-1444	McQueen & March, J. Appl.Phys. 31, 1253 (1960)
Q	Iron (low-carbon steel?)	Deceleration		(Exact)	---	Iron	---	---	8700	Al'tshuler et al., JETP 13, 65 (1962)
R	Copper	Reflection (with flying plate)		"Mirror"(?) + Extrapol.	(Reflected shock)	Iron	L, Q	---	9070	Al'tshuler et al., JETP 13, 65 (1962)
S	Aluminum	Deceleration		Interpolation	(Reflected shock)	Iron	L, Q	---	4930	Kormer et al., JETP 15, 477 (1962)
T	Copper	Deceleration		Extrapolation	(Reflected shock)	Iron	L, Q	---	9550	Kormer et al., JETP 15, 477 (1962)
U	2024 Al	Free surface (?)		Corrected	See van Thiel (1966)	---	---	Fig. A-6	15-1022 (6 points)	Marsh (LASL) (unpublished) quoted in van Thiel (1966)
V	2024 Al	Free surface (?)		Corrected	See van Thiel (1966)	---	---	Fig. A-6a	121-1115	LRL unpublished data quoted in van Thiel (1966)
W	Copper	Deceleration (?)		(Exact)(?)		Cu (?)	---	Fig. A-9	719-1274	Persson and Persson (1964) quoted in van Thiel (1966)
X	Copper	(?)		(?)		(?)		Fig. A-9	740-1500	Berger and Fouquignon (1964) quoted in van Thiel (1966)

[a] See text for discussion of "doubling" and "mirror" approximations "E.S. correction" means that the "cross curves" were generated by making use of an assumed equation of state for the pusher material.
[aa] I.e., for material studied in free-surface method; for pusher material otherwise.
[aaa] The experimental arrangement made use of a tilted lucite block matching a groove in the sample.
[b] The points corresponding, to $u_{24} > 3.5$ km/sec (Fig. A-6) were obtained using the free-run technique.
[g] Result of Experiment J corrected for decay of shock wave in screen and sample.

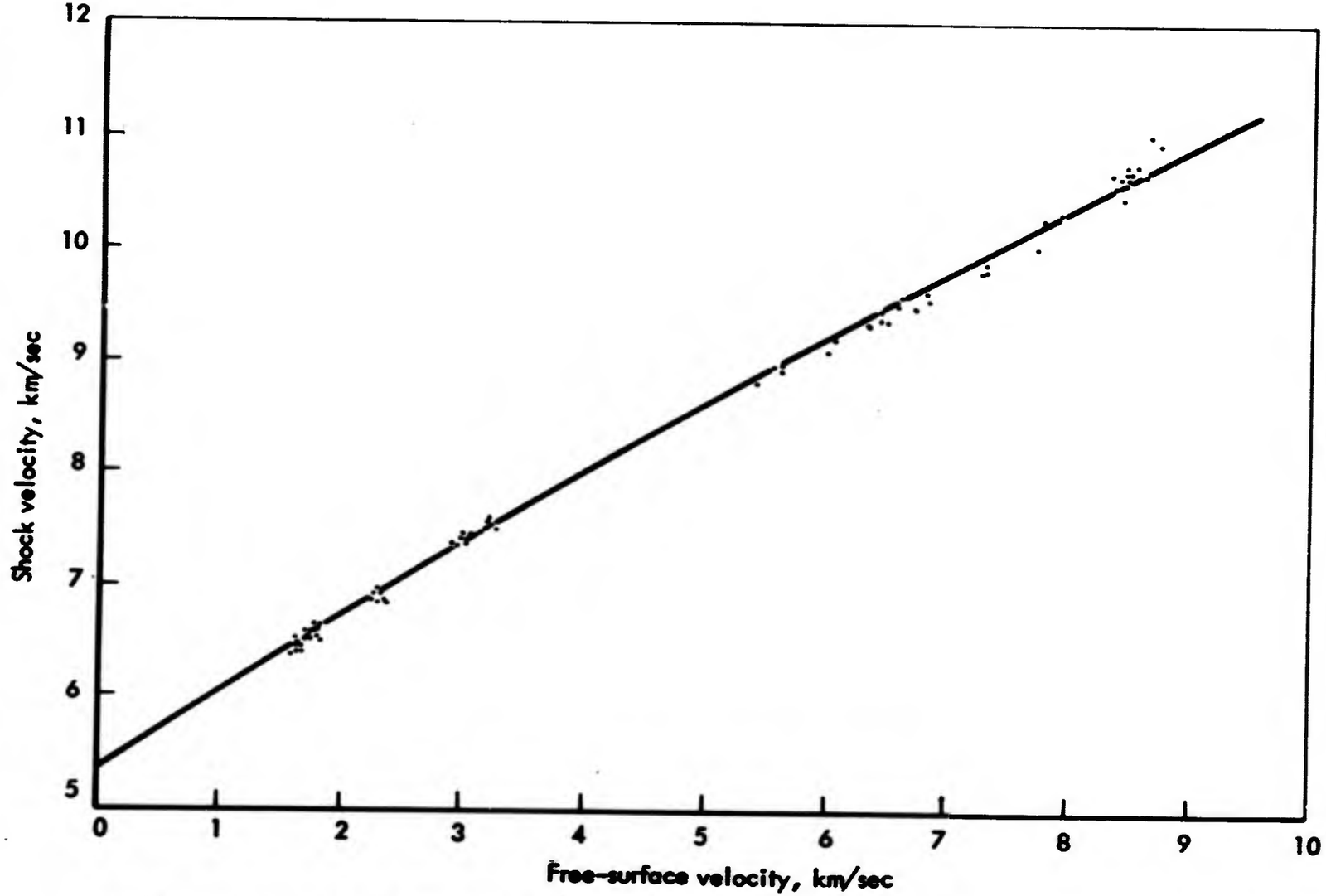

FIGURE C-1 Experimental 24ST Aluminum Shock Velocity Versus Free-Surface Velocity (Experiment "G", Table A-1).

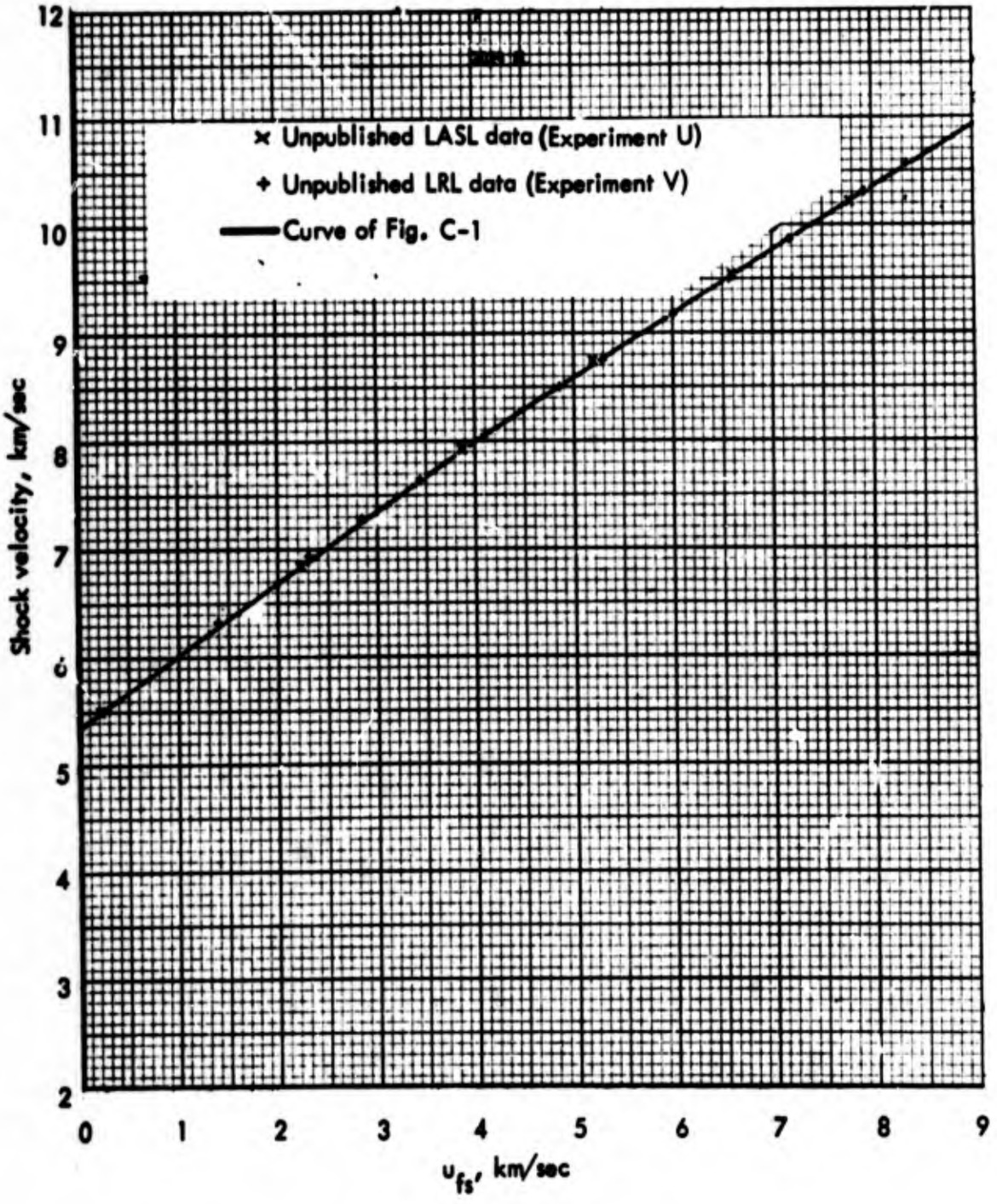

FIGURE C-1a Shock Measurements for 2024 Aluminum (Experiments U and V, Table C-1). Also shown for comparison is the curve of Fig. C-1.

RT-10-67-38

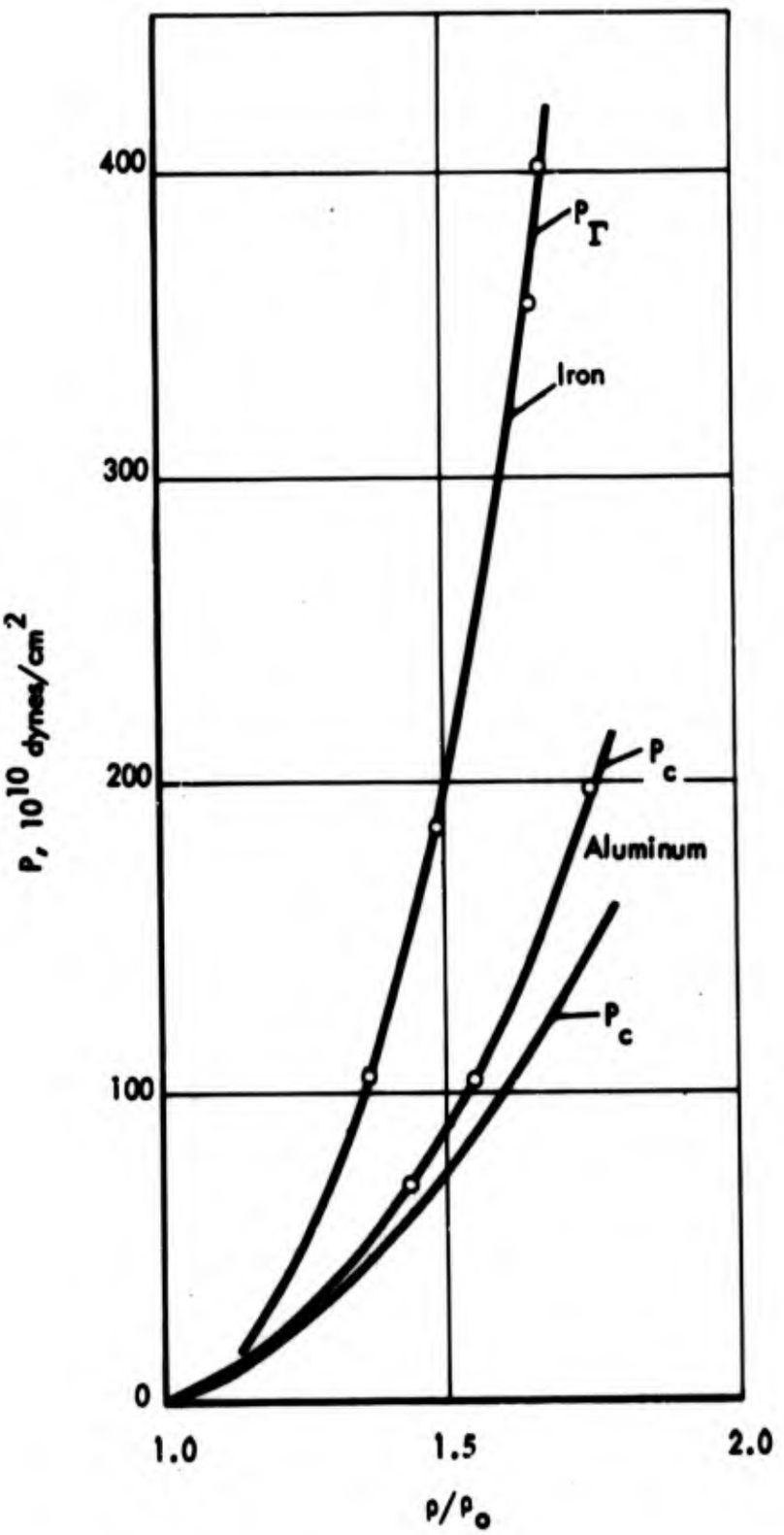

FIGURE C-2 Hugoniot Data for Iron and Aluminum (Experiments K, L). Also shown is T = 0 isotherm for aluminum. (Figure from Al'tshuler, et al., 1960.)

R7-10-67-36

Comparisons of U.S. and Russian measurements for aluminum would not be too useful, since the samples studied may have had different compositions. The data for iron and copper are replotted on a large scale to facilitate comparison in Figs. C-3 and C-4. Estimates by the author of the present report of the uncertainty in the iron and copper Hugoniot curves are indicated in Figs. C-3 and C-4 by the shaded "uncertainty bands." As disucssed below, the data of Experiments H and J are considered to be shifted toward higher mass velocities with respect to the more recent data.* The earlier data for iron (Experiment H) suggest a discontinuity near u_p = 3.7 km/sec. Note that the curve shown in Fig. C-1 does not give a statistically meaningful fit to the 24ST alumirum data for shock velocities greater than 8.75 km/sec. The uncertainty in the Russian aluminum points corresponding to the three highest pressures (Experiments K(2) and S) would be somewhat larger than the uncertainty in the iron points on which the aluminum measurements depend (Experiments L and Q).

For the highest pressure points measured for iron (8700 kilobars) and Cu (9070 kilobars,** the velocity of the steel flyer plate "was determined in 12 experiments" to be 14.68 km/sec "with a probable error of ±1.5 percent. The values of the [shock] wave velocities obtained by averaging 6-8 separate experiments were found with an error of ±1 percent. The resultant inaccuracy in the determination of the degree of compression . . . ($\sigma = \rho/\rho_o$ . . . is equal to ±0.035 for iron and copper."*** (Al'tshuler et al., 1962.)

Note that in Experiment K(2) the solution at P = 1971 kilobars depends on interpolation between the points of the iron Hugoniot at 1855 and 3568 kilobars determined in Experiment L. Similarly, the

---

* Note, however, that the most recent data for copper (Experiments W and X) seem consistent with a data point of Experiment J. Detailed descriptions of Experiments W and X are unavailable.

** Not shown in the figure is a higher pressure point (Experiment T).

*** The 4022-kilobar point (and possibly other points) of Experiment L was revised slightly downward (in pressure) in Al'tshuler et al. (1962) for unspecified reasons.

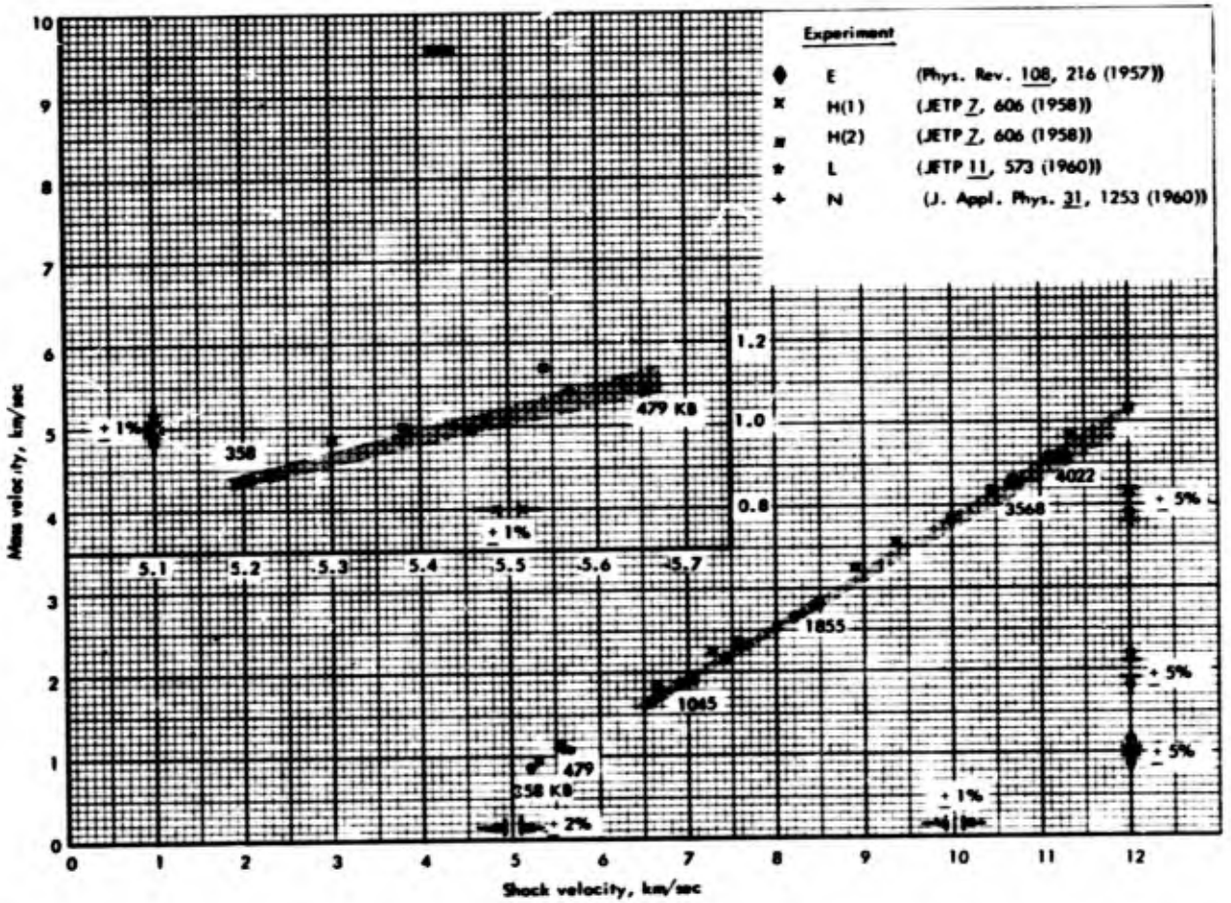

FIGURE C-3 Mass Velocity Versus Shock Velocity Data for Iron (low-C steel) from Experiments Summarized in Table A-1.

The low velocity region is magnified at the left. (For clarity, some of the low velocity points are omitted from the main graph. The data from Experiment E were obtained by the free-surface method. Data corresponding to the four highest velocity points of that experiment obtained by the reflection method agree within 1 percent with the points shown.) The shaded area represents an estimate of the uncertainty associated with the data.

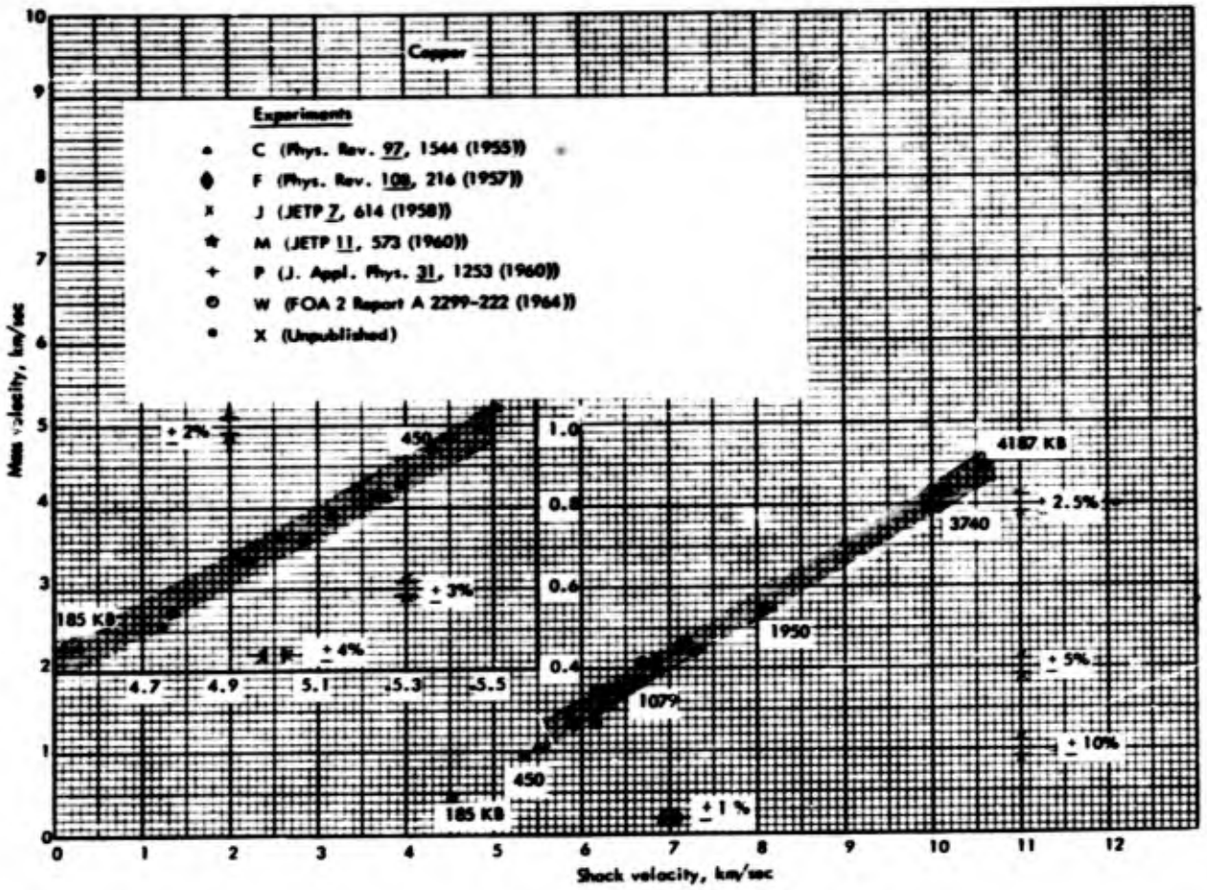

FIGURE C-4 Mass Velocity Versus Shock Velocity Data for Copper from Experiments Summarized in Table A-1

The low velocity region is magnified at the left. (For clarity, some of the low velocity points are omitted from the main graph.) The shaded area represents an estimate of the uncertainty associated with the data.

solutions for Cu in Experiment M depend on extrapolation from points on the aluminum and iron Hugoniots as measured in Experiments K and L.

The Experiments K, L, and M were carried out partly to check possible errors arising from use of the "doubling" approximation in Experiment H and due to decay of the shock wave in the screen protecting the samples, by substituting thinner screens.* According to Al'tshuler et al. (1960), "the inaccuracy in the determination of [the striker and shock wave velocities] did not exceed 1%" (Experiments K, L, M). Each result was obtained as the mean of the values from 4 to 6 experiments. The results for low-C steel and copper are shown along with the earlier results (Experiments H and J) in Figs. C-3 and C-4. Al'tshuler et al (1962) noted that, "in the mean, the mass velocities of [McQueen and Marsh, 1960, results for 8 metals, including Experiments N and P] (for one and the same [shock velocity]) exceed the mass velocities obtained by the present authors by about 2 per cent." The difference was interpreted as being due to the use of the equation of state in the little-studied region $\rho < \rho_o$ to correct the "doubling" approximation for the determination of the mass velocity in the brass screen by McQueen and Marsh (1960). The latter authors, on the other hand, suggest that the difference is due to the use of an experimental geometry characterized by a too-small value of width/thickness by Al'tshuler et al. (1960).

In the earlier experiment (Experiment H), time intervals were recorded with an accuracy of $\pm 5 \times 10^{-9}$ sec, resulting in relative errors for striker and shock velocities, "obtained by averaging data from 3 to 4 experiments, in each of which the measurements were repeated a few times," of ±0.01, corresponding to relative errors in ρ/ρ_o of ±0.01 at $\rho = 1.5\rho_o$ and ±0.03 at $\rho = 2\rho_o$, and relative errors in P of 1.5 - 2 percent. The data for Experiment J depend on the iron data of Experiment H, which are in poor agreement with the later measurements.

*In Experiments K, L, M, a base line of 3 to 4 mm was used for the measurements. Al'tshuler (1958) did not mention the presence of the screen.

Walsh and Christian (1955) discuss the possible inaccuracies in the determinations of the 24ST Al and Cu Hugoniots (Experiments B and C):

> Probable errors for individual velocity determinations are of the order of 0.5 percent. Most of this error (about 0.4 percent) is ascribed to shot assembly uncertainties. Tolerances in this phase of the work are accordingly low, all measurements in the Lucite-metal assembly being made to 0.0001 in. Uncertainty in the analysis if 0.1 percent to 0.5 percent, depending upon record quality. Assembly and analysis measurements are made individually for each experiment, so that the resultant errors should be random and represented by scatter in the final data. Camera writing speed, however, is applied in the determination of all velocities. This parameter has been measured to better than 0.2 percent and is therefore believed to be eliminated as the only possible source of consistent error in the determination of velocities. . . . Overall precisions for experimental Hugoniot points are determined by the accuracy of the ["doubling"] approximation, the precision of the velocity measurements . . ., and the transformation equations to the P-V plane. Results may be conveniently summarized as estimated probable errors in compression for a given pressure, as applied to the curves. These overall uncertainties are estimated at 1 percent for the 24ST-aluminum curve and 2 percent for the copper curve.

For experiments D, E, and F, "the probable error per data point, determined from the observed reproducibility, is 0.7 percent in shock velocity for a given free-surface velocity (about 1 percent in compression, $1 - V/V_o$ at a given pressure)." Refinements to the free-surface data based on an assumed equation of state for 24ST Al reduced the compression offsets (P - V plot) between the "doubling" approximation and reflection method solutions from an average magnitude of 1.1 to 0.7 percent. The results were found to agree with the earlier results (Experiments B and C) "to within 2% or better," and with "shock-wave data [for 24ST Al (Experiment A?)] obtained by another Los Alamos group using an electrical pin-contactor method . . . everywhere better than 1% in compression, [which] is sufficiently good to

indicate freedom from sizable consistent error of either method."* (Walsh et al., 1957)

The error due to the use of the free-surface approximation was bounded by arguments given in Walsh and Christian (1955) for pressures < 400 kilobars in copper and aluminum. (See footnote on the third page of Appendix A.) For the measurements at higher pressures (Experiments G, U, V) corrections calculated on the basis of assumed equations of state were made to the free-surface approximation data.**

It is worth emphasizing that of the experiments summarized in Table C-1, only those data points obtained by the deceleration method do not depend on corrections based on assumed theoretical equations of state.**

Results for 24ST Al obtained by using the wedge technique are shown in Fig. C-6, from Katz et al. (1961). For these experiments a somewhat different recording method was used, utilizing argon flash gaps and a free-run gap. For data reduction purposes the shock was treated as an (infinite) plane shock obliquely incident on the (infinite) wedge face. The doubling approximation $u_{fs} = 2\ u_p$ was made. Note that no mirror "impedance match" was required. The figure shows points from Experiment D (Table C-1) for comparison. "With the exception of points at high velocities, obtained near the explosive-metal interface, agreement among the three shots is within ±1.5% of the shock velocity, consistent with the uncertainty in the detonation velocities which enter directly into the calculation of the shock velocities. . . . A break is observed in the free-surface trace on every shot, free-surface velocity and consequently pressure increasing more rapidly above the break. This break is represented by points to the right of the curves, which have not been extended to include them. Detailed

---

*A compressional elastic wave velocity = 5.72 km/sec has been measured for low-C steel (Katz et al., 1959). No elastic precursor was observed in Experiments E and H.

**The time constraint on the present report precluded investigation of the uncertainties in equation of state for pusher materials.

consideration of the nonuniformity of the shock, produced by the von Neumann spike in the detonation wave [see above], may account for the break in these curves." (Katz et al., 1959) An elastic precursor propagating with velocity 6.2 mm/μs was not observed in these experiments, although it has been measured in other experiments (Lundergan, 1961).

The measurements on aluminum with the wedge technique can be compared directly with isothermal compressibility measurements (Bridgman, 1948), since below 100 kilobars the deviation of the Hugoniot from the 20°C isotherm is small, less than the scatter in the experimental points (Walsh et al., 1957). It is somewhat unsettling that the comparison (Fig. C-5) demonstrated a rather glaring discrepancy between the results of the static and dynamic experiments. This was interpreted by Katz et al. (1959) as being due to the wrong choice "on presumptive ground" of two possible sets of static compression data "obtained under somewhat different experimental conditions."* The rejected data at 98 kilobars were found to agree with the shock measurements.

---

*"Four runs were made: two with an indium sheath and two without. The agreement between the two sets was not as good as desirable, the volume at 100,000 given by the former being 0.903 against 0.915 by the latter. The latter was made the basis of the results in the table, since it is presumptively more correct because of the absence of correction for the sheath. The variation of compressibility given by this series, however, is presumptively not correct, a slight increase of compressibility with increasing pressure being indicated, in opposition to the definitely indicated decrease of compressibility of the much more accurate measurements by the method of linear compressibility, as yet unpublished, to 30,000. The course was therefore adopted of showing a linear decrease of volume in the table between 25,000 and 100,000." (Bridgman, 1948)

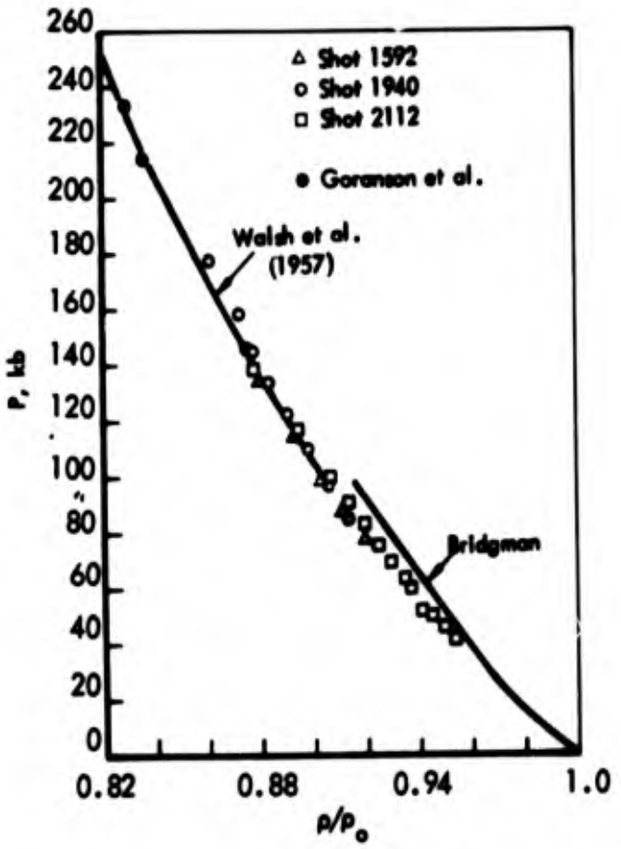

FIGURE C-5 Shock Compression Measurements for 24ST Al. Open symbols represent data of Katz et al. (1959)(wedge technique). Data of Experiments A and D (Table C-1) and static compressibility measurements of Bridgman (1948) are shown for comparison. (Figure from Katz et al., 1959)

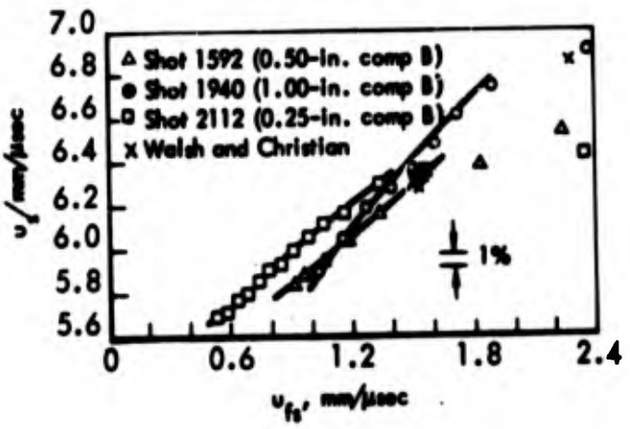

FIGURE C-6 Mass Velocity versus Shock Velocity Data for 24ST Al. Obtained by Wedge Method (Katz et al., 1959). Data of Experiment B (Table C-1) are shown for comparison.

BLANK PAGE

BIBLIOGRAPHY

Abramowitz, M. and I.A. Stegun, eds., Handbook of Mathematical Functions, N.B.S., Applied Mathematics Series, No. 55, Dover Publications Inc., New York, N.Y., 1964.

Adams, J.E., "Permian Salt Deposits of West Texas and Eastern New Mexico," Symposium on Salt, A.C. Bersticker, ed., Northern Ohio Geol. Soc., Inc., 1963.

B.J. Alder, "Physics Experiments with Strong Pressure Pulses," Solids under Pressure, William Paul and D.M. Warschauer, eds., 1963.

Ahrens, T.J. et al., "Dynamic Properties of Rocks," Final Report, SRI Project FGU-4816, DASA-1868 (1966).

Al'tshuler, L.V. et al., Soviet Phys. JETP 7, 606 (1958).

----------, Soviet Phys. JETP 11, 573 (1960).

Al'tshuler, Kormer, Bakanova, and Trunin, Soviet Phys. JETP 11, 573 (1960).

Al'tshuler, L.V. et al., Soviet Phys. JETP 11, 766 (1960).

Al'tshuler, Kuleshova, and Pavlovskii, Soviet Phys. JETP 12, 10 (1961).

Al'tshuler, L.V. et al., Soviet Phys. JETP 15, 65 (1962).

----------, Soviet Phys. Solid State 5, 203 (1963).

Al'tshuler, Pavlovskii, Kuleshova, and Simakov, Soviet Phys. Solid State 5, 203 (1963).

Al'tshuler, L.V., Soviet Phys. USPEKHI 8, 52 (1965).

Bell, J.F. (See discussion in Hauser, 1961).

Berger, J., and C. Fouquignon, unpublished data (1964) quoted in van Thiel (1966).

Born, M. and K. Huang, Dynamical Theory of Crystal Lattices (International Series of Monographs on Physics), Oxford, 1954.

Dothell, L.E. and B.S. Evans, "Shock Front Relation for Air in Thermodynamic Equilibrium for Altitudes from Sea Level to 60 Kilometers and Sea Level to 230 Kilofeet," Report KN-64-326(R), Kaman Aircraft Corp., Nuclear Division, 1964.

Bridgman, P.W., Proc. Am. Acad. Arts Sci., 74, 21-51 (1940).

----------, Proc. Am. Acad. Arts Sci., 76, 9-24 (1945).

----------, Proc. Am. Acad. Arts Sci., 76, 1 (1945).

----------, Proc. Am. Acad. Arts Sci., 76, 71-89 (1948).

----------, Proc. Am. Acad. Arts Sci., 76, 55 (1948).

----------, Proc. Am. Acad. Arts Sci., 77, 187-234 (1949).

----------, The Physics of High Pressures, Macmillan, New York, N.Y., 1952; also Rev. Mod. Phys. 18, 1 (1946).

----------, Proc. Am. Acad. Arts Sci., 84, 131 (1957).

----------, Studies in Large Plastic Flow and Fracture, Harvard University Press, Cambridge, Mass, 1964.

Cohen, E.R. and J.W.M. DuMond, "Our Knowledge of the Fundamental Constants of Physics and Chemistry in 1964," Rev. Mod. Phys., 37, 537-594 (1965).

Christian, R.H., "The Equation of State of the Alkali Halides at High Pressure," Report UCRL-4900, University of California Lawrence Radiation Laboratory, 1957.

Cook, M.A. and L.A. Rogers, "Compressibility of Solids and Liquids at High Pressure," J. Appl. Phys., 34, 2330-2336 (1963).

Cottrell, A.H., Dislocations and Plastic Flow in Crystals, Oxford University Press, Fairlawn, N.J., 1963.

Davidge, R.W. and P.L. Pratt, "Plastic Deformation and Work-Hardening in NaCl," Phys. Stat. Sol., 6, 759-776 (1964).

Deal, W.E., "Measurement of Chapman-Jouquet Pressure for Explosives," J. Chem. Phys., 27, 796 (1957).

Dennen, R.S. "Hugoniot Determination for Granite and Other Geological Samples," Research Institute Report A6040-1, I Illinois Institute of Technology, (1963).

Dugdale, J.S. and K.K.C. MacDonald, Phys. Rev., 89, 832 (1953).

Duvall, G.E., "Propagation of Plane Shock Waves in a Stress-Relaxing Medium." Stress Waves in Anelastic Solids, H. Kolsky and W. Prager, eds., Constable, 1964.

Ekstein, H., Z. Kristallog, 92, 253 (1935). (Results quoted in Seeger, 1958.)

Fatt, "Compressibility of Sandstones at Low to Moderate Pressures," Bull. Am. Assoc. Petrol. Geol., 42, 1924-1957 (1958).

Eshelby, J.D. et al, "Clayed Dislocations and Strength of Ionic Crystals," Phil. Mag., 8th Series, 3, 75-89 (1958).

Fowles, G.R., "Shock Wave Compression of Hardened and Annealed 2024 Aluminum," Report 011-60, Stanford Research Institute, 1960.

Freudenthal, A.M. and H. Geiringer, "Mathematical Theories of the Inelastic Continuum," Encyclopedia of Physics, 6, Springer-Verlag (1958).

Fumi, F.G. and M.P. Tosi, "Born Model Treatment of Polymorphic Transitions of Alkali Halides," J. Phys. Chem. Sol., 23, 359-366 (1962).

Fumi, F.G. amdn M.P. Tosi, "On the Mie-Gruneisen and Hildebrand Approximations to the Equation of State of Cubic Solids," J. Phys. Chem. Vol. 23, 395 (1962).

Fung, Y.C., Foundations of Solid Mechanics, Prentice Hall Inc., Englewood N.J., 1965).

Gogolyev, V.M., Zh. Priklad. Medhan Tekhn. Fiz., 5, 93-98 (1963). Translation by M.E. Backman available: U.S. Naval Ordnance Test Station Report 9043, 1966.

Goguel, J., Introduction à l'Etude Méchanique des Déformations de l'Ecorce Terrestre, 1948.

Goldsmith, W. and C.F. Austin, "Some Dynamic Characteristics of Rocks," Stress Waves in Anelastic Solids, H. Kolsky and W. Prager, eds., Constable, 1964.

Goranson, R.W. et al., "Dynamic Determination of the Compressibility of Metals," J. Appl. Phys., 26, 1472 (1955).

Graf, L. and H. Klatte. Unpublished results quoted in Seeger (1958).

Gregson, V.G., Jr., "Optical Lever Observation of Hypervelocity Impact Shock Waves," J. Appl. Physics 38, 1798 (1967).

Griggs, David et al., Bull. Geol. Soc. Am., 62, 1385 (1961).

Grine, D.R., "Equations of State of Granite and Salt," Report UCRL-13004, SRI/Poulter Labs for Univ. of Calif, Lawrence Radiation Laboratory, Livermore, 1961.

Guide, R.S. and S.E. Warner, "Project COWBOY--Physical Properties of Salt Samples, Report UCRL-6069, Univ. of Calif., Lawrence Radiation Laboratory, Livermore, 1960.

Handin, J., "Application of High Pressure in Geophysics: Experimental Rock Deformation," ASME Trans., 75, 315-324 (1953).

Hauser, F.E., J.A. Simmons, and J.E. Dern, "Strain Rate Effects in Plastic Wave Propagation," Response of Metals to High Velocity Deformation, P.G. Shewmon and V.F. Zackay, eds., Interscience Metallurgical Society of AIME, John Wiley & Sons Inc. New York, N.Y., 1961. (See, especially, discussion following this paper.)

Hauver, G.E. and A. Melani, unpublished data quoted in van Thiel (1966); Ballistic Research Laboratory Report No. 1259, 1964.

Hartman, W.F., "Determination of Unloading Behavior of Uniaxially Strained 6061-T6 Aluminum from Residual Strain Measurements," J. Appl. Phys., 35, 2090-2096 (1964).

Hirschfelder, Curtiss, and Bird, Molecular Theory of Gases and Liquids, John Wiley & Sons Inc., New York, N.Y., 1954).

Hodgman, C.D., ed., Handbook of Chemistry and Physics, 40th ed., 1958.

Höfer, K.H. "Commentary on Paper by E.C. Robertson," International Conference on State of Stress in the Earth's Crust, Proceedings of June 13-14, 1963, W.R. Judd, ed., 1964.

Holzer, F., "Calculations of Seismic Source Mechanisms," Report UCRL-12219, Univ. of Calif., Lawrence Radiation Laboratory, Livermore, 1965.

Hunter, L. and S. Siegel, Phys. Rev. 61, 84 (1942).

Joffé, A., A. Physik, 22, 286 (1924).

Johnston, T.L., R.J. Stokes, and C.H. Li, Phil. Mag. 8th Ser., 4, 1316 (1959).

Katz, S. et al., "Hugoniot Equation of State of Aluminum and Steel from Oblique Shock Measurement," J. Appl. Phys., 30, 568-576 (1959).

Kittel, C., Introduction to Solid State Physics, 3rd ed., John Wiley & Sons Inc., New York, N.Y., 1966.

Knopoff, L., "Approximate Compressibility of Elements and Compounds," Phys. Rev. 138A, 1445-1447 (1965).

Kormer, Sinitsyn, Funtikov, Urlin, and Blinov, Soviet Phys. JETP, 20, 811 (1965).

Kormer, Funtikov, Urlin, and Kolesnikova, Soviet Phys. JETP, 15, 477 (1962).

Kupfer, D.H., "Structure of Salt in Gulf Coast Domes," Symposium on Salt, A.C. Bersticker, ed., Northern Ohio Geol. Soc., Inc., 1963.

Landolt-Börnstein, Physikalisch-Chemische Tabellen (1923).

----------, Zahlenwerte and Funktionen ..., Bd. 2, Teil 4 (1961).

Lee, E.H. and D.F. Liu, "Influence of Yield on High Pressure Wave Propagation," Stress Waves in Anelastic Solids, H. Kolsky and W. Prager, eds., Constable, 1964.

Lennard-Jones, J.E. and A.F. Devonshire, Proc. Roy. Soc. (London) A163, 53 (1937).

Lewis, H.W. and S.B. Treiman, "Seismic Signals from Nuclear Explosions in Overdriven Cavities (U)," Research Paper P-193, Institute for Defense Analyses, 1965.

Likhachev, V.A., Soviet Phys. Solid State, 3, 2314 (1962).

Lombard, D.B., "The Hugoniot Equation of State of Rocks," Report UCRL-6311, Univ. of Calif., Lawrence Radiation Laboratory, Livermore, 1961.

Löwdin, P.O. Thesis, Uppsala Univ., 1948.

Lundergan, C.D., "The Hugoniot Equation of State of 6061-T6 Aluminum at Low Pressures," Report SC-4637 (RR), Sandia Corporation, 1961.

Mayer, J.E., J. Chem. Phys., 1, 270 (1933).

McQueen and S.P. Marsh, "Equation of State for Nineteen Metallic Elements from Shock Wave Measurement to Two Megabars," J. Appl. Phys., 31, 1253-1269 (1960).

Merrill, R.H., "Static Stress Determinations in Salt Site COWBOY," Report APRL 38-31, Bureau of Mines Applied Physics Research Laboratory, 1960.

----------, "Static Stress Determinations - Hockley Salt Mine," Bureau of Mines Applied Physics Research Laboratory (no date).

Negrete, P. and F.E. Prieto, "Lattice Energy of Ionic Crystals," J. Chem. Phys., 40, 255-256 (1964).

Pauling, L., The Nature of the Chemical Bond, 3rd ed., Cornell Univ. Press, Ithica, N.Y., 1960.

Persson, P.A. and L. Persson, FOA Report A 2299-222, Forsvarets Forskningsanstalt, Avdelning, Sweden (1964), UCRL Translation 1173 (L).

Polski Komitet Normalizacyjny, Vocabulary of Mechanics in Five Languages, Pergamon Press, 1962.

Porzel, F.B., "Some Hydrodynamic Problems in Reactor Containment," Paper 434, Vol. 11, Second International Conference on Peaceful Uses for Atomic Energy (1958).

Rawson, D.E., Trans. Am. Geophys. Union, 44, 129 (1963).

Rawson, D. et al., "Post-Explosion Environment Resulting from Salmon Event," Report UCRL-14280, Rev. II, Univ. of Calif., Lawrence Radiation Laboratory, Livermore, 1966.

Reiner, M., "Rheology," Encyclopedia of Physics, 6, Springer-Verlag (1958).

Rice, M.H., R.G. McQueen, and J.M. Walsh, "Compression of Solids by Strong Shock Waves," Solid State Physics, 6 (1958).

Rogers, L.A., "Shock Compression of Several Rock Types," UCRL-12027, Rev. 1, Univ. of Calif., Lawrence Radiation Laboratory, Livermore, 1964.

Schlichta, P.J., "Effects of Predeformation on the Mechanical Properties of Sodium Chloride Crystals," Tech. Report 32-923, Calif. Institute of Technology, Jet Propulsion Laboratory, 1966.

Schmidt, W., Z. Angew. Mineral. 1, 1 (1937).

Seeger, A., "Kristallplastizität," Handbuch der Physik, VII/2, S. Flugge, ed., 1958.

Seidl, F.G.P., "SOC, A Numerical Model for the Behavior of Materials Exposed to Intense Impulsive Stresses," UCID-5033 Univ. of Calif, Lawrence Radiation Laboratory, Livermore, 1964.

Serata, S., "Transition from Elastic to Plastic States of Rocks under Triaxial Compression," Proceedings of Fourth Symposium on Rock Mechanics, Penn. State Univ. Mineral Industries Exper. Sta. Bull. No. 76 (1961).

Serdengecti, S., and G.D. Boozer, "Effects of Strain Rate and Temperature on the Behavior of Rocks Subjected to Triaxial Compression," Proceedings of Fourth Symposium on Rock Mechanics, Penn. State Univ. Mineral Industries Experiment Sta. Bull. No. 76 (1961).

Shook, W.B. and F.W. Niedenfuhr, unpublished work done at Ohio State Univ. Engineering Experiment Station, 1964.

Shreffler, R.G. and W.E. Deal, "Free Surface Properties of Explosive-Driven Metal Plates," J. Appl. Phys. 24, 44-48 (1953)

Siegbahn, M., Spektroskopie der Röntgenstrahlen (1931).

Slater, J.C., Introduction to Chemical Physics, Chap. 13, McGraw, Hightstown, N.J., 1939.

Spangenberg and Haussuhl, Z. Krist. 109, 422 (1957); Z. Phys. 159, 223 223 (1960).

Stepanov, A.V. and I.M. Eidus, Zh. Eksp. Teor. Fiz. 29, 669 (1955); Soviet Phys. JETP 2, 377 (1956).

Stephens, D.R. "Hydrostatic Compression of Eight Rocks," J. Geophys. Res., 69, 2967-2978 (1964).

Stepanow, A.W., Phys. Z. Sowjet., 8, 25 (1934).

"Technical Encyclopedia," Handbook of Physical, Chemical and Technological Properties, Moscow, 1927.

Timoshenko, S. and G.H. MacCullough, Elements of Strength of Materials, 2nd ed., Van Nostrand, Princeton, N.J., 1940.

Tressman, A.H. Kahn, and W. Shockley, "Electronic Polarizabilities of Ion in Crystals," Phys. Rev. 92, 890-895 (1953).

van Thiel, M. et al., eds., "Compendium of Shock Wave Data," UCRL-50108 Univ. of Calif., Lawrence Radiation Laboratory, Livermore, 1966.

Vashchenko, V.Y. and V.N. Zubarev, Soviet Phys. Solid State, 5, 653 (1963).

Voigt, W., Göttinger Nachrichten, 521 (1893).

Walsh, J.M. et al., Phys. Rev., 108, 196 (1957).

Walsh, J.M. nd R.H. Christian, Phys. Rev., 97, 1544 (1955).

Wilkins, M.L., "Calcul de détonations mono et bidimensionnelles," Les Ondes de Détonation, Editions du Centre National de la Recherche Scientifique, 1962.

Wuerker, R.G., "Annotated Tables of Strength and Elastic Properties of Rock," AIME, Petroleum Branch (1956).

Yates, B. and C.H. Panter, ("Thermal Expansion of Alkali Halides at Low Temperatures,") Proc. Phys. Soc. (London), 80, 373 (1962).

Zel'dovich, Ya.B. and Yu. P. Rayzer, Shock Waves and High Temperature Hydrodynamic Phenomena, 1963.

UNCLASSIFIED

Security Classification

DOCUMENT CONTROL DATA - R & D

(Security classification of title, body of abstract and indexing annotation must be entered when the overall report is classified)

1 ORIGINATING ACTIVITY (Corporate author) Institute for Defense Analyses	2a. REPORT SECURITY CLASSIFICATION Unclassified 2b. GROUP --

3 REPORT TITLE

Uncertainties of Equations of State of Explosively Loaded Rock Salt

4 DESCRIPTIVE NOTES (Type of report and inclusive dates)

Study S-267 February 1968

5 AUTHOR(S) (First name, middle initial, last name)

W. David Barfield

6 REPORT DATE February 1968	7a. TOTAL NO OF PAGES 154	7b. NO OF REFS 118
8a CONTRACT OR GRANT NO DAHC15 C 67 0011 b PROJECT NO ARPA Assignment 10 c d.	9a. ORIGINATOR'S REPORT NUMBER(S) Study S-267 9b. OTHER REPORT NO(S) (Any other numbers that may be assigned this report) NA	

10 DISTRIBUTION STATEMENT

This document has been approved for public release and sale; its distribution is unlimited.

11 SUPPLEMENTARY NOTES NA	12. SPONSORING MILITARY ACTIVITY NA

13 ABSTRACT

(U) In connection with a general investigation of uncertainties in prediction capability for close-in ground motion due to buried explosions, rock salt (halite) is selected as an example of rock-like material for purposes of assessing uncertainties associated with methods for determining material properties and with models of material behavior. Uncertainties of techniques for "laboratory" measurement of shock and static compressibility and plastic flow properties and uncertainties of four different equations of state for highly compressed NaCl are discussed.

DD FORM 1 NOV 68 1473

UNCLASSIFIED

Security Classification